DOE/ET/27111-12

CONSOLIDATION OF GEOLOGIC STUDIES OF GEOPRESSURED GEOTHERMAL RESOURCES IN TEXAS

1983 Annual Report

By T. E. Ewing, N. Tyler, R. A. Morton, and M. P. R. Light

Prepared for the U.S. Department of Energy
Division of Geothermal Energy
Contract No. DE-AC08-79ET27111

Bureau of Economic Geology
W. L. Fisher, Director
The University of Texas at Austin
Austin, Texas 78713

June 1984

DISCLAIMER

This report has been produced directly from the best available copy.

Available from the National Technical Information Service, U.S. Department of Commerce, Springfield, Virginia 22161.

Price: Printed Copy A08
Microfiche A01

Codes are used for pricing all publications. The code is determined by the number of pages in the publication. Information pertaining to the pricing codes can be found in the current issues of the following publications, which are generally available in most libraries: Energy Research Abstracts (ERA); Government Reports Announcements and Index (GRA and I); Scientific and Technical Abstract Reports (STAR); and publication NTIS-PR-360, available from NTIS at the above address.

CONTENTS

SECTION I. STRUCTURAL STYLES OF THE WILCOX GROWTH-FAULT TREND IN TEXAS: CONSTRAINTS ON GEOPRESSURED RESERVOIRS 1

ABSTRACT 1

INTRODUCTION 1

KATY STUDY AREA 2

Stratigraphy of the Katy area 5

Structural development of the Katy area 6

Structural constraints on the occurrence of geopressured reservoirs 15

FOSTORIA DIP LINE 15

Stratigraphy of the Fostoria area 18

Structural development of the Fostoria area 20

Structural constraints on the occurrence of geopressured reservoirs 20

ZAPATA STUDY AREA 22

Stratigraphy of the Zapata area 22

Structural development of the Zapata area 24

Structural constraints on the occurrence of geopressured reservoirs 27

CONCLUSIONS 30

ACKNOWLEDGMENTS 31

REFERENCES 31

Figures in Section I

I-1. Location of the study areas in the Wilcox growth-fault trend, Texas Gulf Coast, showing their relationship to the Rockdale and Rosita delta systems 3

I-2. Location map of the Katy study area 4

I-3. Structure section A-A', Austin and Fort Bend Counties 7

I-4. Isopach map of upper and middle Wilcox strata, Katy study area 9

I-5. Schematic palinspastic sections across the San Felipe area, showing the sequence of structural development 11

I-6. Structure map contoured on top of Wilcox, Katy study area 12

I-7. Structure section C-C' across San Felipe dome, Austin, Waller, and Fort Bend Counties 13

I-8. Isopach map of Vicksburg and Jackson strata, Katy study area 14

I-9. Structure map contoured on top of Vicksburg, Katy study area 16

I-10. Map of the Fostoria area, Liberty and Montgomery Counties, showing the approximate locations of the dip section and oil and gas production 17

I-11. Structural well-log cross-section of the Fostoria area 19

I-12. True-depth interpreted section of the Fostoria area 21

I-13. Location map of the Zapata study area. 23

I-14. True-depth sections of the Zapata study area through the Lobo trend and Fandango structure, through North Falcon Lake field, and across Cinco de Mayo anticline 25

I-15. Structure map on top of Wilcox, Zapata study area 26

I-16. Restoration of section over Fandango field 28

I-17. Structure map on base of Yegua, Zapata study area 29

SECTION II. CHEMICAL COMPOSITION OF DEEP FORMATION WATERS, TEXAS GULF COAST 33

ABSTRACT 33

INTRODUCTION. 33

COMPOSITIONAL DIFFERENCES 35

Candelaria field 35

Other fields in area 3 41

DISCUSSION 41

ACKNOWLEDGMENTS 42

REFERENCES 42

Figures in Section II

II-1. Hydrochemical subregions of the Texas Coastal Plain based on composition of deep formation waters 34

II-2. Trilinear plot showing proportions of major cations and anions in formation waters from hydrochemical subregions, Texas Coastal Plain. 36

II-3. Oil and gas fields with water analyses in hydrochemical subregion 3 37

II-4. Structural dip cross section that transects the Rita and Candelaria fields, Kenedy County 38

II-5. Concentrations of total dissolved solids, major ions, and ion ratios in Candelaria field 39

II-6. Trilinear plot showing proportions of chemical constituents in waters from the Candelaria field 40

SECTION III. CONTINUITY AND INTERNAL PROPERTIES OF THREE GULF COAST STRANDPLAIN SANDSTONES: THEIR IMPLICATIONS FOR GEOPRESSURED FLUID PRODUCTION 43

ABSTRACT 43

INTRODUCTION. 43

Facies influence on reservoir continuity 44

Geologic framework. 46

Oil production from the North Markham - North Bay City field 48

METHODS 52

CAYCE RESERVOIR: A COMPOSITE PROGRADATIONAL STRANDPLAIN/ FLUVIAL-DELTAIC COMPLEX 53

Depositional environment 53

Distribution of sandstone 53

Areal distribution of component facies 53

Interpretation 55

Areal stratification trends 58

Reservoir continuity. 58

Integration of production and reservoir-continuity data within the geologic framework 63

Water influx trends 64
Gas-oil ratio trends 64
Reservoir productivity 66
CORNELIUS RESERVOIR: A PROGRADATIONAL CHENIER-PLAIN COMPLEX . . . 66
Depositional environment 68
Distribution of sandstone 68
Areal distribution of component facies 68
Interpretation 68
Reservoir continuity. 71
Integration of production and reservoir-continuity data within the geologic framework. 71
Water influx trends 71
Reservoir productivity 75
CARLSON RESERVOIR: A TRANSGRESSED STRANDPLAIN DEPOSIT 75
Depositional environment 75
Distribution of sandstone 75
Areal distribution of component facies 77
Interpretation 77
Reservoir continuity. 77
Integration of production and reservoir-continuity data within the geologic framework. 79
Water influx and reservoir productivity trends 79
CONCLUSIONS 79
Reservoir-continuity models 79
Implications for geopressured geothermal energy production 82
Summary 83
ACKNOWLEDGMENTS 83
REFERENCES 84

APPENDIX III-1: List of well logs from North Markham - North Bay City field used in this study 86

Figures in Section III

III-1. Depositional framework of the Frio Formation and of major oil fields producing from the Greta/Carancahua barrier-strandplain system. 45

III-2. Dip section of the upper Frio Formation 47

III-3. Structure map of the North Markham - North Bay City field contoured on top of the Cayce sandstone. 49

III-4. Generalized west-east strike section across the North Markham - North Bay City field 50

III-5. Percent-sand map, Cayce reservoir 54

III-6. Log character and net-sandstone map, Cayce reservoir 56

III-7. Facies anatomy of the Cayce sandstone adapted from vertical SP profiles . . . 57

III-8. Stratigraphic-complexity map of the Cayce sandstone 59

III-9. Resistivity cross sections, East Cayce reservoir 60

III-10. Resistivity cross section, West Cayce reservoir 62

III-11. Sequential water-cut maps, East and West Cayce reservoirs 65

III-12. Reservoir-productivity maps, Cayce reservoir, for 1942 through 1965 and 1966 through 1982 67

III-13. Net-sandstone map, Cornelius sandstone 69

III-14. Interpretive facies anatomy of the third Cornelius sandstone 70

III-15. Resistivity strike section, Cornelius sandstone, showing the continuous distribution of hydrocarbons in beach-ridge sandstones of the mud-rich strandplain 72

III-16. Resistivity dip sections, Cornelius sandstone, showing the offlapping relationship of the Co-3 and Co-2 units 73

III-17. Sequential water cut maps, Cornelius reservoir 74

III-18. Reservoir productivity maps, Cornelius reservoir, 1938 through 1965 and 1966 through 1982 76

III-19. Log facies map of the Carlson sandstone illustrating the complex facies architecture of this transgressed strandplain deposit 78

III-20. Reservoir continuity models of simple progradational strandplain sandstones cut by a minor tidal channel and transected by a fluvial-deltaic system 80

III-21. Reservoir continuity model of transgressed strandplain sandstones 81

Table in Section III

III-1. Geologic, fluid-property, engineering, and production characteristics of the principal oil reservoirs of the North Markham - North Bay City field 51

SECTION IV. INTEGRATED GEOLOGIC STUDY OF THE PLEASANT BAYOU - CHOCOLATE BAYOU AREA, BRAZORIA COUNTY, TEXAS--FIRST REPORT 90

ABSTRACT 90

INTRODUCTION. 90

Setting of the Pleasant Bayou - Chocolate Bayou area 91

STRATIGRAPHIC STUDIES 91

Lower Frio sand distribution patterns of the Upper Texas Gulf Coast. 91

Facies analysis and depositional systems 93

STRUCTURAL DEVELOPMENT 97

SANDSTONE CONSOLIDATION HISTORY 99

Effects of internal factors 101

Diagenetic sequence. 105

Origin of permeable aquifers 110

SALIENT FEATURES OF TEST-WELL DATA 113

Distribution of sand and shale pressure 113

Anomalous vitrinite and thermal alteration indices 117

Normal present geothermal gradient 119

Anomalous silica geothermometer temperature 119

Uranium and thorium anomalies in the lower Frio 119

Smectite-illite transformation and geochronometry. 123

High and variable salinity 123

Wet gas in lower Frio shales 125
THERMAL EVOLUTION OF THE PLEASANT BAYOU AREA 125
Modeling of vitrinite and thermal alteration index data. 125
Significance of the illite geochron. 129
Implications for the origin of geopressure 130
POSSIBLE HYDRODYNAMIC MODELS 131
Pressure 131
Temperature 134
Salinity 134
ACKNOWLEDGMENTS 137
REFERENCES 137

Figures in Section IV

IV-1. Simplified depositional architecture of the lower Frio Formation 92
IV-2. Net-sandstone map of the sub-T5 "C" (Andrau) correlation interval 94
IV-3. Facies anatomy of the T2 (Frio A) sandstone based on SP profiles 95
IV-4. Structure map on the T5 marker, Chocolate Bayou - Danbury Dome area . . . 98
IV-5. Faults penetrated by 53 wells on the Chocolate Bayou dome 100
IV-6A. Explanation of symbols and key to abundance of selected sandstone components plotted against depth 102
IV-6B. Detailed core description and petrography of a distributary-channel and delta-plain sequence having an interbedded reworked abandonment phase, sub-T5 interval, Pleasant Bayou No. 2 well 103
IV-7. Detailed core description and petrography of distributary-mouth-bar sandstones, Andrau sandstone, Pleasant Bayou No. 1 and No. 2 wells 104
IV-8. Detailed core description and petrography of a delta-front slump deposit, Pleasant Bayou No. 1 well. 106
IV-9. Detailed core description and petrography of a shoreface sandstone, T3 interval, Pleasant Bayou No. 1 well 107
IV-10. Detailed core description and petrography of abandonment facies sandstone, sub-T5 interval, Pleasant Bayou No. 1 well 108

IV-11. Frio diagenetic sequence in Brazoria County 109

IV-12A. Computer-processed log, compensated neutron log, and density log for the "C" sandstone, Pleasant Bayou No. 2 well 111

IV-12B. Computer-processed log, compensated neutron log, and density log for the "F" sandstone, Pleasant Bayou No. 2 well 112

IV-13. Shale transit time vs. depth for the Pleasant Bayou No. 1 and No. 2 wells . . . 114

IV-14. Formation fluid pressure vs. depth for the Pleasant Bayou No. 1 and No. 2 wells, as estimated from shale transit time, shale resistivity, mud weights, and drill-stem tests 115

IV-15. Observed resistivity vs. effective overburden pressure for Oligocene shales in Brazoria County compared to Miocene and Oligocene shales of southwestern Louisiana 116

IV-16. Vitrinite reflectance and thermal alteration index vs. depth for the Pleasant Bayou No. 1 well 118

IV-17. Well-log temperature corrected to equilibrium values vs. depth, Pleasant Bayou No. 1 and No. 2 wells 120

IV-18. Proportion of illite and smectite in mixed-layer clays vs. depth, Pleasant Bayou No. 1 well; apparent Rb-Sr age of clays < 0.06 μm in diameter vs. depth in the test well; and oxygen isotope values for shale and glauconite vs. depth in the test well 121

IV-19. Salinity and methane solubility vs. depth, Pleasant Bayou No. 1 and No. 2 wells 124

IV-20. Organic geochemistry of shale extracts vs. depth, Pleasant Bayou No. 1 well 126

IV-21. Models for thermal and diagenetic evolution of the Pleasant Bayou No. 2 well, constrained by burial history, present geothermal gradient, and observed vitrinite reflectance 128

IV-22. Shale resistivity vs. depth, Pleasant Bayou No. 1 and No. 2 wells. 133

IV-23. Temperature vs. depth for Chocolate Bayou area wells; measured fluid samples vs. corrected well-log temperatures 135

IV-24. Measured vs. calculated salinities in the Chocolate Bayou area 136

Table in Section IV

IV-1. Potassium, uranium, and thorium distribution in the GCO-DOE Pleasant Bayou No. 2 well 122

SECTION I. STRUCTURAL STYLES OF THE WILCOX GROWTH-FAULT TREND IN TEXAS: CONSTRAINTS ON GEOPRESSURED RESERVOIRS

Thomas E. Ewing, assisted by R. G. Anderson, R. Padilla y Sanchez, and K. Hubby

ABSTRACT

Two major structural styles are identified in the Wilcox growth-fault trend of the Texas Gulf Coast. The style in central and southeast Texas is characterized by continuous, closely spaced growth faults that have little associated rollover despite moderate expansion of section and that show little flattening of the fault plane with depth. Where the growth-fault trend crosses the Houston Diapir Province, growth faults are localized by preexisting salt pillows; however, the piercement salt domes formed after the main phase of faulting, so the salt tectonics "overprints" the growth faults. In South Texas (south of Live Oak County), a narrow band of growth faults having high expansion and moderate rollover lies over and downdip of a ridge of deformed, overpressured shale and lies updip of a deep Tertiary-filled basin formed by withdrawal of overpressured shale. Significant antithetic faulting is associated with this band of growth faults. Also in South Texas, the lower Wilcox Lobo trend is deformed by highly listric normal faults beneath an unconformity that is probably related to Laramide tectonic activity.

Wilcox sandstone reservoirs are predominantly of high-constructive deltaic (distributary-channel and delta-front) origin. This, together with close spacing of faults and characteristically low permeabilities, limits the size of geopressured reservoirs. The largest reservoirs may be in interfault areas or in salt- or shale-withdrawal basins.

INTRODUCTION

Regional studies conducted for the geopressured geothermal research program of the Bureau of Economic Geology have assessed the presence of geopressured geothermal resources within the major growth-fault trends of the Texas Gulf Coast (Bebout and others, 1978, 1982; Weise and others, 1981). Because of the methods used, these studies could assess only the part of the rock column that has been extensively drilled in the search for oil and gas. To assess prospective areas that have been inadequately drilled and to define areas that might be prospective in the future, one needs to understand the different structural styles within the growth-fault trends. A regional synthesis also allows the extrapolation of results from detailed prospect areas to the entire trend.

Structural style and evolution can be best analyzed in areas where both deep well control and seismic coverage are available. Seismic lines obtained by the Bureau include both data grids surrounding geothermal prospect areas and regional dip-oriented seismic lines. The grids for three prospect areas have been previously reported (Winker and others, 1983). The grid for a fourth prospect, and the regional dip lines crossing the Frio growth-fault trend, have been discussed previously (Ewing, 1983b).

The Wilcox trend is the most landward major growth-fault (syndepositional listric normal fault) trend in the Texas Gulf Coast Basin, lying more or less adjacent to the Lower Cretaceous carbonate shelf margin. Major activity on the faults of this trend occurred in Paleocene and early Eocene time, during deposition of Wilcox Group deltaic sands and muds that prograded the shelf margin (Bebout and others, 1982; Winker, 1982). Most of the progradation in southeast Texas occurred in the lower Wilcox Rockdale delta system (Fisher and McGowen, 1967), whereas the major progradation in South Texas was caused by the upper Wilcox Rosita delta system (Edwards, 1982). Lower Wilcox sandstones in South Texas are also geopressured and growth faulted in the distinct Lobo growth-fault trend.

Three areas will be considered in detail in this report (fig. I-1). The Katy area near Houston shows the interplay of growth faults and salt tectonics; two seismic lines are combined with regional well-log correlation. The Fostoria dip line in Liberty County extends the results of the Katy study. The Zapata area in South Texas shows the upper Wilcox growth-fault trend in an area of active shale tectonics. Together with Winker and others' (1983) study of the Cuero area in De Witt County and Edwards' (1980) brief description of faulting in Live Oak County, this study provides a fairly comprehensive view of the entire Wilcox growth-fault trend in Texas.

KATY STUDY AREA

The Katy study area in southeast Texas includes most of Waller and Austin Counties and parts of Harris and Fort Bend Counties (fig. I-2). The area lies between the Colorado geopressured fairway to the southwest and the Harris geopressured fairway to the northeast, as defined by Bebout and others (1982). Correlations within the Wilcox have been extended from the studies of these two fairways. More than 200 well logs were examined and correlated, and 2 regional dip-oriented seismic lines were interpreted. Examination of field data from the Railroad Commission of Texas files improved the mapping of productive structures.

The Katy area lies in the northwestern corner of the Houston Diapir Province (fig. I-1). Two shallow piercement salt domes occur: Hockley dome in Harris County (with salt at -200 ft) and San Felipe, or Brookshire, dome in Waller and Austin Counties (with salt at -2,600 ft;

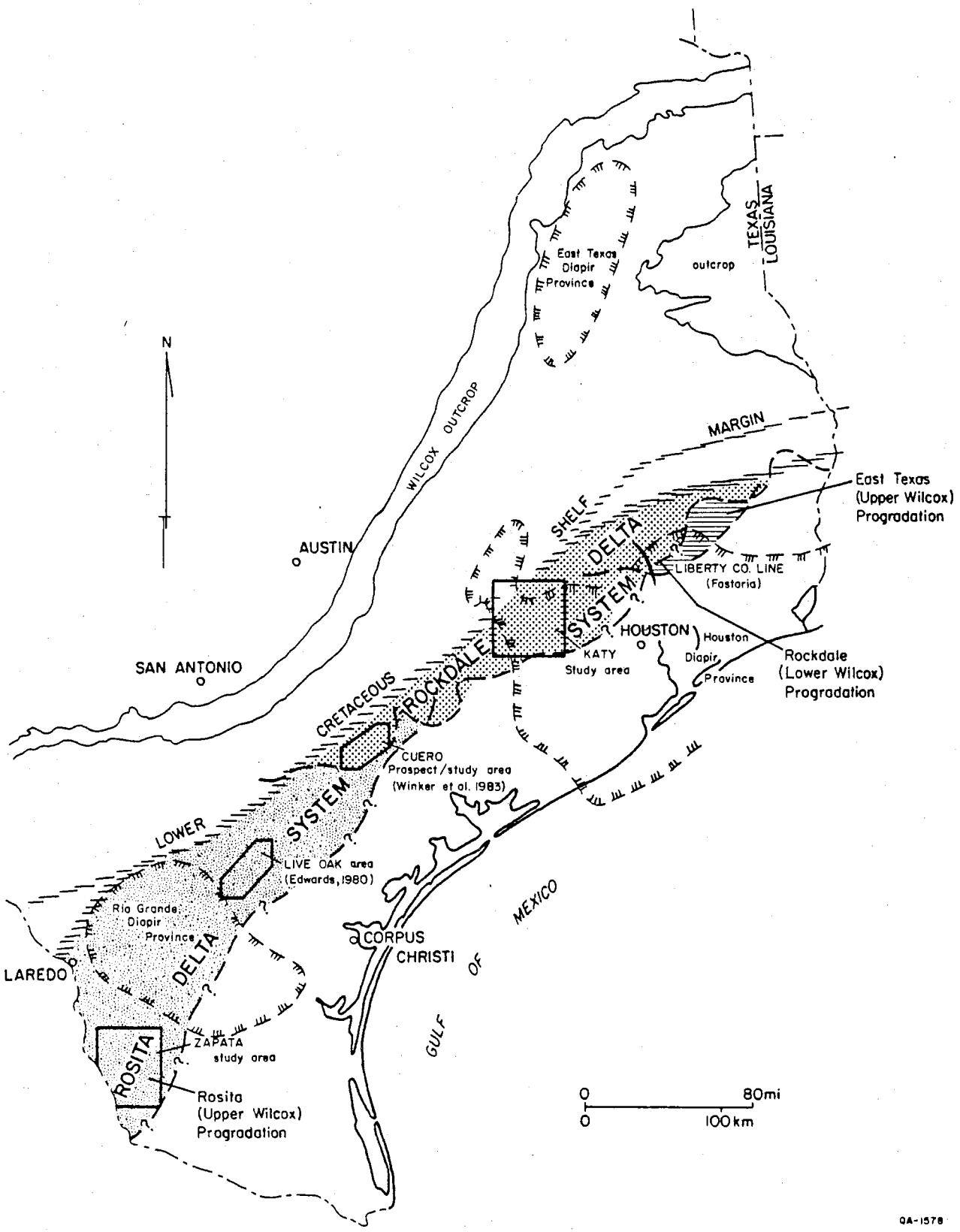

Figure I-1. Location of the study areas in the Wilcox growth-fault trend, Texas Gulf Coast, showing their relationship to the Rockdale and Rosita delta systems.

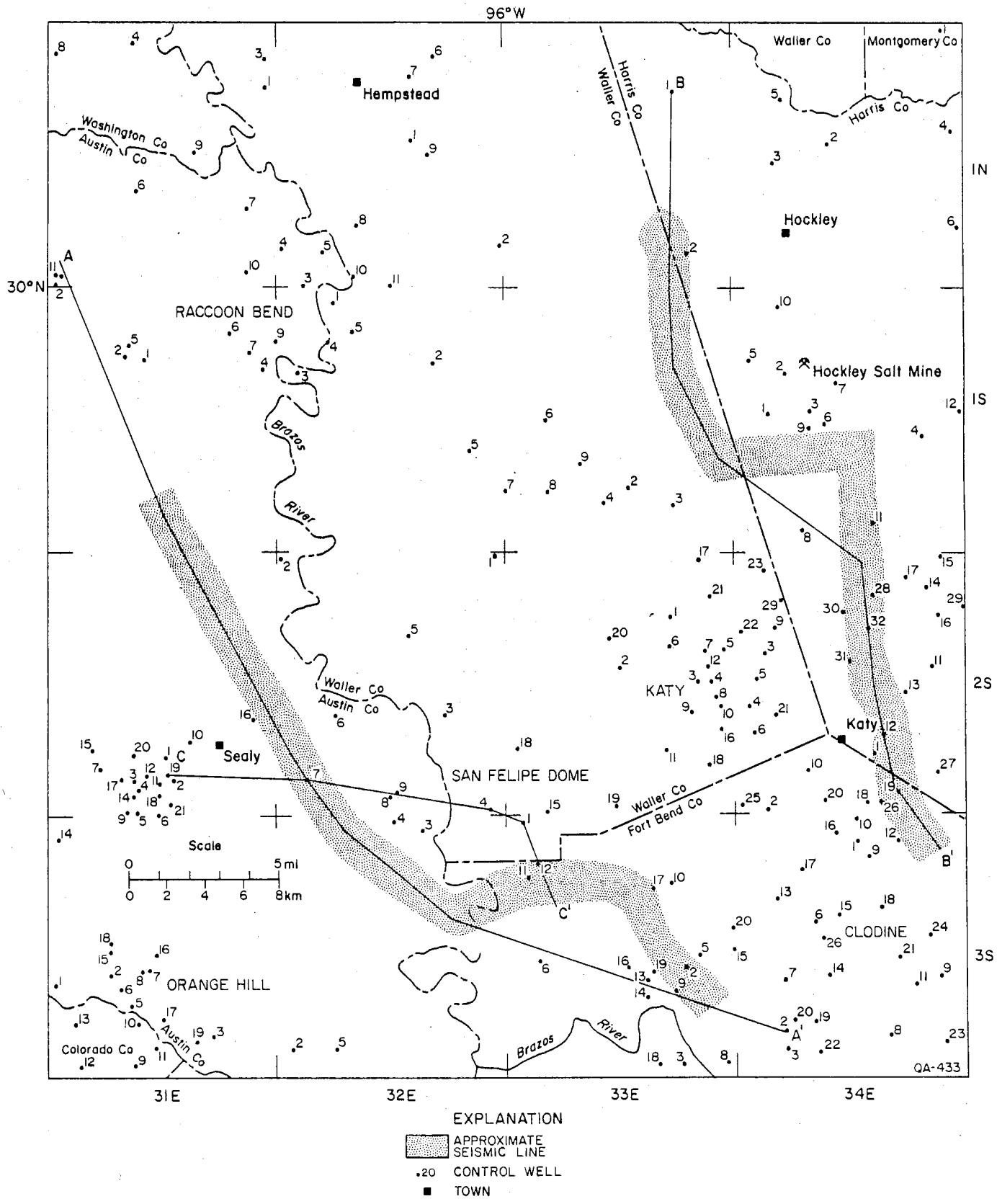

Figure I-2. Location map of the Katy study area.

Halbouty, 1979). Both of these domes have been the site of minor hydrocarbon production. Raccoon Bend field in northeastern Austin County overlies a deep-seated salt diapir (salt at -11,004 ft).

The study area includes significant oil and gas production from the Yegua Formation at Raccoon Bend and Katy fields, as well as from smaller fields such as Fulshear and Clodine in the southeastern corner of the area. The Wilcox has yielded gas at Sealy, Orange Hill, and Katy. Little deep drilling has taken place; of the 200-plus wells examined, only about 95 reach the top of the Wilcox Group. The seismic lines were therefore essential in interpreting the deep structure of the area.

Stratigraphy of the Katy Area

No direct information is available on the sub-Wilcox stratigraphic units in the Katy area; however, the character of seismic reflections together with regional information allows some inferences. The lowest units seen on seismic sections are from Lower Cretaceous carbonates. These carbonates lie seaward of the major Sligo and Stuart City (Edwards) reef trends and are inferred to represent their basinal facies equivalents. Undifferentiated marine strata of Gulfian (Upper Cretaceous) and Midway (Lower Paleocene) ages overlie these carbonates. Seismic sections show a sequence of prograding clinoforms in the upper Midway and basal Wilcox Groups, representing the seaward advance of the Wilcox shelf margin.

The lower Wilcox Group is a sandstone-rich (more than 60 percent sandstone) clastic sequence that was deposited in the Rockdale delta system (Fisher and McGowen, 1967). Sandstone percentage in the upper part of the lower Wilcox remains high as far to the southeast as it has been penetrated, suggesting that deltaic progradation continued well to the southeast of the Katy area. Seismic data indicate that the lower Wilcox Group ranges in thickness from 3,600 ft to more than 6,000 ft updip of the first major growth fault.

The middle Wilcox Group is a sandstone-shale sequence, probably of deltaic origin, having less sandstone than the units below and above (generally 20 to 40 percent). To the northwest, this unit becomes less distinct. The upper Wilcox Group is a sandstone-rich (40 to 75 percent) clastic sequence. It is part of a regional sandstone maximum in southeast Texas (mapped by Bebout and others, 1982) that is inferred to represent a delta system that succeeded the lower Wilcox Rockdale delta system. The combined middle and upper Wilcox Group ranges from 1,700 ft to more than 5,000 ft in thickness.

The overlying lower Claiborne Group consists of 1,500 to 2,000 ft of neritic shale. Sandstones and siltstones of the Sparta and Queen City Formations are found in the area northwest of Raccoon Bend but do not persist basinward. The overlying Yegua Formation

(upper Claiborne Group) consists of 1,500 to 2,000 ft of sand and shale (10 to 60 percent sand). Mapping of sand percentage shows that the northern half of the area was dominated by a fluvial regime having dip-oriented sand maxima, which fed a delta system in the southern half of the area.

The Jackson Group overlies the Claiborne strata. Although mostly marine shale, it contains important sandstones in the northwestern part of the area. The overlying Vicksburg Formation (lower Oligocene) is a sandstone-shale sequence in which minor fluvial axes in Austin and Waller Counties merge southward to form a strike-oriented deltaic sand maximum (Gregory, 1966). The overlying Catahoula and younger strata are nonmarine fluvial-streamplain sediments.

The velocity structure of these sedimentary units has been derived from velocity analyses made during routine processing of the seismic lines. In general, the velocity structure is similar to that of the Cuero area to the southwest (Winker and others, 1983). However, in the Katy area, the Sparta horizon yields a very strong reflector that masks the distinctiveness of the top Wilcox reflector. The Sparta reflector is probably related to constructive interference, as no large velocity break exists. Velocities in the Wilcox vary across the area, with lower velocities in the basinward areas, as in the Cuero area. This is probably related to a combination of decrease in the amount of sand and rise in the first occurrence of geopressure. Although no detailed study of the distribution of geopressure has been made, the data presented by Bebout and others (1982) indicate that the lower Wilcox interval is geopressured in the central and southeastern parts of the Katy area. The upper Wilcox is hydropressured over most of the area.

Structural Development of the Katy Area

Detailed well-log correlation and seismic interpretation have been combined to produce structure maps on the Vicksburg, Yegua, and upper Wilcox horizons; isopach maps of the Vicksburg, Jackson, Claiborne, and upper and middle Wilcox units; and true-depth structural sections paralleling the seismic lines and crossing San Felipe dome. Three phases of structural development are indicated: a Mesozoic salt-pillow phase; a Wilcox phase of growth faulting associated with shelf-margin progradation; and a post-Wilcox phase of piercement salt diapirs.

Evidence for the nature and scope of pre-Wilcox tectonics in the area is confined to the seismic data. On dip-oriented seismic lines (fig. I-3), a thinning of the Gulfian strata is noted in the area of the later withdrawal basins around the salt domes. This suggests that an early, broad, salt-cored uplift was present at and updip of each of the two domes. Such uplifts may have been underlain by nondiapiric salt pillows similar to those in the East Texas Basin (Seni and Jackson, 1983). The Raccoon Bend structure, as well as the Sealy structure to the southwest,

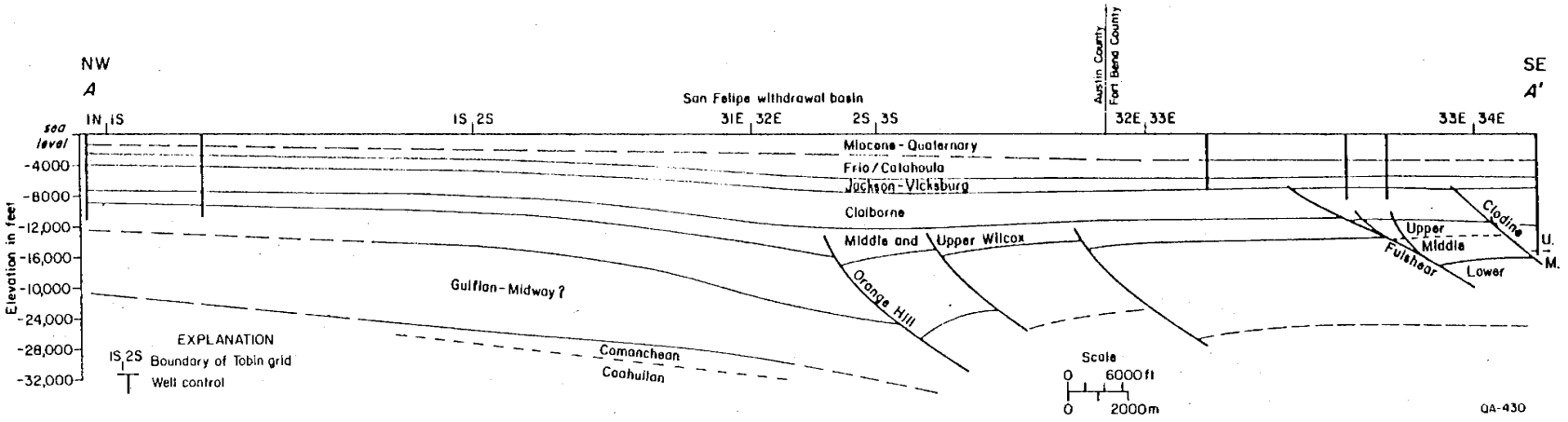

Figure I-3. Structure section A-A', Austin and Fort Bend Counties; line of section is shown in figure I-2.

may be similar in geologic history to the Brenham line of salt domes (including Brenham, Clay Creek, and Millican domes) in Washington and Burleson Counties to the northwest, which appear to have a Cretaceous diapiric history.

The pillows that are inferred to underlie the San Felipe and Hockley salt domes and their related salt-withdrawal basins lie on trend with two large, oil-productive domal structures, Conroe and Tomball, to the northeast. Conroe dome is the site of a marked gravity low (Hammer, 1983, p. 222). It seems reasonable that these large features are also salt pillows that failed to develop into piercement salt domes after progradation of the Wilcox shelf margin. This northeast-trending alignment of pillows may have developed along an early salt-cored ridge seaward of and parallel to the Lower Cretaceous carbonate shelf margin.

The Wilcox phase of tectonic activity is shown by the upper Wilcox isopach map (fig. I-4). A series of three or four large growth faults trend southwest-northeast across the San Felipe and Hockley dome areas. These faults were previously known from the Orange Hill field. The base of the lower Wilcox is not well defined basinward of these faults; however, faint baselapping reflectors in one seismic line suggest that the lower Wilcox section has undergone at least a twofold expansion across this fault system (fig. I-3). Upper and middle Wilcox growth on these faults is also considerable, with expansion indices (downthrown/upthrown) of 1.3 to 1.6 on each fault (fig. I-4). These faults flatten downward somewhat, suggesting a décollement plane above the Lower Cretaceous carbonates; however, the quality of the seismic data is insufficient to fully demonstrate this. The lower and middle Wilcox units in the fault zone show dip reversal (landward dip). Another belt of large growth faults is found in the southeastern corner of the area, including the Fulshear and Clodine faults. These faults were active during middle and upper Wilcox deposition; expansion indices ranged from 1.7 to greater than 2.5. These faults may have a shallower dip and less curvature than do the lower Wilcox faults.

Salt tectonism was less important than growth faulting during Wilcox deposition. The anomalous thickening of the lower Wilcox strata landward of the Orange Hills fault near San Felipe dome suggests that a withdrawal basin had developed. However, much of the development of this basin was masked by large-displacement growth faulting. On the basis of present data, it appears that the salt stocks at San Felipe and Hockley were probably not present during the main phase of growth faulting. This is similar to the growth history of Danbury Dome in the Brazoria fairway of the Frio trend (Winker and others, 1983). The Sealy and Raccoon Bend structures were persistent sediment thins during Wilcox deposition, suggesting that these salt domes, although they failed to diapirically intrude the massive clastic influx of the Wilcox, continued to be uplifted.

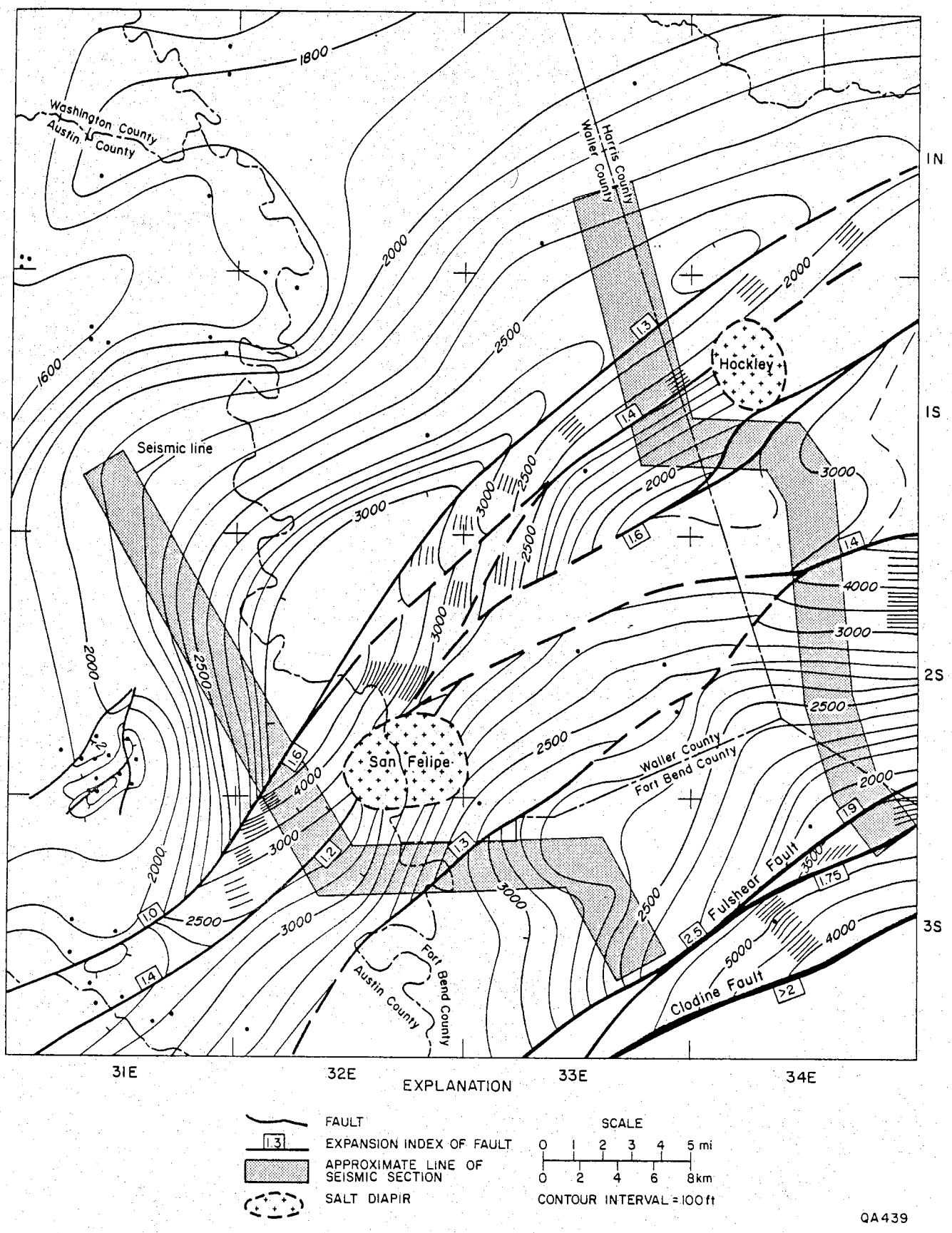

Figure I-4. Isopach map of upper and middle Wilcox strata, Katy study area.

The identification of large-displacement growth faults of early to middle Wilcox age (the Orange Hill system) and of middle to late Wilcox age (the Fulshear-Clodine system) is consistent with the stratigraphic record of substantial early Wilcox (Rockdale) and late Wilcox deltaic shelf-margin progradation. These deltaic systems prograded from northwest to southeast, burying the salt pillows in a mass of unstable clastic sediment. In the wake of the shelf-margin progradation, the growth faults stabilized and salt stocks grew from the pillows, leading to the post-Wilcox structural phase.

Unlike the Cuero and Live Oak areas (Edwards, 1980; Winker and others, 1983), the first Wilcox-age growth faults do not occur immediately downdip from the Cretaceous reef trend, but rather 20 or more miles basinward. Most previous work has assumed that the first progradation of the Wilcox sand package over thick basinal shales started growth faulting; however, the history appears to have been more complex in the Katy area. The location of the Orange Hill fault system may have been controlled by the line of nondiapiric salt pillows, much as other growth-fault systems are controlled by shale ridges (Bruce, 1973). Instability updip of the pillows may have been inhibited by the buttressing effect of the pillows, despite the presence of 6,000 ft of Gulfian shale and marl. Instability was concentrated atop the pillows, and a décollement surface developed on their basinward slopes (fig. I-5).

After Wilcox time, salt tectonics became the dominant feature of the area. The two piercement salt domes, each associated with a deep, crescentic salt-withdrawal basin, pierced and deformed the Wilcox (fig. I-6) and Claiborne strata. Both domes are located along the Orange Hill fault system, piercing the major fault planes. The associated basins lie updip from the salt stocks; the deep basin and the stock together outline the original pillow shape. The Katy domal anticline originated after Wilcox time as a residual high between the two withdrawal basins and the area of continuing growth faulting to the southeast. This high may be a sediment-cored turtle structure formed by infilling of a pre-Wilcox interpillow withdrawal basin. The Sealy and Raccoon Bend structures continued to be slightly uplifted during Claiborne time, testifying to the continued buoyancy of their underlying salt masses.

Activity during Jackson and Vicksburg time was largely confined to continued uplift of the salt stocks, slight uplift of the Raccoon Bend and Sealy structures, and sinking of the withdrawal basins (fig. I-7). After Vicksburg deposition, the Claiborne and Jackson strata were pushed up and overturned along the western flank of San Felipe dome (fig. I-8), developing a local unconformity upon which Frio/Catahoula sediments were deposited (Halbouty and Hardin, 1954). Multiple cap rocks on Hockley dome (Canada, 1962) suggest an episodic uprise of the salt stock there as well.

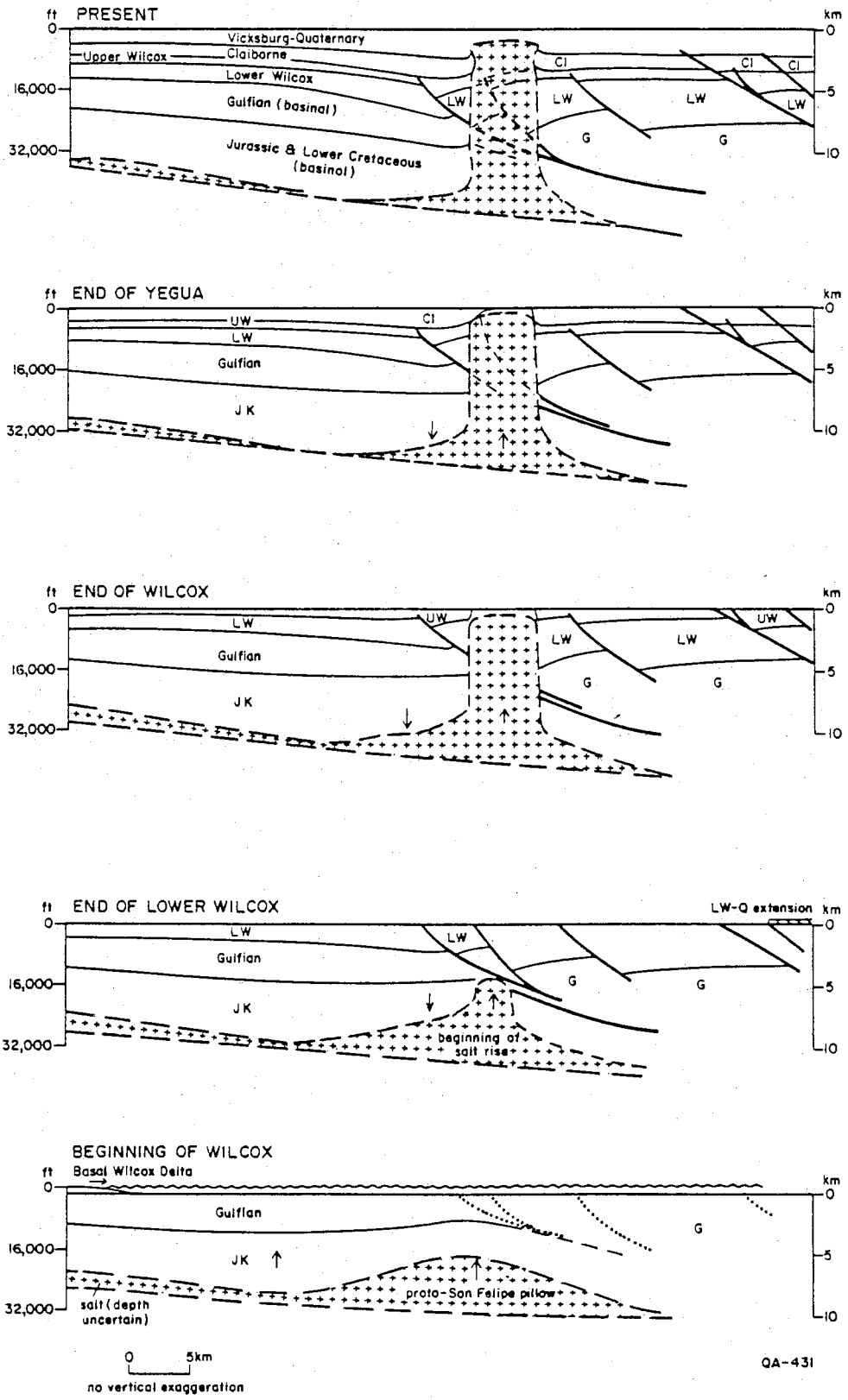

Figure I-5. Schematic palinspastic sections across the San Felipe area, showing the sequence of structural development.

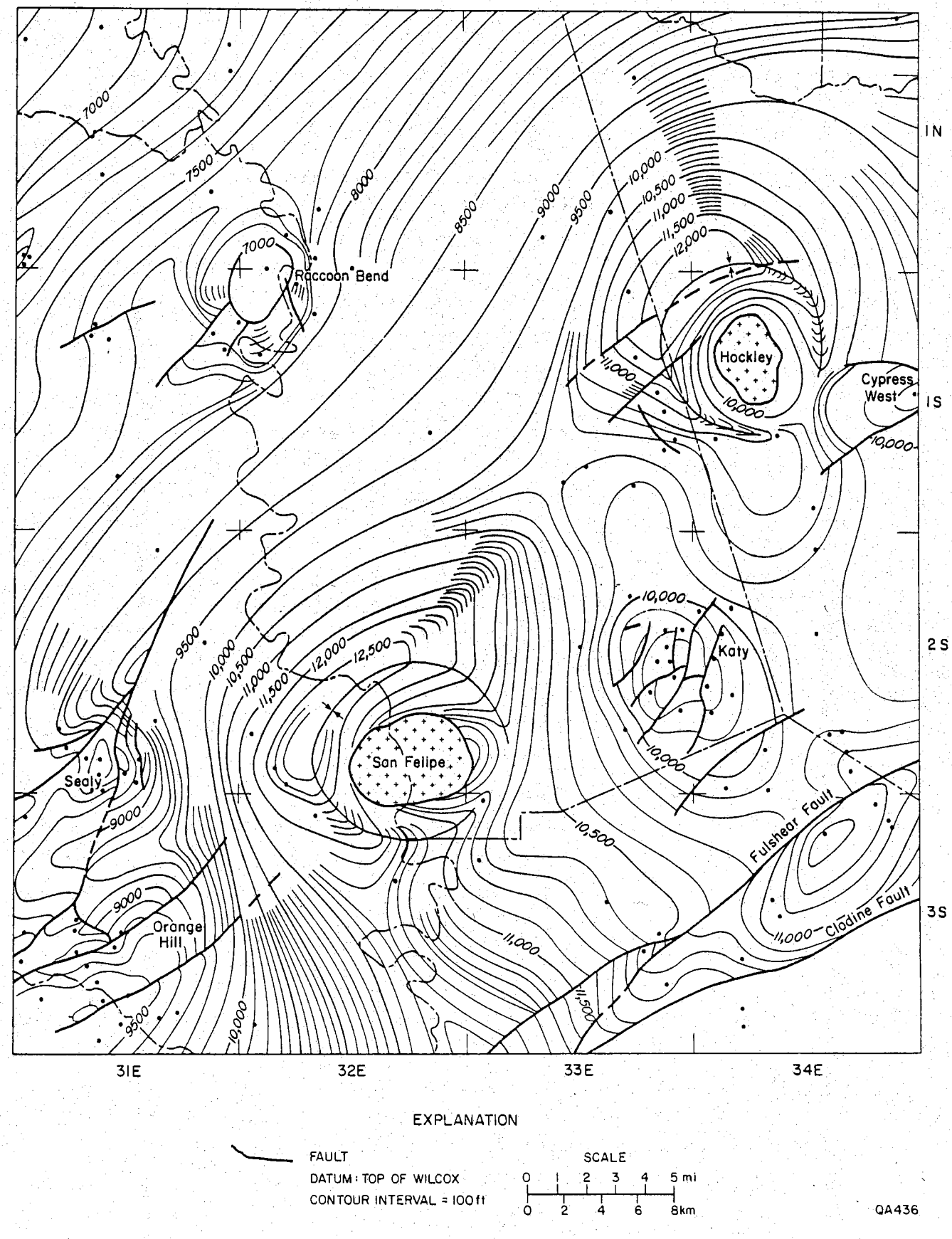

Figure I-6. Structure map contoured on top of Wilcox, Katy study area.

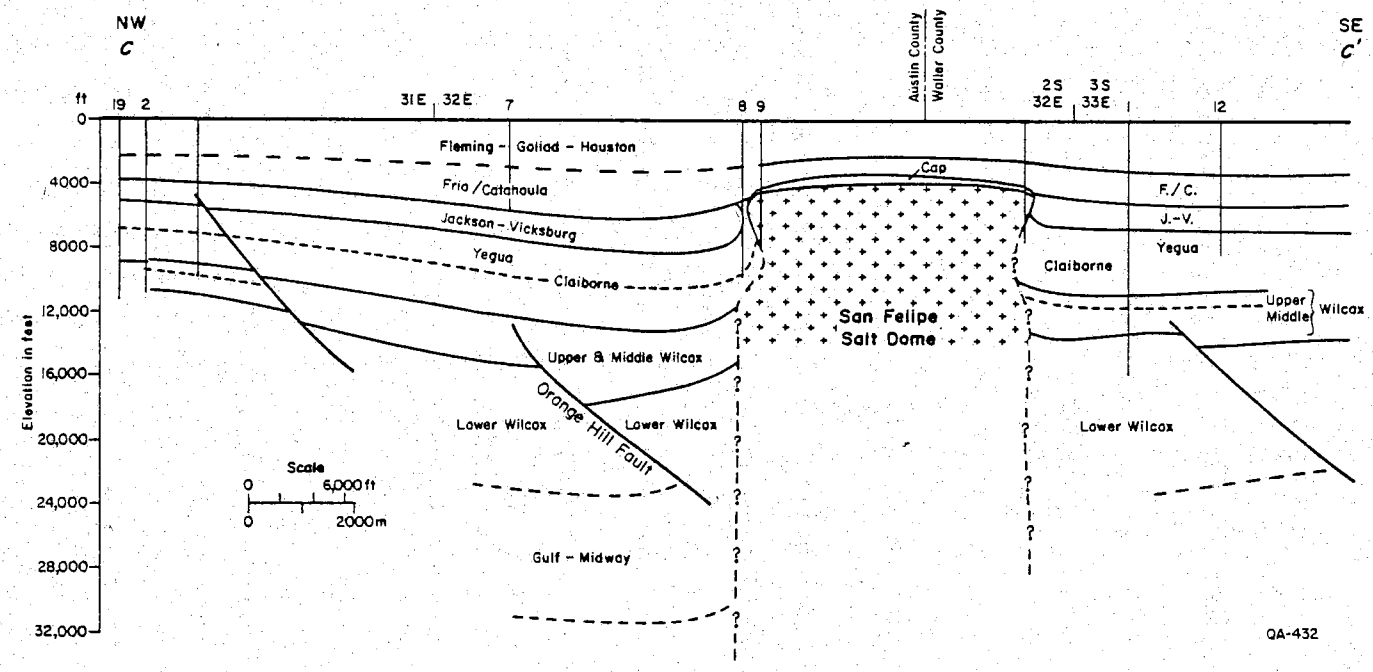

Figure I-7. Structure section C-C' across San Felipe dome, Austin, Waller, and Fort Bend Counties; line of section is shown in figure I-2.

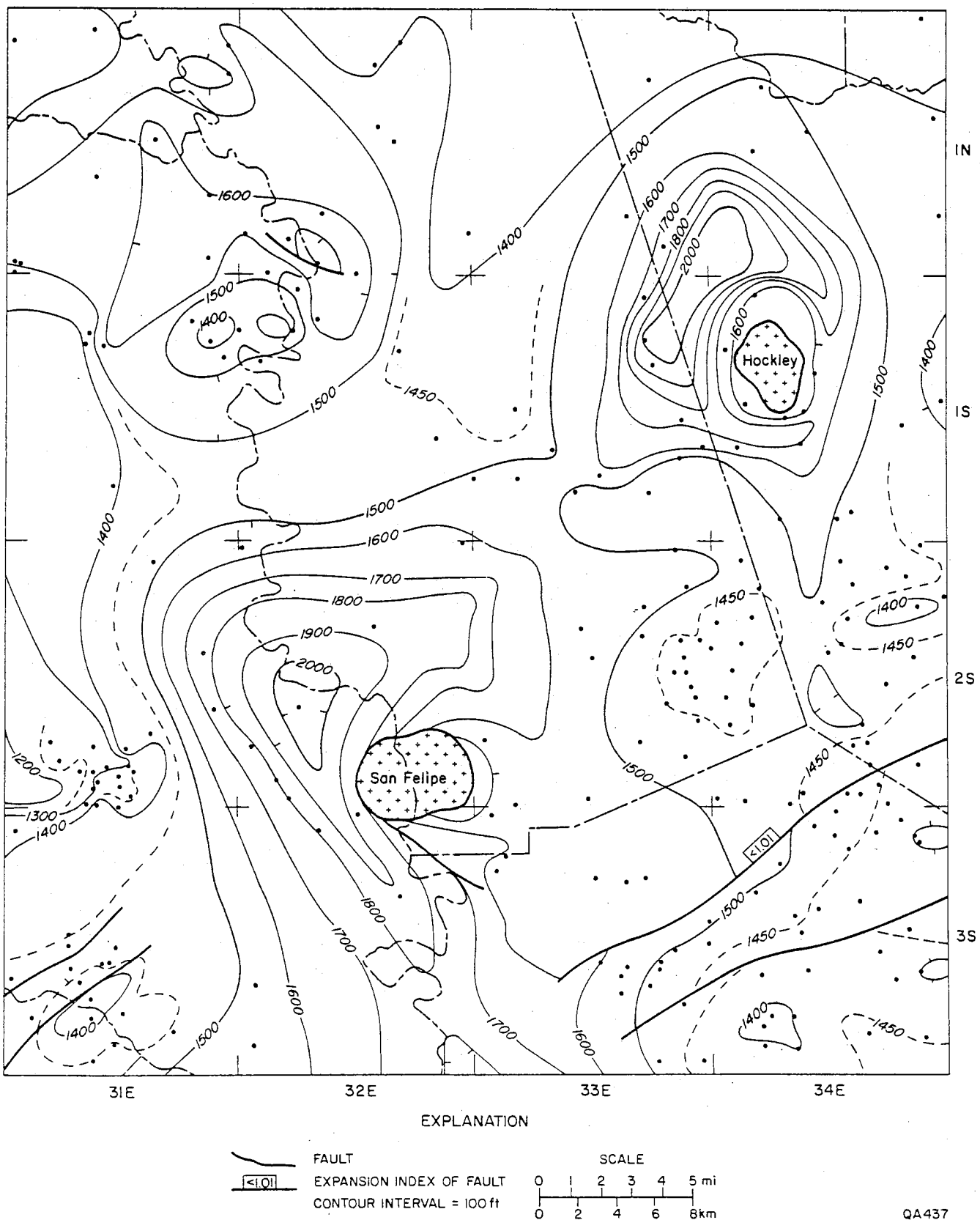

Figure I-8. Isopach map of Vicksburg and Jackson strata, Katy study area.

Post-Vicksburg structural activity continued the Jackson and Vicksburg patterns (fig. I-9). Growth of San Felipe dome apparently ceased in Frio/Catahoula time, as it is buried by Frio/Catahoula and younger sediments. Hockley dome, however, continued to pierce and deform sediments to Pleistocene time. Southeastward dip, probably caused by loading of the large Frio depocenter to the southeast, tilted the entire region.

Structural Constraints on the Occurrence of Geopressured Reservoirs

Geopressured sandstone reservoirs are found downdip of the Orange Hill fault system in the Wilcox Group. Wilcox sandstones updip of this fault system have not been tested but are probably not highly geopressured because of aquifer continuity updip. The growth-fault trends of the Wilcox in the Katy area (fig. I-4) are similar to those that have yielded large quantities of geopressured natural gas to the southwest. In Austin and Waller Counties, these fault trends have been deformed by salt tectonism, but gas-productive reservoirs should still exist; the deep potential of the area has not been adequately determined (Ewing, 1983a).

Although the lower Wilcox has been penetrated only in a few wells in the Katy area, those penetrations, along with regional considerations, suggest that the typical geopressured reservoirs may be distributary-channel and related delta-front sandstones similar to those in the Cuero area (Winker and others, 1983). Fault-block geometry within the fault systems is expected to be similar to that at Cuero: highly elongate with limited dip extent. This combination limits aquifer volumes. The area between the two fault systems, however, has a much broader dip extent and may favor larger aquifer volumes. Large geopressured aquifers may exist in the area of Katy field and south of San Felipe dome.

Low permeabilities are reported from Wilcox sandstones in both the Harris and Colorado fairways (Bebout and others, 1982), and these inhibit the flow rates necessary for geopressured geothermal energy production. This reduces the quality of geopressured geothermal reservoirs in the sand-rich Wilcox sequence in the Katy area.

FOSTORIA DIP LINE

A dip-oriented section across the Wilcox growth-fault trend in western Liberty County has been constructed using a regional seismic line and all available well information. The line (fig. I-10) extends from southern San Jacinto County across the Fostoria fault block southward into the rim syncline of North Dayton salt dome. The line lies on the northern flank of the Houston Diapir Province (fig. I-1), and within the Harris geopressured geothermal fairway (Bebout and others, 1982).

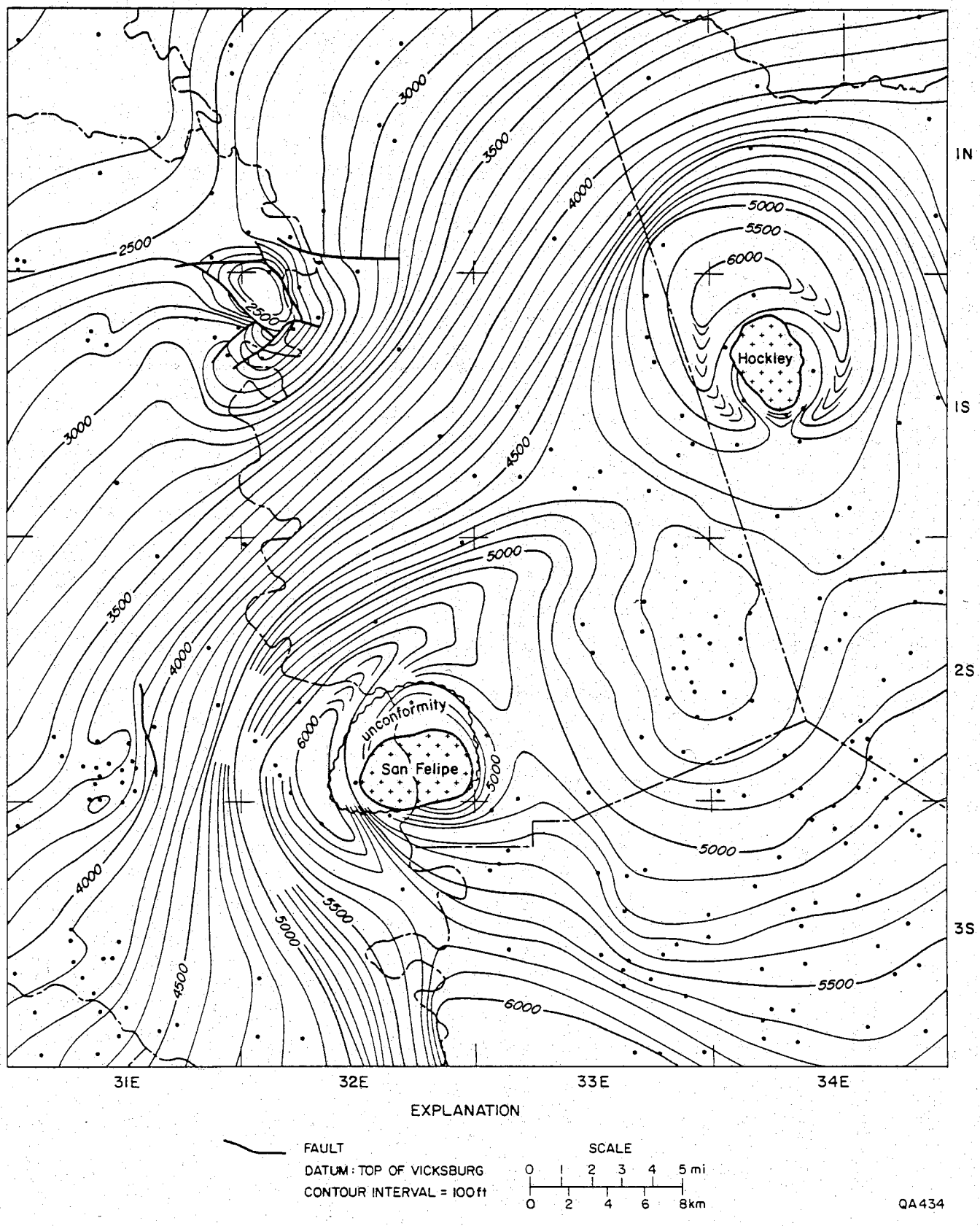

Figure I-9. Structure map contoured on top of Vicksburg, Katy study area.

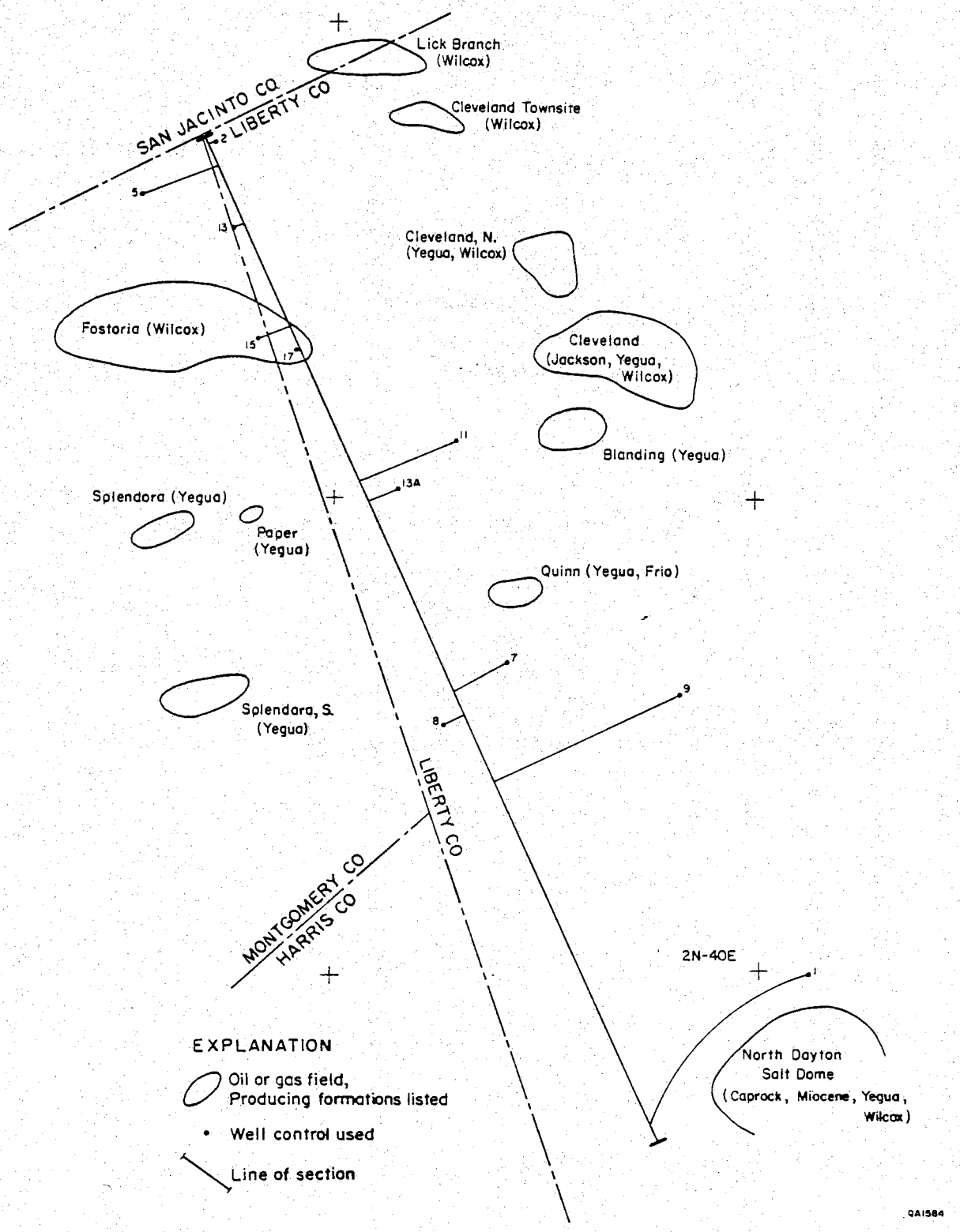

Figure I-10. Map of the Fostoria area, Liberty and Montgomery Counties, showing the approximate locations of the dip section and oil and gas production.

In addition to the lower Wilcox gas produced at Fostoria field, significant gas has been produced from the Wilcox in Cleveland Townsite and Lick Branch fields; Yegua oil and gas also have been produced in Quinn and Splendora fields. Many wells penetrate the upper Wilcox in the updip part of the area, but no wells completely penetrate the lower Wilcox.

Stratigraphy of the Fostoria Area

Neither the sub-Wilcox strata nor the marginal-marine base of the lower Wilcox have been drilled. The area is about 20 mi basinward of the Lower Cretaceous reef trend. Although the area lies downdip of some mapped faults of the Wilcox growth-fault trend, the deep Cretaceous yields some distinctive reflections on the seismic line north of Fostoria. Prograding clinoforms in the Midway interval are not observed on the seismic section; the base of the Wilcox is picked at a change in reflection character from less-continuous reflectors in the fluvial-deltaic Wilcox to more-continuous reflectors in the Midway or Gulfian section. Downdip this pick is arbitrary.

The lower Wilcox Group is a sand-rich clastic sequence (fig. I-11) forming part of the Rockdale delta system (Fisher and McGowen, 1967). Sand percentage remains high in the lower Wilcox to the downdip limit of well control; the final deltaic shelf margin is therefore inferred to lie basinward of this limit (south of Fostoria field). The continuous reflections in the deep basin northwest of North Dayton dome suggest that the interval may have passed into a marginal-marine to marine facies. The thickness of the lower Wilcox strata is unknown but probably ranges from 4,000 ft updip to perhaps as much as 8,000 ft downdip.

The middle Wilcox Group is a slightly less sand-rich sequence, probably of deltaic origin. It is less distinctive here than farther to the west and southwest (as in the Katy or Cuero areas). The upper Wilcox Group is a sand-rich clastic sequence forming part of the regional sand maximum in southeast Texas mapped by Bebout and others (1982). Thickness of the combined upper and middle Wilcox Group ranges from 2,400 to more than 7,000 ft.

The stratigraphic sequence above the Wilcox is basically the same as that in the Katy area. Strong continuous seismic reflectors are noted in the lower Claiborne Group, perhaps near the Sparta horizon, and in the Jackson Group marine strata above the Yegua deltaic(?) sequence. A thin interval of Vicksburg strata occurs in the downdip part of the section, overlain by the Catahoula Formation and by Neogene nonmarine strata.

Velocities derived from the seismic stacking velocities were used for time-depth conversion of the seismic data. The velocity structure, as in the Katy and Cuero areas, shows a downdip decrease in Wilcox interval velocity. This decrease is most marked downdip of Wilcox penetrations and may reflect either a decrease in sand content or an increase in the degree of overpressuring. The top of geopressure rises downsection from within the lower Wilcox interval into the middle Wilcox; the nature of geopressure in the southern part of the line is unknown.

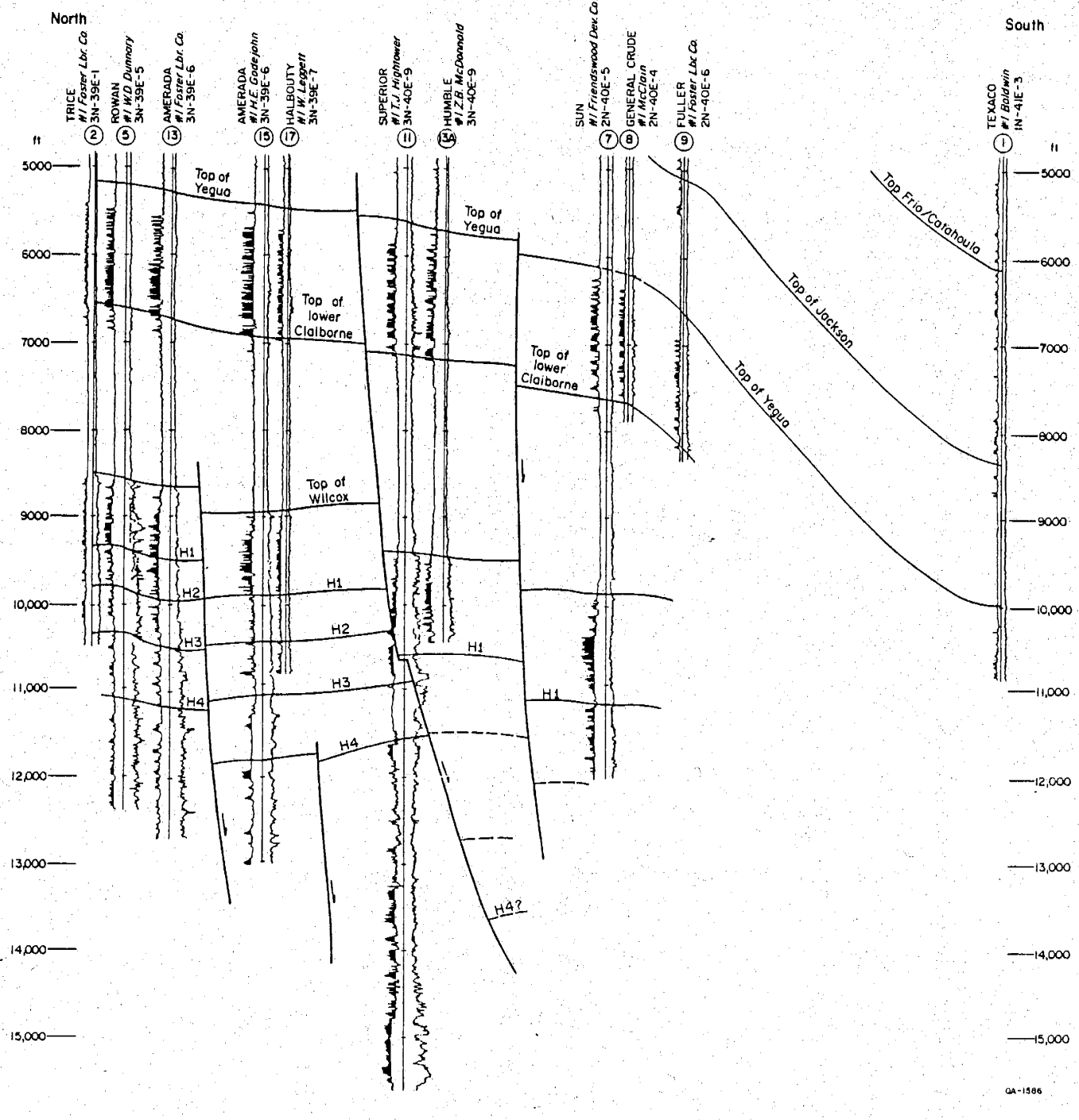

Figure I-11. Structural well-log cross-section of the Fostoria area.

Structural Development of the Fostoria Area

There are two distinct phases of structural development in the Fostoria area: one primarily affecting the Wilcox Group and the other of post-Claiborne age (fig. I-12). The deeper structure consists of four growth faults and a deep basin. The two updip faults expand the lower Wilcox section substantially but show only minimal movement in younger units. They have very little associated rollover, similar to the Wilcox trend at Cuero (Winker and others, 1983). The two downdip faults formed on the northern flank of a deep basin. They show large expansion of the upper and middle Wilcox sequence (as interpreted from seismic data) and continued to move through Claiborne time. The faults appear to become parallel with seismic reflectors in the lower Wilcox(?) interval, suggesting that they may sole out near the base of the lower Wilcox. The deep basin shows strong reflections down to 28,000 ft, but stratigraphic assignment is uncertain. Much of the basin, however, is filled with Wilcox-age rocks. This deep basin stopped subsiding at about the end of the Wilcox; Claiborne and Jackson strata are uniform in thickness across the section.

The post-Claiborne strata dip generally basinward, except that Catahoula and Neogene strata markedly thicken into the rim syncline surrounding North Dayton salt dome. This thickening indicates that the North Dayton dome became a piercement diapir during Oligocene (Frio/Catahoula) time, even though Wilcox and Yegua sand deposition substantially preceded this.

The deep Wilcox basin disclosed by the seismic data may, because of its location relative to North Dayton dome, represent a primary peripheral sink related to a salt pillow. The general form of the structural high underlying the growth faults at Fostoria field (strengthened by the upturned deep reflector in the Cretaceous) suggests the presence of a pillow. A gravity low underlies the Cleveland field east of the line (Hammer, 1983). The shelflike appearance of the Claiborne structure in the Quinn area is thus due to an incomplete turtle structure. Some of the deep-basin reflectors may represent an intraslope basin developed before progradation of the Wilcox shelf margin. The deep basin, however, is also similar to structures in South Texas, described below, which appear to be due largely to shale mobilization and withdrawal.

Structural Constraints on the Occurrence of Geopressured Reservoirs

Geopressured sandstone reservoirs are thought to be sparse in the Fostoria area. The lower Wilcox deltaic sand sequence is very sand rich; geopressure occurs in the sequence only at great depth. However, neither the deeper parts nor the downdip extension of the sequence have been tested, and more significant overpressures may occur there.

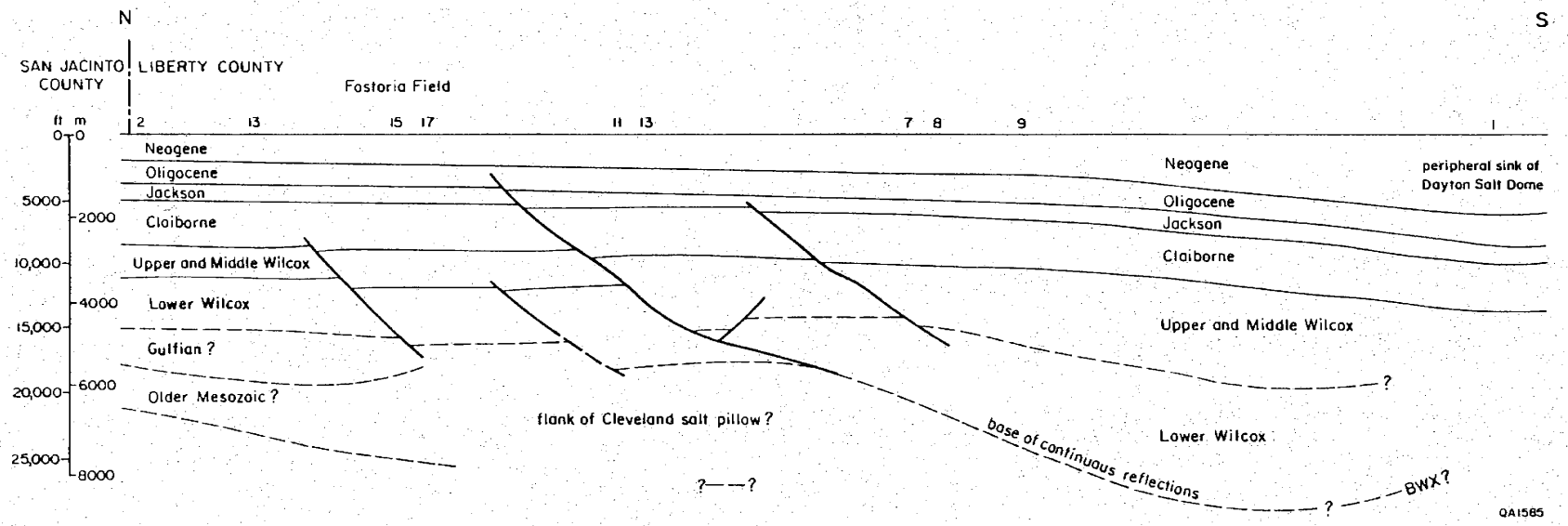

Figure I-12. True-depth interpreted section of the Fostoria area.

The part of the Wilcox that has been drilled is dominated by fluvial or distributary-channel sand bodies, which are expected to be low-volume, dip-oriented reservoirs. However, if these sand bodies occur and are geopressured in the deep basin, they could be high-volume reservoirs. The basal and downdip parts of the lower Wilcox are expected to contain more continuous sands of marginal-marine (delta-front and strandplain) origin; these constitute a significant but untested hydrocarbon and geothermal play. As in the Katy area, the deep Wilcox sandstones may have low permeabilities.

ZAPATA STUDY AREA

The Zapata study area includes most of Zapata County in South Texas, the western edge of Jim Hogg County, and a small part of Starr County (fig. I-13). The area lies within the Zapata geopressure fairway described by Bebout and others (1982). The well-log correlations used in the previous study were checked and extended to all available wells in the area; proprietary seismic lines also were examined.

The Zapata area lies at the western margin of the Tertiary Rio Grande Embayment. The area contains complex structures associated with upper Wilcox shelf-margin progradation of the Zapata delta of the Rosita delta system (Edwards, 1982). In the western half of the area, structures associated with the lower Wilcox Lobo trend occur, as do gentle anticlines probably related to Laramide deformation.

Stratigraphy of the Zapata Area

Rock units older than Late Cretaceous have not been drilled in the Zapata area. Proprietary lines disclose that Jurassic-age salt is present, forming low-amplitude pillows and shallow withdrawal basins overlying a fairly flat basement surface. No salt diapirs are found in the area; the nearest diapirs are to the north and northeast (Pescadito in Webb County and Piedras Pintas in Duval County). Overlying the salt are high-amplitude reflectors representing a basinal carbonate sequence, which thickens northwestward into Upper Jurassic and Lower Cretaceous carbonates and related clastics. The basinal carbonates appear to thin markedly within 40 to 60 mi of the Lower Cretaceous reef trend, and salt underlay only a thin veneer of sediment in middle Cretaceous time. The Upper Cretaceous strata in the area consist of shale and marl, including the basinal equivalents of the San Miguel and Olmos deltas of southwest Texas and Mexico.

Lower Wilcox sandstones known as the Lobo sands occur in the northwestern part of the Zapata area. Limited information suggests that they formed in a strike-fed sand system related

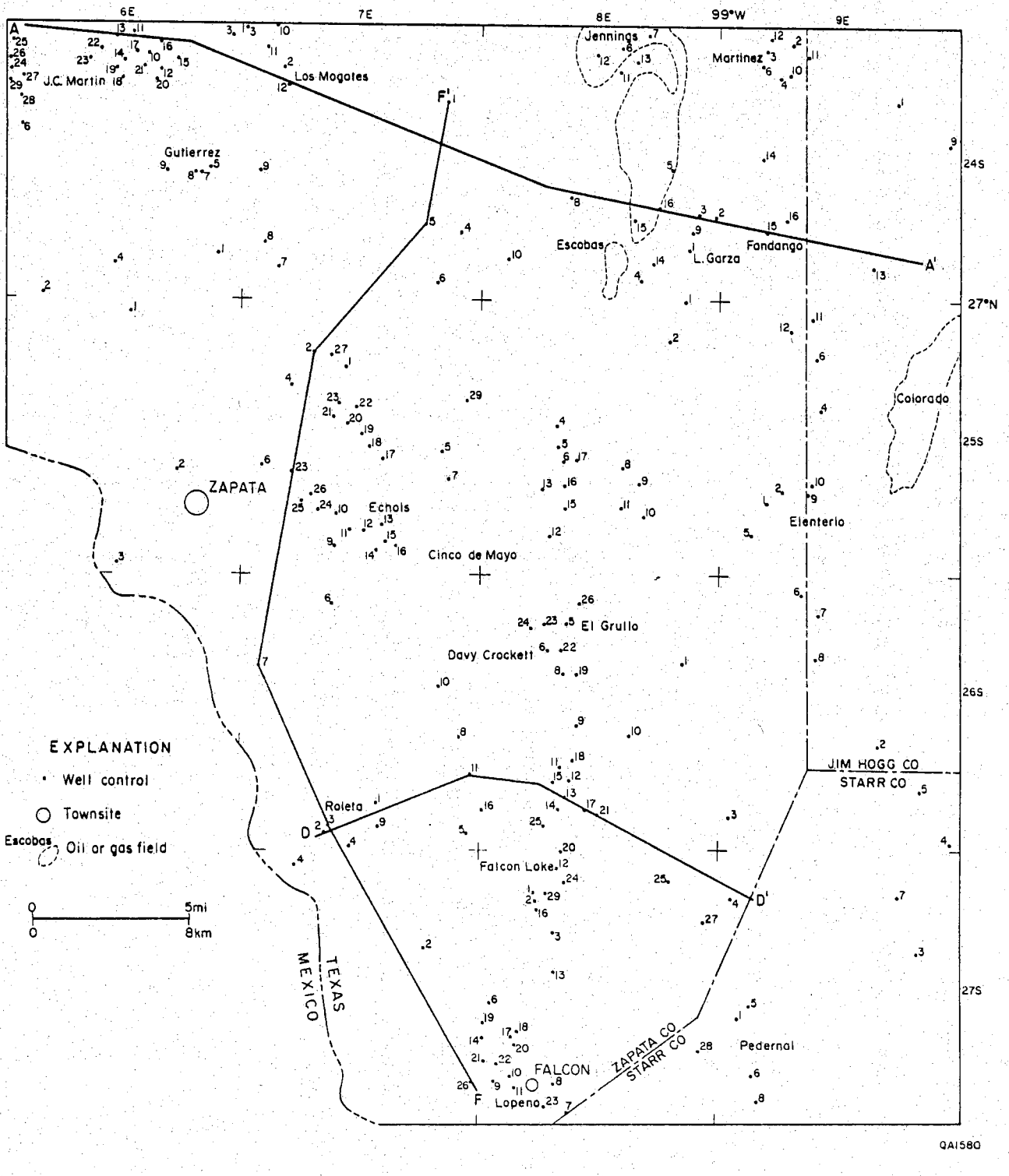

Figure I-13. Location map of the Zapata study area.

to the Cotulla barrier-bar/strandplain system of Fisher and McGowen (1967). The lower Wilcox is separated from the middle and upper Wilcox by an unconformity in Webb and Zapata Counties and adjacent Mexico.

The upper Wilcox is a sand-rich progradational clastic unit, described by Edwards (1982) as the Zapata delta complex of the Rosita delta system. Updip, in the western part of the area, it is very thin but thickens markedly to 4,000 to 8,000 ft over a series of growth faults. Sand content decreases downdip, but the final seaward extent of shallow-water sand deposition is unknown.

The overlying Eocene units consist of strike-fed barrier-bar/strandplain sandstones and related shallow-marine shales of the Queen City (Guevara and Garcia, 1976) and Yegua (Fisher, 1969) Formations and the Jackson Group (Fisher and others, 1969). Yegua and Jackson units are exposed over most of the study area.

Velocity information from two wells in the main growth-fault trend shows a fairly constant interval velocity of 10,000 to 11,000 ft per second below about 2,000 ft. Available information on seismic velocity is inadequate to show any decrease of interval velocity basinward. The top of geopressure, in the middle Wilcox west of the growth-fault trend, rises above the Wilcox in and east of the trend (Bebout and others, 1982).

Structural Development of the Zapata Area

Three major structural elements are found in the Zapata area (fig. I-13): the lower Wilcox Lobo trend in the northwest; the upper Wilcox growth-fault trend in the east; and gentle anticlinal folds in the west, which affect strata as young as the outcropping Yegua.

The lower Wilcox Lobo sands of the Zapata area are complexly faulted. Faults in this area appear to be listric normal faults that flatten into Midway or Upper Cretaceous shales at shallow depth. The faulted and folded lower Wilcox strata are unconformably overlain by smoothly basinward-dipping strata: the relation is shown diagrammatically on section A-A' (fig. I-14A). Correlations in this area are difficult, and seismic data were not examined; hence, this area is not discussed here in detail.

The upper Wilcox growth-fault trend extends north-south through eastern Zapata County (fig. I-15). Where it is best known, it consists of two to four major growth faults, commonly with more than threefold expansion of section (Bebout and others, 1982). This expansion, coupled with abundant antithetic faulting, makes regional structure mapping below the top of the Wilcox difficult. Substantial dip reversal occurs in the narrow, complex fault compartments between major faults (fig. I-14). This narrow band of growth faults lies over and on the downdip side of a shale ridge distinguished on seismic sections by chaotic reflections. Downdip of this

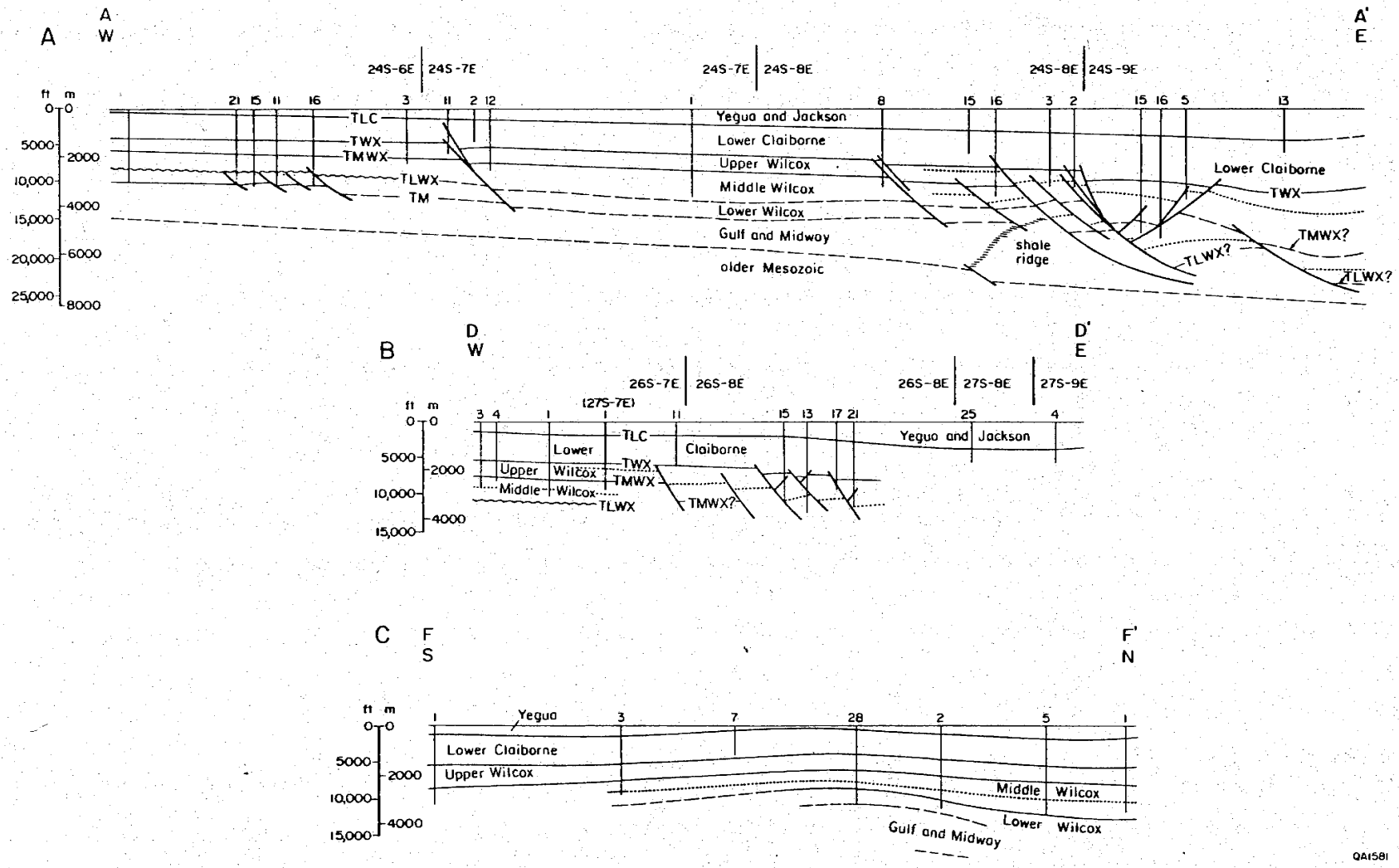

Figure I-14. True-depth sections of the Zapata study area. (A) Section A-A' through the Lobo trend and Fandango structure. (B) Section D-D' through North Falcon Lake field. (C) Section F-F' across Cinco de Mayo anticline.

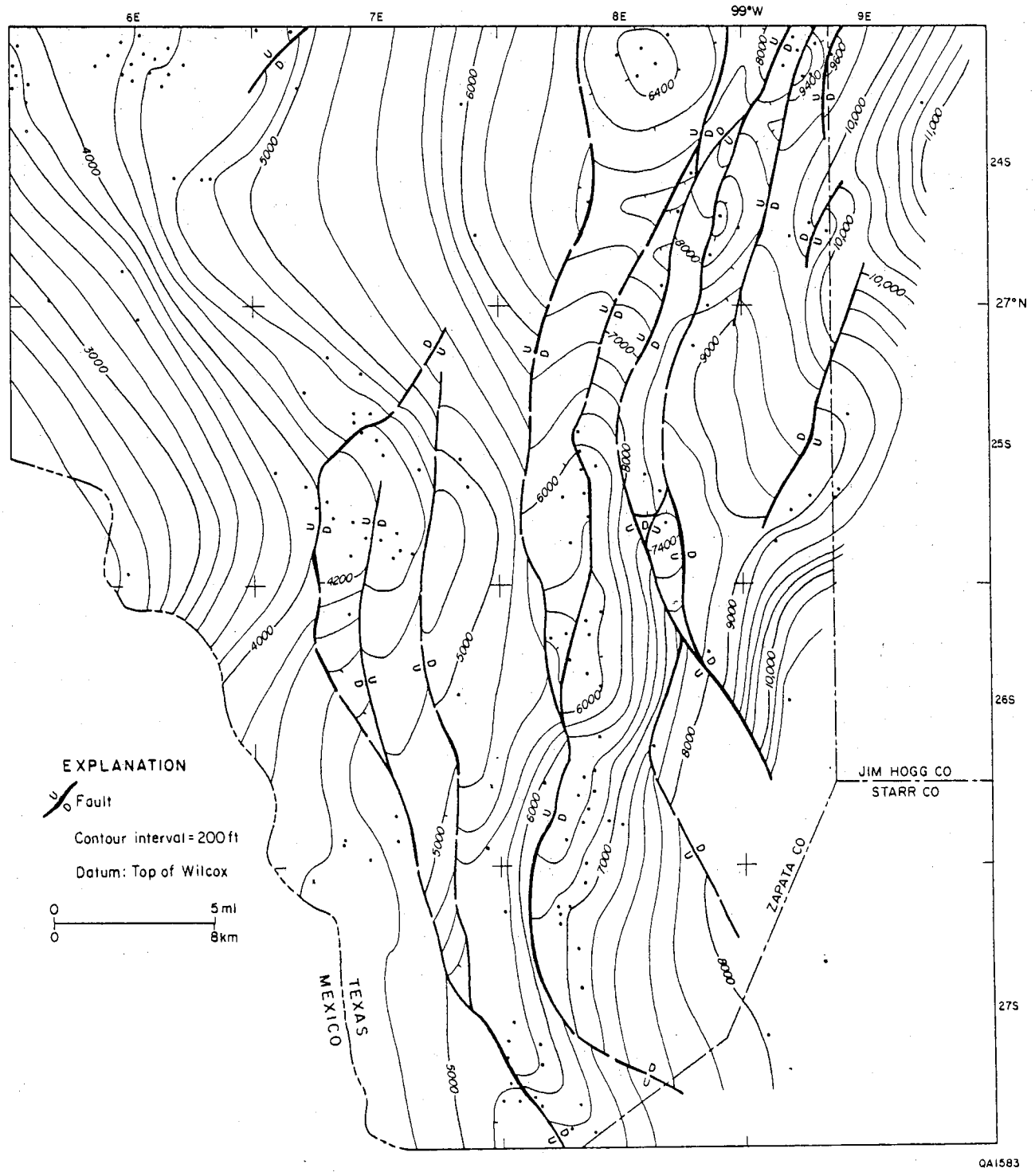

Figure I-15. Structure map on top of Wilcox, Zapata study area.

shale ridge lies a deep synclinal basin filled with Wilcox and lower Claiborne sediments to depths of nearly 20,000 ft; another shale ridge lies east of this basin. Locally, large antithetic faults have formed on the downdip side of the shale ridge, producing large, deep traps such as that at Fandango.

Reconstruction of a section at Fandango field (fig. I-16) shows that the shale ridge, the growth-fault system with antithetic faulting, and the deep basin developed concurrently during upper Wilcox deposition. The shale ridge was apparently passive, although upward forcing may have helped to form the large antithetic fault near its crest in the latest Wilcox. Very thick sediment, inferred to be shale, must be added in the older sections to balance them. This mobile shale may have been forced out of the area below the deep basin, either into the updip shale ridge or, more likely, into the next shale ridge to the east. This deep basin is thus a linear shale-withdrawal basin related to the formation of shale ridges.

Broad anticlinal noses occur updip of and within the upper Wilcox growth fault trend; they are expressed without interference by growth faults at the lower Claiborne (base Yegua) horizon (fig. I-17). The two anticlines, the Cinco de Mayo and the Lopeno, are mapped in outcrop (Barnes, 1976). Relief on the Cinco de Mayo anticline (fig. I-14C) decreases from the top Lobo unconformity to the top of the Wilcox, with nearly constant low relief to the surface. These folds may be compressional, related either to the open Tamaulipas folds, such as the Sierra Picachos to the west, or to the low-amplitude fold belt seen to the northwest in Maverick and Val Verde Counties and adjacent Coahuila (Chittim, Del Rio, and Trevino anticlines). The anticline may have been developed by deformation of either Upper Cretaceous shale or Mesozoic salt or by basement warping. Post-Wilcox deformation may be related to compaction or to continued movement of incompetent sediments.

Structural Constraints on the Occurrence of Geopressured Reservoirs

Geopressured sandstone reservoirs are expected in two structural locations: within the narrow growth-fault belt or downdip in the deep shale-withdrawal basin. Reservoirs within the growth-fault belt will be complexly faulted and limited in dip extent; hence, sand volumes in the deltaic setting will be limited. However, strike-oriented sandstones within the trend, as at Northeast Thompsonville field (Morton and others, 1983), may have significant volume.

Sandstone reservoirs downdip of the fault trend, either near the significant antithetic faults or in the deep basin, may be unfaulted and hence have substantial volumes of sand. The critical control on sand distribution is the location of the final shelf margin established by the Zapata delta. Well control is nearly nonexistent; however, high-continuity seismic reflectors in the basin and over the downdip shale ridge are more characteristic of shelf-slope shale

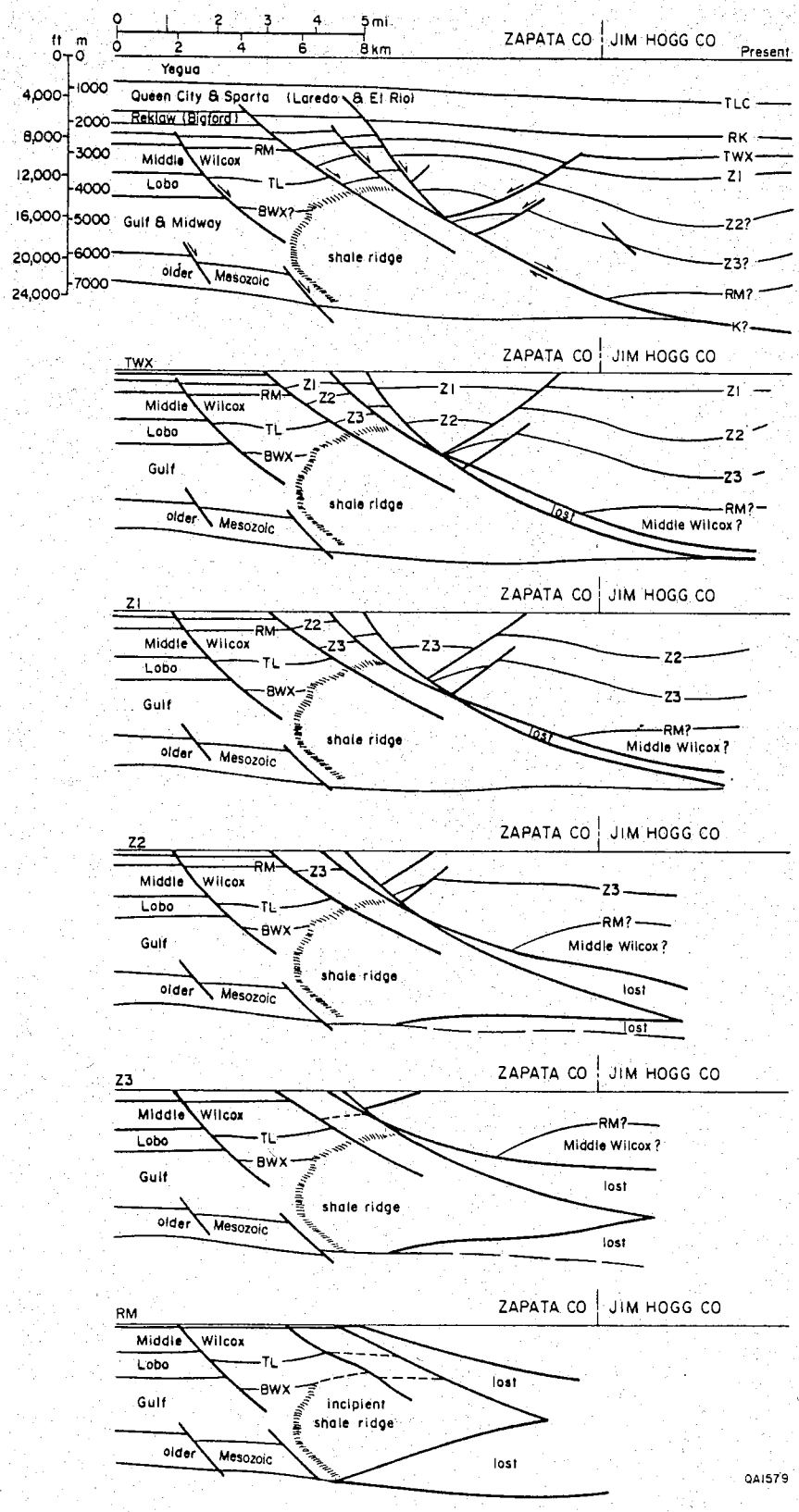

Figure I-16. Restoration of section over Fandango field.

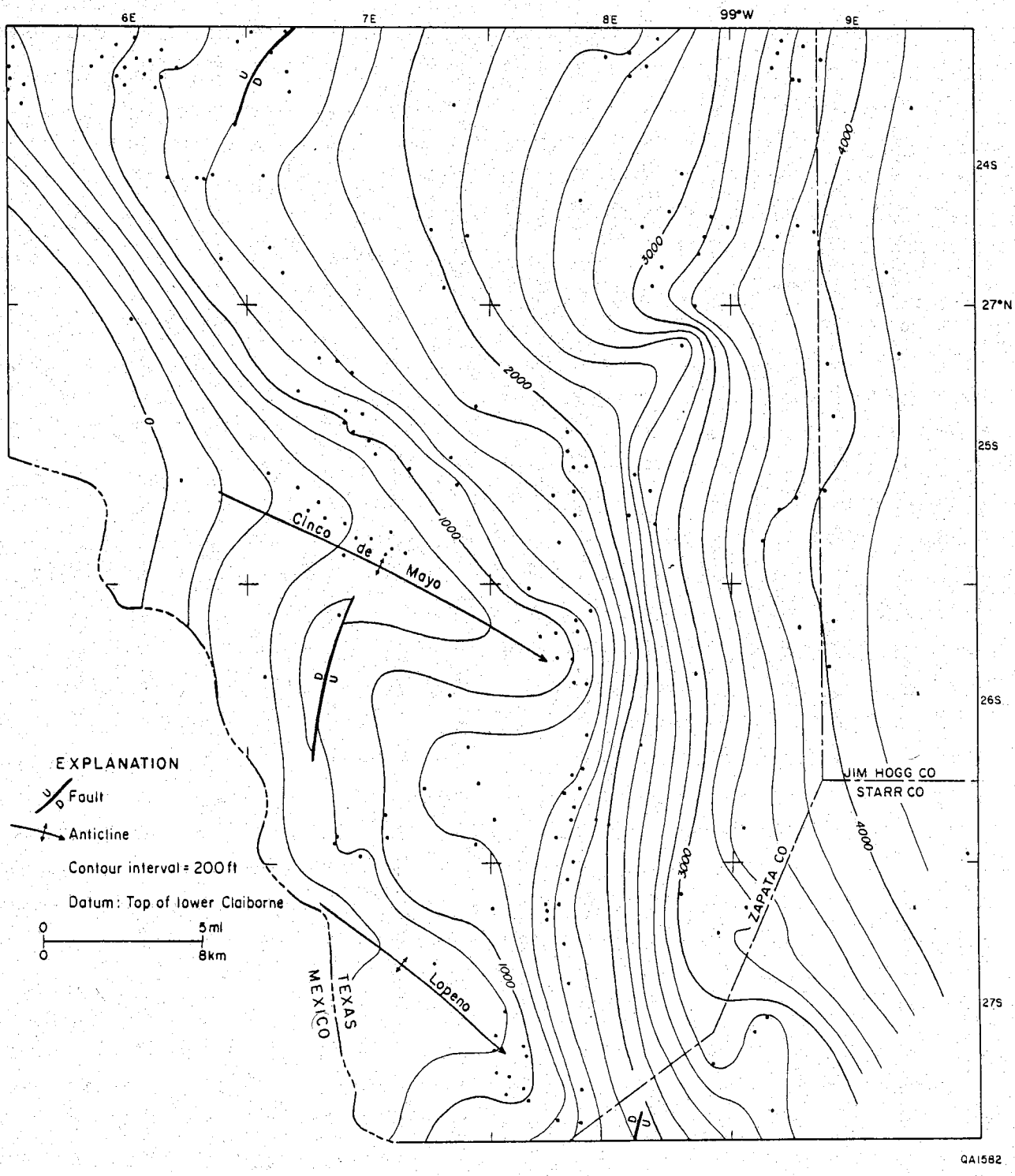

Figure I-17. Structure map on base of Yegua, Zapata study area.

sequences than of deltaic sand sequences. Lack of permeable reservoir rocks may therefore limit geopressured reservoirs in this area. Additional drilling should help to clarify this.

CONCLUSIONS

Two areas of contrasting structural style are outlined within the Wilcox growth-fault trend of the Texas Gulf Coast. One style is typically developed at the Cuero study area (Winker and others, 1983) and, modified by salt tectonics, at Katy and Fostoria. This style is characterized by several fairly straight growth faults that show little flattening with depth and that bound highly elongate fault compartments. Expansion across the faults is moderate (indices of 2 to 3), but rollover, except in the most basinward faults, is minor. Salt, where diapirically active, pierces the growth-fault trend after the main phase of growth faulting. Early salt pillows, however, localize the growth-fault trend. A similar style occurs in Live Oak County (Edwards, 1980) and probably extends eastward into Louisiana.

The other structural style is developed in the Zapata area. It is characterized by a narrow belt of growth faults that has great expansion and related antithetic faults and is localized on a linear shale ridge updip of a deep shale-withdrawal basin. A similar style extends northeast into Duval County and possibly into the South Chapa area of Live Oak County. This trend lies east of the lower Wilcox Lobo trend of highly listric faulting beneath an unconformity.

The South Texas Wilcox structural style appears to require more shale mobility than does the Cuero style. This may result from closeness to the Sierra Madre, which was undergoing Laramide deformation during Wilcox deposition. Thick Upper Cretaceous and Paleocene shales (the Mendez and equivalents) fill a foredeep basin in northeastern Mexico and may extend into South Texas. The mid-Wilcox unconformity in the Lobo area and the gentle anticlines in Zapata County also indicate more structural activity in South Texas, which might have helped to create a concentrated belt of higher-magnitude sliding near the Eocene shelf margin. The Cuero style, by contrast, shows little mobilization of the underlying shales; in fact, the Wilcox faults may pass through the Lower Cretaceous strata into the Jurassic or into salt.

Exploration for geopressured gas resources is active along the entire Wilcox growth-fault trend. The currently active frontiers of exploration are the Fandango-type antithetic structures in South Texas and the deep lower Wilcox in Central and southeast Texas. The base of the lower Wilcox is very poorly known in most of southeast Texas but has potential to produce from marginal-marine sandstones.

Most geopressured reservoirs in the Wilcox trend are deltaic (except for the Lobo). Most of the trend consists of highly elongate fault compartments having limited downdip extent; hence, reservoir sizes are limited. The largest reservoirs may be found in areas between major

growth-fault trends, such as the deep shale-withdrawal basin in South Texas or the interfault parts of the Katy and Fostoria areas. Permeabilities in both of these areas, unfortunately, are very poor (Bebout and others, 1982).

ACKNOWLEDGMENTS

Thanks are due to M. B. Edwards and C. D. Winker, who provided insights into Wilcox structural styles. The manuscript was typed by Dottie C. Johnson under the direction of Lucille Harrell. Illustrations were drafted by John T. Ames, Thomas M. Byrd, Jeff Horowitz, and Jamie McClelland under the supervision of R. L. Dillon. This work was funded by the U.S. Department of Energy, Division of Geothermal Energy, under Contract No. DE-AC08-79ET27111.

REFERENCES

Barnes, V.E., 1976, McAllen-Brownsville sheet: The University of Texas at Austin, Bureau of Economic Geology, Geologic Atlas of Texas, scale 1:250,000.

Bebout, D.G., Loucks, R.G., and Gregory, A.R., 1978, Frio sandstone reservoirs in the deep subsurface along the Texas Gulf Coast, their potential for the production of geopressured geothermal energy: The University of Texas at Austin, Bureau of Economic Geology Report of Investigations No. 91, 100 p.

Bebout, D.G., Weise, B.R., Gregory, A.R., and Edwards, M.B., 1982, Wilcox sandstone reservoirs in the deep subsurface along the Texas Gulf Coast, their potential for production of geopressured geothermal energy: The University of Texas at Austin, Bureau of Economic Geology Report of Investigations No. 117, 125 p.

Bruce, C.H., 1973, Pressured shale and related sediment deformation: mechanism for development of regional contemporaneous faults: American Association of Petroleum Geologists Bulletin, v. 57, p. 878-886.

Canada, W.R., 1962, Hockley field, Harris County, Texas, in Denham, R. L., ed., Typical oil and gas fields of southeast Texas: Houston Geological Society, p. 76-79.

Edwards, M.B., 1980, The Live Oak delta complex: an unstable shelf/edge delta in the deep Wilcox trend of South Texas: Gulf Coast Association of Geological Societies Transactions, v. 30, p. 71-79.

_____ 1982, The upper Wilcox Rosita delta system of South Texas: record of growth-faulted shelf-edge deltas: American Association of Petroleum Geologists Bulletin, v. 65, no. 1, p. 54-73.

Ewing, T.E., 1983a, Growth faulting and salt tectonics in the Houston Diapir Province: timing and exploration significance: Gulf Coast Association of Geological Societies Transactions, v. 33, p. 83-90.

_____ 1983b, Structural styles and structural evolution of the Frio growth-fault trend in Texas: constraints on geopressured reservoirs: in Morton, R.A., Ewing, T.E., Kaiser, W.R., and Finley, R.J., Consolidation of geologic studies of geopressured geothermal resources in Texas: The University of Texas at Austin, Bureau of Economic Geology, report prepared for the U.S. Department of Energy, Contract No. DE-AC08-79ET27111, p. 1-61.

Fisher, W.L., 1969, Facies characterizaton of Gulf Coast delta systems, with some Holocene analogues: Gulf Coast Association of Geological Societies Transactions, v. 19, p. 239-261.

Fisher, W.L., and McGowen, J.H., 1967, Depositional systems in the Wilcox Group of Texas and their relationship to occurrence of oil and gas: The University of Texas at Austin, Bureau of Economic Geology Geological Circular 67-4, 20 p.

Fisher, W.L., Proctor, C.V., Jr., Galloway, W.E., and Nagle, J.S., 1970, Depositional systems in the Jackson Group of Texas--their relationship to oil, gas, and uranium: The University of Texas at Austin, Bureau of Economic Geology Geological Circular 70-4, 28 p.

Gregory, J.L., 1966, A lower Oligocene delta in the subsurface of southeastern Texas: Gulf Coast Association of Geological Societies Transactions, v. 16, p. 227-241.

Guevara, E.H., and Garcia, R., 1972, Depositional systems and oil-gas reservoirs in the Queen City Formation of Texas: The University of Texas at Austin, Bureau of Economic Geology Geological Circular 72-4, 22 p.

Halbouty, M.T., 1979, Salt domes, Gulf Region, Texas and Mexico (2nd ed.): Houston, Gulf Publishing, 561 p.

Halbouty, M.T., and Hardin, G.C., Jr., 1954, New exploration possibilities on piercement-type salt domes established by thrust fault at Boling salt dome, Wharton County, Texas: American Association of Petroleum Geologists Bulletin, v. 38, no. 8, p. 1725-1740.

Hammer, S., 1983, Airborne gravity is here!: Geophysics, v. 48, no. 2, p. 213-223.

Morton, R.A., Ewing, T.E., and Tyler, Noel, 1983, Continuity and internal properties of Gulf Coast sandstones and their implications for geopressured fluid production: The University of Texas at Austin, Bureau of Economic Geology Report of Investigations No. 132, 70 p.

Seni, S.J., and Jackson, M.P.A., 1983, Evolution of salt structures, East Texas Diapir Province, part I: sediment record of halokinesis: American Association of Petroleum Geologists Bulletin, v. 67, no. 8, p. 1219-1244.

Weise, B.R., Edwards, M.B., Gregory, A.R., Hamlin, H.S., Jirik, L.A., and Morton, R.A., 1981, Geologic studies of geopressured and hydropressured zones in Texas: test-well site selection: The University of Texas at Austin, Bureau of Economic Geology, contract report to the Gas Research Institute under Contract No. 5011-321-0125, 308 p.

Winker, C.D., 1982, Cenozoic shelf margins, northwestern Gulf of Mexico: Gulf Coast Association of Geological Societies Transactions, v. 32, p. 427-448.

Winker, C.D., Morton, R.A., Ewing, T.E., and Garcia, D.D., 1983, Depositional setting, structural style, and sandstone distribution in three geopressured geothermal areas, Texas Gulf Coast: The University of Texas at Austin, Bureau of Economic Geology Report of Investigations No. 134, 60 p.

SECTION II. CHEMICAL COMPOSITION OF DEEP FORMATION WATERS, TEXAS GULF COAST

Robert A. Morton, assisted by R. L. Kugler and J. F. O'Connell

ABSTRACT

Four hydrochemical subregions previously identified on the basis of total dissolved solids and single ion concentrations are substantiated with the use of trilinear plots. These plots illustrate the proportions of major cations and anions dissolved in formation water and allow comparisons of brine composition regardless of concentration. The plots also show that mixing of NaCl and CaCl brines is common in subregion 3 (Kenedy and Hidalgo Counties). Zones of brine mixing occur downdip of the Vicksburg fault zone and correspond to sand-rich intervals of the Vicksburg and Frio Formations. Sediments within the transition zone (0.465 - 0.7 psi/ft) and highly overpressured sediments (> 0.7 psi/ft) both contain modern pore waters having intermediate compositions.

INTRODUCTION

During the past two years (1982-83), chemical analyses of deep subsurface brines revealed that concentrations of total dissolved solids and single ions may vary substantially in both lateral and vertical directions. Many of these variations in water chemistry coincide with subsurface changes in physical state such as temperature gradient, pressure gradient, or lithology (Morton and others, 1981, 1983). When viewed regionally, the chemical analyses define four hydrochemical subdivisions that approximately correspond to the principal structural elements that were active and that controlled deposition during the Tertiary Period.

The four subregions (fig. II-1) and their primary geological significance are as follows: Area 1 (Jefferson County to Brazoria County) corresponds to the Houston Embayment and related salt dome province. Formation waters exhibit high salinities derived partly from dissolution of underlying and adjacent salt. Waters in area 2 (Matagorda County to Kleberg County) are moderately saline and exhibit unusually high alkalinities. These alkalinities are most likely associated with organic acids and perhaps are derived from underlying shale masses that characterize the interdeltaic embayment area corresponding to the San Marcos platform. Area 3 and area 4 waters are markedly different even though they both reside within the South Texas Rio Grande Embayment. Waters in area 3 (Kenedy County and western Hidalgo County)

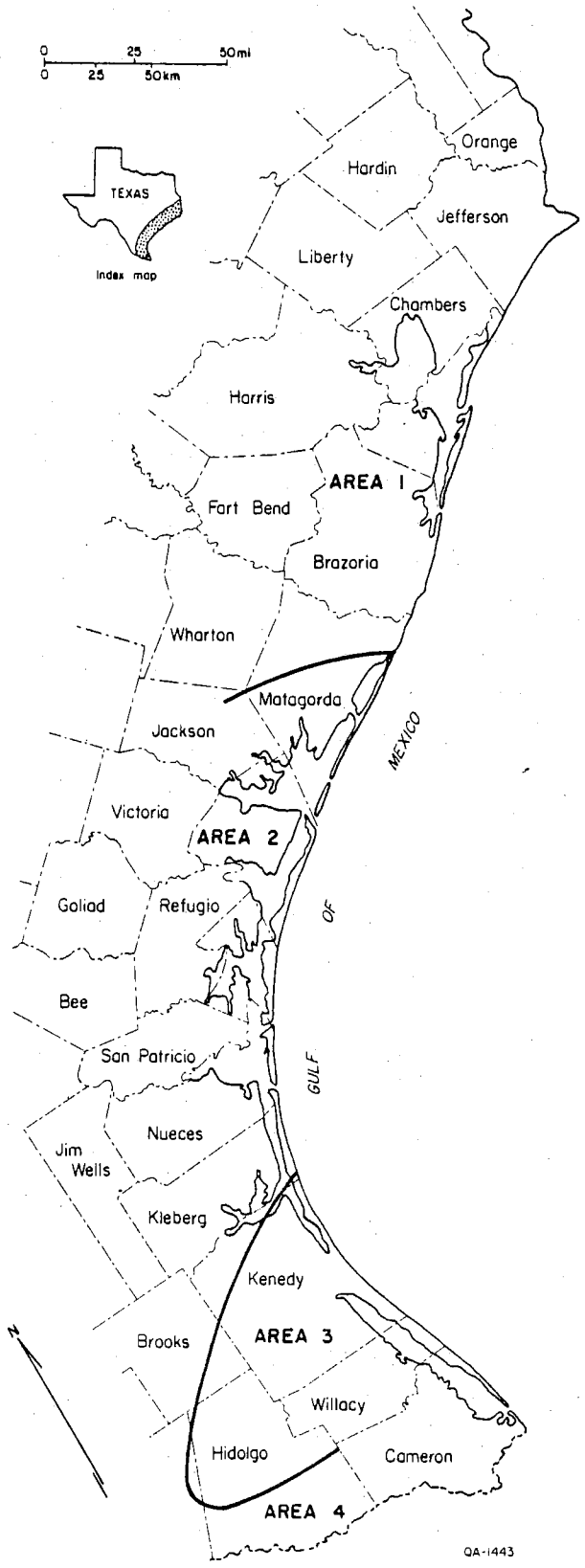

Figure II-1. Hydrochemical subregions of the Texas Coastal Plain based on composition of deep formation waters.

vary in composition; however, they commonly have high concentrations of calcium and high total dissolved solids. These waters may owe their high salinity to deep-seated salt, even though diapiric salt has not been reported within the subregion. In contrast, waters of area 4 (southern Hidalgo County) exhibit uniformly low salinities over a broad range of depths, suggesting that underlying salt, if present, is negligible or thin.

COMPOSITIONAL DIFFERENCES

The four subregions were originally identified on the basis of salinity and concentrations of major cations. However, ternary plots (Hem, 1970) are a more accurate method of identifying waters with different compositions, regardless of solution concentration. These plots also have the advantage of distinguishing mixtures of different water types if sample density is sufficient.

Partitioning of water analyses by trilinear diagrams for each subregion (fig. II-2) illustrates that chemical compositions within a subregion are similar, whereas they are considerably different for adjacent areas. Waters from areas 1 and 4 are sodium chloride types that vary little in composition. Area 2 also produces sodium chloride waters; however, some of the waters contain greater proportions of calcium and have higher alkalinities than do waters from the other two areas. Waters from area 3 (fig. II-2) range in composition from NaCl type to CaCl type, suggesting that modern pore waters may record widespread mixing of subsurface brines. Disaggregation of the data for area 3 (fig. II-3) tends to confirm that mixing of water types is largely responsible for the lateral and vertical changes in composition and concentration.

Candelaria Field

Sandstone reservoirs in the Candelaria field (fig. II-3) contain waters that are demonstrably different in composition at depths between 8,500 and 16,000 ft. The systematic changes in composition (figs. II-4 through II-6) suggest that mixing of two brines having separate evolutionary histories has formed a third brine of intermediate composition. At shallow depths, NaCaCl waters of moderately high salinities are enriched with CaCl and progressively pass from CaNaCl to CaCl type, then to NaCaCl, and finally to a NaCl type at the deepest sampling point near 16,000 ft (figs. II-5 and II-6). Highest calcium concentrations occur at intermediate depths (about 10,000 ft), where thermal gradients are substantially higher than in overlying or underlying strata (fig. II-4). Pressure gradients are also abnormally high, but less than 0.7 psi/ft (fig. II-5). This transition zone below the top of geopressure corresponds with the base of a sand-rich middle Frio progradational sequence (fig. II-4).

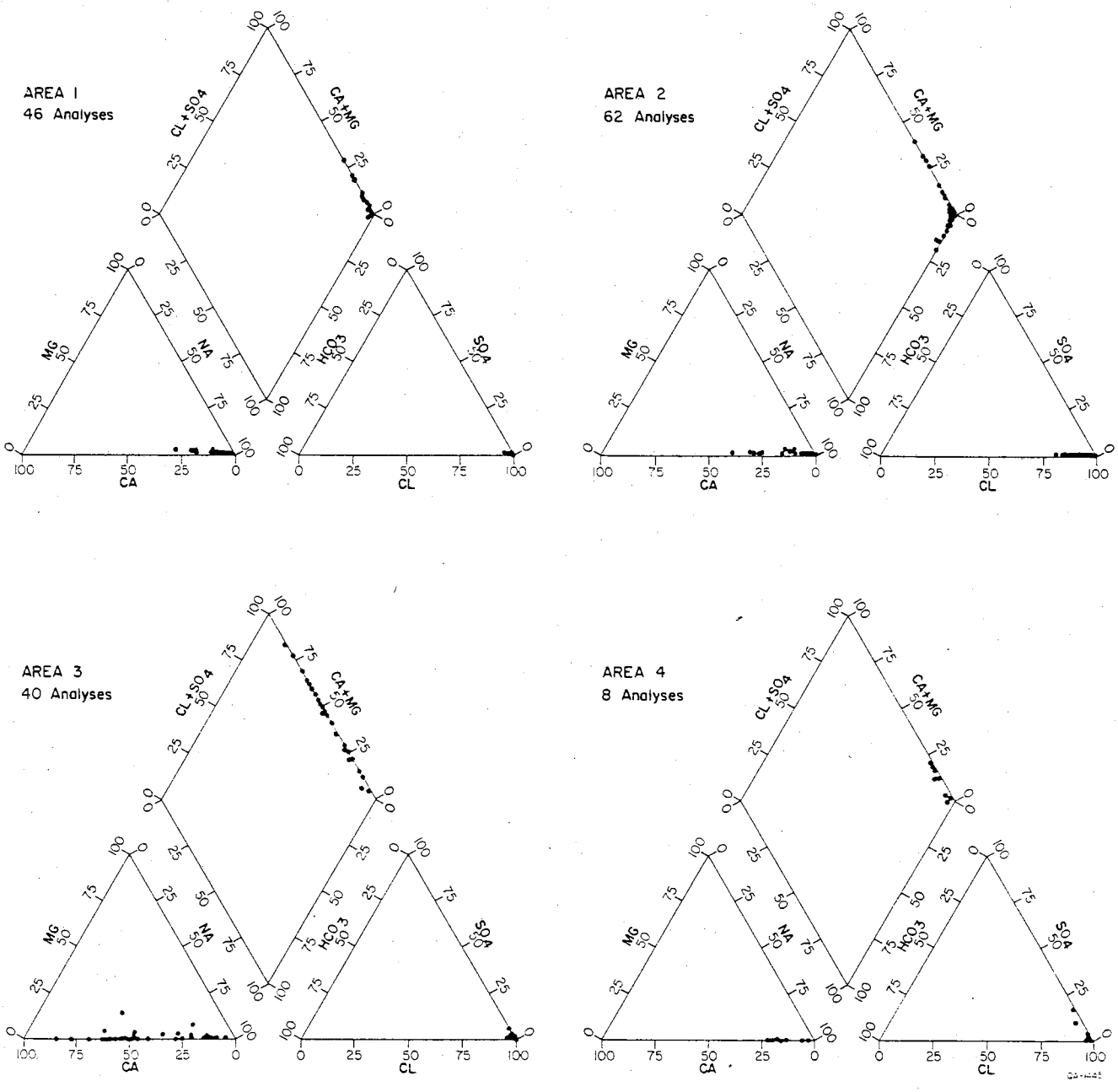

Figure II-2. Trilinear plot showing proportions of major cations and anions in formation waters from hydrochemical subregions, Texas Coastal Plain.

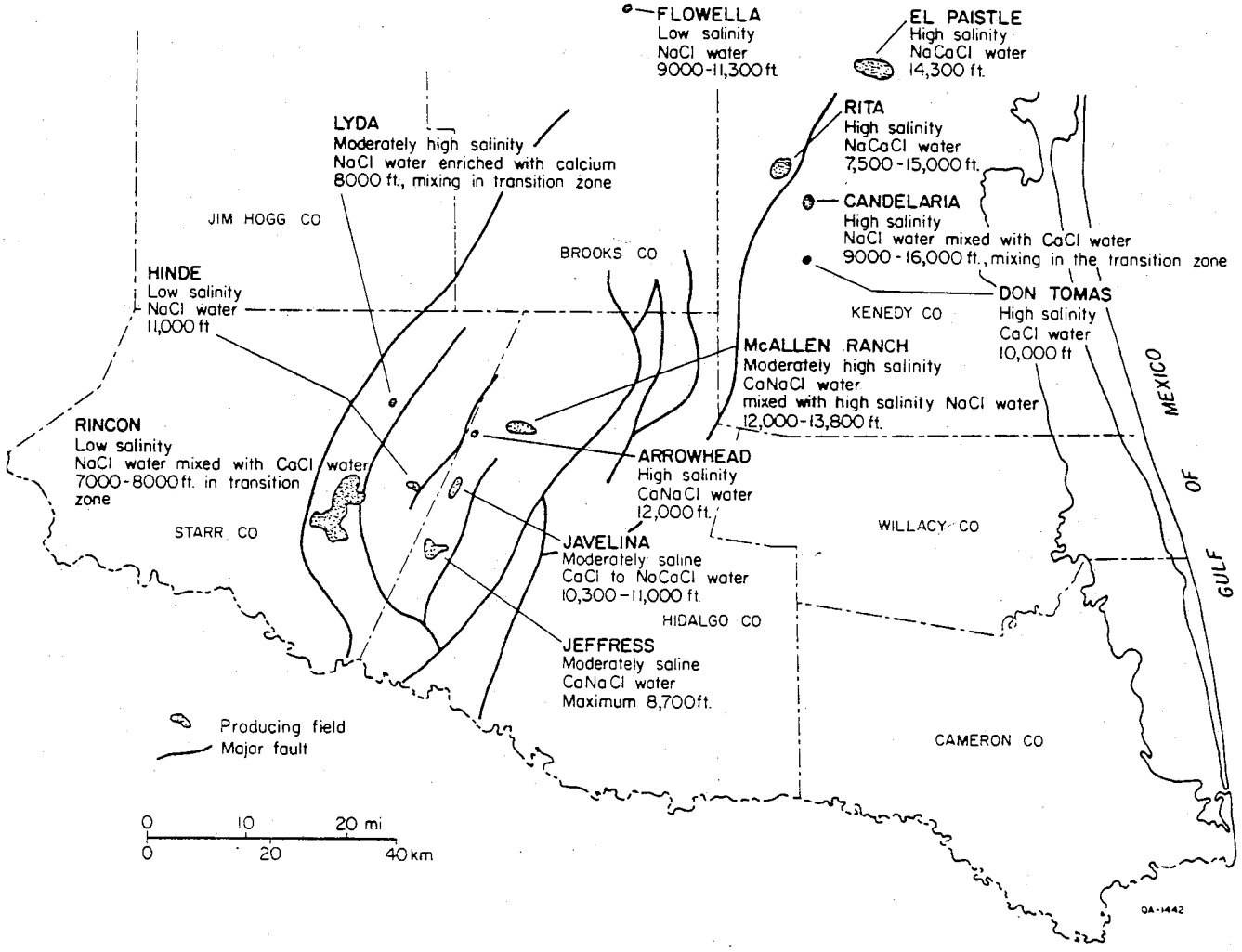

Figure II-3. Oil and gas fields with water analyses in hydrochemical subregion 3.

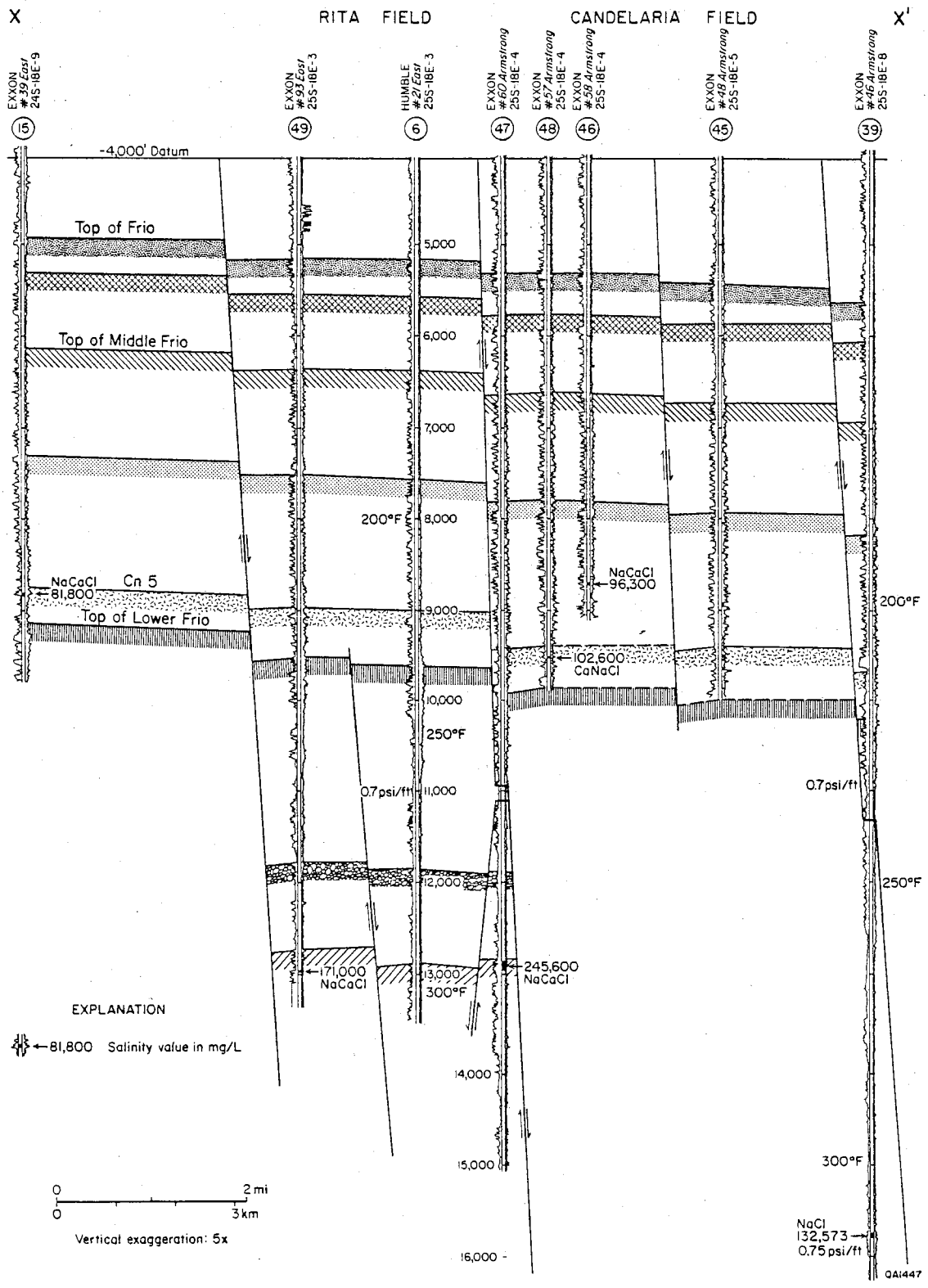

Figure II-4. Structural dip cross section that transects the Rita and Candelaria fields, Kenedy County. Modified from Morton and others (1981). Field locations shown in figure II-3.

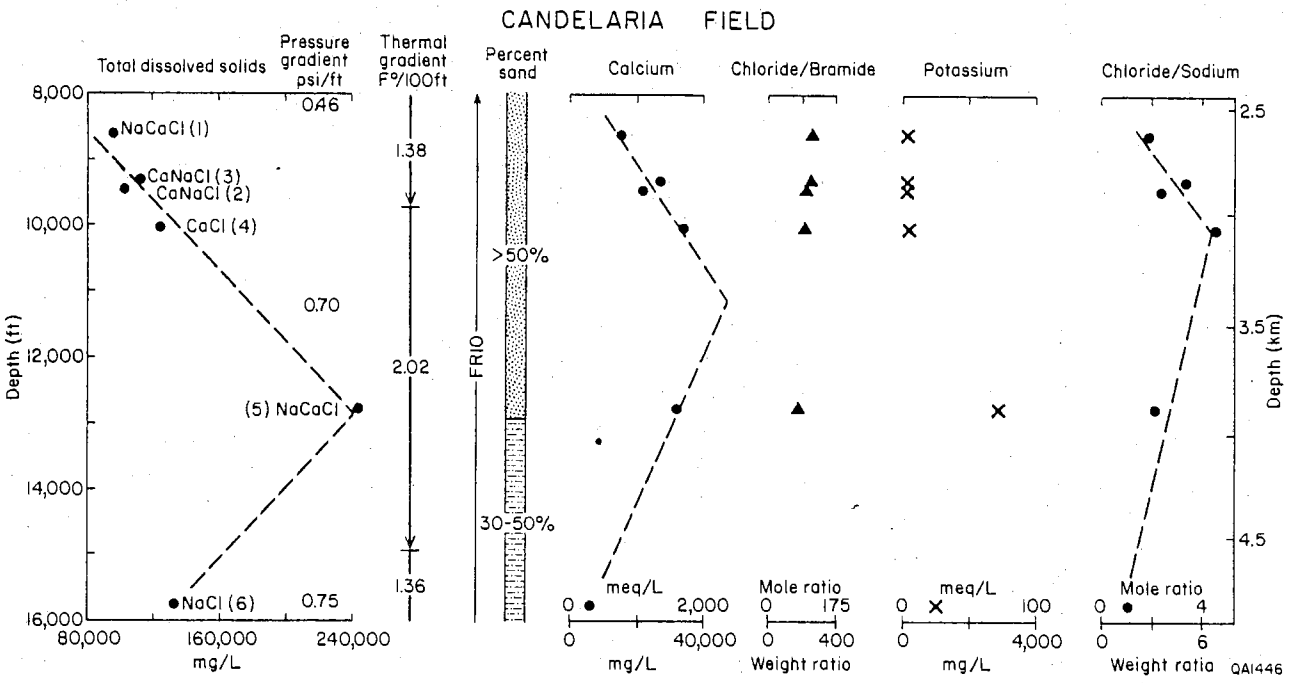

Figure II-5. Concentrations of total dissolved solids, major ions, and ion ratios in Candelaria field. Modified from Morton and others (1981). Sample numbers correspond to those in figure II-6.

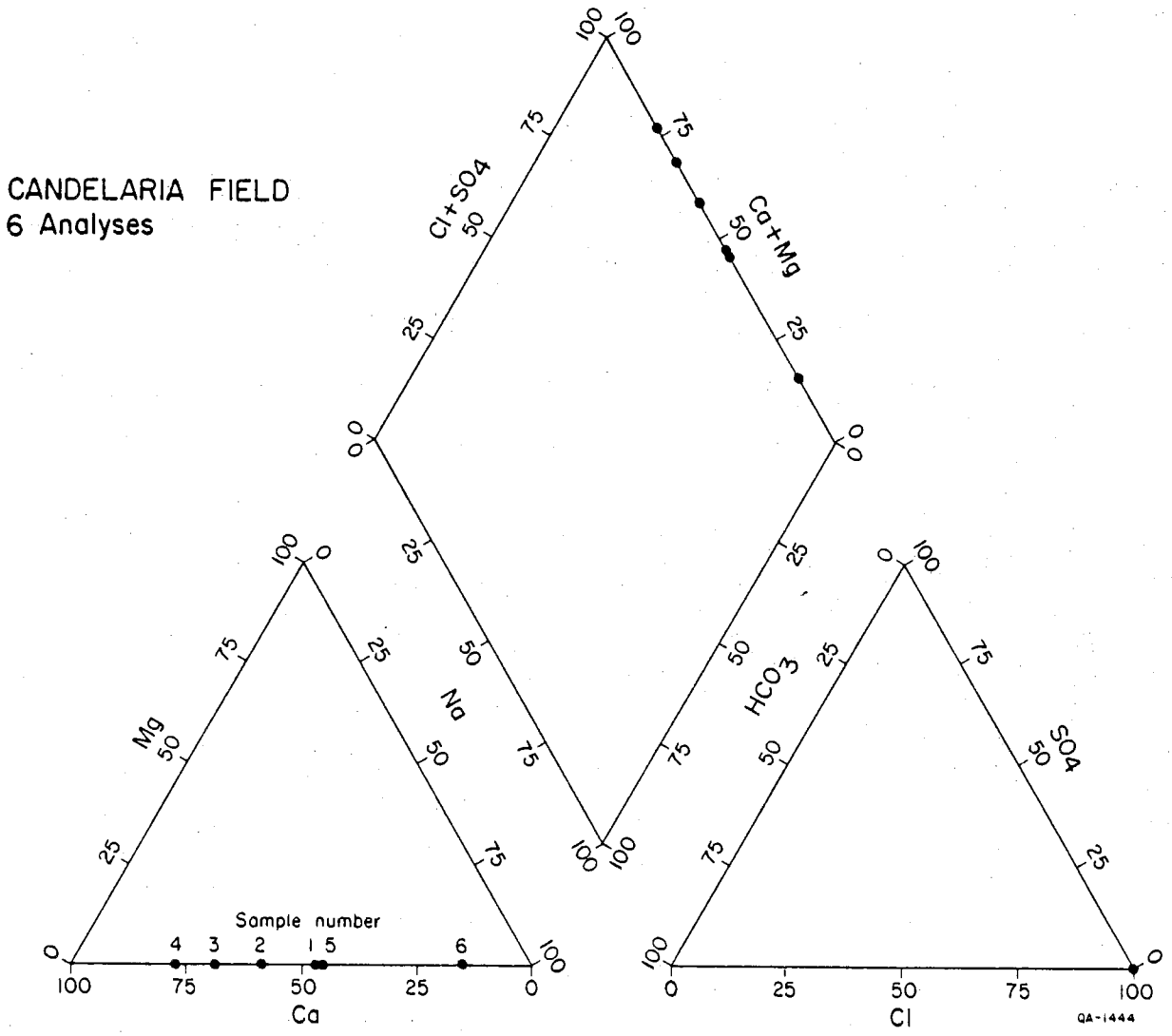

Figure II-6.. Trilinear plot showing proportions of chemical constituents in waters from the Candelaria field. Sample numbers correspond to those in figure II-5.

These factors suggest that a plume of hot CaCl water has invaded and mixed with older NaCl pore waters. Apparently the younger water mass migrated preferentially through the basal middle Frio sandstones at depths of about 10,000 ft (figs. II-4 and II-5).

Other Fields in Area 3

Mixing of subsurface brines like that documented for the Candelaria field is also apparent in other fields in hydrochemical subregion 3. Additional examples are illustrated by water analyses from Lyda, Arrowhead, North Rincon, Jeffress, and McAllen Ranch fields (fig. II-3). Water samples from massive sandstone reservoirs of Vicksburg age in the Lyda field range from 6,300 to 9,300 ft. NaCaCl waters of moderately high salinity occupy the shallowest and deepest horizons, whereas CaNaCl waters are present at depths of about 8,000 ft. As at Candelaria, the enrichment with respect to calcium occurs within the transition zone at pressure gradients less than 0.7 psi/ft. Mixing of CaCl and NaCl brines within the transition zone also occurs in the North Rincon field. At North Rincon, formation waters are produced at depths between 4,300 and 8,400 ft. Moderate- to low-salinity NaCl waters are produced from lower Frio sandstones near the top of geopressure, whereas low- to moderate-salinity CaNaCl and CaCl waters come from upper Vicksburg reservoirs. Maximum concentrations of calcium occur at depths around 8,000 ft, where CaCl brines are present.

In contrast to composition at other area 3 fields, CaCl waters predominate where pressure gradients are extremely high, such as at Jeffress and McAllen Ranch fields. Moderately saline CaNaCl brines are produced from sand-rich Vicksburg sediments at depths between 8,700 and 10,000 ft in the Jeffress field. Sandstone reservoirs at those depths have pressure gradients greater than 0.7 psi/ft.

At the McAllen Ranch field, sand-rich sediments of the Vicksburg Formation produce moderately to highly saline brines from depths between 12,000 and 14,000 ft. Systematic increases in total dissolved solids and sodium between 12,000 and 13,000 ft and decreases in both variables below 13,000 ft suggest subsurface mixing of brines. The data indicate that NaCl and CaCl brines have come in contact. Most likely, moderately saline CaCl brines were intruded by highly saline NaCl brines, changing composition of both water masses by forming predominantly CaNaCl brines and leaving a NaCaCl brine at intermediate depths.

DISCUSSION

Chemical analyses of formation waters in subregion 3 (fig. II-3) are adequate for demonstrating brine mixing; however, sparse data and complex histories of fluid movement and water-rock interactions make interpretation of the spatial relationships difficult. Although regional

patterns are less coherent than site-specific patterns, trends do emerge that appear reasonable.

Physical mixing of brines is evident in all fields with samples from more than two reservoirs. Low-salinity NaCl waters mark the perimeter of subregion 3 and serve as the chemical baseline. These unaltered waters are found in eastern Hidalgo County in the Frio Formation and in the Vicksburg Formation updip of the Vicksburg flexure. Downdip of the Vicksburg flexure, the influence of moderate- to high-salinity CaCl brines is widespread. The CaCl brines have mixed with low-salinity NaCl waters to form CaNaCl solutions, such as in western Hidalgo County, or highly saline NaCl waters have been converted to NaCaCl types such as in Kenedy County.

According to these data, mixing zones correspond to stratigraphic intervals that have intermediate to high sandstone percents and are below the top of geopressure. Preferential fluid movement within the transition zone (pressure gradients between 0.465 and 0.7 psi/ft) is apparent; however, fluid movement is also evident within sediments that are now highly overpressured.

ACKNOWLEDGMENTS

Water samples for this study were collected by James F. O'Connell and chemical analyses were performed by Dorothy Gower under the supervision of Clara Ho, Mineral Studies Laboratory of the Bureau of Economic Geology. The text was typed by Dottie C. Johnson under the direction of Lucille C. Harrell, and illustrations were prepared by Margaret R. Day and Jeff Horowitz under the direction of R. L. Dillon. Funding for this research was provided by the U.S. Department of Energy, Division of Geothermal Energy, under Contract No. DE-AC08-79ET27111.

REFERENCES

Hem, J. D., 1970, Study and interpretation of the chemical characteristics of natural water: U.S. Geological Survey Water Supply Paper 11473, 358 p.

Morton, R. A., Garrett, C. M., Jr., Posey, J. S., Han, J. H., and Jirik, L. A., 1981, Salinity variations and chemical compositions of waters in the Frio Formation, Texas Gulf Coast: The University of Texas at Austin, Bureau of Economic Geology, report to the U.S. Department of Energy, Contract No. DE-AC08-79ET27111, 96 p.

Morton, R. A., Han, J. H., and Posey, J. S., 1983, Variations in chemical compositions of Tertiary formation waters, Texas Gulf Coast, in Morton, R. A., Ewing, T. E., Kaiser, W. R. and Finley, R. J., Consolidation of geologic studies of geopressured geothermal resources in Texas: The University of Texas at Austin, Bureau of Economic Geology, report prepared for the U.S. Department of Energy, Contract No. DE-AC08-79ET27111, p. 63-135.

SECTION III. CONTINUITY AND INTERNAL PROPERTIES OF THREE GULF COAST STRANDPLAIN SANDSTONES: THEIR IMPLICATIONS FOR GEOPRESSURED FLUID PRODUCTION

Noel Tyler, assisted by W. A. Ambrose

ABSTRACT

Study of three oil-productive strandplain sandstones in the Frio Formation of Matagorda County yields models of progradational mud-rich strandplain, composite fluvial/deltaic/strandplain, and transgressed strandplain sandstone reservoirs. These models, based on sandstones with relatively abundant well penetrations, serve as guides for evaluation of deep geopressured reservoirs.

Progradational and transgressed strandplain sandstones (such as parts of the Cayce and Carlson reservoirs) are characterized by laterally continuous geometries. Internal physical and textural variability exerts only a minor influence on production except where crosscutting fluvial-deltaic systems interrupt the continuity of the sandstones. Component facies of composite fluvial/deltaic/strandplain systems (such as the Cayce reservoir) exhibit widely divergent fluid migration and production characteristics; fluvial sandstones, insulated from adjacent deposits by physical and textural contrasts, act as foci for channelized fluid influx. By contrast, the strandplain sandstones are characterized by broad fronts of water influx. Mud-rich strandplain (Cornelius) reservoirs are composite bodies with complex fluid-migration histories.

Macroscopic heterogeneity is least in simple progradational and transgressed strandplain sandstones. Extensive deposits such as these would provide an attractive completion target for production of geopressured geothermal energy in areas where permeability, temperature, pressure, and structural constraints are satisfied.

INTRODUCTION

A principal objective of the reservoir continuity study is to examine the facies architecture of potential geopressured geothermal reservoirs along the Gulf Coast in order to determine which facies would promote and which would hinder the production of the vast quantities (40,000 bbl/day or more) of geothermally heated brines necessary for the production of geothermal energy. The study focused initially on the continuity of component facies of wave-modified high-constructive deltaic sandstones in the Pleasant Bayou test well area of

Brazoria County (Tyler and Han, 1982; Morton and others, 1983). Because deep geopressured reservoirs generally have poor well control and undetailed production histories, it was decided to examine the continuity of shallower reservoirs that could serve as generic models for sandstones of the same origin within the geopressured zone.

The Greta/Carancahua barrier-strandplain system of the Frio Formation (fig. III-1) was selected for detailed study. Regional analysis of sandstone facies and the structural fabric of the Gulf Coast Basin suggested that large and relatively continuous reservoirs, from which optimum magnitudes and rates of fluid production could be obtained, occur within this trend (Morton and others, 1983).

Facies Influence on Reservoir Continuity

The impact of physical and textural variations in reservoir lithology on reservoir performance is attracting increasing attention (Polasek and Hutchinson, 1967; Alpay, 1972; Hartman and Paynter, 1979; and others). In the past, engineering practice either assumed reservoirs to be homogeneous and isotropic or allowed for simple anistropy (Alpay, 1972). However, the hard lessons learned from several decades of enhanced recovery have confirmed that a detailed understanding of the internal architecture of reservoir facies is needed to develop realistic models for predicting reservoir behavior. Variations in the internal properties of depositional units (grain-size distribution, pore-space distribution, permeability, internal porosity stratification, and frequency and position of shale breaks) are responses to changes in the nature of the sedimentary processes responsible for their deposition. Where process changes are of a sufficient magnitude, depositional environments will change location or be abandoned and replaced by environments compatible with the new regime. Amalgamation and superposition of depositional facies in this manner results in composite sandstone bodies and, ultimately, heterogeneous reservoirs. Evidence from studies of modern environments (Pryor, 1973) and production characteristics of oil fields (for example, Hartman and Paynter, 1979) indicates that physical and textural characteristics of sand facies and abrupt changes in these parameters at facies boundaries clearly influence rates and paths of fluid flow.

Three levels of reservoir heterogeneity affect or control fluid flow in sandstones (Alpay, 1972). Megascopic heterogeneity describes fieldwide (inter-reservoir) or regional variation in sandstone character; macroscopic heterogeneity refers to well-to-well intraformational variation; and microscopic heterogeneity describes pore-to-pore variability. Macroscopic textural differences arranged areally and vertically in the reservoir and megascopic heterogeneities, such as facies extent and geometry, are the principal concerns of this study. Elements that determine the presence and extent of macroscopic heterogeneities in a reservoir are stratifica-

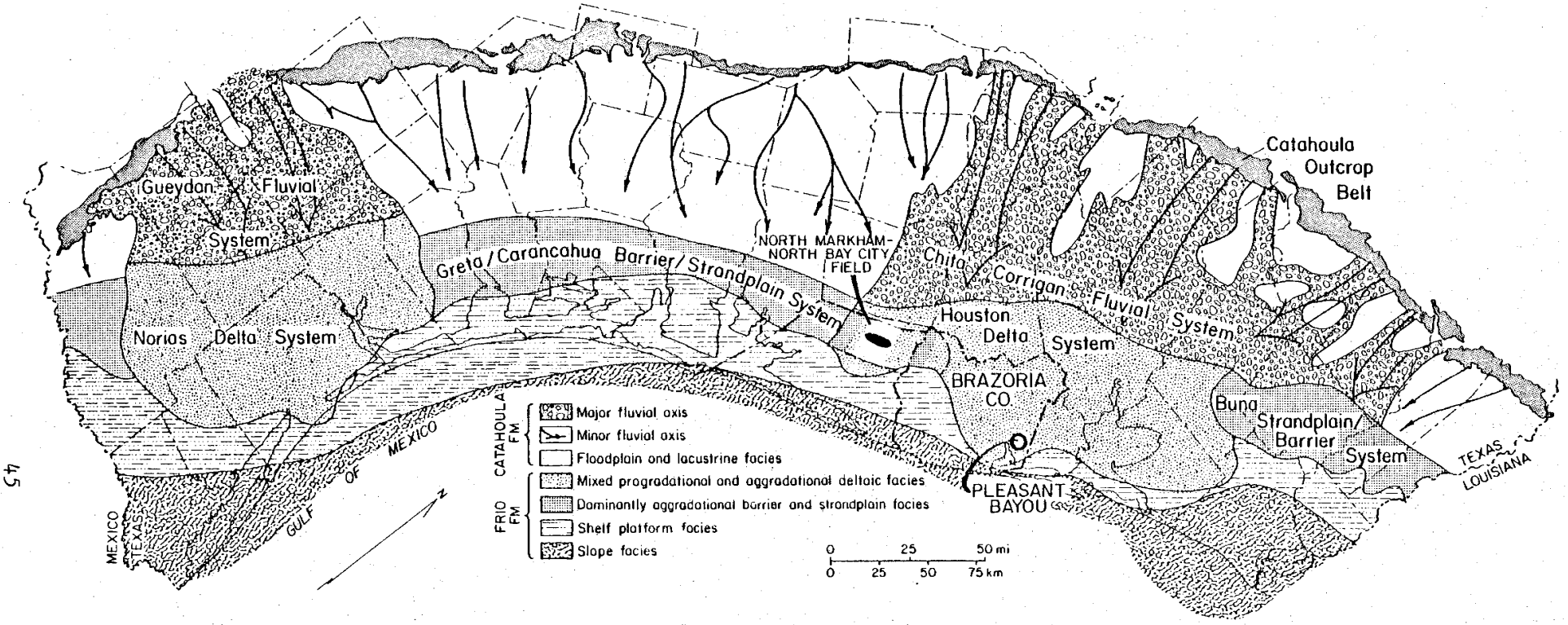

Figure III-1. Depositional framework of the Frio Formation (Galloway and others, 1982) and of major oil fields producing from the Greta/Carancahua barrier-strandplain system (Galloway and others, 1983). The North Markham - North Bay City field is located in northwest Matagorda County.

tion characteristics, such as nonuniform stratification and stratification contrast, and permeability characteristics, such as permeability trends and directional or anisotropic permeability (Alpay, 1972).

Geologic Framework

The North Markham - North Bay City field in Matagorda County is one of a trend of major oil fields that tap syndepositionally faulted Oligocene sandstones along the Vicksburg and Frio fault zones of the central Texas Gulf Coast. The field produces from multiple barrier and strandplain sandstones of the Frio Formation. The Frio and its updip equivalent, the Catahoula Formation, form one of the principal progradational wedges of the Gulf Coast Basin. The formations consist of deposits of two large fluvial-deltaic systems centered in the Houston and Rio Grande Embayments (Galloway and others, 1982). Separating the embayments is an area of lesser subsidence (the San Marcos Arch), where vertically stacked, strike-parallel sandstones of the Greta/Carancahua barrier-strandplain system were deposited (Boyd and Dyer, 1964; Galloway and others, 1982). This curvilinear sandstone belt separates marine shale from lagoonal and streamplain mudstone and sandstone. Both the northern and southern limits of the barrier-strandplain system are gradational with adjacent delta systems (fig. III-1).

Deposition of the Greta/Carancahua barrier-strandplain system was characterized by aggradation (Galloway and others, 1982). However, various levels of transgressive and regressive cycles are present in the upper Frio in the North Markham - North Bay City field area (fig. III-2). The two sandstone thicks near the Wharton-Matagorda county line, which together compose the axis of barrier-strandplain sedimentation, were deposited during a transgressive phase in shorezone sedimentation, as indicated by the onlap of the thickest sandstones. A minor regression characterized mid- to late-stage sedimentation of the cycle 1 sandstone. The thick succession of mudstone landward of this offlapping sandstone indicates that this lower sequence was deposited as an accreting barrier (fig. III-2).

The cycle 2 sequence does not contain thick lagoonal mudstone. Instead, thin sandstones and mudstones of the back shorezone setting are locally truncated by thick fluvial-channel sands. The absence of lagoon mudstone facies suggests that the upper sandstones are of strandplain origin, such as those of the Nayarit coastal plain in Western Mexico (Curray and others, 1969). The final pulse of Frio sedimentation was the deposition of the Greta barrier-lagoon system (cycle 3). Greta sandstones were subsequently transgressed by the Anahuac sea.

Minor onlap and offlap events are also documented by analysis of the reservoir sandstones. The North Markham - North Bay City field is located shoreward of the principal axis of sand accumulation in the Frio Formation (fig. III-2). The three oil sandstones of interest were

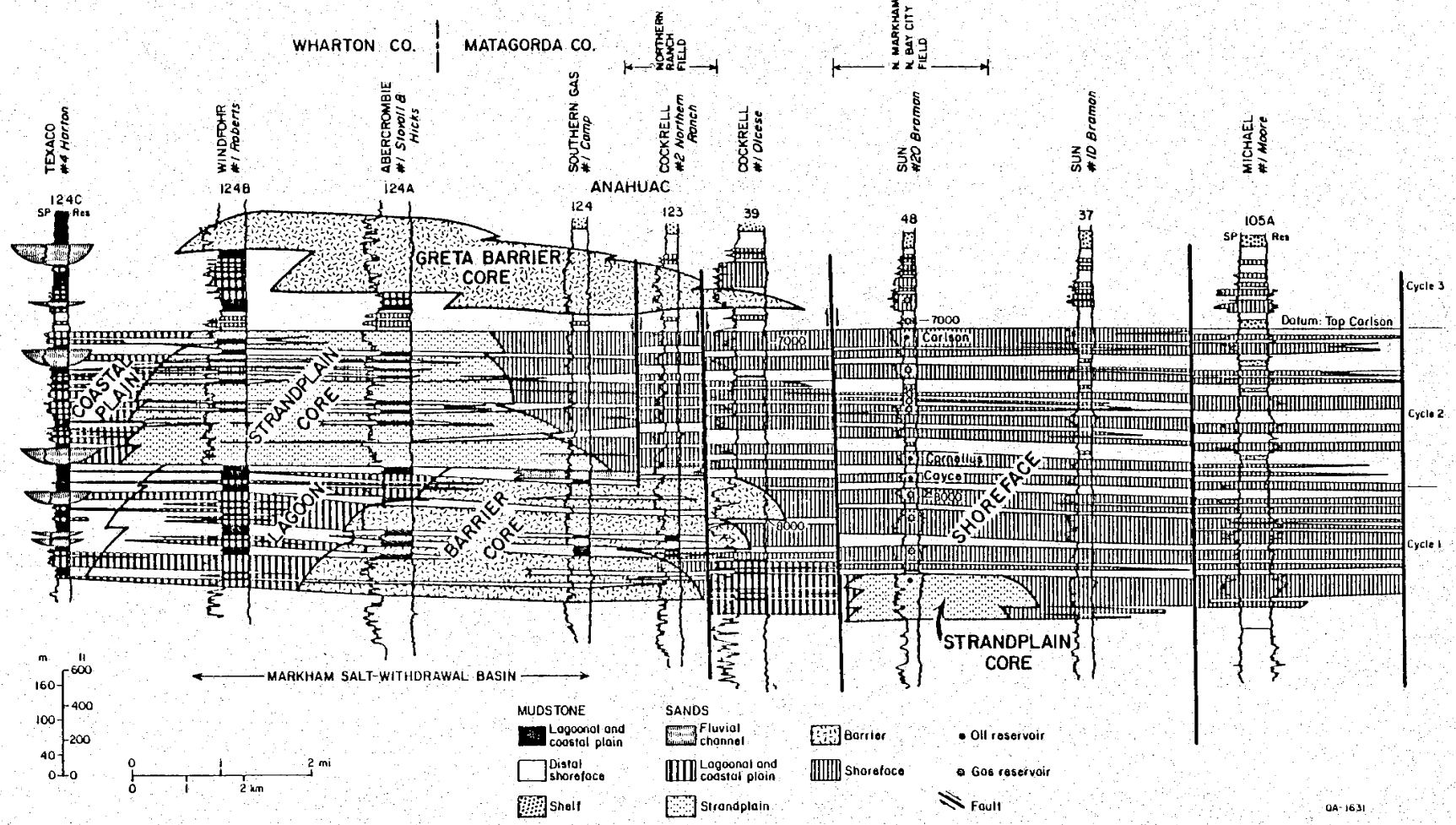

Figure III-2. Dip section of the upper Frio Formation. The North Markham - North Bay City field lies basinward of the Greta/Carancahua depositional axis. Principal oil reservoirs are the Carlson, Cornelius, and Cayce.

deposited under conditions of strandplain accretion and local deltaic progradation (Cornelius and Cayce sands) and coastal onlap (Carlson sand).

Contemporaneous growth faulting was the dominant structural process during deposition of the Frio Formation. The Vicksburg and Frio growth-fault zones are oriented subparallel to the Greta/Carancahua barrier-strandplain axis accentuating the strongly strike-parallel orientation of facies (Galloway and others, 1982). Locally, as in the North Markham - North Bay City field area, the principal growth faults are aligned obliquely to the strandplain axis. Displacement along the updip fault deformed sediments at North Markham - North Bay City field into an elongate rollover anticline with two culminations (fig. III-3). The structural elevation of both domes varies with depth (fig. III-4). Because the structural closure of the west dome is greatest in the shallower sandstones, oil and gas in these reservoirs (including the Carlson) is confined to the western half (North Markham) of the field. Hydrocarbons occur in both domes at intermediate depths (including the Cornelius and Cayce reservoirs); however, the deep gas reservoirs produce only from the east dome.

Oil Production from the North Markham - North Bay City Field

In the early years of oil production, the North Markham and North Bay City field areas were operated separately. The western half of the field (North Markham) was discovered in 1938 with the completion of the Ohio Cornelius No. 1 well in the Cornelius reservoir. Production from the eastern dome was established in 1942 by the completion of the Ohio McDonald Account No. 1 well in the Cayce reservoir. For the following 10 years, the two domes were produced as discrete fields under two sets of field rules.

Recognition of continuous hydrocarbon zones and pressure continuity between the two domes in reservoirs of intermediate depths led to a joint engineering study by the operators. In 1952, the two fields were consolidated and unitized to form the North Markham - North Bay City field. By 1969, a total of 20 separate hydrocarbon reservoirs had been recognized by the Railroad Commission of Texas; 9 are principally oil reservoirs, and the remaining 11 are gas reservoirs. Cumulative oil production from discovery to the end of 1982 was 44.4 million bbl, and total gas production including casinghead gas for 1982 only was 1.1 million Mcf (Railroad Commission of Texas, 1983). The Carlson (cumulative production of 13.1 million bbl oil), Cornelius (17.4 million bbl), and Cayce (9.8 million bbl) sandstones are the principal oil reservoirs and the focus of this study.

Geologic, engineering, and fluid characteristics of the three reservoirs are summarized in table III-1. Reservoir energy is supplied by water drives supplemented by gas-cap expansion. Average porosities range from 24 to 31 percent, and average permeabilities range from 750 to

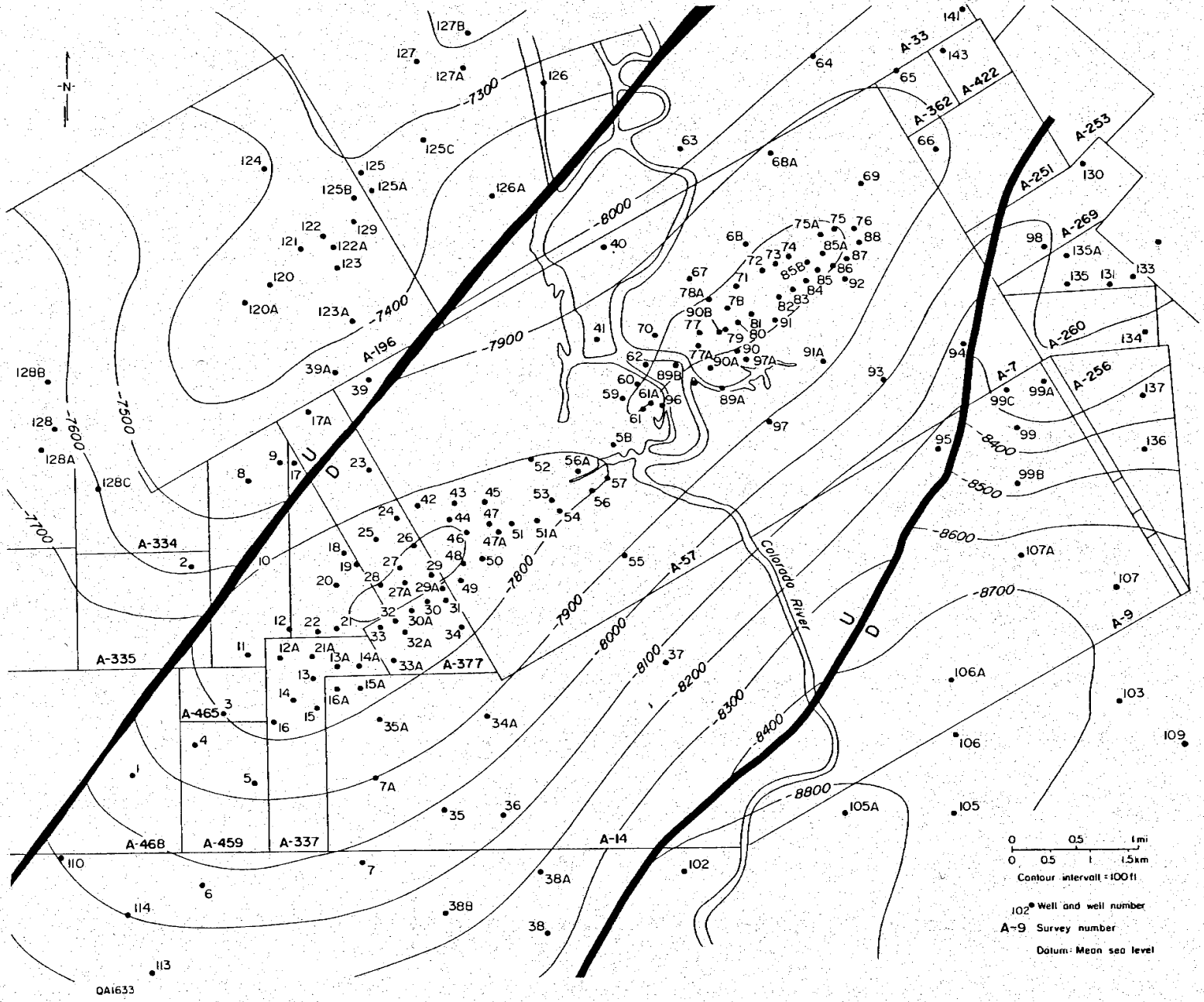

Figure III-3. Structure map of the North Markham - North Bay City field contoured on top of the Cayce sandstone. All legal surveys and lease boundaries are shown.

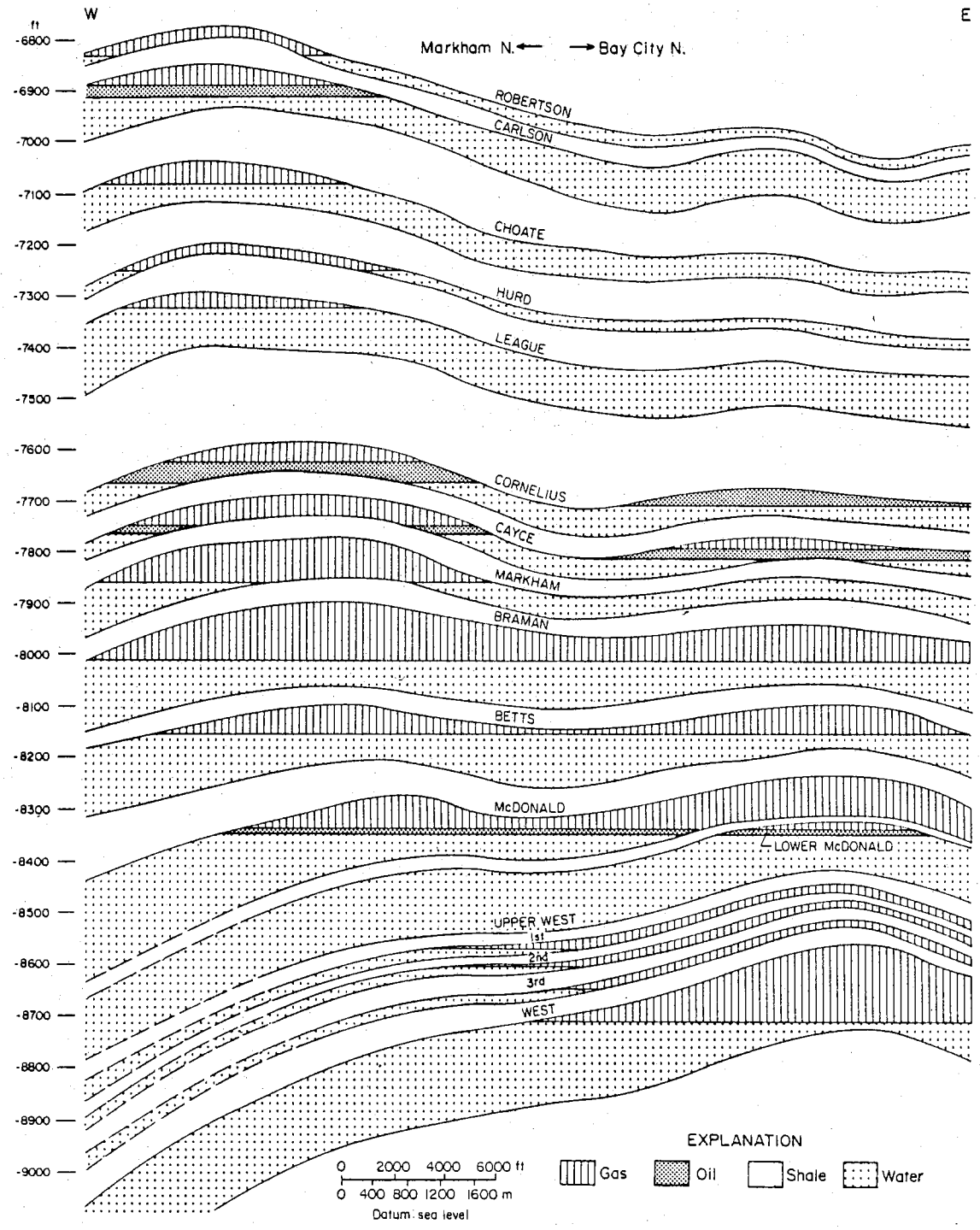

Figure III-4. Generalized west-east strike section across the North Markham - North Bay City field (modified from Marathon Oil Company, Railroad Commission of Texas Docket No. 3-23116, exhibit 2).

Table III-1. Geologic, fluid-property, engineering, and production characteristics of the principal oil reservoirs of the North Markham - North Bay City field.*

	Carlson	Cornelius	Cayce**
Discovery date	1938	1938	1942
Lithology	SS	SS	SS
Trap	ROA	ROA	ROA
Drive	WD + GCE	WD + GCE	WD + GCE
Depth (ft)	7,000	7,700	7,800
Oil column (ft)	25	40	20
Porosity (%)	31	24	28.5
Permeability (average md)	3,333	750	1,737
Permeability (log range)	2-3	2-3	2-3
Water saturation (%)	26	28	30
API gravity (°)	36	36	35
Initial GOR (ft^3/bbl)	600	640	628
Initial pressure (Psig)	3,175	3,572	3,623
Temperature (°F)	182	193	201
Secondary production	PMG	PMG	PMG
Unitization date	52	52	52
Well spacing (acres)	40	40	40
Residual oil saturation	28 (?)		
OOIP (MMbbl)	20	36	15.7
Cumulative production (MMbbl)	13.1	17.4	9.8
Ultimate recovery (MMbbl)	14.0	22.0	10.4
Recovery efficiency (%)	70	61	66

ROA = rollover anticline
WD = water drive
OOIP = original oil in place
GCE = gas-cap expansion
PMG = pressure maintenance via gas injection
ROS = residual oil saturation

*Data obtained from the hearing files of the Railroad Commission of Texas.
**Data are for the East Cayce reservoir.

3,300 md for the three reservoirs. The reservoirs produce moderately high gravity oil (35° to 36° API) with low original gas-oil ratios (600 ft^3/bbl) and have undergone pressure maintenance via gas injection. Ultimate recovery of oil ranges from 61 percent for the Cornelius reservoir to 70 percent for the Carlson reservoir.

METHODS

Analysis of reservoir compartmentalization in the North Markham - North Bay City field is based on the electric log (spontaneous potential and resistivity) response to the sandstones, supplemented by production data supplied by Marathon Oil Company. Almost 200 logs were used in the study (appendix III-1). This field was initially chosen for detailed study because of an extensive coring program carried out in the 1940's and early 1950's. Unfortunately, these cores are no longer available.

The geologic framework of the three oil reservoirs was mapped using 10 strike and dip sections and interval thickness, net-sand, and percent-sand maps. Fence diagrams are particularly useful in documenting lateral and vertical log-facies changes in the Carlson and Cornelius reservoirs; high variability and rapid facies changes diminish the usefulness of this technique in the Cayce reservoir. Log character (facies) maps, developed by Galloway and others (1982), proved particularly useful in mapping the areal distribution of the component sandstone facies in all three reservoirs. This technique was invaluable in unraveling the complicated facies architecture of the Cayce reservoir.

The areal variation in vertical heterogeneity in each reservoir was examined using maps of stratigraphic complexity. These maps reflect the number of beds in the reservoir irrespective of total thickness. The term "beds" is used here to refer to sandstone units that are differentiated from underlying and overlying sands by shale beds or cemented zones. Bed boundaries are indicated by spontaneous potential (SP) and resistivity deflections. Both the number of beds in the main reservoir sand and the number of beds within the entire genetic package were mapped. The figures obtained in this manner for each well represent the stratigraphic complexity (analogous to the heterogeneity factor of Polasek and Hutchinson, 1967) in the area. They do not imply that actual physical boundaries exist in the reservoir where contours are drawn (Alpay, 1972).

Production data supplied by Marathon Oil Company were compiled onto a suite of maps. Paths of water influx in each reservoir were documented using watercut maps for 1950, 1960, 1970, and 1980. These are useful in confirming facies control on fluid-flow characteristics in the reservoir. Gas-oil ratio (GOR) maps for 1960, 1970, and 1980 were less instructive. Reservoir productivity maps contoured in bbl/yr were drawn for two periods: from reservoir

discovery to 1965 and from 1966 to 1982. Finally, data from all three suites of maps were synthesized onto reservoir-compartment maps for each reservoir.

Compilation of cross sections on which the long-normal resistivity profiles are contoured has been found to be particularly effective in documenting reservoir heterogeneity. Resistivity logs are used to determine hydrocarbon versus water-bearing zones (Asquith and Gibson, 1982). The framework components and matrix of rocks are nonconductive. The transmission of electrical currents through the sandstone is thus due to water contained in the pores. Hydrocarbons are also nonconductive; therefore, an increase in the resistivity reading can be used as an indicator of increasing hydrocarbon saturation (Asquith and Gibson, 1982). The magnitude of the resistivity deflection was mapped throughout the field area for the three reservoirs, and the location and magnitude of the resistivity "kick" were plotted on combined SP/long-normal resistivity cross sections. Subtle changes in log facies character that are difficult to recognize on SP logs are emphasized by changes in the magnitude and location of the resistivity peak. The effect of differing mud types on the resistivity response was found to be minor.

CAYCE RESERVOIR: A COMPOSITE PROGRADATIONAL STRANDPLAIN/FLUVIAL-DELTAIC COMPLEX

Depositional Environment

Distribution of Sandstone

The updip bounding growth fault strongly influences interval thickness trends in the Cayce; thickness is greatest immediately adjacent to the fault. The entire interval thins over the anticlinal crest, and the isopach contours mimic structure contours. This suggests that the anticline was topographically positive during deposition of the Cayce. The interval expands downdip of the anticline and thins towards the south. A downdip fault, which has a displacement of 200 to 400 ft, did not influence the thickness of the Cayce and thus was not active during deposition of this sandstone.

Decreases in net-sandstone and percent-sandstone contents accompany thinning of the interval over the anticline (fig. III-5). Thicker accumulations of sandstone lie on the updip and downdip sides of the anticline; the major zone of sandstone deposition is downdip and east of the anticline. A second area of sandstone accumulation lies on the updip side of the growth fault as indicated by high sandstone percentage.

Areal Distribution of Component Facies

The SP log character of the Cayce sandstone varies greatly throughout the field area. In the western half of the fault block, log patterns are commonly serrate, with thin sandstones

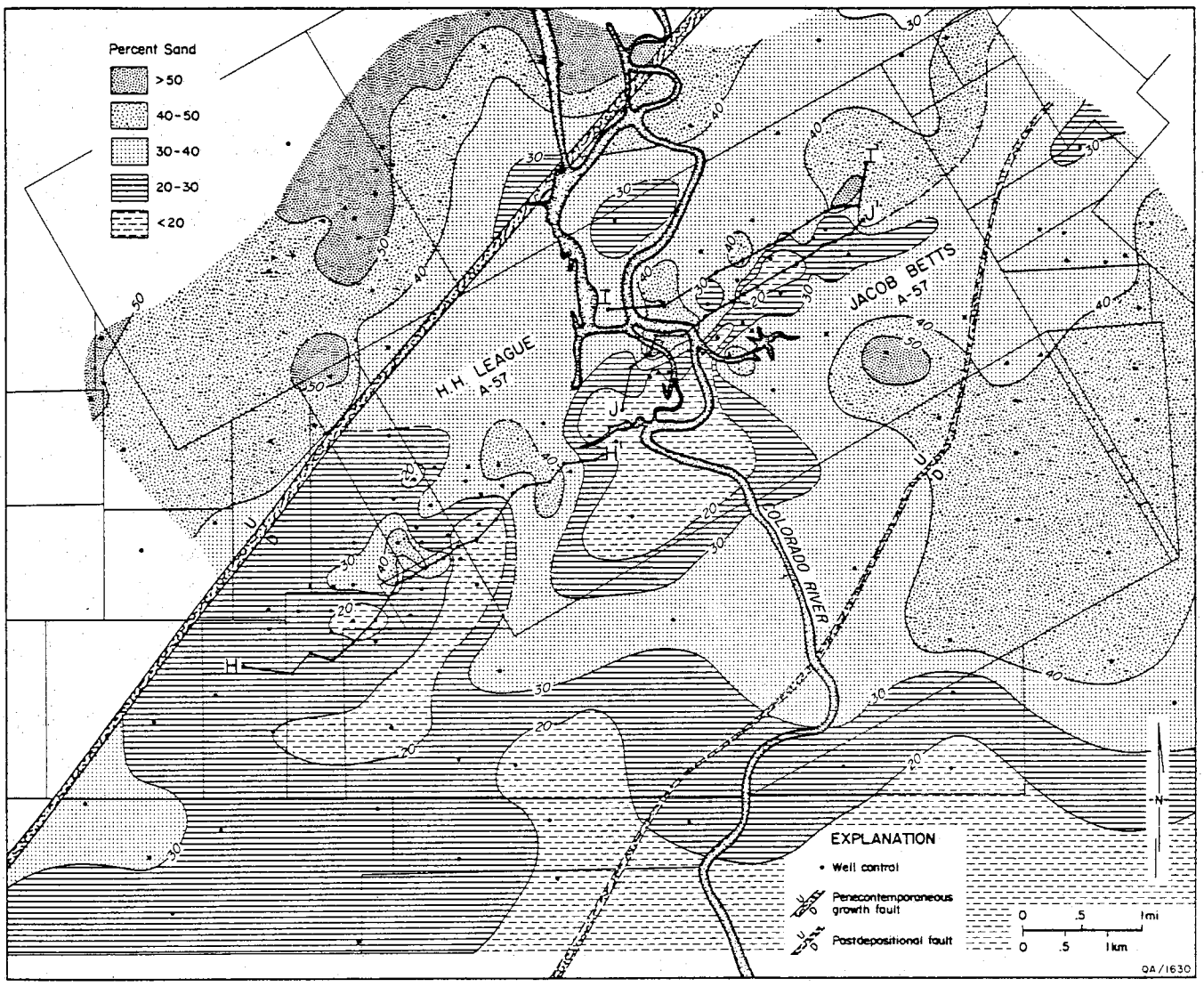

Figure III-5. Percent-sand map, Cayce reservoir. The main area of sand accumulation downdip of the principal growth fault lies southeast of the rollover anticline. Total thickness and sand content of the Cayce decrease over the crest of the anticline. Sections H, I, and J are shown in figures III-9 and III-10.

defining upward-coarsening cycles (fig. III-6). Upward-fining and blocky patterns, locally present in the western half of the field, dominate the eastern half. Characterization of the SP profiles (fig. III-6) into progradational and aggradational facies helps to map the architecture of the component facies (fig. III-7) that make up this composite sandstone body.

Progradational facies are divided into two principal categories: blocky or upward coarsening. These are in turn subdivided into a more detailed breakdown, as is illustrated in the explanation of figure III-7. Progradational facies provide the framework of the Cayce sandstone, which is characterized by variations of a blocky SP response over much of the area. Upward-coarsening log patterns are concentrated basinward. Transecting the suite of progradational facies is a north-south-oriented aggradational system consisting of simple and serrate upward-fining sandstones. Downdip, this aggradational facies becomes strike-oriented. In this area, SP logs retain their dominantly upward-fining character but become more blocky. Both sandstone-rich serrate and mudstone-rich serrate logs are closely associated with the cross-cutting system.

Interpretation

The Cayce sandstone was deposited in a prograding strandplain system. The sandstones characterized by blocky SP patterns that compose the bulk of the unit were deposited as beach ridges on a strandplain; locally developed interbedded sandstones and mudstones represent sedimentation in ephemeral ponds or marshes. Modern and recent strandplain coastlines that provide analogs are the coastal plain of Nayarit on the Pacific Coast of Mexico (Curray and others, 1969; McCubbin, 1982), and parts of the Pleistocene Ingleside Formation along the central Texas Gulf Coast (Winker, 1979). The Cayce prograding strandplain system was transected by a river that eroded and redeposited the strandplain sediments into typically upward-fining fluvial sandstones. Log facies in areas of dense well control indicate that the upward-fining fluvial sandstones are flanked by sandstone-rich and sandstone-poor zones that have a serrate SP response; these probably represent levee and floodplain deposits. The upper part of the river system consists of three discrete channels merging seaward into a single channel; these separate channels probably represent different positions of the river. Remnant strandplain deposits separate the channels. Immediately adjacent to the convergence of the channels is a local area of upward-coarsening sandstones. The restricted distribution and lobate geometry of these sandstones suggest deposition as a crevasse splay.

Downdip, the orientation of the aggradational system changes to strike parallel (fig. III-7), with a concomitant increase in the "blockiness" of the SP response. Adjacent basinward sandstones have the typical upward-coarsening, progradational character of shoreface and delta-front deposits. The entire strike-parallel system is interpreted as a highly wave-reworked

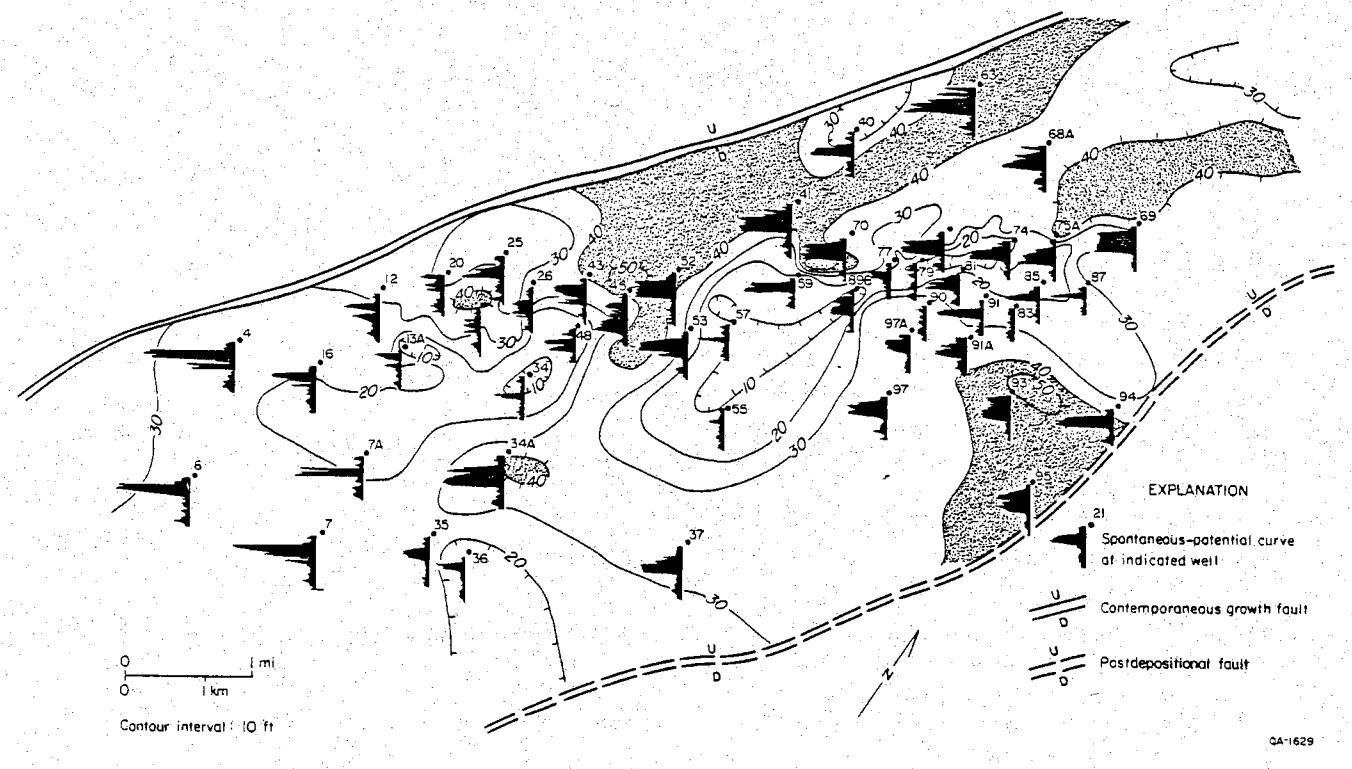

Figure III-6. Log character and net-sandstone map, Cayce reservoir.

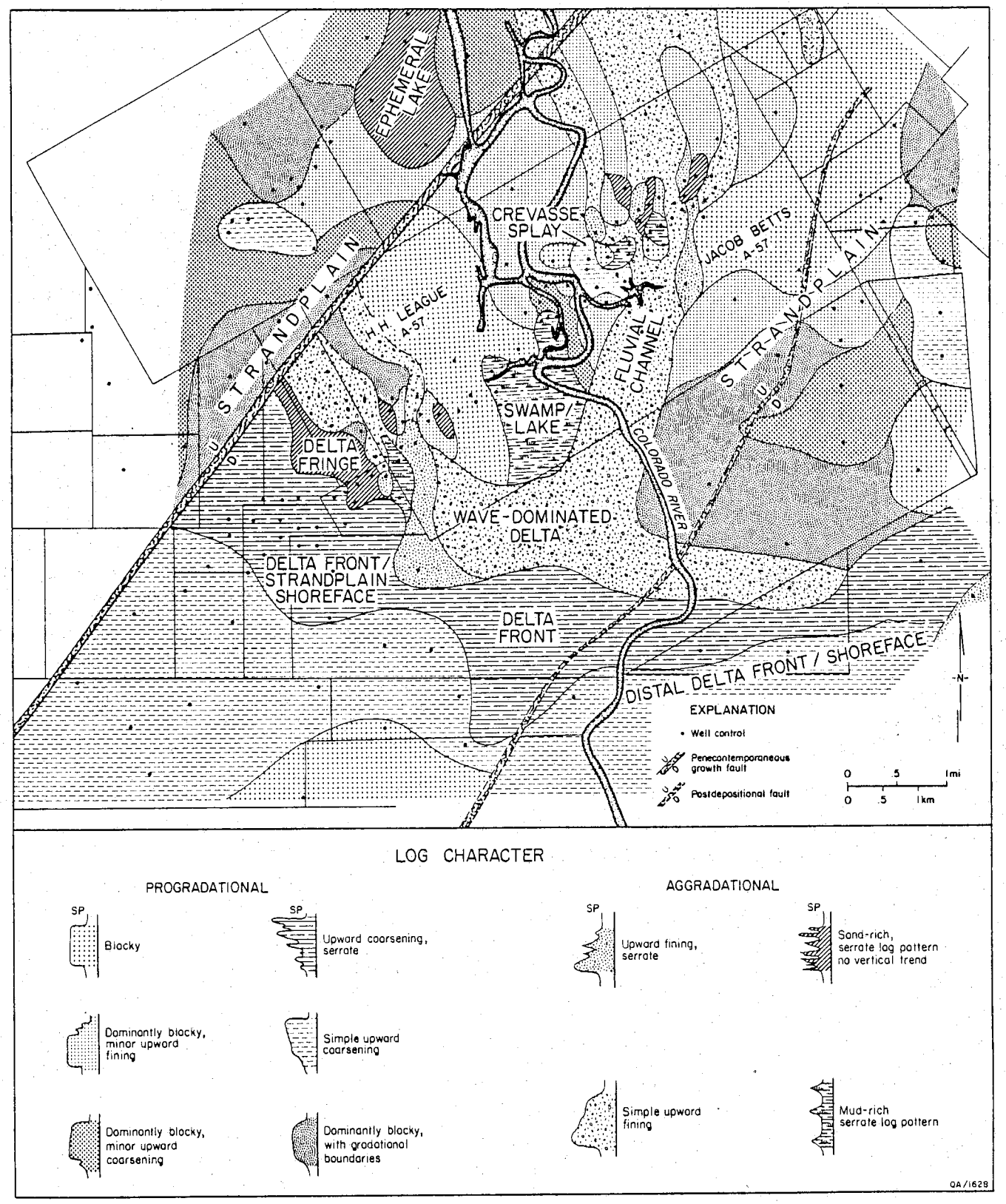

Figure III-7. Facies anatomy of the Cayce sandstone adapted from vertical SP profiles. Strandplain sandstones are crosscut by a fluvial-deltaic system that grades downdip into upward-coarsening delta-strandplain deposits.

delta that had a second fluvial entrant west of the principal channel. Wave-dominated deltas commonly occur along strandplain shorelines. The Cayce delta is very similar in geometry and areal extent to the modern wave-dominated Brazos delta of the Upper Texas Gulf Coast, which owes its cuspate geometry to the rapid reworking of materials in the Gulf basin by waves and currents (Morton and McGowen, 1980).

Areal Stratification Trends

Stratigraphic complexity maps, which focused on the immediate field area (fig. III-8), examine the areal distribution of the number of strata that compose the Cayce reservoir. When the entire Cayce progradational genetic unit is considered (from the top of the Markham to the top of the Cayce, fig. III-4) a systematic decrease in the number of beds takes place from updip, where there are 10 discrete strata, to downdip, where there are only 2 stacked sandstones. When only the main sandstone is considered, a more complicated pattern emerges that matches the complex facies architecture (fig. III-8). Both dip- and strike-oriented elements are represented. The channel sandstones generally contain few discrete strata (that is, low heterogeneity factors), whereas the strandplain, delta-fringe, and delta-front sandstones have a moderate to large number of interbeds. The low in the center of the field area corresponds to the marsh or lake deposits that lay adjacent to the main channel.

Reservoir Continuity

Contoured resistivity cross sections proved to be most useful in documenting the lateral continuity of the component facies and facies control on the areal distribution of hydrocarbons. Twelve cross sections (three of which are presented in the report, figs. III-9A, III-9B, and III-10) were compiled. Figures III-9A and III-10 are hung on a structural datum to show the relatively gentle doming of the East and West Cayce reservoirs, as well as the distribution of the hydrocarbon resistivity peaks relative to the gas-oil and oil-water contacts. However, because this analysis is primarily concerned with facies control on reservoir continuity, many of the sections were hung on a stratigraphic datum (in this instance the top of the Cayce).

In the East Cayce reservoir, the lateral continuity of the sandstones is greatest in the strandplain setting, as shown on the left side of section J-J' (fig. III-9B). The crosscutting fluvial-deltaic complex disrupts the continuity of the strandplain deposits, imparting considerable macroscopic lateral heterogeneity to the reservoir. The strike-parallel resistivity cross sections across the East Cayce reservoirs (figs. III-9A and B) illustrate the compartmentalization of the strandplain sandstones by the crosscutting channel complex. Even though both the strandplain and channel deposits are sandstone-rich, the boundaries between these deposits act

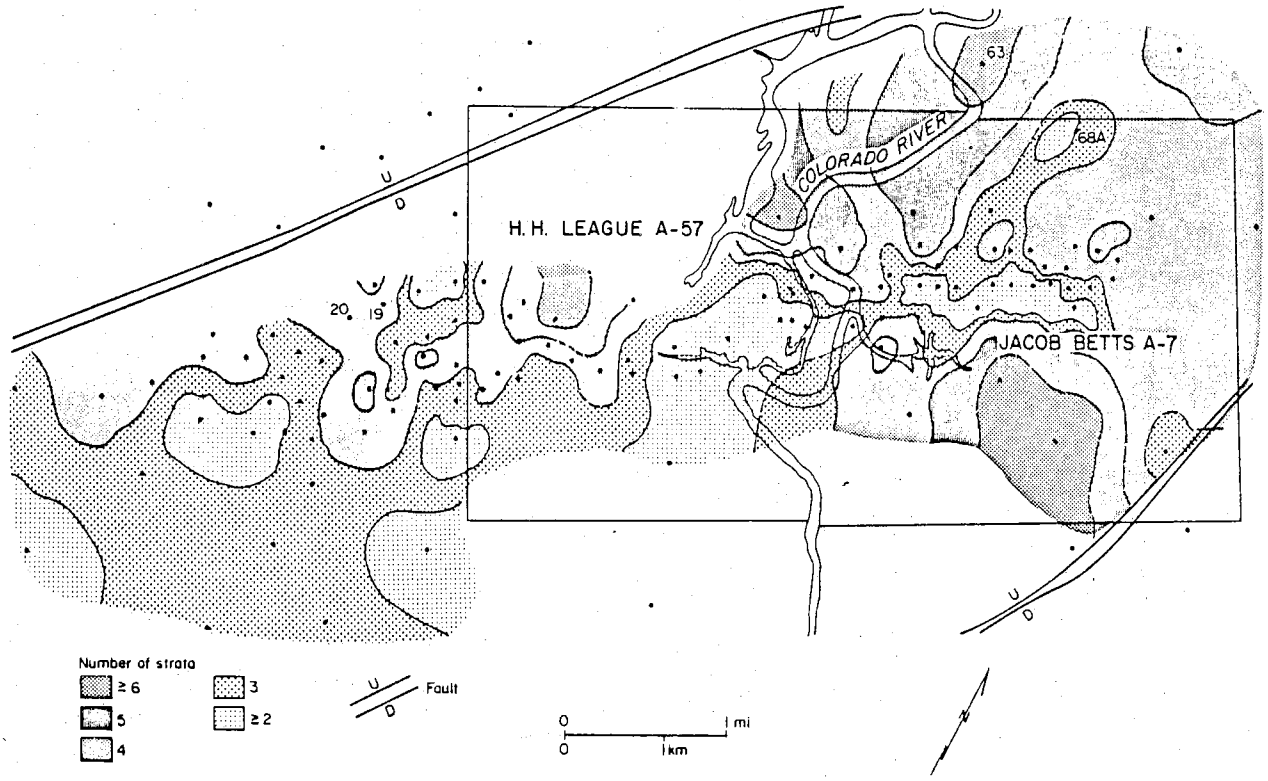

Figure III-8. Stratigraphic-complexity map of the Cayce sandstone. Resistivity and SP deflections are used to distinguish individual strata. In general, strandplain sandstones have a greater number of interbeds (that is, higher vertical heterogeneity) than fluvial-channel sandstones.

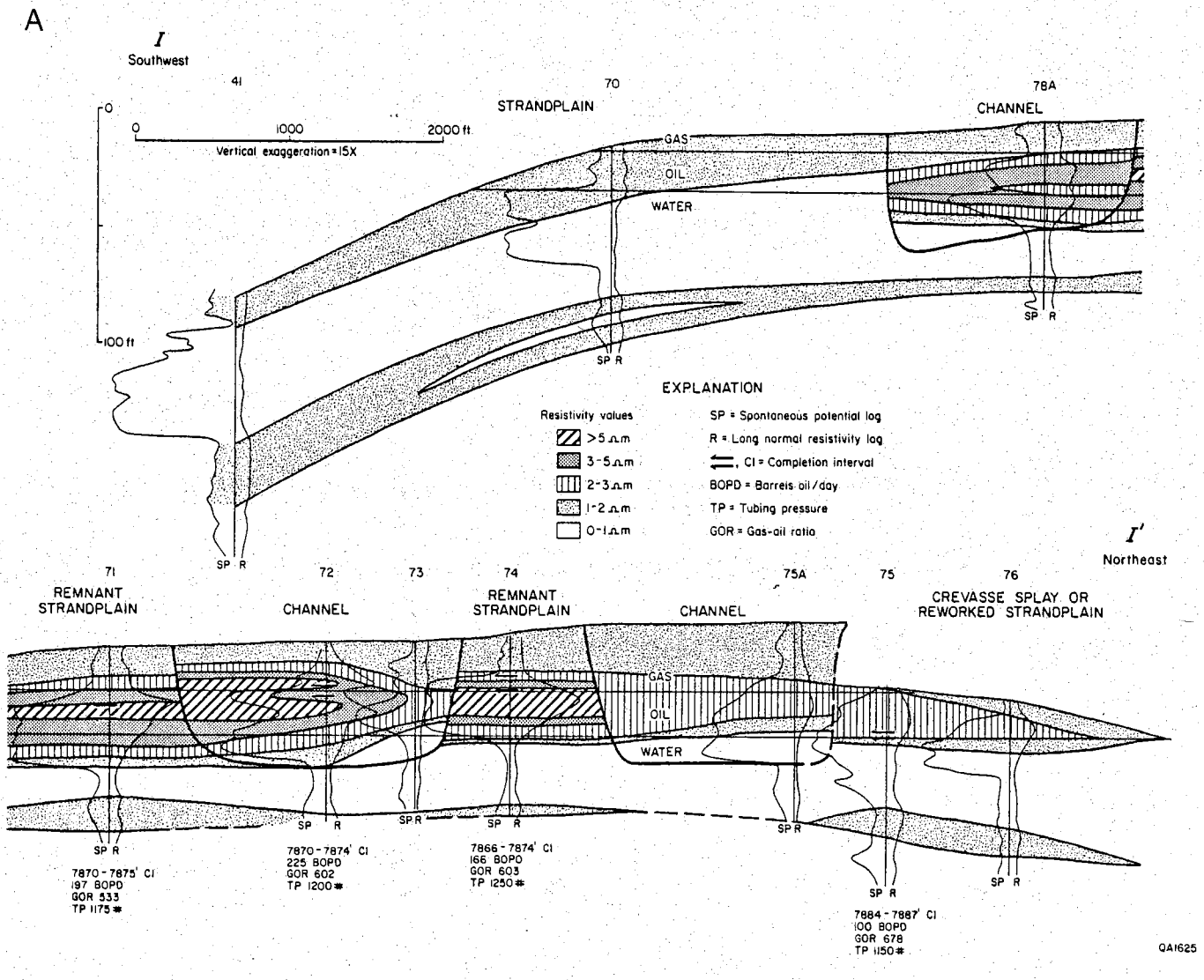

Figure III-9. Resistivity cross sections, East Cayce reservoir: (A) Section I-I' is drawn on a structural datum. (B) Section J-J' is hung on the top of the Cayce sand. Contouring of resistivity deflections allows the evaluation of the internal continuity of sandstone facies. Lines of section shown in figure III-5.

B

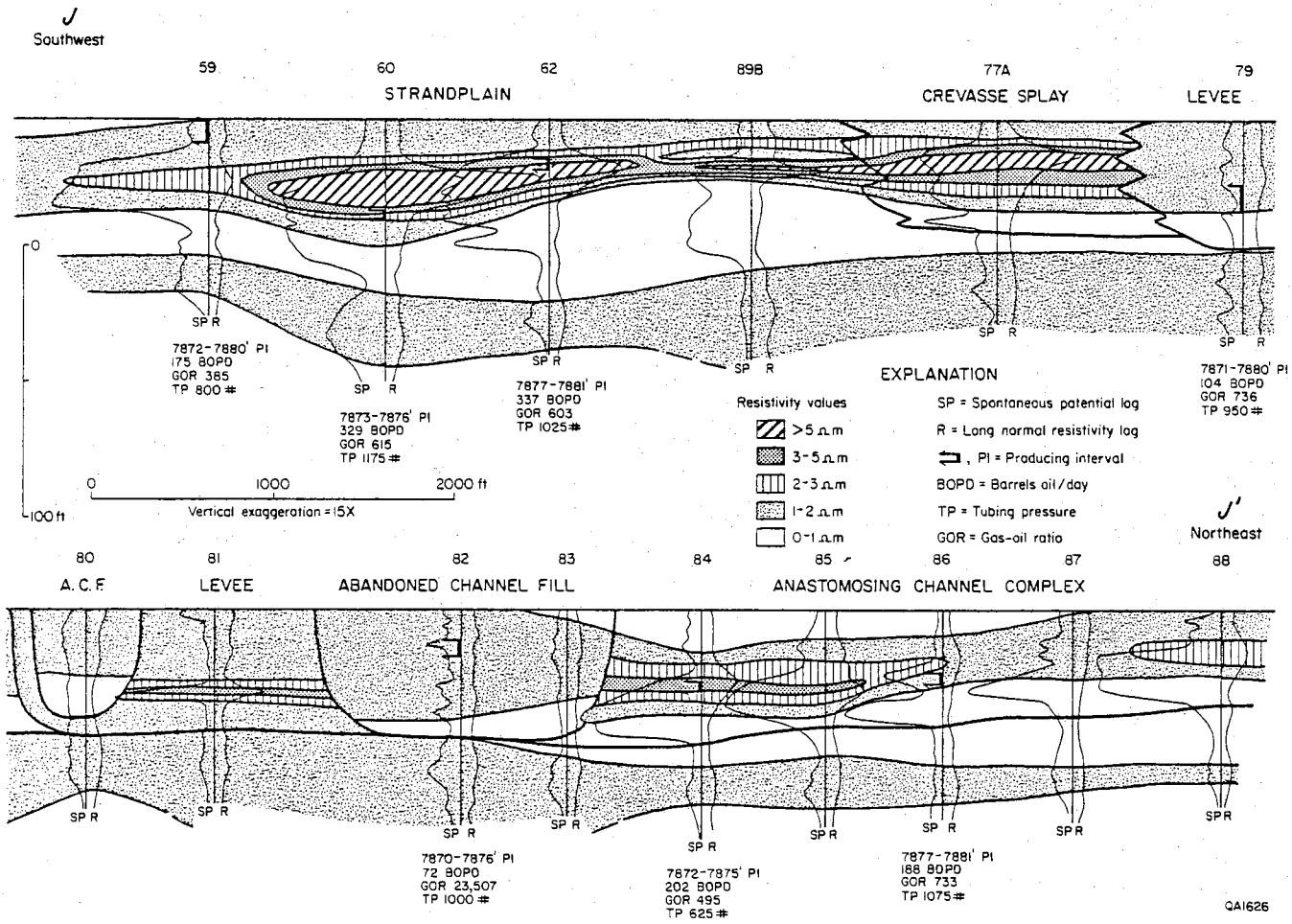

Figure III-9 (cont.)

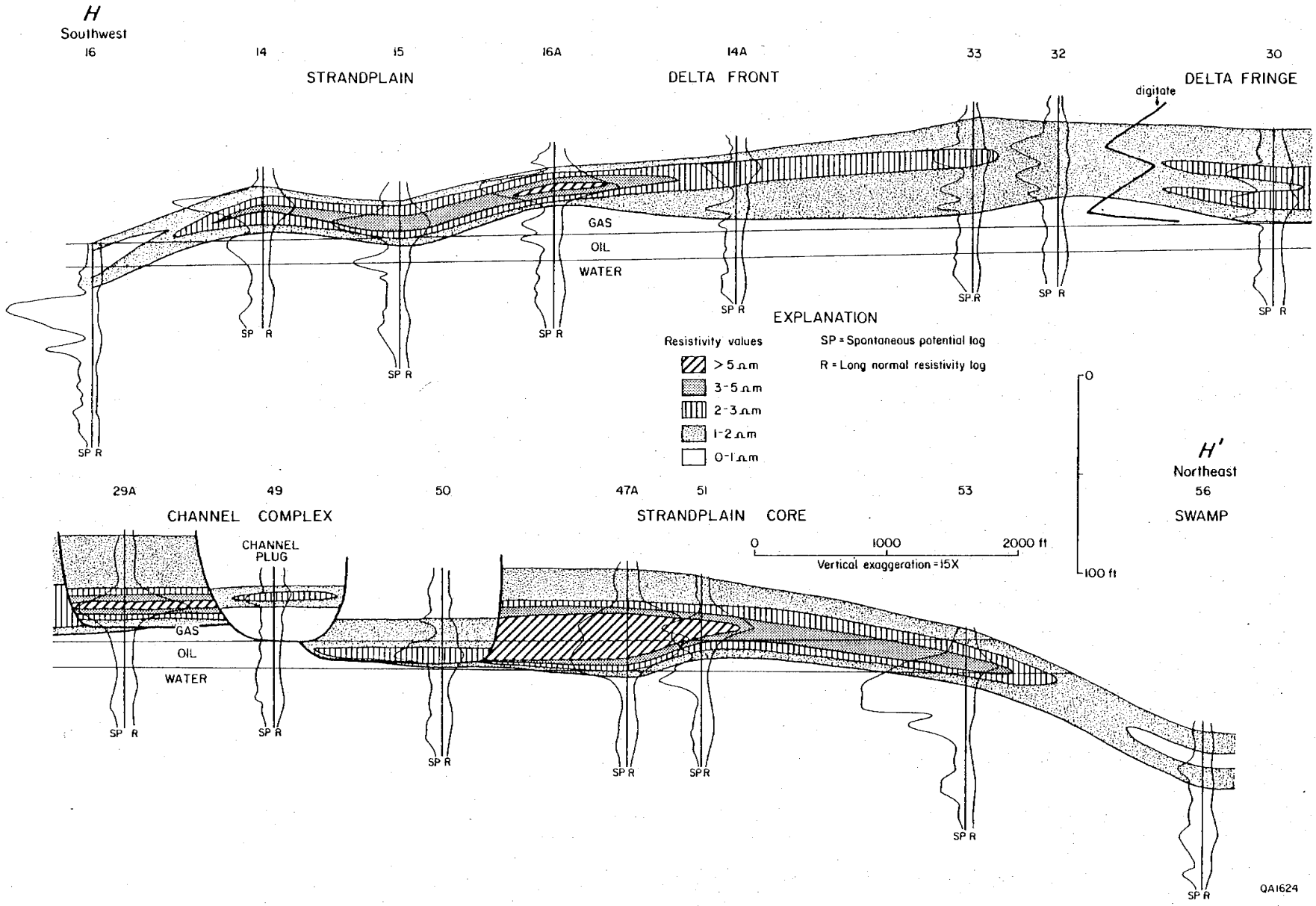

Figure III-10. Resistivity cross section, West Cayce reservoir. Hydrocarbon distribution is most continuous in strandplain sandstones. Line of section shown in figure III-5.

as flow and pressure boundaries. Completion data show that remnant strandplain deposits isolated within the channel complex have lower initial production than do the adjacent channel sandstones. For example, wells 71 and 74, which were both completed in remnant strandplain deposits, had an average initial production of 182 bbl/day whereas well 72, completed in the channel sandstone separating the two strandplain remnants, yielded 225 bbl/day (fig. III-9A). The two facies clearly have different production characteristics. Without whole core data, it is difficult to determine whether the differences result from permeability variations or from disparity in original in-place oil distribution. However, the boundaries that separate facies clearly restrict fluid flow.

The lower production from the remnant strandplain sandstones isolated in the fluvial complex is anomalous when compared to production from strandplain sands over the entire East Cayce reservoir. Average initial production from strandplain deposits for the entire East Cayce exceeds that from fluvial-channel sandstones by 50 bbl/day ($\bar{P}_{sp}$ = 248 bbl/day; $\bar{P}_{c}$ = 194 bbl/day; $\bar{P}_{cs}$ = 90 bbl/day), which in turn exceeds production from the associated crevasse-splay sandstones by 100 bbl/day. The higher production from strandplain deposits is illustrated on figure III-9B, where wells on the southwest side of section J-J' completed in strandplain sandstones have consistently higher productions than do fluvial deposits.

Reservoir continuity trends in the West Cayce reservoir match those in East Cayce reservoir; hydrocarbon saturation is most persistent in the strandplain/delta-front sandstones and least continuous in the channel sandstones (fig. III-10). At the northeast contact between channel and strandplain deposits (between wells 50 and 47A), a thick zone of hydrocarbon saturation in the strandplain core flanks the channel complex. Had fluids been able to move freely across this facies boundary, hydrocarbon saturations would have equilibrated. Instead, the boundary provides an intrareservoir trap that pools hydrocarbons downdip of the low-permeability boundary, providing further evidence of the flow-resistant nature of facies boundaries.

Integration of Production and Reservoir-Continuity Data Within the Geologic Framework

Monthly production data including water cut, oil production, and gas-oil ratios for wells in the three reservoirs are shown on a series of maps that chart the evolution of the produced fluids over the life of the field. These maps test the hypothesis that the facies architecture of the sandstone controls patterns of fluid migration within, and hydrocarbon recovery from, the reservoir.

Water Influx Trends

Water-cut maps show the amount of water produced as a percentage of the total fluid production (oil, gas, and water) from each test well. The progressive influx of water over 40 years is shown on figures III-11A through III-11D. Water influx in the East Cayce reservoir took place by two distinct mechanisms with different geometries. A broad zone of edge-water influx had begun in the northwest section by 1950 (fig. III-11A). This swath of higher water cuts migrated progressively southward. However, channelized migration was the dominant mode of water influx in the eastern part of East Cayce (fig. III-11A). With time, the dip-oriented channel of water invasion expanded laterally (fig. III-11B); by 1970, most of the East Cayce wells were producing over 90 percent water. Abandoned wells are also shown in figure III-11; the pattern of abandonment of watered-out wells follows the same trends shown during early water invasion. In West Cayce, channelized water influx dominated and minor edge water occurred on the west side of the field (fig. III-11C).

The relation of water influx trends to the architecture of the reservoir sand is well defined. Zones of channelized invasion correspond remarkably well with the crosscutting, upward-fining, fluvial-channel system in both reservoirs (fig. III-11C). The broad zones of edge-water invasion take place within the laterally continuous and widespread strandplain sandstones in East Cayce and within delta-front and strandplain-shoreface sands of West Cayce. Certain facies retard water invasion, most notably the serrate delta-fringe sands of West Cayce. This central zone of low production may also be due to the structurally high position of the facies of the crest of the dome. Other low-permeability facies are levee and sand-poor abandoned-channel-fill and marsh deposits.

Gas-Oil Ratio Trends

The gas-oil ratio (GOR) is a function of two parameters: the decrease in reservoir pressure with time and the level of completion in the hydrocarbon column. Of these, reservoir pressure exerts a greater influence on GOR trends. As a result, the GOR patterns shown in the East Cayce reservoir exhibit little or no correlation with facies architecture and sand content. Furthermore, the geometry and orientation of the GOR highs and lows have varied greatly with time, possibly as a result of gas injection for pressure maintenance.

In the West Cayce reservoir, the GOR patterns remained dip-oriented with time, although the widths and position of the high GOR axes changed during production. In general, the GORs in argillaceous interbedded sand and mud facies (delta fringe, delta front, and strandplain shoreface) are considerably higher than in the associated fluvial-channel and strandplain sands.

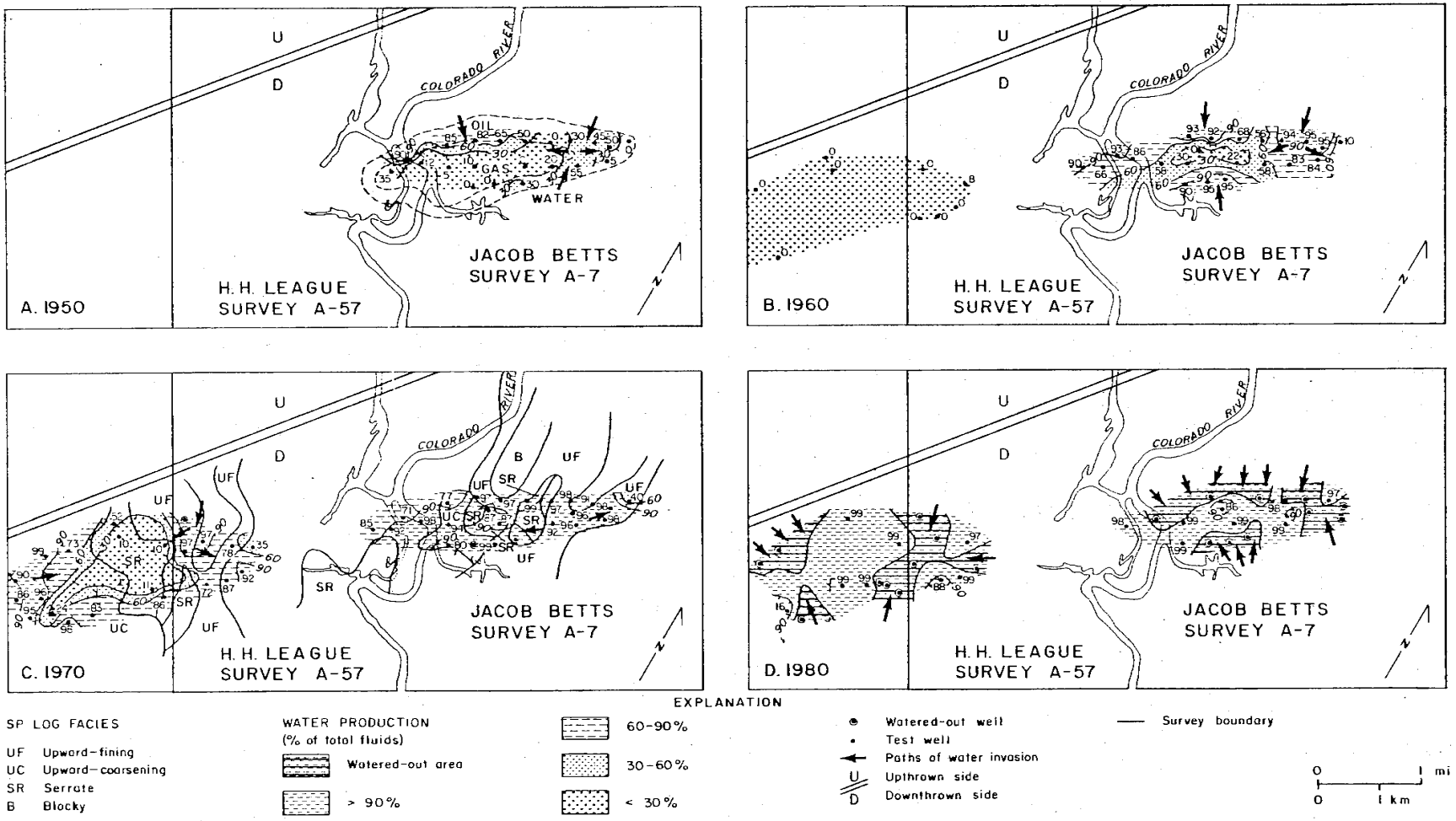

Figure III-11. Sequential water-cut maps, East and West Cayce reservoirs. Crosscutting fluvial-channel sandstones clearly act as foci for channelized water influx. In contrast, strandplain sandstones are characterized by broad water influx fronts.

Reservoir Productivity

The average annual production from each well for the periods (1) from the discovery of the reservoir through 1965 and (2) 1966 through 1982 were contoured to construct reservoir-productivity maps (fig. III-12). Productivity trends that emerge are digitate in geometry and strongly dip oriented, particularly in the early production from East Cayce reservoir. Similar geometries and orientations are suggested in West Cayce. However, because this reservoir is oil productive only from a thin oil rim, production patterns are ill defined.

During the early years of production (1942-1965) the East Cayce yielded a little over 8.0 million bbl of oil. Much of the oil was derived from two major dip-oriented trends (fig. III-12A): the western trend produced from laterally continuous strandplain and crevasse-splay deposits, whereas the northeastern trend tapped fluvial and associated remnant strandplain sandstones (compare with fig. III-6). The central low-yield area that separates the axes of high oil productivity centers on mud-rich swamp and abandoned-channel-fill deposits and adjacent levee sandstones. More recent production trends (1966-1982) are more closely related to structure than stratigraphy, with the central high being localized over the crest of the anticline and decreasing toward the encircling oil-water contacts (fig. III-12B).

The channel-like dip-oriented zone of high oil production in the east flank of West Cayce reservoir (fig. III-12B) corresponds approximately with the thick zone of hydrocarbon saturation as illustrated by the resistivity cross section (fig. III-10). On the basis of resistivity relations, an intrareservoir trap was inferred in which the seal for hydrocarbons in the strandplain sandstones was provided by a crosscutting fluvial channel. However, the two most prolific wells are located in the channel sandstone. Closer examination of wells 50 and 47A on figure III-10 shows that the base of channel sandstone lies below the gas-oil contact, whereas most of the hydrocarbons in the strandplain sand lie within the gas cap. The oil-saturated zone at the base of the strandplain sandstone probably lies within immature and bioturbated shoreface deposits that were laid down during initial strandplain progradation. Thus oil production from the channel sandstone took place from the most coarse grained deposits, presumably of better reservoir quality, whereas strandplain production was from poor-quality reservoir sandstones.

CORNELIUS RESERVOIR: A PROGRADATIONAL CHENIER-PLAIN COMPLEX

The Cornelius reservoir is separated from the Cayce reservoir by a 50-ft-thick lower shoreface to shelf mudstone in the North Markham - North Bay City field area. The mudstone pinches out updip and the Cayce and Cornelius sandstones merge into a single unit in the strandplain core (fig. III-2). Crosscutting channel complexes are of local importance in the Cornelius reservoir, and reservoir continuity greatly exceeds that in the Cayce.

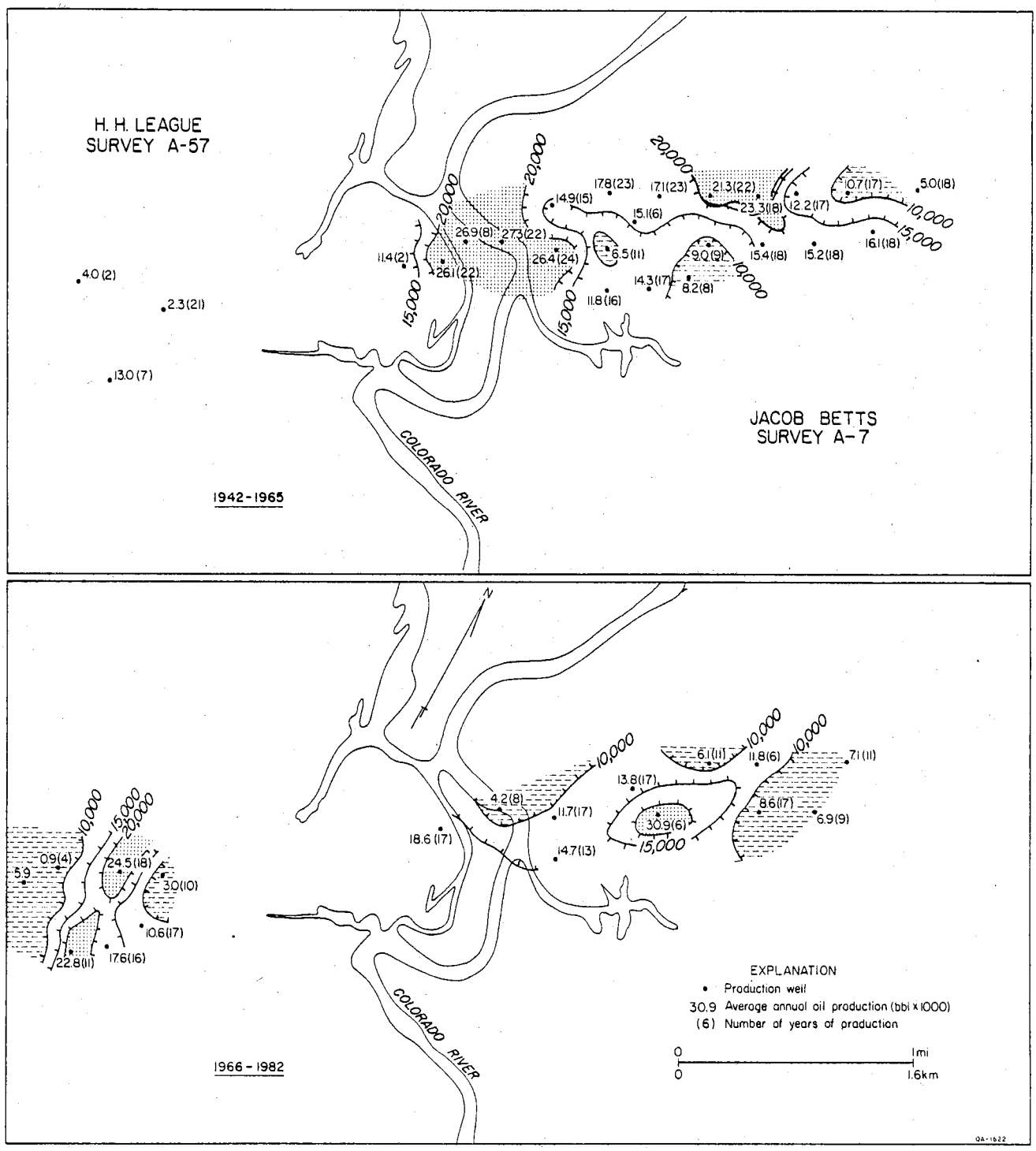

Figure III-12. Reservoir-productivity maps, Cayce reservoir, for 1942 through 1965 and 1966 through 1982.

Depositional Environment

Sandstone Distribution

Sandstone distribution in the Cornelius interval is strongly strike parallel and oblique to the growth fault (fig. III-13). The area of major sandstone accumulation lies updip, immediately adjacent to the fault; however, expansion across the fault is minor. Net-sandstone and percent-sandstone maps both show a systematic decrease seaward.

Areal Distribution of Component Facies

The orientation of the component facies is similar to that of sandstone accumulation trends (fig. III-14). The principal progradational facies (blocky and upward coarsening) are concentrated in the updip parts of the North Markham - North Bay City area, whereas upward-fining and "spiked" aggradational patterns are more common in the downdip part of the area. This particular sand (the Co-3, fig. III-14 inset) pinches out near the southeastern fault. Note that the log-character map shows the facies architecture of only the Co-3 sand, the principal reservoir sand in the Cornelius, and not the log character of the entire Cornelius unit.

Interpretation

The strongly strike-parallel orientation of component facies and the seaward decrease in sandstone content suggest deposition in a prograding shorezone system. Reservoir-specific resistivity dip sections used to examine reservoir continuity (figs. III-16A, B) substantiate the progradational nature of the deposit. Taking into account the weaknesses inherent in environmental inferences not reinforced by studies of whole core, the Cornelius sandstone is interpreted as the product of prograding mud-rich strandplain sedimentation. The Cornelius, which contains between 20 and 60 percent sandstone, displays much higher sandstone contents than do modern chenier plains such as the west coast of Louisiana (Beall, 1968). Yet the physiography of the reservoir is similar to that displayed by chenier plains. Consequently, the Cornelius is considered to be intermediate in composition, between sand-rich Nayarit-type strandplains and mud-rich chenier plains, and is classified as a mud-rich strandplain. Specific environments (fig. III-14) that were probably present during deposition of the sandstone include beach ridges (blocky SP response), fresh- to brackish-water marshes deposited in inter-ridge swales and landward of the breaker bar (upward-fining SP response), lakes (sand-poor, serrate SP response), and strandplain flats (upward-coarsening, composite SP patterns). Sand was supplied to the interridge marshes by washover fans and by flattening out of the beach ridges. As the elevation of the ridges decreased, sand supply declined, resulting in an upward-fining sand character. The zone of spiked SP response probably reflects breaker-bar sedimentation on

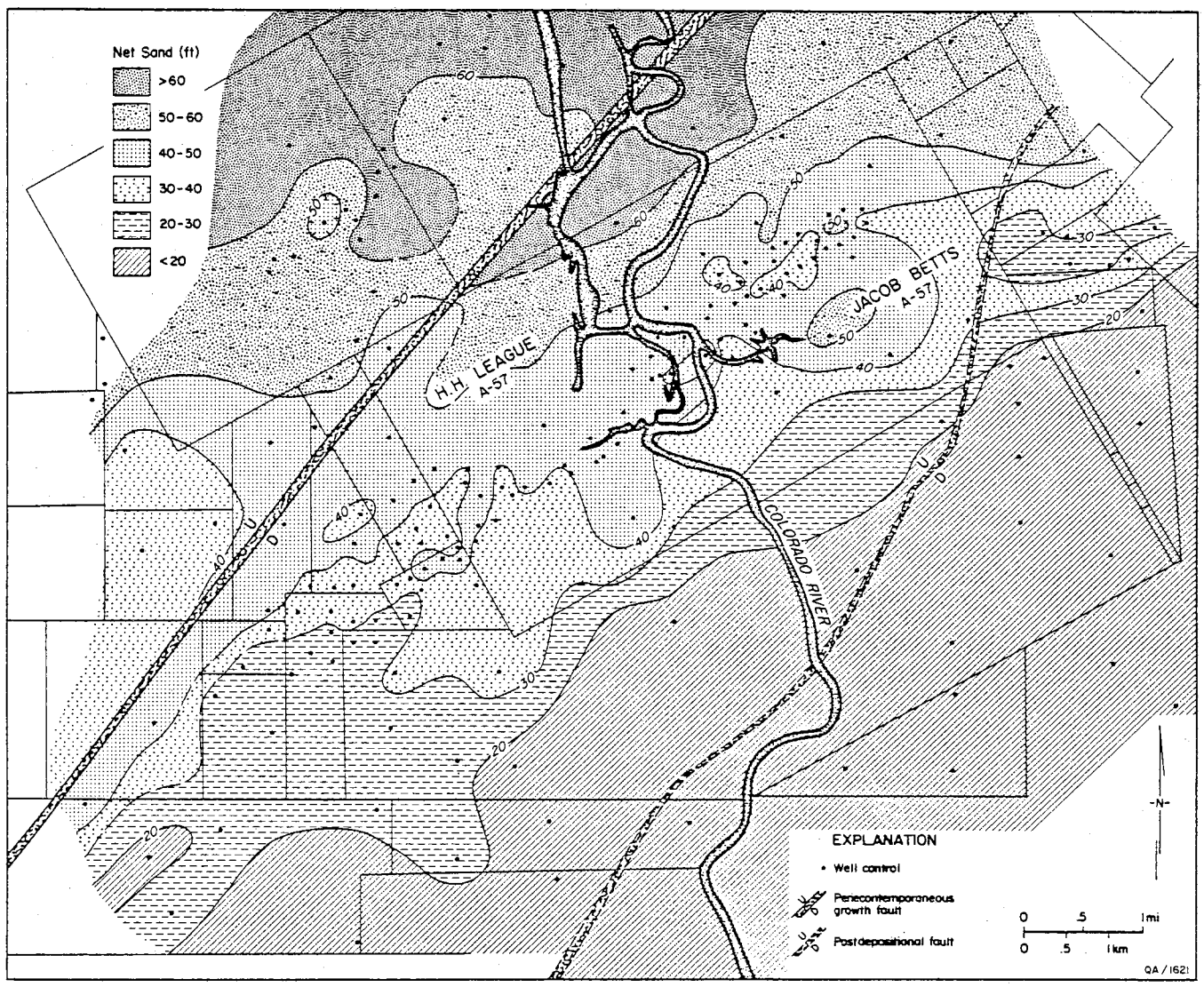

Figure III-13. Net-sandstone map, Cornelius sandstone, showing a simple and systematic basinward decrease in sandstone content.

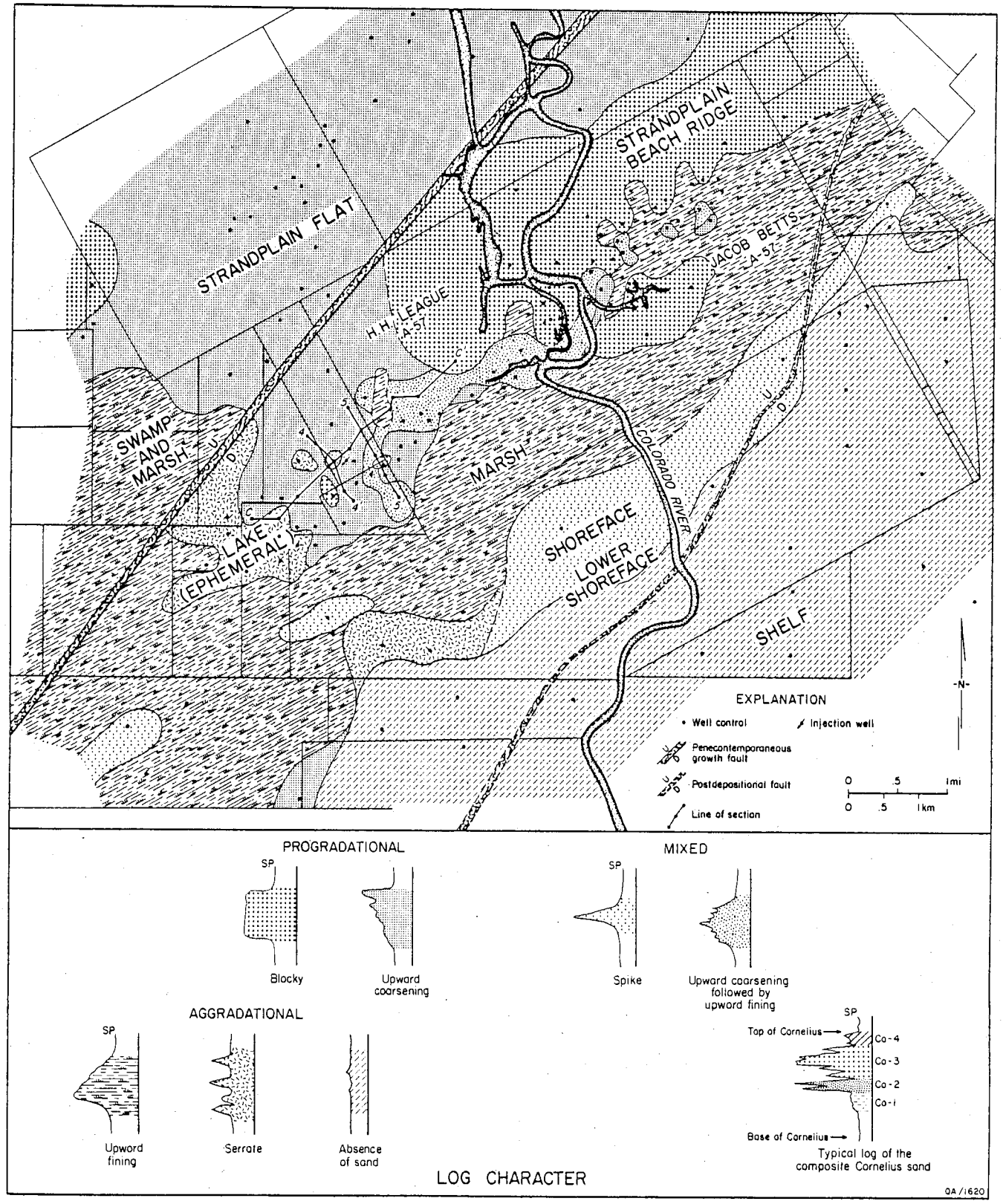

Figure III-14. Interpretive facies anatomy of the third Cornelius sandstone (Co-3, see inset). The strike-parallel architecture of the component facies matches net-sandstone trends, suggesting shorezone sedimentation. Cross sections C-C', 4-4', and 5-5' are shown in figures III-15 and III-16.

the shoreface, and the broad area of mud deposition seaward represents lower shoreface to shelf sedimentation.

Reservoir Continuity

Reservoir continuity varies within the progradational mud-rich strandplain sandstones. A resistivity cross section across the West Cornelius reservoir shows that hydrocarbon distribution is highly continuous in sand-rich facies but is interrupted by the intervening swales (fig. III-15). Two distinct hydrocarbon subreservoirs are present. The upper widespread subreservoir is largely contained in the Co-3 sandstone, whereas the lower, less continuous subreservoir has maximum resistivity values in the Co-2 sandstone. Resistivity values of the lower unit decrease with a drop in stratigraphic level from the Co-2 to the Co-1 sandstone.

Dip sections illustrate the relationship between the upper and lower hydrocarbon subreservoirs (fig. III-16). The upper zone of hydrocarbon saturation lies in strandplain sandstones (Co-3) that have prograded across more distal and slightly older strandplain deposits (Co-2). The updip part of the Co-2 sandstone appears to have been partly reworked into the younger cycle so that the older cycle pinches out against the base of the Co-3 sandstone. Resistivity trends follow this pattern, indicating two zones of hydrocarbon saturation. Completion data indicate that the sandstones are in pressure continuity as tubing pressures are fairly similar irrespective of level of completion. However, the average initial oil yield from wells completed in the upper sandstone (wells 24, 31, 43; 290 bbl/day) was 25 percent higher than those completed in the lower sandstone (wells 19, 26, 27, 28, 29; 219 bbl/day).

The facies element that segments the hydrocarbon distribution in the Co-3 sandstone shows the upward-fining SP response characteristic of aggradational interridge swales (fig. III-15). The well completed in the swale deposits displayed the poorest production attributes of all the Cornelius completions. Initial oil production was only 51 bbl/day; its tubing pressure was 190 psi, approximately 5 to 6 times less than adjacent wells, and GOR was significantly higher than that of the nearby wells. Initially there was little or no fluid or pressure communication between the ridge sandstones and swale deposits within this reservoir.

Integration of Production and Reservoir-Continuity Data Within the Geologic Framework

Water Influx Trends

The paths of water influx based on sequential water-cut maps are shown in figures III-17A through III-17D. Early water influx in the West Cornelius reservoir took place dominantly from the northeast. Minor incursion also took place in the southwest and from point sources in the

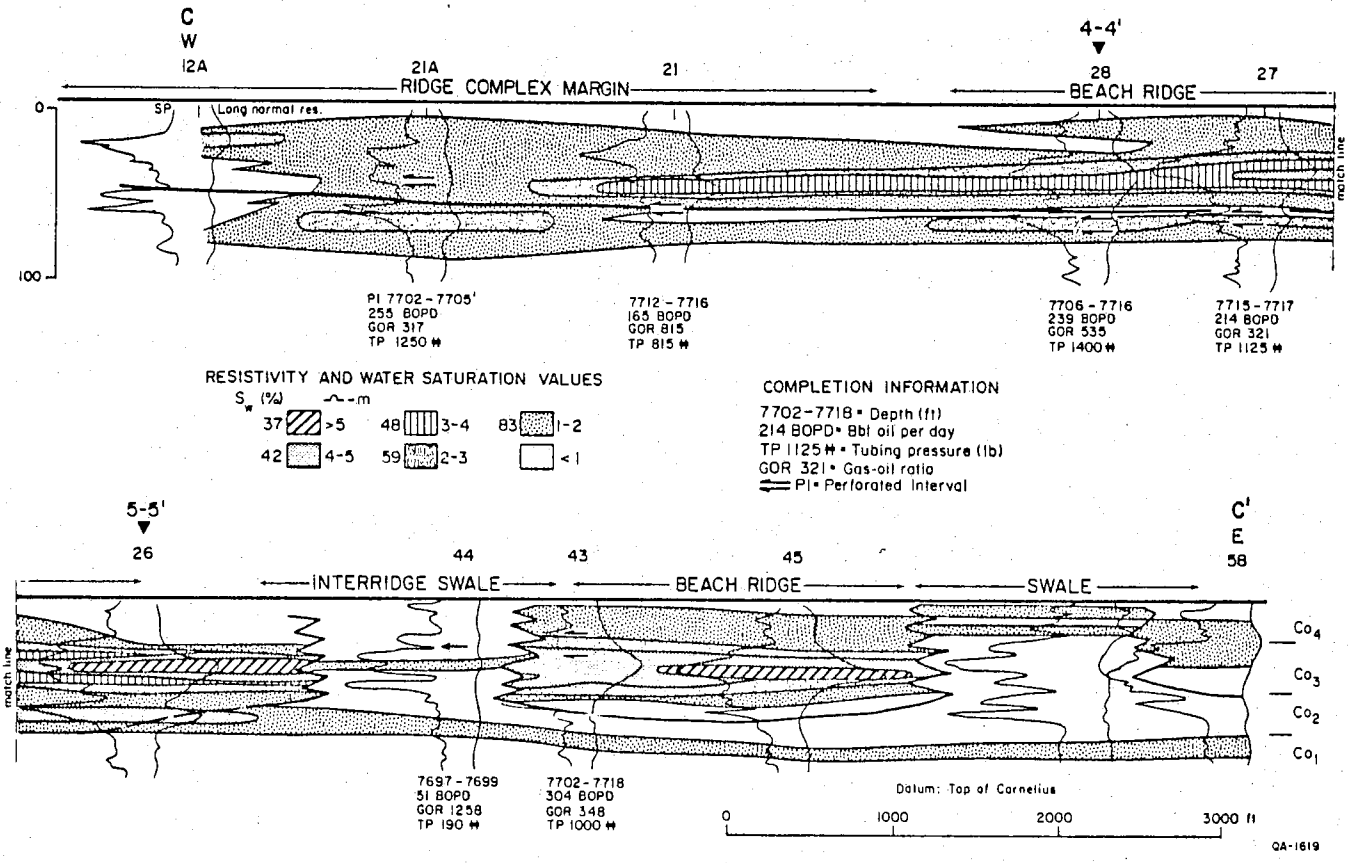

Figure III-15. Resistivity strike section, Cornelius sandstone, showing the continuous distribution of hydrocarbons in beach-ridge sandstones of the mud-rich strandplain. Intervening swales disrupt interridge communication. Line of section shown in figure III-14.

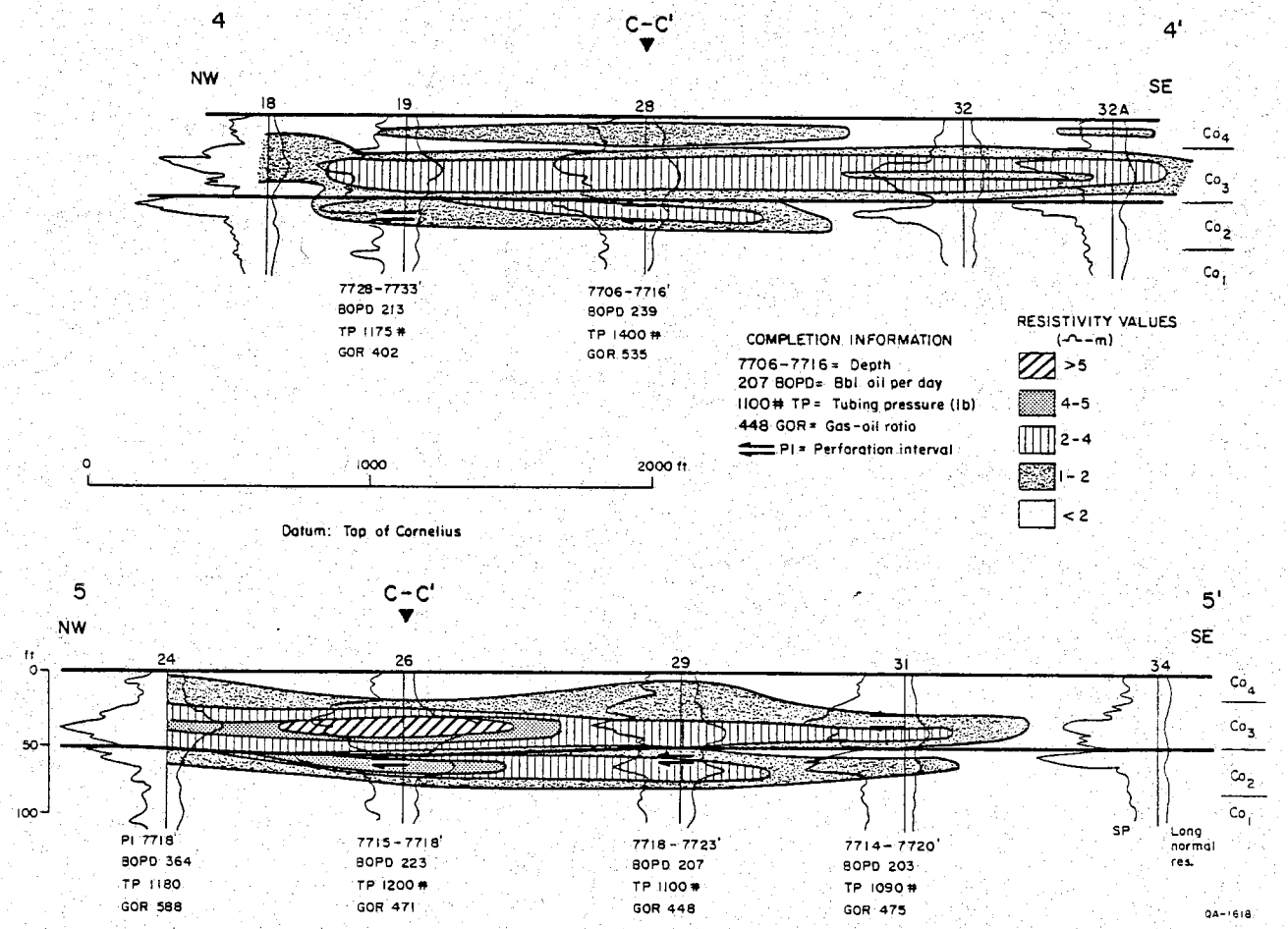

Figure III-16. Resistivity dip sections, Cornelius sandstone, showing the offlapping relationship of the Co-3 and Co-2 units. Hydrocarbons in the lower sandstone are trapped against the bounding surface. Line of section shown in figure III-14.

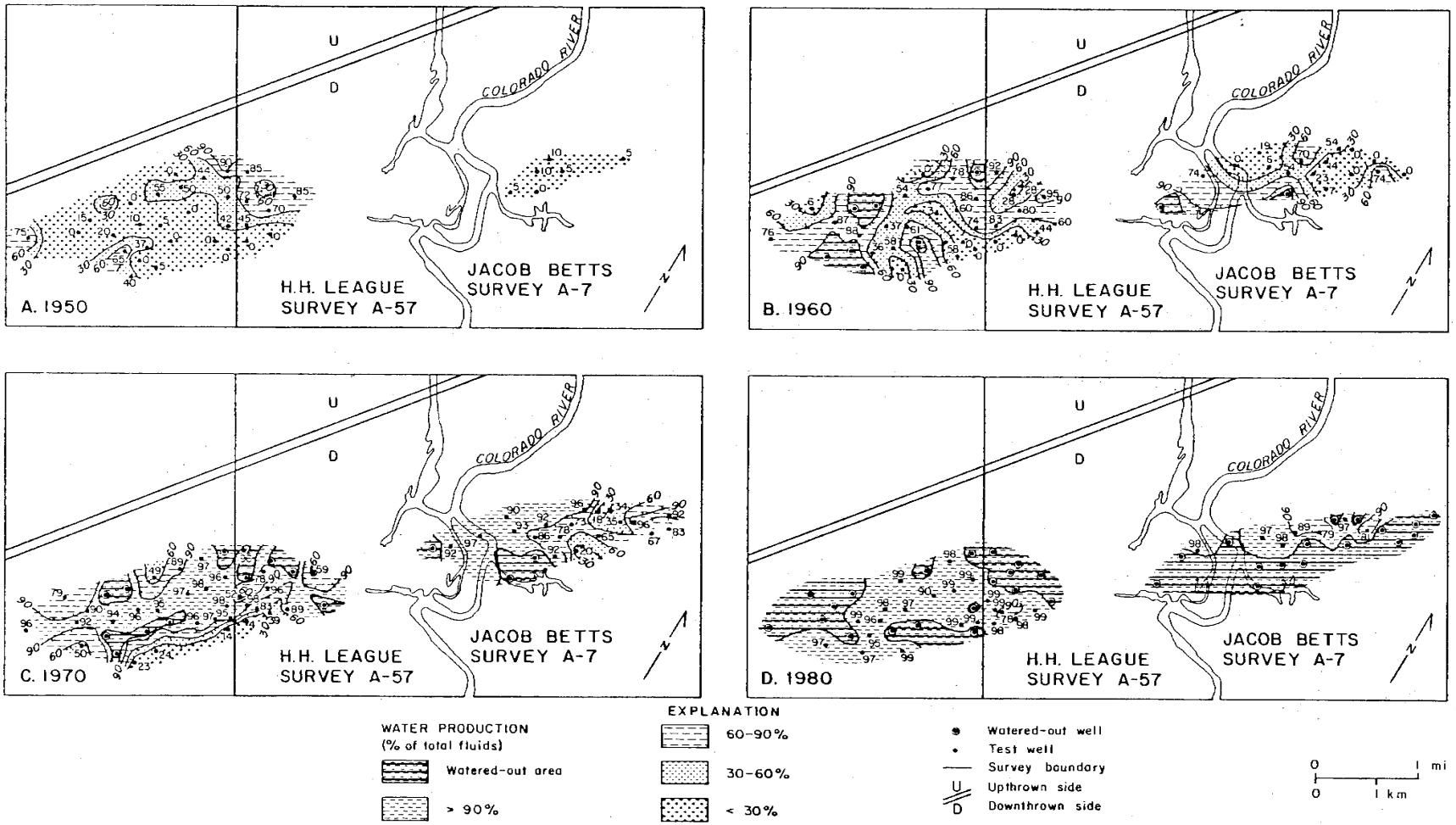

Figure III-17. Sequential water cut maps, Cornelius reservoir.

northwest and west (fig. III-17A). By 1970, almost the entire reservoir was producing over 90 percent water except for a few areas of low watercut on the northern and southern flanks of the reservoir. In 1980, much of the reservoir had watered out, and abandoned areas coincided closely to the areas of early high water cut (fig. III-17D).

In the East Cornelius reservoir, particularly in the later years of production (1970-1980) aggradational facies (swales) were areas of lower water cut, progradational facies (ridges) with a blocky SP response were characterized by higher water cuts. Early water influx in the reservoir was more closely related to sand-rich areas. During later production, water encroachment was more widespread, and irregularities in sandstone content had less effect. The serrate sandstones of lacustrine origin on the west margin of the reservoir exerted a moderate influence on water cut; these remained low producers of water throughout the first 30 years of production.

Reservoir Productivity

The principal control on well-to-well variability in the Cornelius is the ridge and swale topography of the beach-ridge complex (figs. III-18A and III-18B). Ridges remained areas of high oil production throughout the life of the reservoir whereas the intervening swales were more rapidly depleted. The dip-oriented area of low to moderate production on the west side of West Cornelius (fig. III-18) corresponds to serrate sandstones of possible lacustrine origin. The eastern part of the field that coincides with the zone of upward-coarsening sandstones characterized by low GOR oil production was an area of consistently high yield.

CARLSON RESERVOIR: A TRANSGRESSED STRANDPLAIN DEPOSIT

The Carlson sandstone represents the penultimate phase of major sandstone deposition in the upper Frio (fig. III-2). It is overlain by lower shoreface and shelf mudstones, which are in turn overlain by the Greta barrier sandstone. Carlson SP curves typically suggest an early progradational phase followed by aggradation during coastal onlap.

Depositional Environment

Distribution of Sandstone

Sandstone distribution in the Carlson interval exhibits a well-defined strike-parallel orientation similar to that of the Cornelius sandstone. The area of maximum sand accumulation lies adjacent to (both updip and downdip of) the major growth fault in the field area. Sandstone content systematically decreases southeastward from the fault, with the exception of an elongate high-sand finger that is oriented subparallel to the principal axis of sandstone

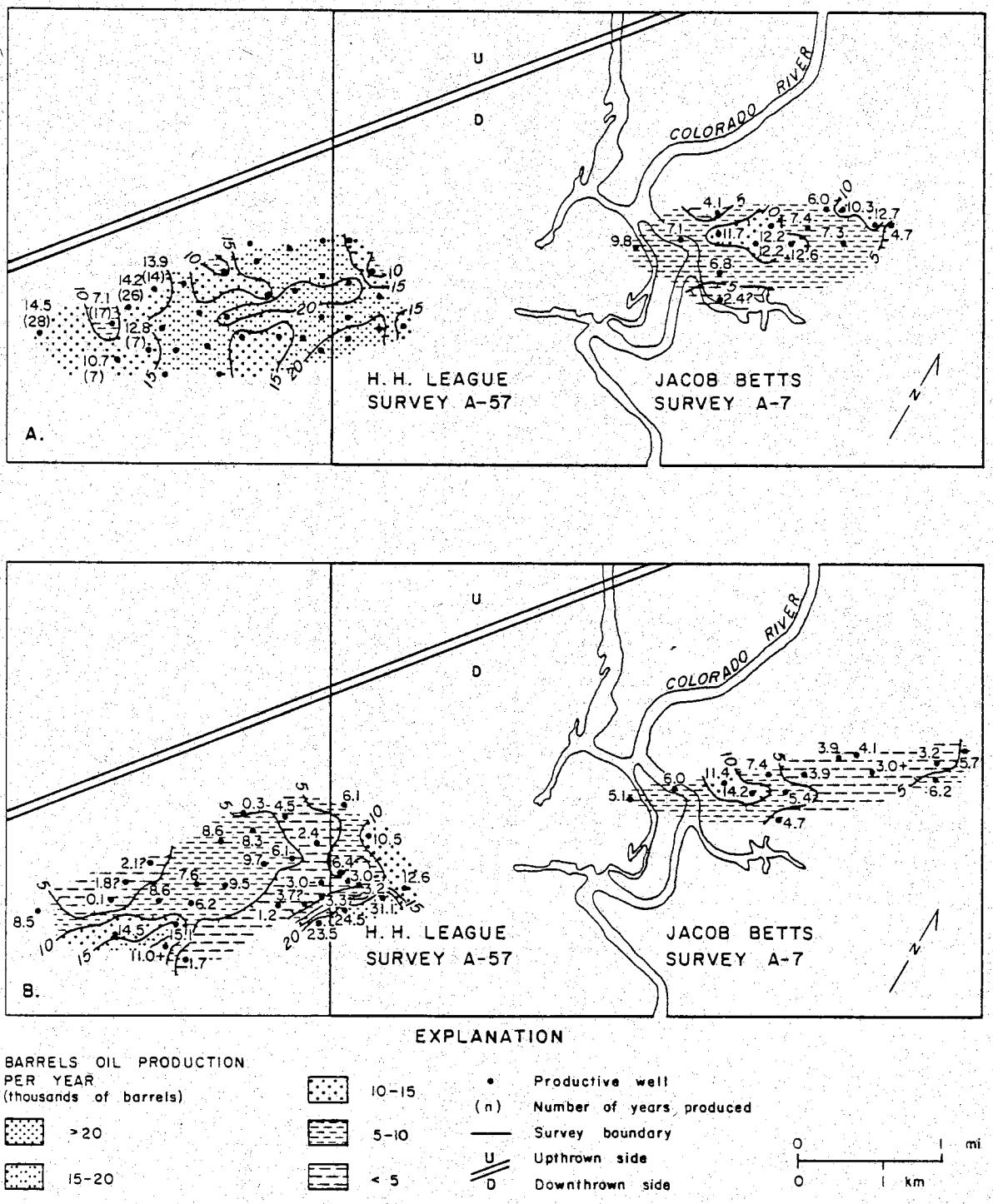

Figure III-18. Reservoir-productivity maps, Cornelius reservoir: (A) 1938 through 1965 and (B) 1966 through 1982. Production trends for the early period show both dip and strike orientations. The southeast part of West Cornelius remained an area of high yield throughout both time periods.

accumulation. As in the Cayce reservoir, sandstone contents decrease over the crest of the rollover anticline.

Areal Distribution of Component Facies

Vertical profiles in the Carlson sandstone based on analysis of SP logs generally show a lower thick, upward-coarsening sand overlain by a thinner, upward-fining sand (see fig. III-2, well 48). However, there are at least five variations on this mixed progradational-aggradational theme (fig. III-19). Simple aggradational facies are present but are only locally developed. Note that the log facies map was compiled using the entire Carlson genetic package.

The facies architecture of the Carlson sandstone is dominated by three principal components (fig. III-19). In the southern and southeastern parts of the field area, upward-coarsening progradational facies are prevalent. Much of the rest of the area is characterized by a basal serrate, upward-coarsening sandstone overlain by a "blocky" sandstone, which is overlain in turn by an upward-fining cycle (facies pattern PA-3, fig. III-19). At the interface between these two major facies components is a sandstone in which the basal progradational cycle is capped by a well-defined "blocky" sandstone (facies pattern PA-2, fig. III-19). This latter log facies has a well-defined strike-parallel geometry; sandstones adjacent to it along strike have simple or serrate upward-fining upper zones.

Other log facies of note are the narrow, dip-oriented aggradational facies and the localized progradational facies over the crest of the rollover anticline.

Interpretation

The Carlson is a composite sandstone deposited within a prograding strandplain system and subsequently reworked during transgression. The lower progradational phase has a simple and widespread distribution of upward-coarsening sands, in contrast to the more complex facies architecture of the overlying transgressive deposits. Upward-fining patterns reflect deposition under conditions of decreasing energy and increasing water depths. Interbedded strike-parallel sandstones with blocky SP responses are thought to be of wave-dominated deltaic origin. Fluvial feeder systems may include the aggradational system updip of the deltaic sandstones and a second channel system characterized by dip-oriented "blocky" sandstones to the southwest (fig. III-19). Note that the former of these two feeder systems consisted of aggradational sandstones even during the progradation of the older strandplain deposits. This suggests that the fluvial system was fairly stable.

Reservoir Continuity

Although the facies architecture of the upper part of the Carlson sand is complex, the distribution of hydrocarbons within the sandstones is laterally continuous both in strike and dip

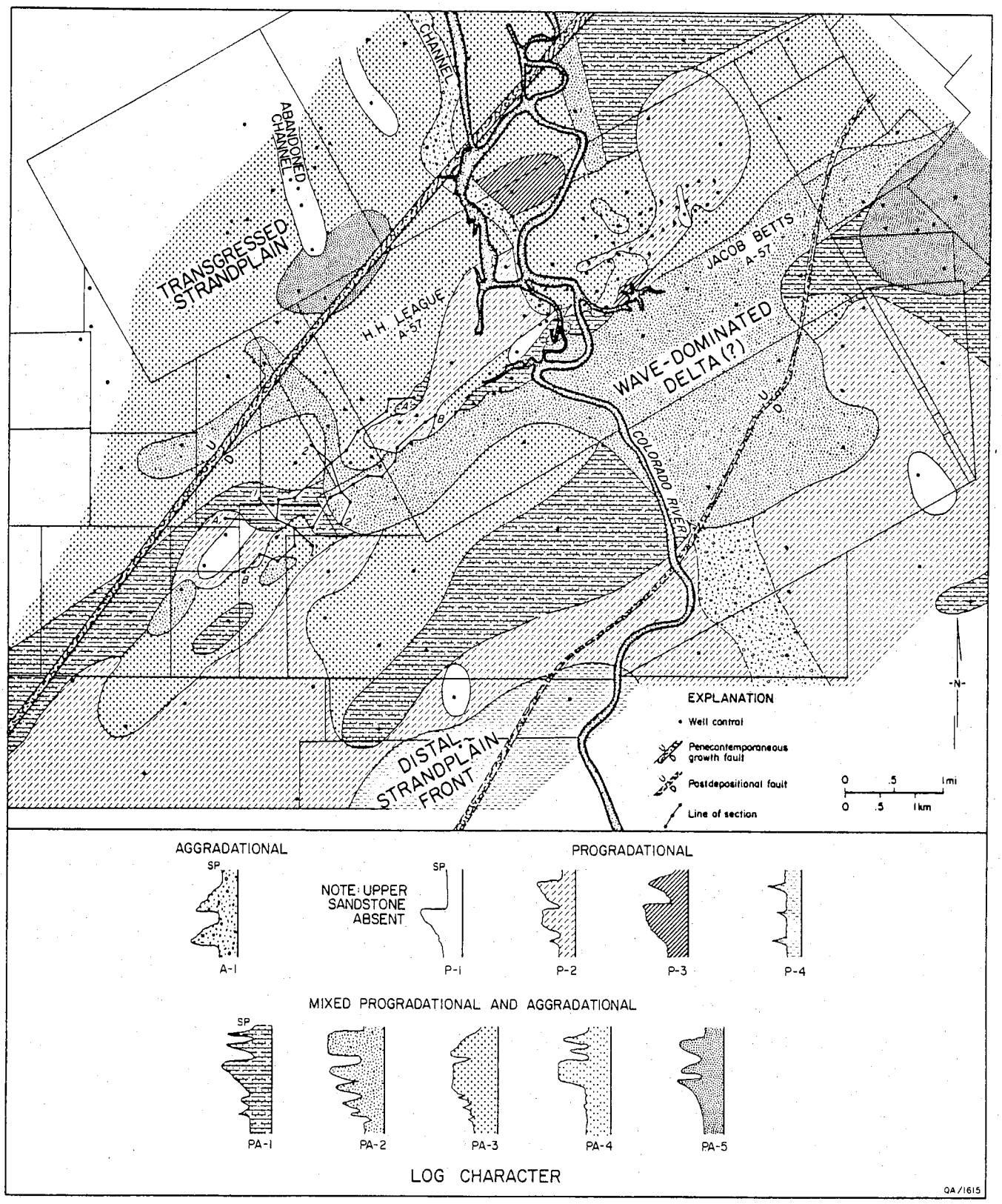

Figure III-19. Log facies map of the Carlson sandstone illustrating the complex facies architecture of this transgressed strandplain deposit. Log facies patterns most commonly exhibit upward-coarsening (progradational) overlain by upward-fining (aggradational) trends. Purely progradational patterns downdip reflect shoreface or delta-front sedimentation, or both.

directions. The distribution of hydrocarbons is uninterrupted by facies changes, but the thickness and vertical continuity of the hydrocarbon-bearing zone is influenced by facies. The thickest and most vertically homogeneous hydrocarbon distributions occur in "blocky" or simple upward-fining sandstones; hydrocarbon distribution in wells characterized by serrate upward-fining patterns is thinner and heterogeneous. The overall pattern is one of uniform lateral continuity and variable vertical continuity within the transgressed strandplain sandstones.

Integration of Production and Reservoir-Continuity Data Within the Geologic Framework

Water Influx and Reservoir Productivity Trends

Water influx into the Carlson reservoir is largely by edge-water encroachment rather than by channelized flow. Early water incursion took place in two broad zones that gradually expanded toward the crest of the reservoir. Watered-out and abandoned areas closely correspond with the early areas of water encroachment. Broad areas of similar production histories further indicate that the facies anatomy of the Carlson sandstones exerted little influence on production trends. The widespread patterns of water influx and uniform production trends confirm the conclusion that the reworked strandplain sandstones have uniform lateral continuity and that facies changes in this setting do not impart strong lateral heterogeneity to the sandstone body.

CONCLUSIONS

Reservoir-Continuity Models

Reservoir-continuity models for sand deposits resulting from two major coastal processes (progradation and coastal onlap) have been constructed, based on the beach-ridge/strandplain reservoirs of the North Markham - North Bay City field (figs. III-20 and III-21). The surface features shown on the models are adapted from modern studies (see Morton and McGowen, 1980, and Hayes and Kana, 1977, for reviews of morphologies and processes of modern coastal systems). Shorezone sandstones deposited by a prograding strandplain system are further subdivided into a simple strandplain model (fig. III-20A) based on the character of parts of the Cayce reservoir and a strandplain crosscut by a delta distributary/wave-dominated delta system (fig. III-20B) modeled on the Cayce reservoir. The reservoir-continuity model of composite progradational/transgressed strandplain sandstones (fig. III-21) uses the continuity relations of the Carlson reservoir.

Lateral reservoir continuity is greatest in simple and sand-rich progradational strandplain and transgressed strandplain systems. Reservoir compartmentalization increases with the

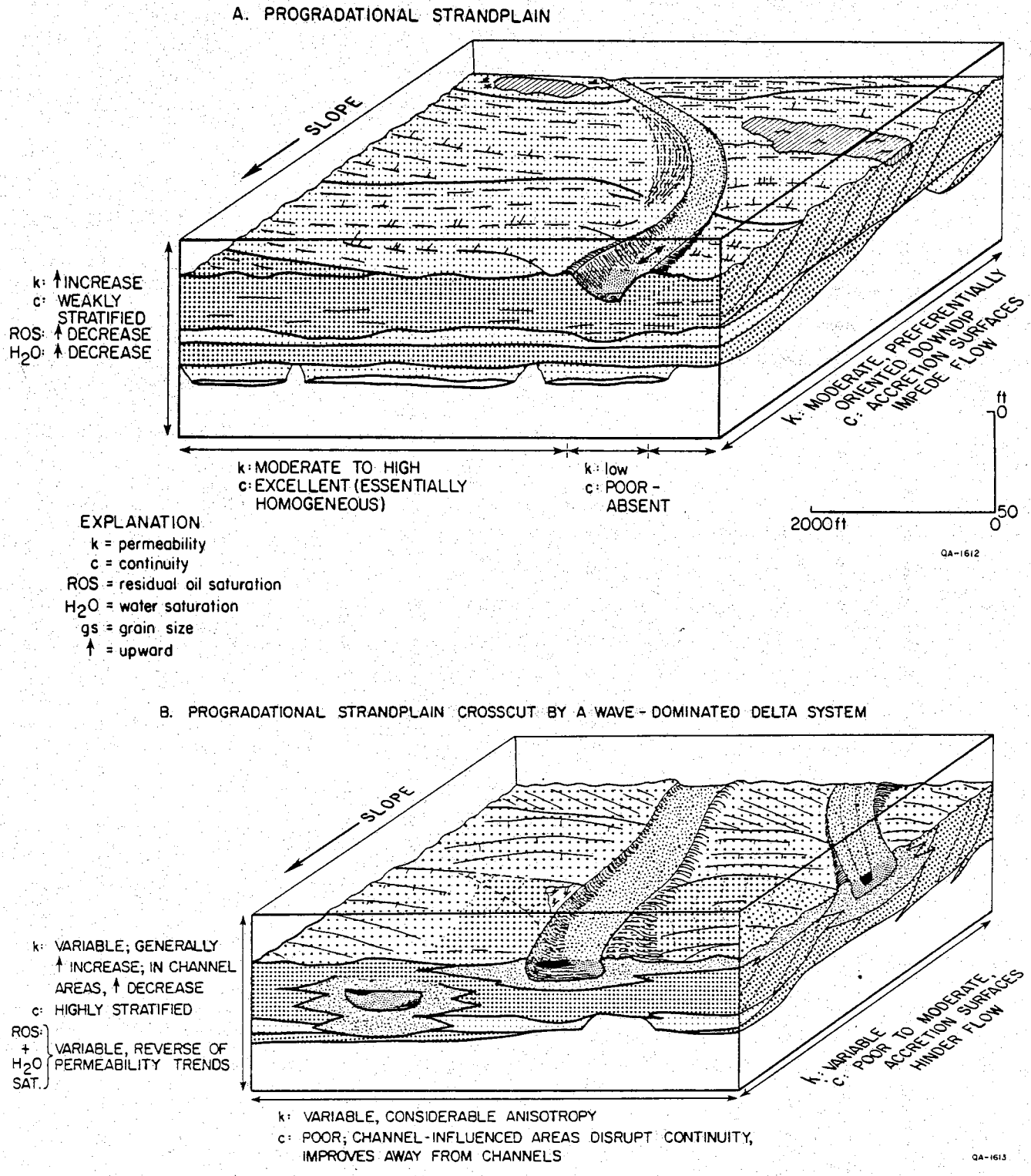

Figure III-20. Reservoir continuity models of simple progradational strandplain sandstones (A) cut by a minor tidal channel and (B) transected by a fluvial-deltaic system. Reservoir continuity decreases with increasing complexity of the crosscutting systems such that macroscopic heterogeneity is at a maximum at the interface between the fluvial, deltaic, and strandplain systems. Reservoir quality improves with height in strandplain and deltaic sandstones, but basal fluvial sandstones are the most porous and permeable.

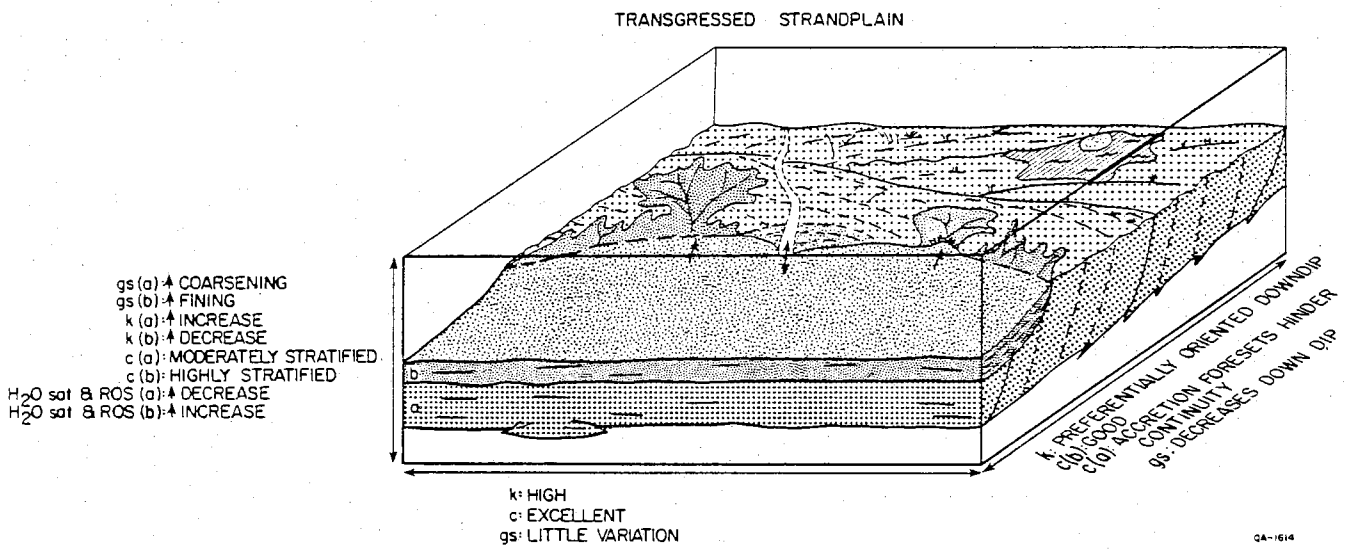

Figure III-21. Reservoir continuity model of transgressed strandplain sandstones. Although the facies architecture of the sandstones is complex, the physical and textural characteristics of juxtaposed facies are similar, allowing continuous hydrocarbon distributions and broad fronts of water incursion (similar to simple progradational strandplain deposits).

presence of crosscutting units. The greater the complexity of the transecting system the higher the degree of compartmentalization. Thus sandstones of mixed progradational strandplain/delta distributary heritage display the most compartmentalization within sand-rich strandplain systems (fig. III-20B).

On the basis of log facies mapping, the Carlson reservoir would be predicted to display a lower continuity than is mapped using resistivity cross sections. Broad patterns of edge-water influx and uniformly low initial GORs further confirm that the reservoir behaves homogeneously. Studies of modern transgressive shorezones along the Texas coast have shown that barriers are reworked during transgression via shoreline erosion and storm washover (Morton and McGowen, 1980). These processes result in stratified sheet-like sands of good lateral continuity. Thus, although progradational facies of limited extent are present in the lower half of the unit, the sheet-like transgressive part of the sequence is responsible for the continuity of the sands and the persistence of the hydrocarbon-saturated zones.

Muddy strandplain systems intermediate between sand-rich beach plains of the Nayarit type and the mud-rich chenier plains of the west Louisiana coastline exhibit good continuity along strike but poor continuity perpendicular to the depositional axes of the system. The beach ridge and swale topography clearly restricts fluid migration to well-defined trends parallel to the long dimensions of the sand ridges.

Implications for Geopressured Geothermal Energy Production

The implications of the study are twofold. First, progradational and transgressed sand-rich strandplain systems exhibit a tabular geometry. The great lateral continuity of simple strandplain deposits has been described elsewhere (Curray and others, 1969; Winker, 1979). Individual and composite strandplain deposits of the Frio Formation are continuous in a downdip direction (fig. III-2). Thus, megascopic heterogeneities are not a limiting factor for the production of geopressured geothermal energy. Structural boundaries, rather than depositional limits, impose the primary constraints on the extent of potential strandplain geothermal aquifers. The lateral continuity of these sandstones is analogous to the distributary-mouth-bar deposits (Andrau sandstone) currently being tested in the Pleasant Bayou test well.

Secondly, the internal complexity of component facies (macroscopic heterogeneity) does not appear to influence the production histories of simple progradational and transgressed sand-rich strandplain deposits. Fluids migrate through the sandstones along broad fronts, indicating that the deposits behave isotropically with respect to fluid flow and that log facies boundaries do not act as barriers to through-flow. Furthermore, the nature of water influx suggests that radial drainage would characterize geothermal completions in simple strandplain sandstones.

In contrast, evidence from production histories of internally complex, composite fluvial/deltaic/strandplain sandstones and muddy strandplain systems clearly indicate the anisotropic behavior of these aquifer systems. Crosscutting fluvial channels act as foci for early water influx into oil and gas reservoirs. They also influence the distribution of hydrocarbons by acting as intra-reservoir traps preventing hydrocarbon migration in the adjacent strandplain deposits. Boundaries between facies may be characterized by lithologic changes (channel sandstone/floodplain mudstone) where mudstone acts as an aquitard, or by sand-on-sand contacts (channel-sandstone/beach-ridge deposits). The flow-resistant behavior of these facies boundaries is a consequence of contrasting physical and textural parameters on either side of the boundary. Divergent grain-size distributions, pore-space distributions, internal stratification, frequency and position of shale breaks, and possibly permeability distributions and directional permeability all hinder communication between facies and contribute to different production characteristics. In addition to physical and textural differences, thin mud coatings such as those that occur on lateral accretion surfaces may impede flow across facies boundaries. Detailed subsurface analysis of the Rio Grande delta clearly shows channel sands separated from adjacent sand facies (channel and floodplain) by a thin mud sheath (Fulton, 1975, fig. 17) that would act as a barrier to fluid flow between facies. While reasons for the flow resistance of facies boundaries have not been clarified in the literature, an increasing number of papers are being devoted to describing anomalous drainage patterns in composite sandstone bodies.

Summary

The tabular geometry and macroscopic homogeneity of simple progradational and transgressed sand-rich strandplain deposits enhance the favorability of these sandstones as prospective geopressured geothermal exploration targets if all other constraints are satisfied. Composite fluvial/deltaic/strandplain sandstones and mud-rich strandplains, which may be intimately associated with prograding strandplain systems, exhibit anisotropic fluid flow and in all probability would yield restricted drainage patterns. Completions in these complex sandstones require careful well siting to achieve adequate drainage. For geothermal energy production from strandplain deposits, perforations should be located at the crest of upward-coarsening and upward-maturing sandstone cycles.

ACKNOWLEDGMENTS

Funding for this work was provided by the U.S. Department of Energy, Division of Geothermal Energy, under Contract No. DE-AC08-79ET27111. Partial support was also

obtained from the Texas Energy and Natural Resources Advisory Council, Energy Development Fund, Project No. 82-O-U-1. Marathon Oil Company, Shreveport, Louisiana, supplied production data from the North Markham - North Bay City field. Dr. R. A. Morton reviewed the manuscript. Word processing was by Jana McFarland under the supervision of Lucille C. Harrell. The figures were drafted by John T. Ames, Mark T. Bentley, Margaret R. Day, Jeff Horowitz, Jamie McClelland, and Kerza A. Prewitt under the supervision of R. L. Dillon.

REFERENCES

Alpay, O. A., 1972, A practical approach to defining reservoir heterogeneity: Journal of Petroleum Technology, v. 24, p. 841-848.

Asquith, G., and Gibson, C., 1982, Basic well log analysis for geologists: American Association of Petroleum Geologists, Methods in Exploration Series, 216 p.

Beall, A. O., 1968, Sedimentary processes operative along the western Louisiana shoreline: Journal of Sedimentary Petrology, v. 38, no. 3, p. 869-877.

Boyd, D. R., and Dyer, B. F., 1964, Frio barrier-bar system of South Texas: Gulf Coast Association of Geological Societies Transactions, v. 14, p. 309-322.

Curray, J. R., Emmel, F. J., and Crampton, P. J. S., 1969, Holocene history of a strandplain, lagoonal coast, Nayarit, Mexico, in Castañares, A. A., and Phleger, F. B., eds., Coastal Lagoons, a Symposium: Universidad Nacional Autónoma de México, p. 63-100.

Fulton, K. J., 1965, Subsurface stratigraphy, depositional environments, and aspects of reservoir continuity--Rio Grande delta, Texas: University of Cincinnati, Ph.D. dissertation, 330 p.

Galloway, W. E., Ewing, T. E., Garrett, C. M., Tyler, N., and Bebout, D. G., 1983, Atlas of major Texas oil reservoirs: The University of Texas at Austin, Bureau of Economic Geology Special Publication, 139 p.

Galloway, W. E., Hobday, D. K., and Magara, Kinji, 1982, Frio Formation of the Texas Gulf Coast Basin--depositional systems, structural framework, and hydrocarbon origin, migration, distribution, and exploration potential: The University of Texas at Austin, Bureau of Economic Geology Report of Investigations No. 122, 78 p.

Hartman, J. A., and Paynter, D. D., 1979, Drainage anomalies in Gulf Coast Tertiary sandstones: Journal of Petroleum Technology, v. 31, p. 1313-1322.

Hayes, M. O., and Kana, T. W., 1977, Terrigenous clastic depositional environments, some modern examples: American Association of Petroleum Geologists field course, Coastal Research Division, University of South Carolina, 315 p.

McCubbin, D. G., 1982, Barrier-island and strand-plain facies, in Scholle, P. A., and Spearing, D., eds., Sandstone depositional environments: American Association of Petroleum Geologists Memoir 31, 410 p.

Morton, R. A., Ewing, T. E., and Tyler, Noel, 1983, Continuity and internal properties of Gulf Coast sandstones and their implications for geopressured fluid production: The University of Texas at Austin, Bureau of Economic Geology Report of Investigations No. 132, 70 p.

Morton, R. A., and McGowen, J. H., 1980, Modern depositional environments of the Texas coast: The University of Texas at Austin, Bureau of Economic Geology Guidebook 20, 167 p.

Polasek, T. L., and Hutchinson, C. A., Jr., 1967, Characterization of non-uniformities within a sandstone reservoir from a fluid mechanics standpoint: Proceedings, Seventh World Petroleum Congress, v. 2, p. 397-407.

Pryor, W. A., 1973, Permeability-porosity patterns and variations in some Holocene sand bodies: American Association of Petroleum Geologists Bulletin, v. 57, p. 162-189.

Railroad Commission of Texas, 1983, Annual report of the oil and gas division for 1982: Austin, 733 p.

Tyler, Noel, and Han, J. H., 1982, Elements of high constructive deltaic sedimentation, lower Frio Formation, Brazoria County, Texas: Gulf Coast Association of Geological Societies Transactions, v. 32, p. 527-540.

Winker, C. D., 1979, Late Pleistocene fluvial-deltaic deposition, Texas coastal plain and shelf: The University of Texas at Austin, Master's thesis, 187 p.

APPENDIX III-I

List of well logs from North Markham - North Bay City field used in this study.

Number	Operator and Lease
1	Texas Gulf Sulphur & Goodell #1 W. D. Cornelius
2	Bay City Drilling Co. #1 Northern Ranch
3	Ohio Oil Co. #B-1 Cornelius
4	Petro Corp. of Delaware #1 Cornelius
5	W. Earl Rowe #1 C. D. Cornelius
6	E. Cockrell, Jr. #1 D. S. Prinzing
7	R. O. Mangun and P. H. Welder #1 W. D. Cornelius
7A	Rowan Drilling and Texas Gulf #1 Clara Mason
8	Draper, Goodale & Co. #5 J. L. Camp
9	Draper, Goodale & Co. #5 (5H) J. L. Camp
10	Group Oil Co. #1 J. C. Carlson
11	Ohio Oil Co. #1 Carlson
12	Ohio Oil Co. #8 Carlson
12A	Ohio Oil Co. #3 Carlson
13	Ohio Oil Co. #3 W. L. Cornelius
13A	Ohio Oil Co. #5 J. C. Carlson
14	Ohio Oil Co. #4 Cornelius
14A	Ohio Oil Co. #7 Carlson
15	Ohio Oil Co. #5 Cornelius
15A	Sun Oil Co. #2 Braman
16	Ohio Oil Co. #6 Cornelius
16A	Sun Oil Co. #1 Braman
17	Bright & Schiff #1 J. L. Camp et al.
17A	C. J. Barber et al. #1-A J. L. Camp
19	Ohio Oil Co. #16 J. C. Carlson
20	Ohio Oil Co. #12 Carlson
21	Ohio Oil Co. #6 Carlson
21A	Ohio Oil Co. #4 Carlson
22	Ohio Oil Co. #25 Carlson
23	Draper, Goodale & Co. #B-1 J. L. Camp
24	Ohio Oil Co. #19 Carlson
25	Ohio Oil Co. #20 Carlson
26	Ohio Oil Co. #18 Carlson
27	Ohio Oil Co. #15 Carlson
27A	Ohio Oil Co. #A-29 Ohio-Sun Unit
28	Ohio Oil Co. #13 Carlson
29	Ohio Oil Co. #21 Carlson
29A	Ohio Oil Co. #24-A Ohio-Sun Unit
30	Ohio Oil Co. #1 Pietz
30A	Ohio Oil Co. #14 Carlson
31	Ohio Oil Co. #2 Pietz
32	Ohio Oil Co. #27 Carlson
32A	Ohio Oil Co. #23 Carlson
33	Ohio Oil Co. #9 Carlson
33A	Ohio Oil Co. #25-A Ohio-Sun Unit

Number	Operator and Lease
34	Ohio Oil Co. #3 Pietz
34A	Monsanto & Clark #1 Miller
35	Coastal States #1 Holman
35A	Sun Oil Co. #3 Braman
36	Cosden Petroleum #1 W. D. Cornelius, Jr.
37	Sun Oil Co. #D-1 Braman
38	Cosden Petroleum #1 W. D. Cornelius Unit #2
38A	Cosden Petroleum #1 Farthing-Thompson
38B	Monsanto #1 Cornelius Cattle Co.
39	E. Cockrell, Jr. #1 Olcese
39A	Draper, Goodale & Co. #3 J. L. Camp
40	Sun Oil Co. #1 Olcese
41	Brewster & Bortie #1 Olcese
42	Sun Oil Co. #5 Braman
43	Sun Oil Co. #7 Braman
44	Sun Oil Co. #16 Braman
45	Sun Oil Co. #11 Braman
46	Sun Oil Co. #12 Braman
47	Ohio Oil Co. #21 Braman
47A	Ohio Oil Co. #23-J Ohio-Sun Unit
48	Sun Oil Co. #20 Braman
49	Sun Oil Co. #13 Braman
50	Sun Oil Co. #14 Braman
51	Sun Oil Co. #8 Braman
51A	Sun Oil Co. #22-J Ohio-Sun Unit
52	Sun Oil Co. #19 Braman
53	Sun Oil Co. #9 Braman
55	Bradco Oil & Gas #1 Elizabeth Burkhart
56	Sun Oil Co. #18 Braman
56A	Marathon Oil Co. #26-J Ohio-Sun Unit
57	Sun Oil Co. #17 Braman
58	Sun Oil Co. #B-6 Braman
59	Sun Oil Co. #B-4 Braman
60	Sun Oil Co. #B-3 Braman
61	Sun Oil Co. #B-5 Braman
61A	Marathon Oil Co. #9-K Ohio-Sun Unit
62	Sun Oil Co. #B-1 Braman
63	Davis Oil & Gas #1 Pierce Runnels
64	Perry R. Bass et al. #2 Armour-Duncan Ranch
65	M.P.S. Production Co. - Van Dyke et al. #1 G. Krueger
66	R. E. Hibbert #1 C. T. Dye
67	Marathon Oil Co. #15 McDonald Acct. #1
68	Ohio Oil Co. #6 E. L. McDonald Acct. #1
68A	Ohio Oil Co. #1 E. L. McDonald Acct. #3
69	Sun Oil Co. #1 Ross
70	Ohio Oil Co. #4 McDonald Acct. #1
71	Ohio Oil Co. #3 McDonald Acct. #1
72	Ohio Oil Co. #5 McDonald Acct. #1
72A	Ohio Oil Co. #13 McDonald Acct. #1
73	Ohio Oil Co. #11 McDonald Acct. #1

Number	Operator and Lease
74	Ohio Oil Co. #7 McDonald Acct. #1
75	Ohio Oil Co. #9 McDonald Acct. #1
76	Ohio Oil Co. #8 McDonald Acct. #1
77	Sun Oil Co. #4L McDonald
77A	Sun Oil Co. #1L McDonald
78	Ohio Oil Co. #12 McDonald Acct. #1
78A	Ohio Oil Co. #2 McDonald Acct. #1
79	Ohio Oil Co. #1 McDonald Acct. #2
80	Ohio Oil Co. #11 McDonald Acct. #2
81	Ohio Oil Co. #3 McDonald Acct. #2
82	Ohio Oil Co. #4 McDonald Acct. #2
83	Ohio Oil Co. #13 McDonald Acct. #2
84	Ohio Oil Co. #6 McDonald Acct. #2
85	Ohio Oil Co. #12 McDonald Acct. #2
85A	Ohio Oil Co. #14L McDonald
85B	Ohio Oil Co. #15 McDonald Acct. #2
86	Ohio Oil Co. #5 McDonald Acct. #2
87	Ohio Oil Co. #14 McDonald Acct. #2
88	Ohio Oil Co. #7 McDonald Acct. #2
89	Marathon Oil Co. #5-L Ohio-Sun Unit
89A	Sun Oil Co. #3L McDonald
89B	Marathon Oil Co. #2K Ohio-Sun Unit
90	Ohio Oil Co. #2 McDonald Acct. #2
90A	Sun Oil Co. #2L McDonald
91	Ohio Oil Co. #10 McDonald Acct. #2
91A	Ohio Oil Co. #8 McDonald Acct. #2
92	Ohio Oil Co. #16 McDonald Acct. #2
93	G. Mitchell & Assoc. #1 E. H. Taylor
94	Cyprus Oil #1 Ella Hawkins Taylor
95	Cyprus Oil #1 Rugley
96	Sun Oil Co. #B-2 Braman
97	Sun Oil Co. #A-1 McDonald
97A	Marathon Oil #17 McDonald Acct. #2
98	Skelly Oil #1 Morris
99	Cyprus Oil #1 L. N. Miller
99A	Rutherford #1 Birkner
99B	Cyprus Oil #1 R. M. Cole
99C	Cyprus Oil #1 Curry-Green
101	Stanolind Oil #1 First National Bank
102	Fidelity Oil & Houston Natural Gas #1 Doman
103	Pan American Petroleum #1 Sherill Gas Unit
104	Stanolind Oil #1 Barth
105	Pan American Petroleum #1 Grover Moore
105A	J. S. Michael #1 Layton Moore
106	U. M. Harrison #1 R. P. Moore est.
106A	Shubuta Oil #1 Epstein et al
107	Cerro de Pasco #1 J. C. Lewis
107A	Cyprus Oil #1 F. L. Railsback
108	J. M. Huber #1 George Serrill
109	Tenneco Oil #2 H. E. Le Tulle

Number	Operator and Lease
110	SoRelle & SoRelle #1 Le Tulle
111	J. M. Huber and H. S. Cole #1 Sam Le Tulle
112	Colorado Oil & Gas #1 Sam Le Tulle
113	E. G. Catlett #1 Sam Le Tulle
114	Cardoil, Inc. #1 D. S. Prinzing
116	Wm. K. Davis & Texas Gas Exploration #1 S. V. Le Tulle
120	E. Cockrell, Jr. #1 Northern Ranch
120A	Oil & Gas Prop. #1 John Camp
121	E. Cockrell, Jr. #5 Northern Ranch
122	E. Cockrell, Jr. #4 Northern Ranch
122A	E. Cockrell, Jr. #8 Northern Ranch
123	E. Cockrell, Jr. #2 Northern Ranch
123A	Mangum & Chimm #1 Northern Ranch
124	Southern Natural Gas Co. #1 J. L. Camp
125	Stewart & Gouger #1 M. E. Crouch
125A	McCarrick, Gouger, & Mitchell #B-1 M. E. Crouch
125B	E. Cockrell, Jr. #7 Northern Ranch
125C	Hunt Oil #1 Crier-Braman
126	Sunray D-X #1 E. L. McDonald
126A	Michael T. Halbouty and Claud Hamill #1 M. Crouch
127	H. L. Hunt #1 D. H. Braman
127A	Michael T. Halbouty #3 M. Crouch
127B	E. Cockrell, Jr. #1 Crouch
128	Viking Drilling #2 John Camp
128A	Goodale, Bertman & Co. #1 Northern Ranch
128B	Goodale, Bertman & Co. #2 Northern Ranch
128C	British-American Oil #1 John Camp
129	E. Cockrell, Jr. #6 Northern Ranch
130	Skelly #8-30 Cobb
131	Skelly #6 Moore
132	Skelly #14-B F. G. Cobb
133	Skelly #1 Moore
134	Skelly #3 First National Bank
135	Skelly #5 Moore
135A	Skelly #4 Moore
136	J. P. Owen, H. Hurt, and Cyprus Oil #1 M. G. Langham
137	J. P. Owen and H. Hurt #1 Annie Silva
141	Frio Drilling #1 Runnels-Pierce
143	Canus Petroleum #1 Mrs. P. Krueger
144	T. M. Quigley #1 Runnels-Pierce

SECTION IV. INTEGRATED GEOLOGIC STUDY OF THE PLEASANT BAYOU - CHOCOLATE BAYOU AREA, BRAZORIA COUNTY, TEXAS-- FIRST REPORT

Thomas E. Ewing, Malcolm P. R. Light, and Noel Tyler, assisted by V. Lombeida

ABSTRACT

Drilling and logging of the Pleasant Bayou No. 1 and No. 2 test wells and the study of their samples, in conjunction with the study of data from the Chocolate Bayou oil and gas field, yield the most complete picture of a geopressured geothermal aquifer system yet obtained for the Texas Gulf Coast. The main geothermal reservoir, the "C" (Andrau) sandstone, owes its outstanding porosity and permeability to initially high porosity caused by deposition in a distributary-mouth-bar complex; to enhancement by secondary leaching by acidic waters migrating through the system; and to preservation from late carbonate cementation, perhaps because it is located in a thermally immature section. The anomalous maturity profile obtained for the test well can be modeled using either today's geothermal gradient, modified by cooling of the lower Frio section, or anomalously cool past geothermal gradients, modified by warm waters in the middle Frio section. Either model indicates a fairly late origin for secondary porosity. Examination of errors inherent in regional pressure, temperature, and salinity mapping places severe limitations on using these maps to detect fluid flow paths in the shallow geopressure zone.

INTRODUCTION

Studies conducted by the Bureau related to geopressured geothermal resources on the Texas Gulf Coast have generated a large amount of regional and local information on structural style, depositional systems, sandstone petrology and diagenesis, and fluid properties such as salinity, pressure, and temperature. In addition, the drilling of the Pleasant Bayou test well led to a wide variety of studies on shale mineralogy, organic geochemistry, vitrinite reflectance, and reservoir continuity and diagenesis.

The present project attempts to draw together all of the information available for the area of the Pleasant Bayou test well, to analyze its limitations, and to integrate it into a comprehensive geologic history. In particular, we wish to answer these questions:

--Can we determine the timing and causes of geopressure in the area?

--Why are certain reservoirs highly porous and permeable and others in a similar position impermeable?

--How has the maturation of organic matter in overpressured shales affected porosity and permeability of the reservoirs?

--Is information on the fluid properties of pressure, temperature, and salinity sufficiently accurate to construct meaningful maps of fluid flow regimes?

Setting of the Pleasant Bayou - Chocolate Bayou Area

The Oligocene Frio Formation forms one of the principal progradational clastic wedges of the Tertiary Gulf Coast Basin in Texas. This unit thickens basinward from several hundred feet of outcropping fluvial deposits of the Catahoula Formation to 15,000 ft of deltaic, barrier-strandplain, shelf, and slope deposits (Galloway and others, 1982b). Two deltaic depocenters (the Norias and Houston delta systems, fig. IV-1) are separated by the Greta/Carancahua barrier-strandplain system. The Pleasant Bayou geopressured geothermal test well lies in the Houston delta system in eastern Brazoria County (fig. IV-1). Thick geopressured sandstones occur in the lower Frio Formation below the T5 correlation marker (Bebout and others, 1978, 1980) in the Anomalina bilateralis zone.

The area of main interest lies between two large syndepositional normal faults that displace and isolate lower Frio strata. The eastern part of the Chocolate Bayou oil and gas field occurs atop a broad dome between these faults; the western part of the field is located in a small fault block immediately to the northwest. The Pleasant Bayou geothermal test well was drilled in a basin between the broad dome and the Danbury piercement salt dome to the west. In the area of interest, the lower and middle Frio sandstones (intervals T3 and below) are overpressured, having geostatic ratios (pore-fluid pressure/lithostatic pressure) of 0.7 or greater below T5 in the lower Frio sandstones.

STRATIGRAPHIC STUDIES

Lower Frio Sand Distribution Patterns of the Upper Texas Gulf Coast

The Anomalina bilateralis zone in Galveston and Brazoria Counties is characterized by comparatively high sandstone contents (Bebout and others, 1976). The area lies downdip of the main T5-T6 depocenter, a narrow (10-30 mi wide) belt containing more than 40 percent sandstone. Basinward of the depocenter, the sandstone content decreases to zero in a short distance, with the exception of scattered areas generally on the downdip side of growth faults. The Pleasant Bayou No. 2 well is testing a high sandstone area of this nature.

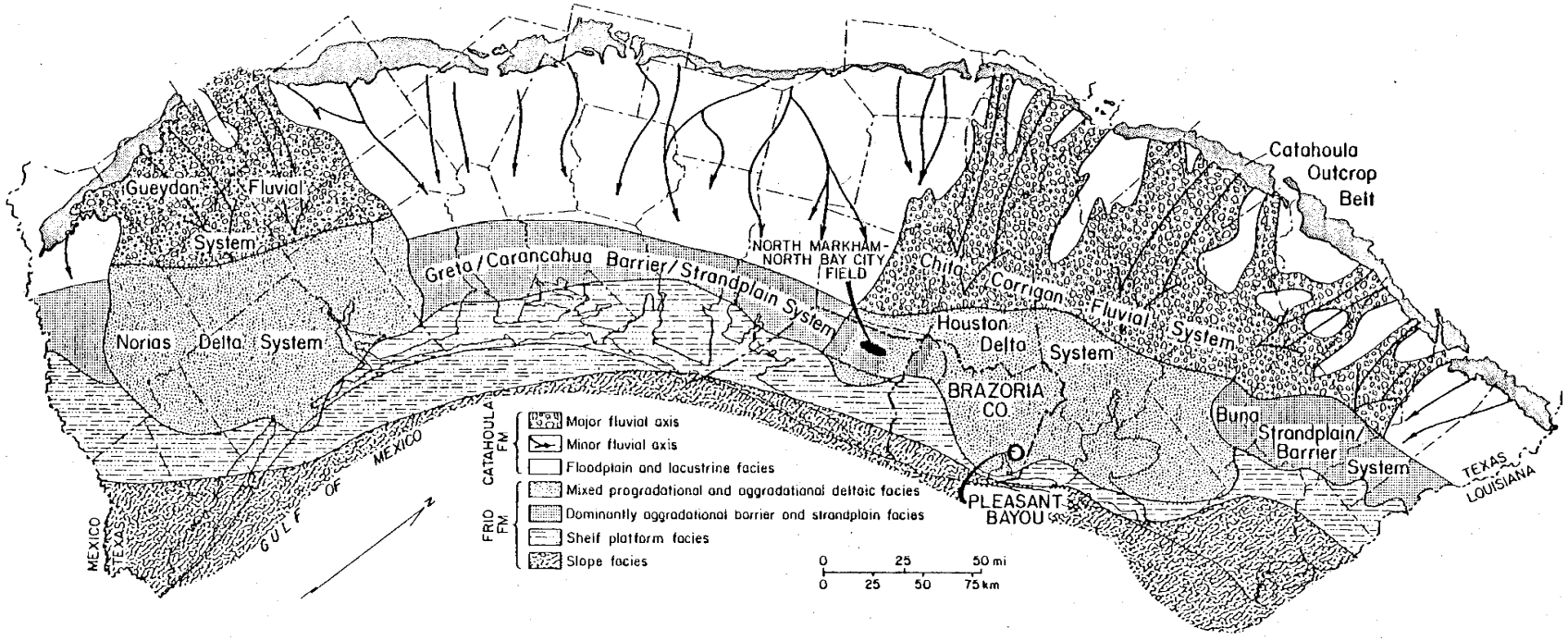

Figure IV-1. Simplified depositional architecture of the lower Frio Formation, modified from Galloway and others (1982b). Location of the Pleasant Bayou area is shown. North Markham - North Bay City field area is discussed in section III of this report.

Total sandstone thickness in the T5-T6 interval varies from more than 1,200 ft in the Danbury Dome area to less than 200 ft northeast of Chocolate Bayou field (Bebout and others, 1978). Seven major sandstone-shale depositional sequences (A-G) of variable electric log character occur in the interval. The geometry of the depositional sequences as indicated by net-sandstone mapping (fig. IV-2) was dominantly lobate with local dip-elongate elements. The main axis of sediment transport across the fault system was near Danbury Dome (fig. IV-2) throughout the deposition of the lower Frio; all of the sequences exhibit large amounts of sandstone in this area. Another axis over the Chocolate Bayou field is evident during deposition of the "C" interval.

In contrast to the sand-rich lower Frio, middle and upper Frio strata are shale-rich having less abundant thin sandstone beds. Thus the Frio in the western part of the Houston delta system reflects two major depositional episodes (Frazier, 1974; Bebout and others, 1978): an early progradational event from the base of the Frio Formation to the top of T5 and a transgressive event from the top of T5 to the top of the Frio.

Regional subsidence is considered to have been moderate during deposition of the lower Frio, allowing progradation of the high-constructive deltaic system. During the later stages of Frio sedimentation, subsidence exceeded sedimentation.

Facies Analysis and Depositional Systems

The well-defined lobate to elongate net-sandstone patterns supplemented by log character analysis led Bebout and others (1978) to conclude that the sand-shale sequences of the lower Frio were deposited by high-constructive lobate deltas. Their conclusions were later substantiated by interpretation of the Pleasant Bayou cores (Tyler and Han, 1982) and by micropaleontological analysis of cuttings and cores from the two wells (Boulden and Walk, 1979; C. C. Albers, personal communication, 1982). The architecture of the component facies of each deltaic sequence mimics the curvilinear to lobate sand distribution patterns (fig. IV-3). It may be possible to predict favored paths of fluid migration from log facies maps. For example, laterally continuous distributary-mouth-bar sandstones have a higher production potential than do interstratified sandstones and mudstones of the distal delta front, even though cumulative sandstone thicknesses may be equivalent.

A variety of subenvironments representing constructive and destructive phases of delta formation are recognized in the Pleasant Bayou No. 1 and No. 2 and in adjacent Phillips cores, as described by Tyler and Han (1982). These phases can be distinguished in cores by geometry, areal extent, and appearance.

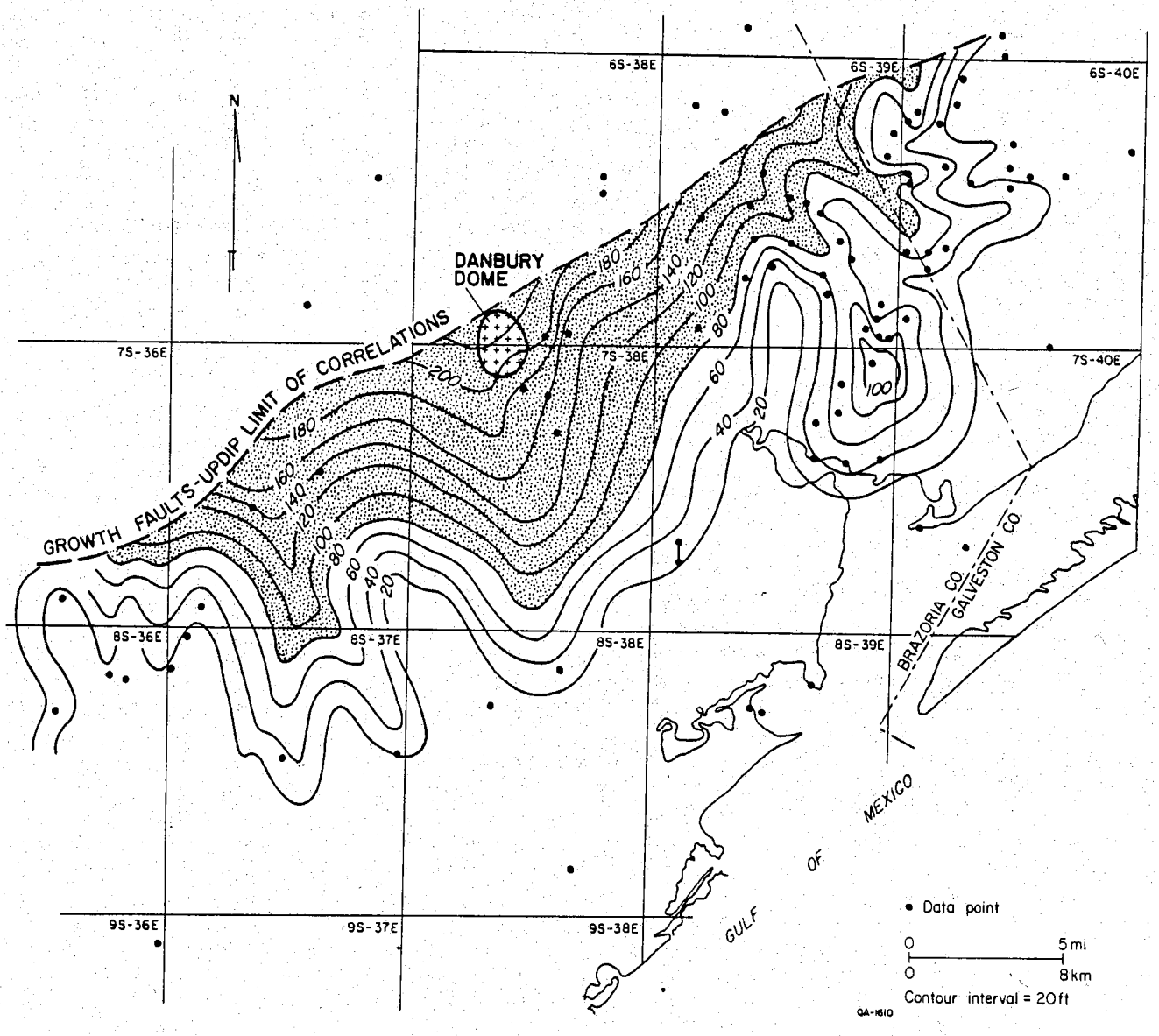

Figure IV-2. Net-sandstone map of the sub-T5 "C" (Andrau) correlation interval, modified from Bebout and others (1978).

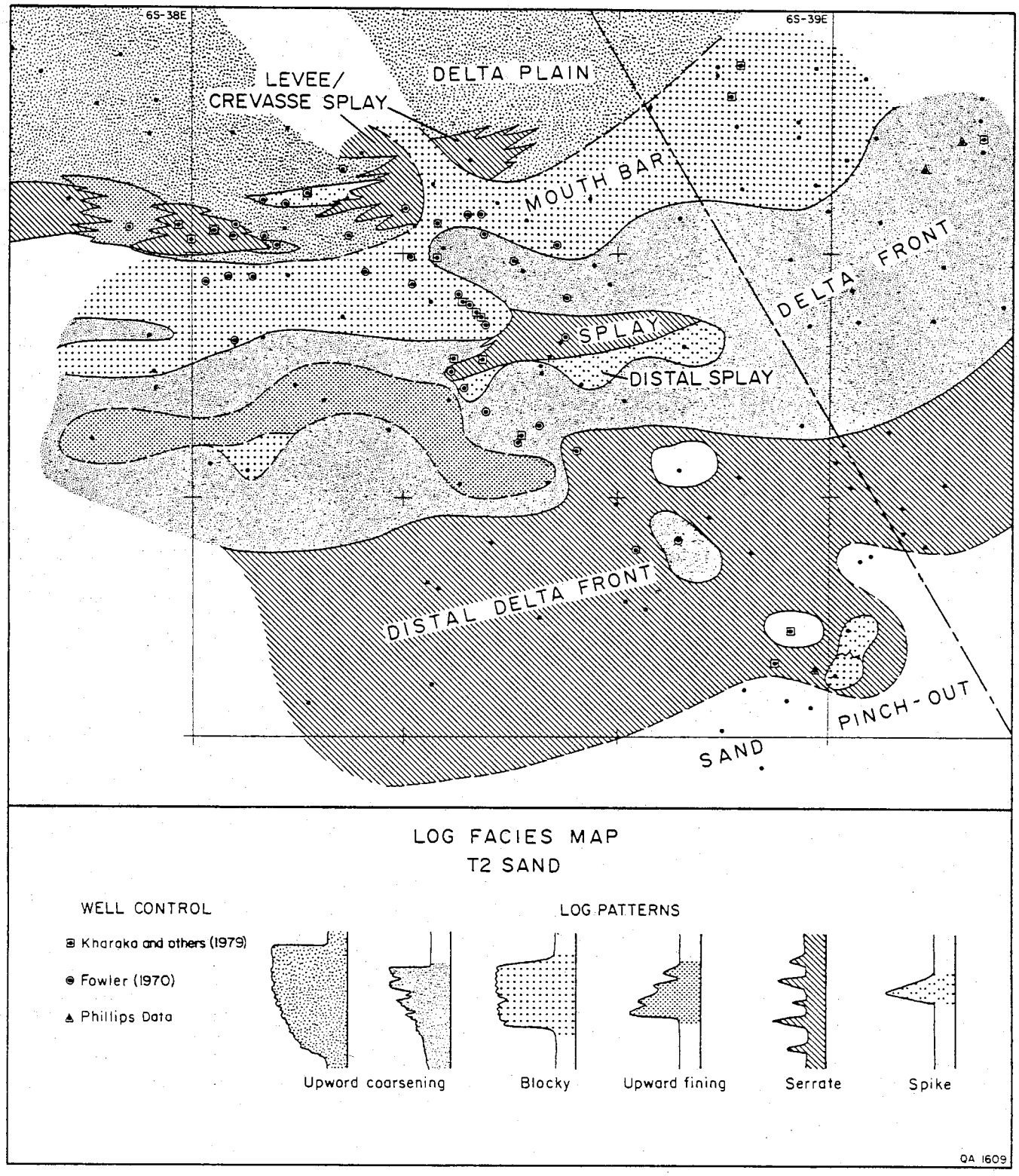

Figure IV-3. Facies anatomy of the T2 (Frio A) sandstone based on SP profiles. All major sandstone systems in the area exhibit a transition from thick, composite upward-coarsening sandstones updip to serrate sandstones downdip. The curvilinear strike parallel to the distribution of facies is characteristic of wave-modified, sand-rich constructive deltas.

Delta-front splays occur as thin, upward-fining cycles interbedded in prodelta mudstones and siltstones near the bases of depositional sequences. The vertical profile of the splay is identical to that of classic turbidite sequences, suggesting deposition by turbidity currents (Walker, 1979). However, delta-front splays are a response to onshore storms. Sediment- and leaf-laden floodwaters entered the receiving basin under conditions of hyperpycnal flow (water-sediment mixture more dense than seawater) and continued moving down the delta-front slope until waning current strengths caused sedimentation.

Highly contorted interbedded delta-front mudstones and sandstones that rest on and are overlain by undeformed beds are interpreted to be local slump deposits (as noted in the "A" sand at Pleasant Bayou). The sands are very fine grained and moderately sorted. Subaqueous gravity-induced mass movements are a common phenomenon in modern deltas, particularly those having high depositional rates and large quantities of fine-grained sediment (Coleman and Prior, 1980).

Crossbedded, poorly to moderately sorted, rather coarse-grained distributary-mouth-bar sandstones of the "C" correlation interval (Andrau sandstone) form the test interval in the Pleasant Bayou No. 2 well. Spontaneous-potential logs indicate rapidly upward-coarsening to blocky sandstone that is extensive in both dip and strike directions. The Andrau coalesced distributary-mouth-bar complex was characterized by high rates of sedimentation. Winnowed and reworked sandstones in the lower part of the sequence give way to sandstones of variable texture and maturity at the bar crest; the paucity of trace fossils is consistent with conditions of vigorous sedimentation. Very coarse sandstones cap the succession, representing distributary-channel deposits that eroded into the bar crest during continued progradation of the delta system.

Fine to very coarse grained sandstones interbedded with highly carbonaceous mudstone and thin coal seams rest on a thick progradational sequence in the "F" correlation interval of the Pleasant Bayou well. The sandstones are poorly sorted and cross-stratified and compose several upward-fining cycles. The truncated upward-fining sandstone sequences reflect cyclic fluvial or distributary-channel sedimentation. Thick, rooted sandstones reflect substantial levee deposits, suggesting that the channels were meandering and were flanked by, and meandered over, extensive delta-plain marshes.

Marine reworking and winnowing of the progradational deltaic sequence followed lobe abandonment and foundering of the delta platform. Two abandonment subfacies are recognized in the Pleasant Bayou cores: a proximal (upper shoreface-foreshore) subfacies and a distal shoreface to shelf subfacies (Tyler, 1981; Tyler and Han, 1982). Abandonment facies are

characteristically more intensely bioturbated, finer grained, and better sorted relative to constructional facies. However, abandonment facies are volumetrically insignificant.

Sandstones of the lower Frio Formation in Brazoria County were deposited in a high-constructive deltaic environment within the Houston delta system. Lobate to elongate sandstone distribution patterns, log patterns, and core analysis indicate high rates of deltaic progradation. Furthermore, the lateral continuity of coalesced mouth-bar deposits, coupled with the lobate geometries of the delta lobes, points to considerable wave modification. Constructive elements include storm-induced delta-front splays, distributary-mouth-bar deposits, and aggraded distributary-channel and floodplain deposits (fig. IV-3). Delta-front slumping, considered an integral facet of delta progradation by Coleman and Prior (1980), was also an active constructional process. Crevasse splays, although not intersected in cores, are also important in extending the delta plain.

STRUCTURAL DEVELOPMENT

The structural evolution of the Pleasant Bayou - Chocolate Bayou area was thoroughly studied by Winker and others (1983), using well-control and seismic data. Additional well control within and east of the Chocolate Bayou area was later used by Han (in Morton and others, 1981) to somewhat revise the structural interpretation. This work has been reviewed and integrated with the previous study, and some supplementary information has been added near Danbury Dome, to produce a refined interpretation. The major structural features expressed at the T5 level (fig. IV-4) are Danbury Dome, Chocolate Bayou dome, the Chocolate Bayou growth fault (and lesser faults), and the South Chocolate Bayou growth fault.

Danbury Dome is a piercement salt dome; the tip of the salt stock pierces basal Miocene strata at a depth of approximately 4,500 ft. The zone around the salt stock has also been lifted up to 4,000 ft above adjacent areas. Winker and others (1983) showed that the uplift (and, by inference, the intrusion of the salt stock) began in late Frio time; the strata below T3 are not significantly affected. The dome rose along and through the Chocolate Bayou growth fault; strata on the downthrown side of the fault have been affected by the uplift.

Origin of the Chocolate Bayou dome is uncertain; Winker and others (1983) speculated that it may represent a turtle structure cored by strata of pre-Frio age. All correlation intervals of the Frio and Anahuac Formations thin across the dome, indicating that it subsided less than the surrounding areas. However, the dome's closure to the east, where no salt-withdrawal basin is recognized, suggests that the dome may represent a deep-seated salt dome or salt pillow that has retained a small degree of positive buoyancy.

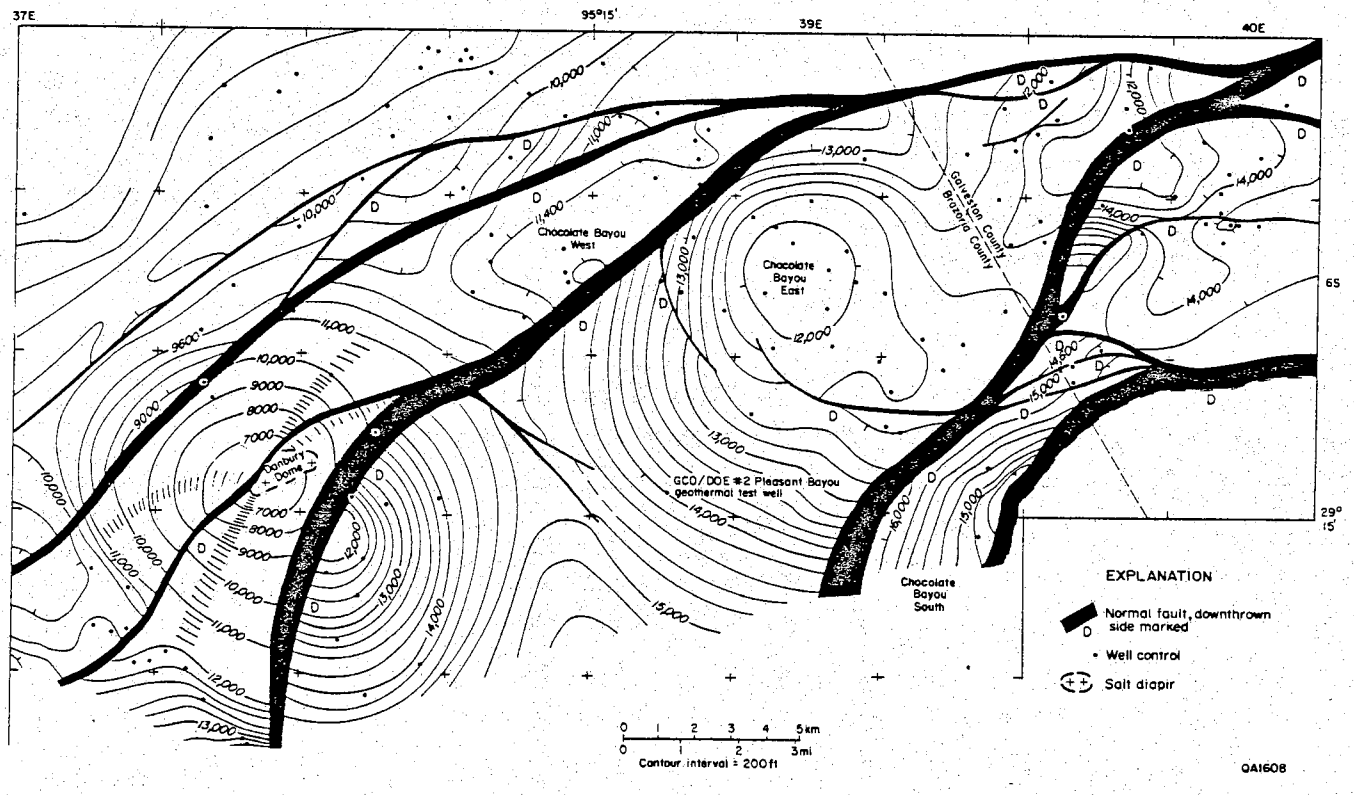

Figure IV-4. Structure map on the T5 marker, Chocolate Bayou - Danbury Dome area.

Wells drilled on the dome have intersected faults on 64 occasions, as determined by detailed log correlation (fig. IV-5). Most of these faults have less than 100 ft of displacement and cannot be correlated with any confidence from well to well. It is suspected that these represent crestal faults formed during dome growth. They are found throughout the Frio and Anahuac Formations but appear (after correction for the smaller number of deep wells) to be more abundant below 10,500 ft (approximately between T3 and T4). Two faults with displacement greater than 100 ft can be correlated on the west and south sides of the dome, with displacement down to the salt-withdrawal basin. These faults probably represent basin-marginal faults caused by subsidence of the salt-withdrawal basin. They do not appear to be continuous across the flank, as they do not seal the Chocolate Bayou reservoirs from the downdip basinal aquifers.

The Chocolate Bayou growth fault is the updip bounding fault of the Pleasant Bayou - Chocolate Bayou fault block. During lower Frio deposition, this major growth fault had expansion indices (downthrown thickness/upthrown thickness) of 3 to 6, causing rotation of the downdip fault compartment. The fault is the updip seal of overpressure in the lower Frio sandstones in Chocolate Bayou (East) and Pleasant Bayou areas (Fowler, 1970). The fault became inactive in later Frio time and was pierced by the Danbury salt stock. Smaller faults northwest of the main fault were active during deposition of the middle and upper Frio strata; they bound the Chocolate Bayou (West) fault block, among others, and contribute to a certain degree of overpressuring in that field (Fowler, 1970).

The South Chocolate Bayou growth-fault system forms the downdip limit of the Pleasant Bayou - Chocolate Bayou block and bounds the Chocolate Bayou South field. It merges to the northeast with the Chocolate Bayou fault. This fault system was active throughout Frio deposition, with expansion indices of 1.4 to 2.0. Southeast of the fault, the entire Frio section is overpressured.

SANDSTONE CONSOLIDATION HISTORY

The diagenetic evolution of the Frio Formation has been intensively studied as a direct consequence of the geopressured geothermal research program. Early studies (Lindquist, 1977; Loucks and others, 1977; Bebout and others, 1978; Loucks and others, 1979a and 1979b) established regional trends in sandstone composition and a generalized diagenetic sequence for Tertiary strata of the Texas Gulf Coast. More recent studies focused on specific aspects of diagenesis in the Pleasant Bayou area (Loucks and others, 1981; Land and Milliken, 1981; Milliken and others, 1981) and on the impact of water-rock interaction (Kaiser and Richmann, 1981; Kaiser, 1983).

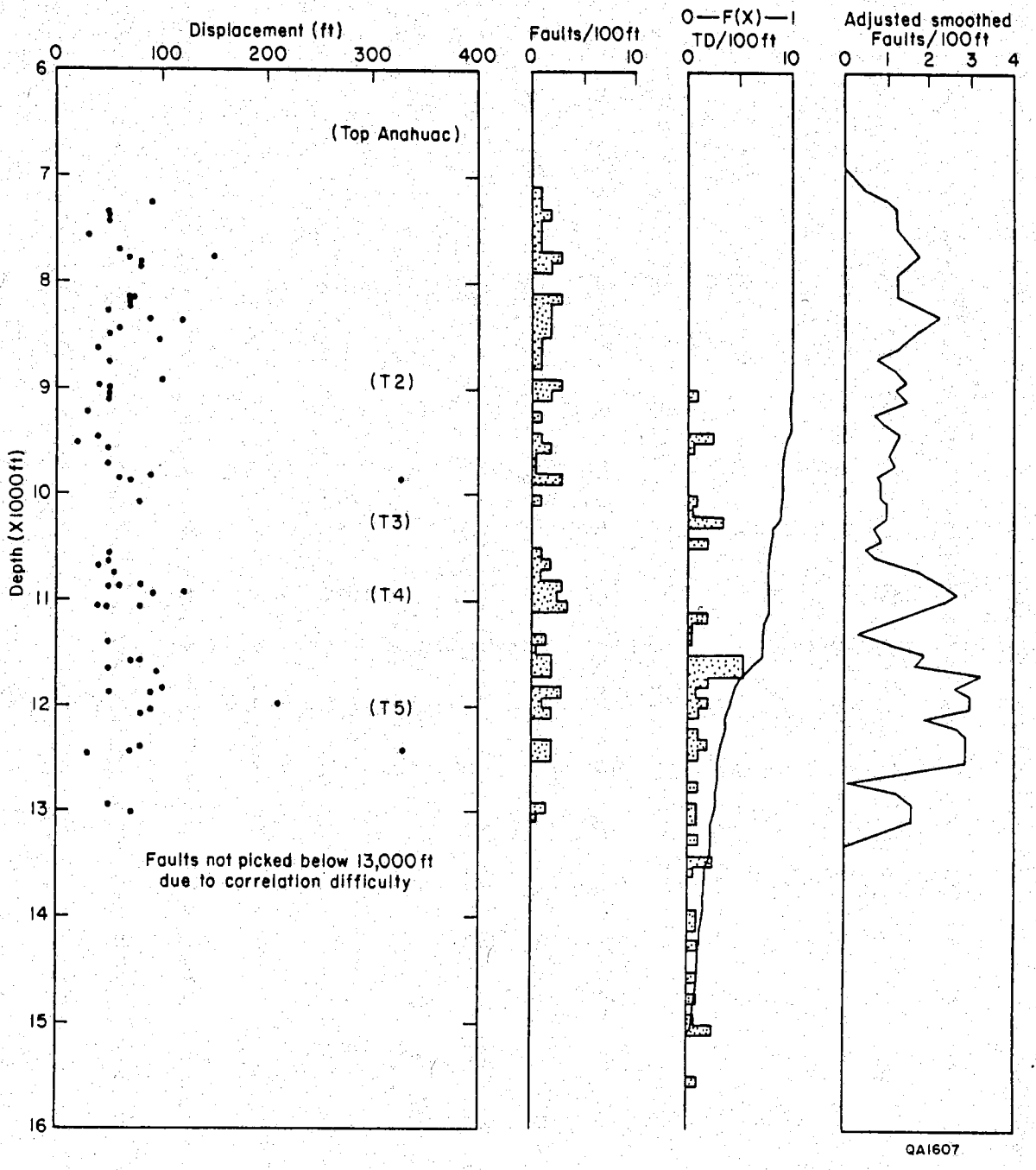

Figure IV-5. Faults penetrated by 53 wells on the Chocolate Bayou dome. Most fault intersections show less than 100 ft of omitted section. The histogram of faults vs. depths is corrected for the smaller number of wells reaching greater depths by multiplying by 1/F(x), where F(x) is the fraction of wells reaching a depth x.

Diagenetic processes, including cementation, replacement, and leaching, are influenced by both internal and external factors (Loucks and others, 1981). Internal factors include sediment provenance, climate, depositional environment, subsidence history, and evolution of organic matter; external parameters include geothermal gradient, fluid pressure gradient, and pore-fluid chemistry. Interaction between these factors results in complex diagenetic histories that include repeated alternations of dissolution and precipitation of framework and authigenic minerals.

The Frio Formation shows great regional variation in mineral composition (Loucks and others, 1983). South Texas sandstones are poorly sorted, fine-grained feldspathic litharenites to lithic arkoses rich in volcanic rock fragments (Lindquist, 1977) and locally derived caliche clasts. Middle Texas Gulf Coast (Greta/Carancahua system) sandstones are moderately to well sorted, fine-grained, quartzose lithic arkoses having smaller amounts of volcanic and carbonate rock fragments. Metamorphic fragments, possibly derived from the Llano Uplift, are common in some samples. Upper Texas Gulf Coast sandstones are moderately sorted, fine-grained lithic arkoses and feldspathic litharenites to subarkoses (Loucks and others, 1981). The abundant volcanic fragments of South Texas were derived from active volcanic areas to the west; smaller amounts of this detritus survived transport to the Middle and Upper Texas Gulf Coast (Loucks and others, 1983). Sandstones of the Frio Formation thus display a gradient of increasing compositional maturity from South Texas to the Upper Texas Gulf Coast; this is matched by improved reservoir quality.

Effects of Internal Factors

Regional studies of reservoir quality of deep Frio sandstones have described a progressive increase in deep reservoir quality from the Lower to the Upper Texas Gulf Coast (Bebout and others, 1978; Loucks and others, 1983). Most permeabilities in the deep subsurface of South Texas are less than a few millidarcys, increasing to several hundred millidarcys in the Upper Texas Gulf Coast. Shallow oil reservoirs display a similar trend (Galloway and others, 1982a). Changes in rock composition, climate, and to a lesser extent geothermal gradient account for this change.

Correlation of depositional environment with diagenesis-related reservoir quality can best be demonstrated at the Pleasant Bayou test well using the data of Loucks and others (1979b) and Morton and others (1983a). Distributary-channel and subaerial-levee sandstones are matrix-poor with well-developed quartz overgrowths and have low permeabilities (fig. IV-6). Distributary-mouth-bar and delta-front sandstones contain both quartz overgrowths and kaolinite filling leached pore spaces but have higher porosities and good permeabilities (fig. IV-7). High matrix

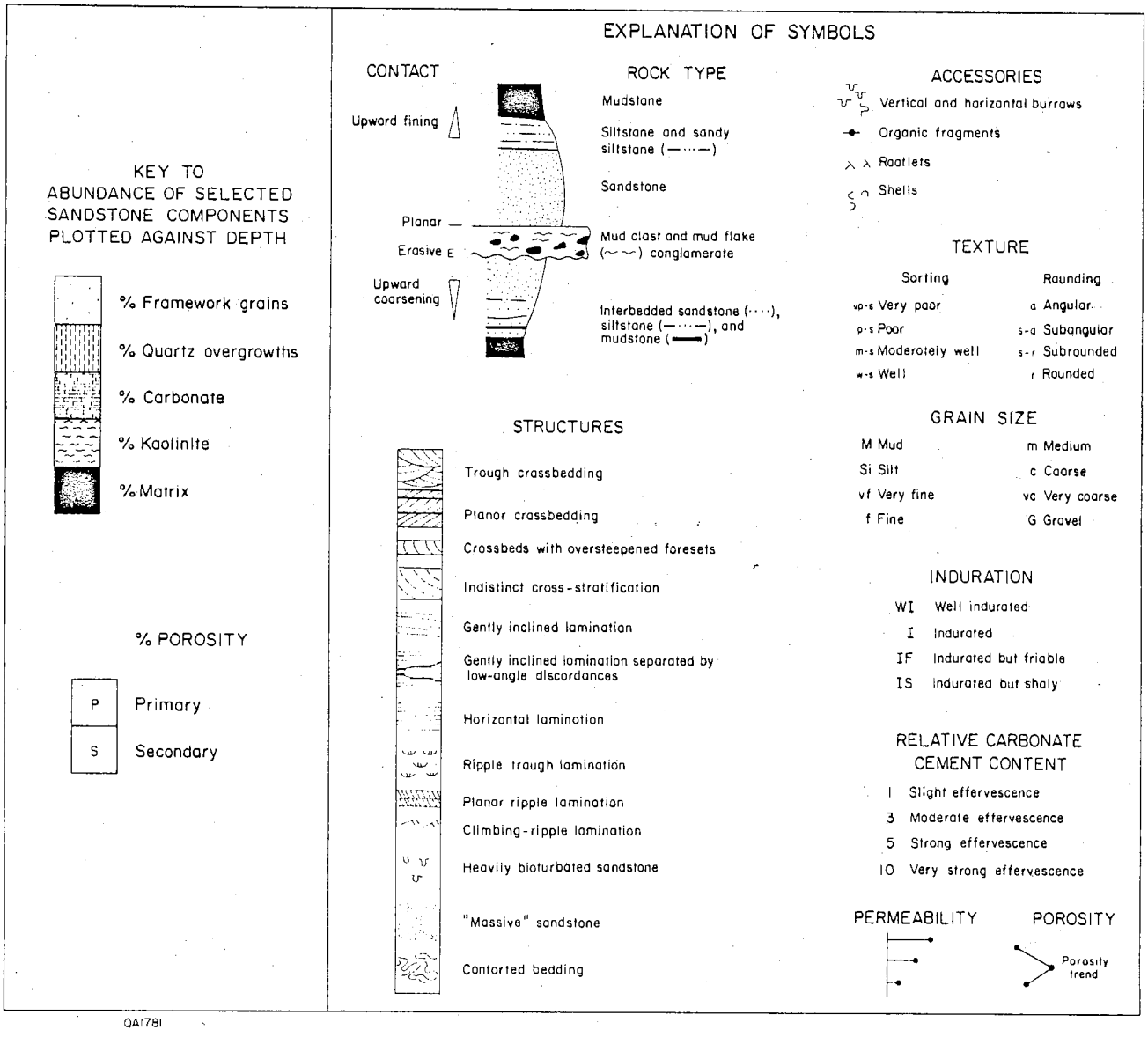

Figure IV-6A. Explanation of symbols and key to abundance of selected sandstone components plotted against depth.

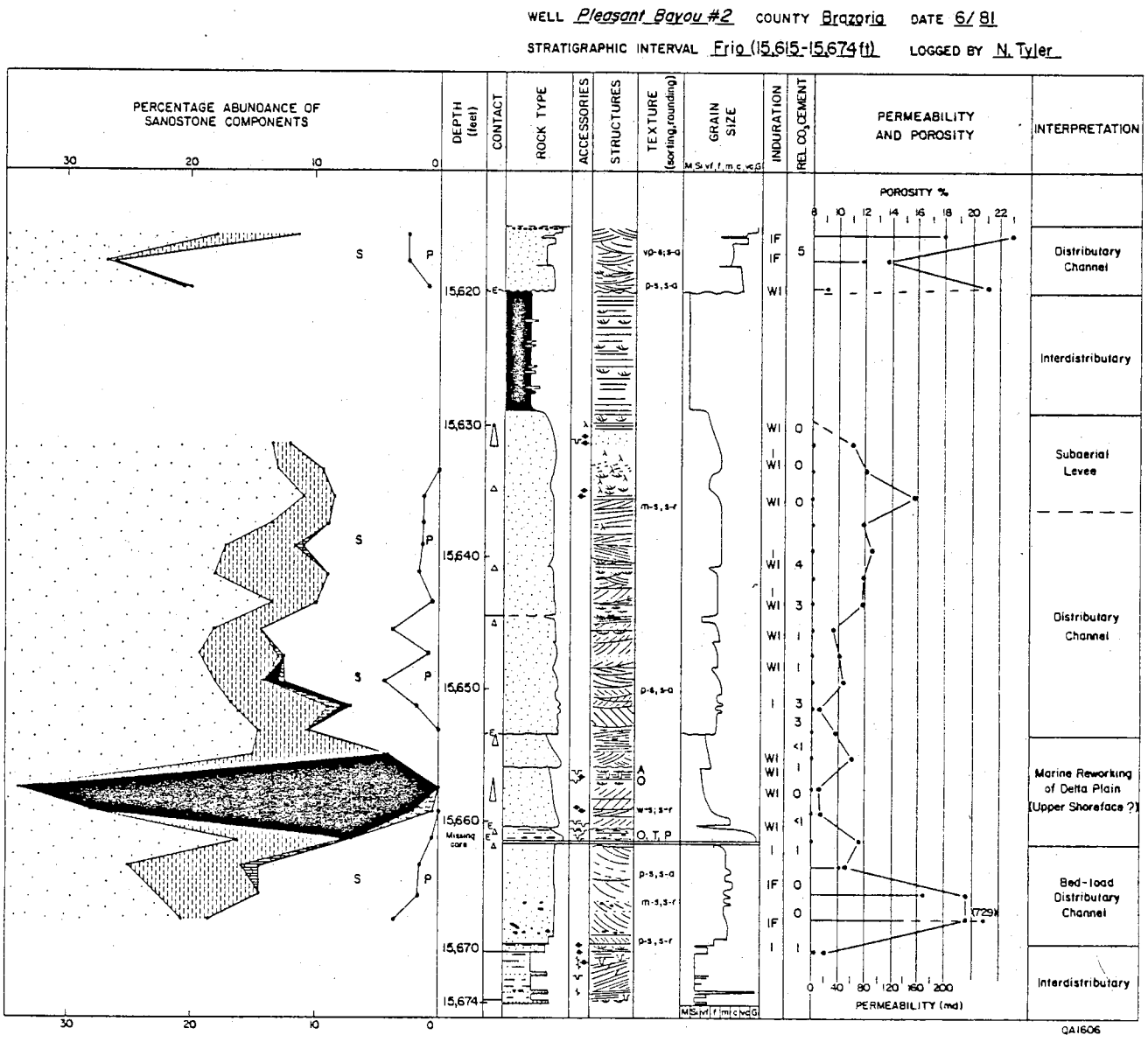

Figure IV-6B. Detailed core description and petrography of a distributary-channel and delta-plain sequence having an interbedded reworked abandonment phase, sub-T5 interval, Pleasant Bayou No. 2 well. Modified from Morton and others (1983).

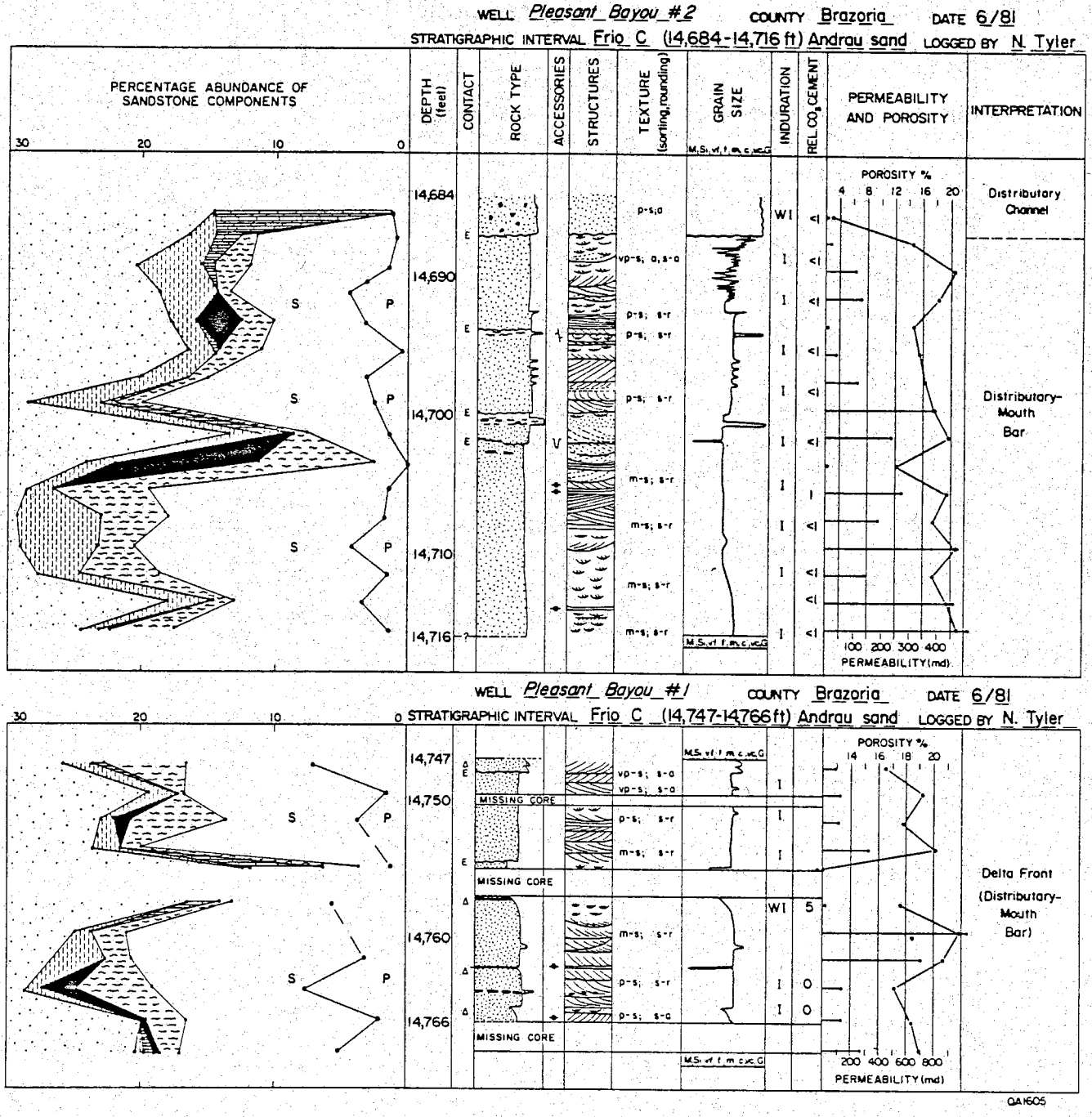

Figure IV-7. Detailed core description and petrography of distributary-mouth-bar sandstones, Andrau sandstone, Pleasant Bayou No. 1 and No. 2 wells. Modified from Morton and others (1983).

contents are mainly associated with mud-clast conglomerates. Delta-front slump deposits exhibit a very great amount of matrix, which yields a very low permeability (fig. IV-8), because of intermixing of mud and silt by slumping and burrowing (Morton and others, 1983a). Shoreface sandstones contain quartz overgrowths, carbonate cement, and kaolinite in varying amounts; burrowed zones are matrix-rich (fig. IV-9). Permeability is erratic but fairly good except where either matrix or carbonate cement is present. Sandstones of the delta-abandonment facies show low porosity and permeability (fig. IV-10). Proximal abandonment sandstones contain abundant carbonate, which probably represents a shelly beach. Distal abandonment sandstones, as well as delta-plain reworked sandstones, contain abundant matrix probably due to bioturbation.

Diagenetic Sequence

Several attempts have been made to create a general Frio diagenetic sequence (Lindquist, 1977; Loucks and others, 1977, 1979a, 1979b, 1980, and in preparation). Paragenetic sequences using isotopic temperatures derived for the Pleasant Bayou area (Loucks and others, 1981; Milliken and others, 1981) show substantial departures from these general sequences, especially in their estimates of depth of formation. However, the overall evolution of Tertiary diagenesis is similar.

Diagenesis of Tertiary sandstones in Brazoria County has been subdivided into an upper zone of passive diagenesis (zone 1) overlying zones of active diagenesis (zones 2a, 2b, 3) (fig. IV-11; Milliken and others, 1981). Zone 1 includes near-surface to moderate subsurface compaction and precipitation of authigenic minerals within pores. Cements formed include carbonates, quartz, rare feldspar, and possible kaolinite. Carbonate authigenesis is complex, with periods of precipitation and leaching over the entire range of depths of Frio diagenesis (Loucks and others, 1981). The top of geopressure lies near the base of zone 1.

Active diagenesis involves the reaction of aqueous solutions with unstable detritus, as well as continued precipitation in pore spaces. In this region, metastable components (smectite and Ca-plagioclase) shift toward equilibrium with the pore waters and the rock (Milliken and others, 1981). Three processes occur: the gradual change of smectite to illite, maturation of organic matter, and albitization of detrital feldspars. Incipient transformation of smectite to illite marks the top of the zone.

Maturation of organic matter is of paramount importance not only for hydrocarbon generation but also because acids responsible for leaching and formation of secondary porosity may be produced (Schmidt and MacDonald, 1979; but see Lundegard and others, in press). Secondary porosity in the Chocolate Bayou area is extensively developed below 10,000 ft

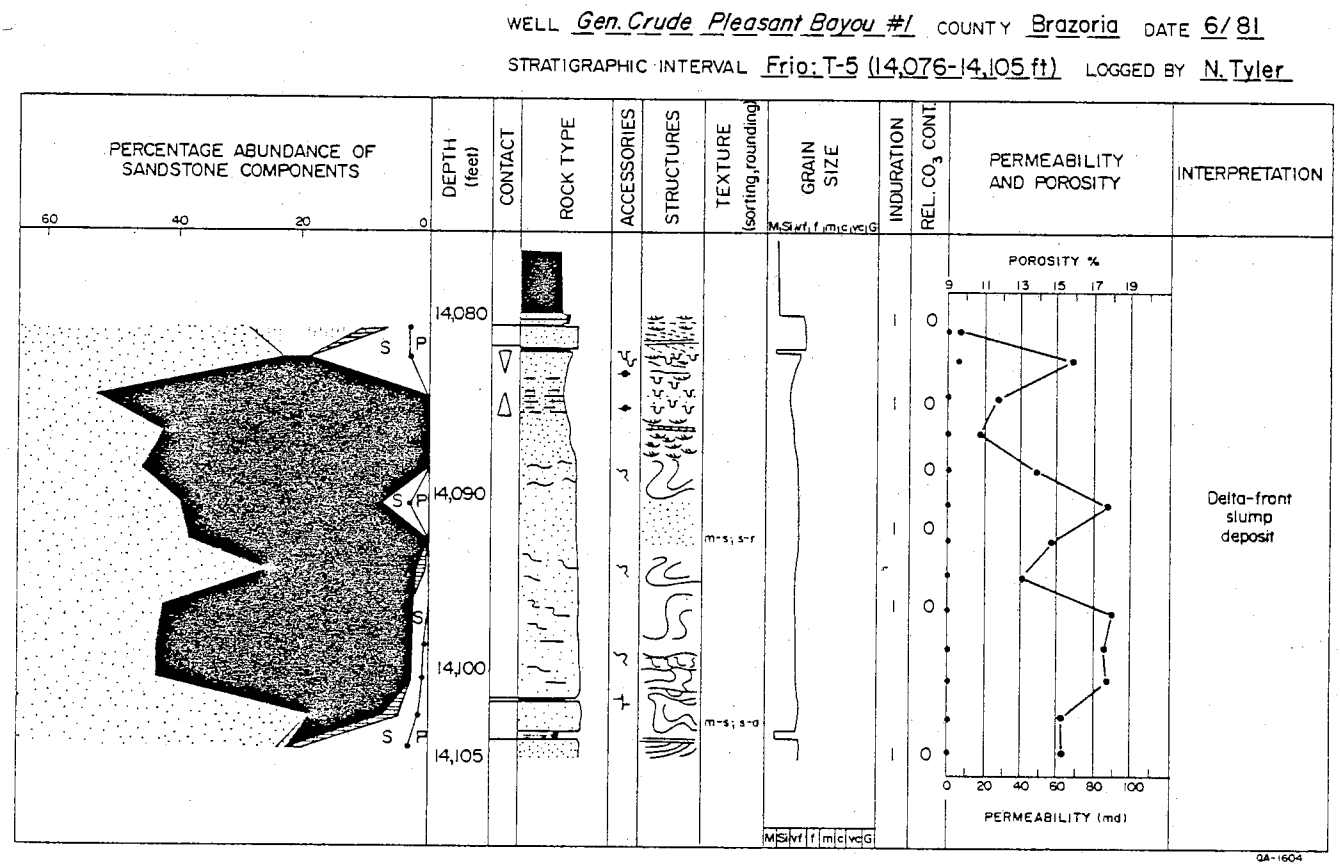

Figure IV-8. Detailed core description and petrography of a delta-front slump deposit, Pleasant Bayou No. 1 well. Modified from Morton and others (1983).

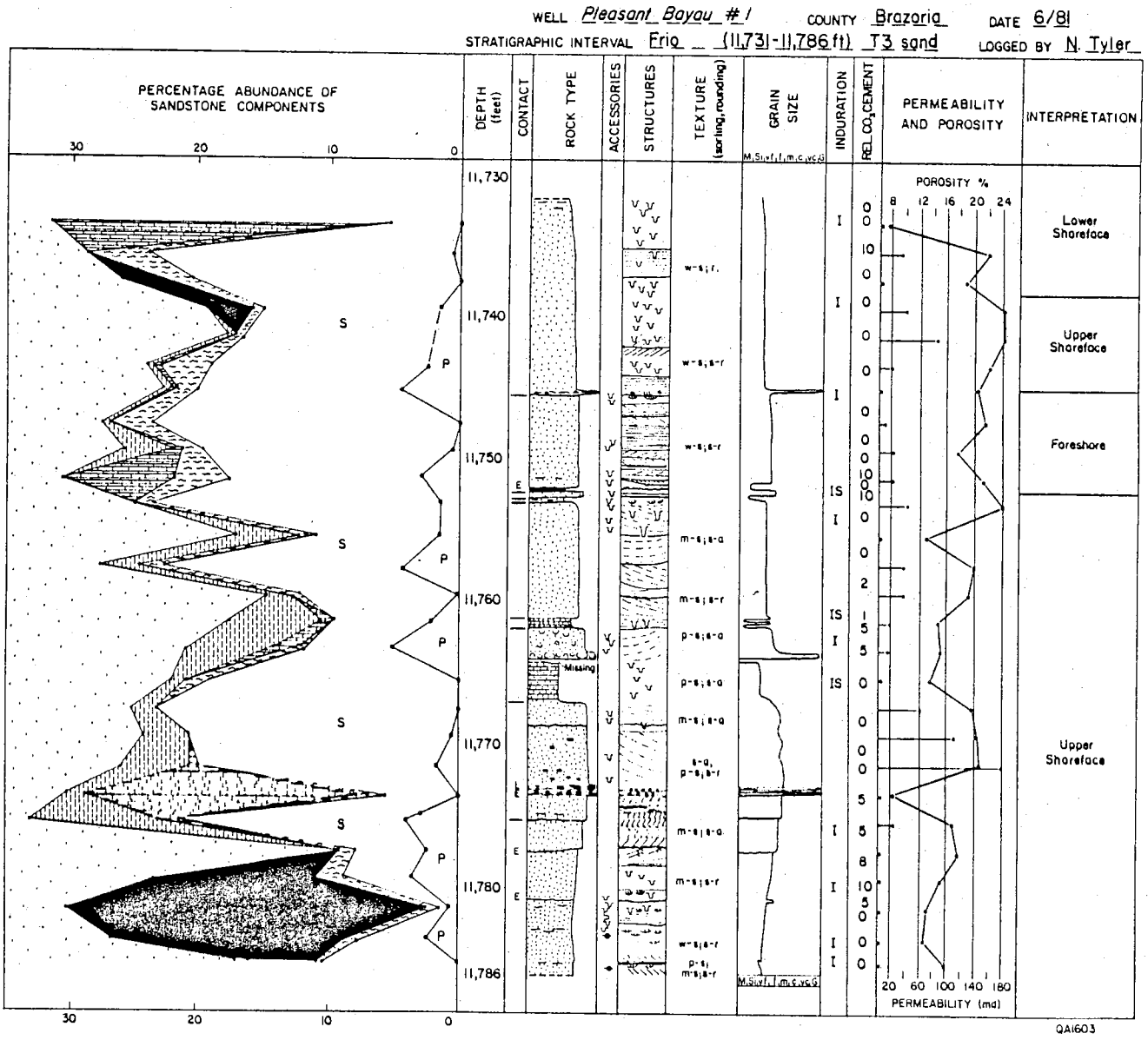

Figure IV-9. Detailed core description and petrography of a shoreface sandstone, T3 interval, Pleasant Bayou No. 1 well. Modified from Morton and others (1983).

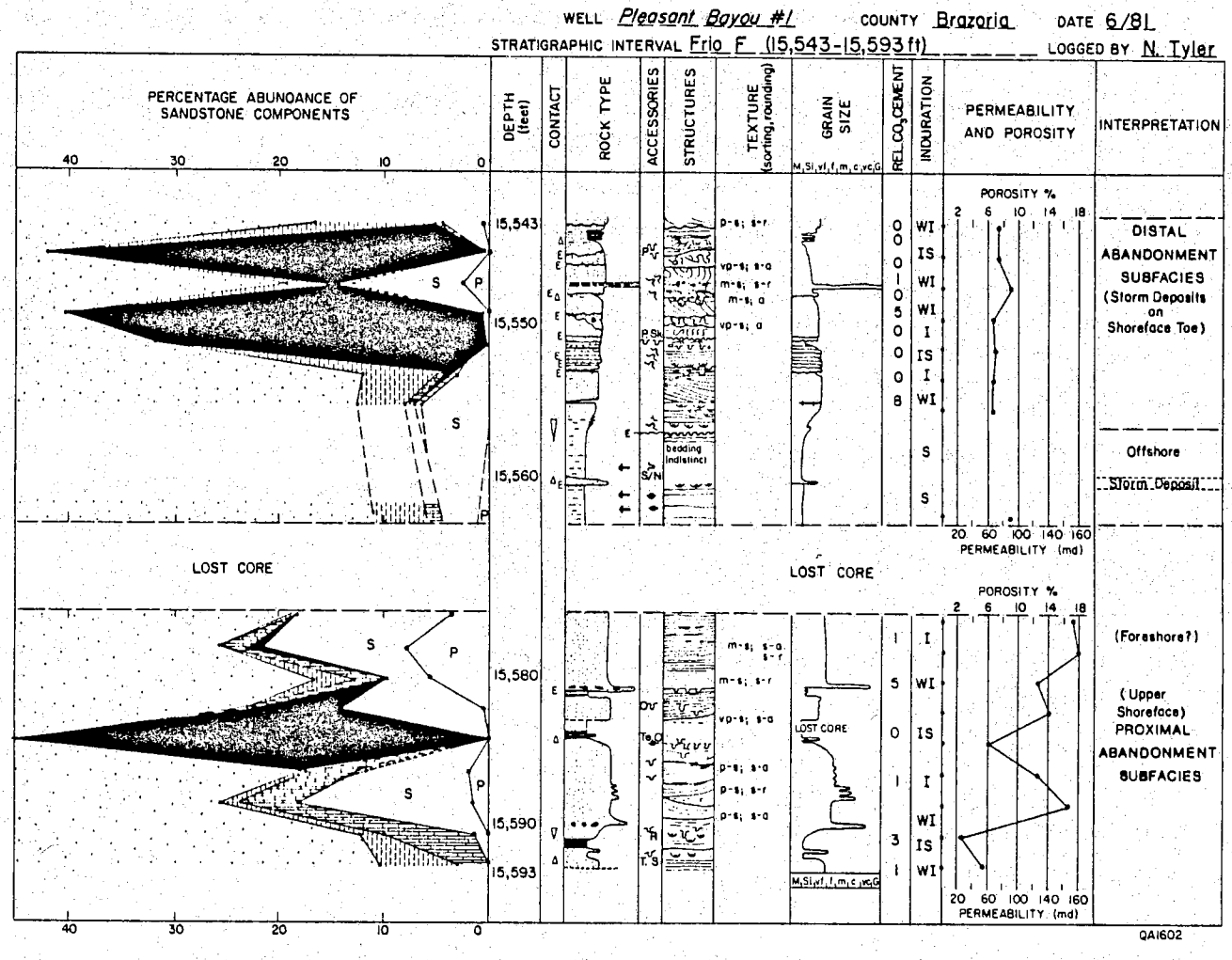

Figure IV-10. Detailed core description and petrography of abandonment facies sandstone, sub-T5 interval, Pleasant Bayou No. 1 well. Modified from Morton and others (1983).

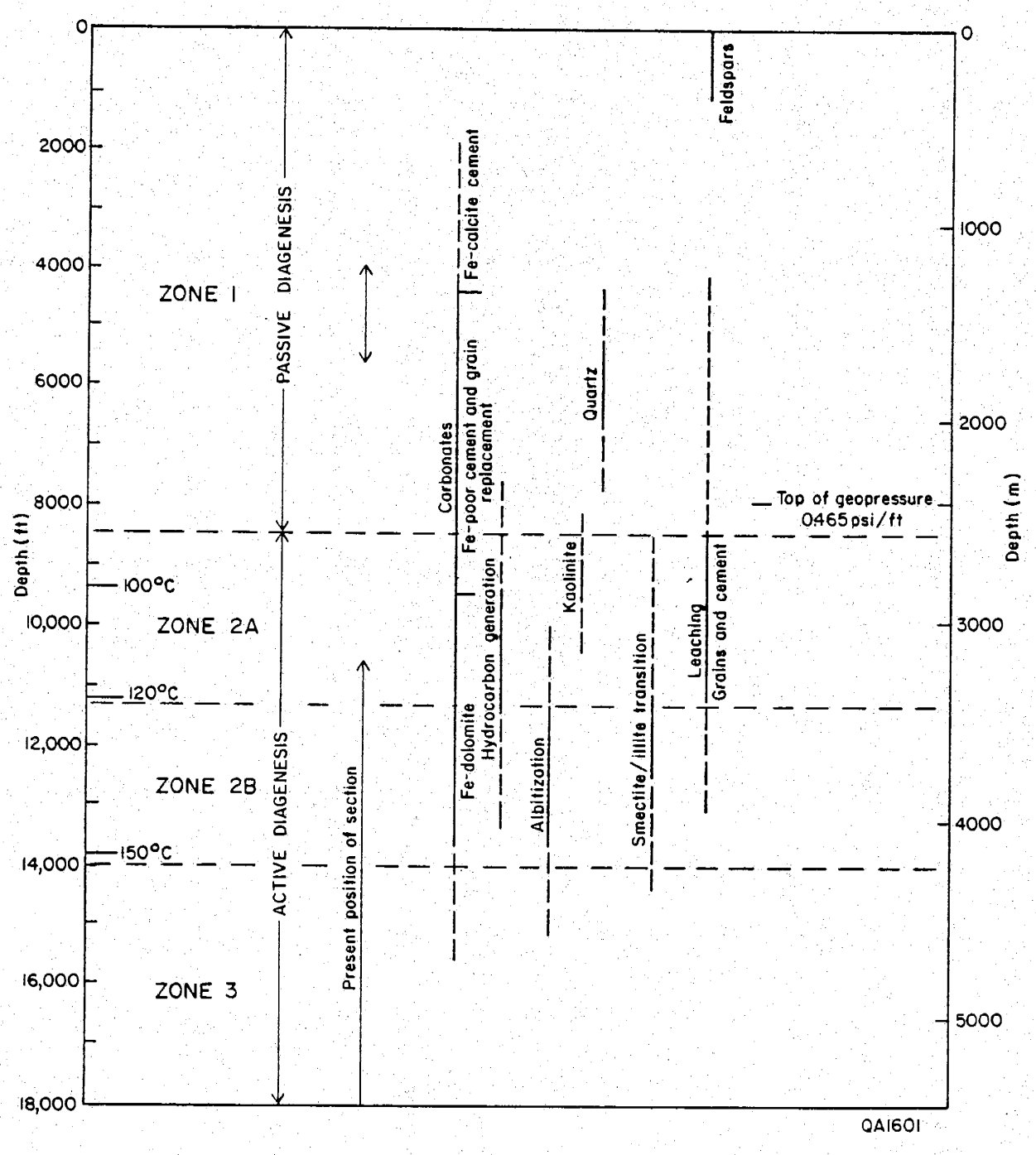

Figure IV-11. Frio diagenetic sequence in Brazoria County, modified from Loucks and others (1981) and Milliken and others (1981).

(Loucks and others, 1981). This porosity postdates quartz overgrowths, which are enriched in O^{18} consistent with their formation at lower temperatures than at present. Pervasive leaching of carbonate rock fragments and calcite cement is responsible for the generation of much of the observed secondary porosity; leaching of feldspars and volcanic fragments is also significant. These leaching processes resulted in the observed dominance of secondary porosity over primary porosity (Bebout and others, 1978) and in the anomalous positive correlation between cement content and porosity (Loucks and others, 1980). Secondary porosity ranges from 40 to 100 percent of total porosity, as shown on figures IV-6 through IV-10.

In zone 3, the illitization and albitization processes are nearly complete. Leaching is minor to absent, but minor ferroan dolomite and possibly kaolinite precipitation continues. Progressive albitization of plagioclase occurs; the sodium required for reaction is derived from sodium-rich saline brines (Land and Milliken, 1981). At Pleasant Bayou, kaolin formed at around 100°C, filling secondary pores or replacing feldspar (Loucks and others, 1981). Albitization took place primarily at temperatures greater than 120°C (Loucks and others, 1981). South Texas Frio sandstones show nearly complete occlusion of secondary porosity with ferroan carbonate and kaolinite (Lindquist, 1977). Organic maturation may be responsible in part for this occlusion by acting as a source of dissolved CO_3^{2-} in subsurface fluids that reacts with calcium derived from albitization.

Origin of Permeable Aquifers

Although regional studies of Frio diagenesis determined that deep reservoir quality improves eastward along the Texas Gulf Coast, they failed to emphasize that even in the better areas, sandstones having permeabilities high enough to allow geopressured geothermal production are atypical. The Andrau, or "C," sandstone in particular displays anomalously high permeabilities (1 to 1,000 md, averaging 232 md) over its entire cored thickness (fig. IV-7) and over much of its lateral extent. Permeability and facies stratification are lacking in this remarkably continuous sandstone (fig. IV-12A; Morton and others, 1983a). In contrast, other lower Frio sandstones in the geopressured interval, even at Pleasant Bayou, have uniformly low permeabilities (fig. IV-10) or extreme permeability stratification (fig. IV-6). As discussed above, these variations in permeability appear to be related to depositional environment; yet 78 percent of the Andrau sandstone porosity and 88 percent of the "F" sandstone porosity are secondary.

In the case of the "F" sand, it is possible that acids released during thermal maturation of organic matter in adjacent shales leached metastable grains and cements, creating secondary porosity. This porosity could have been preserved by hydrocarbons generated by continued

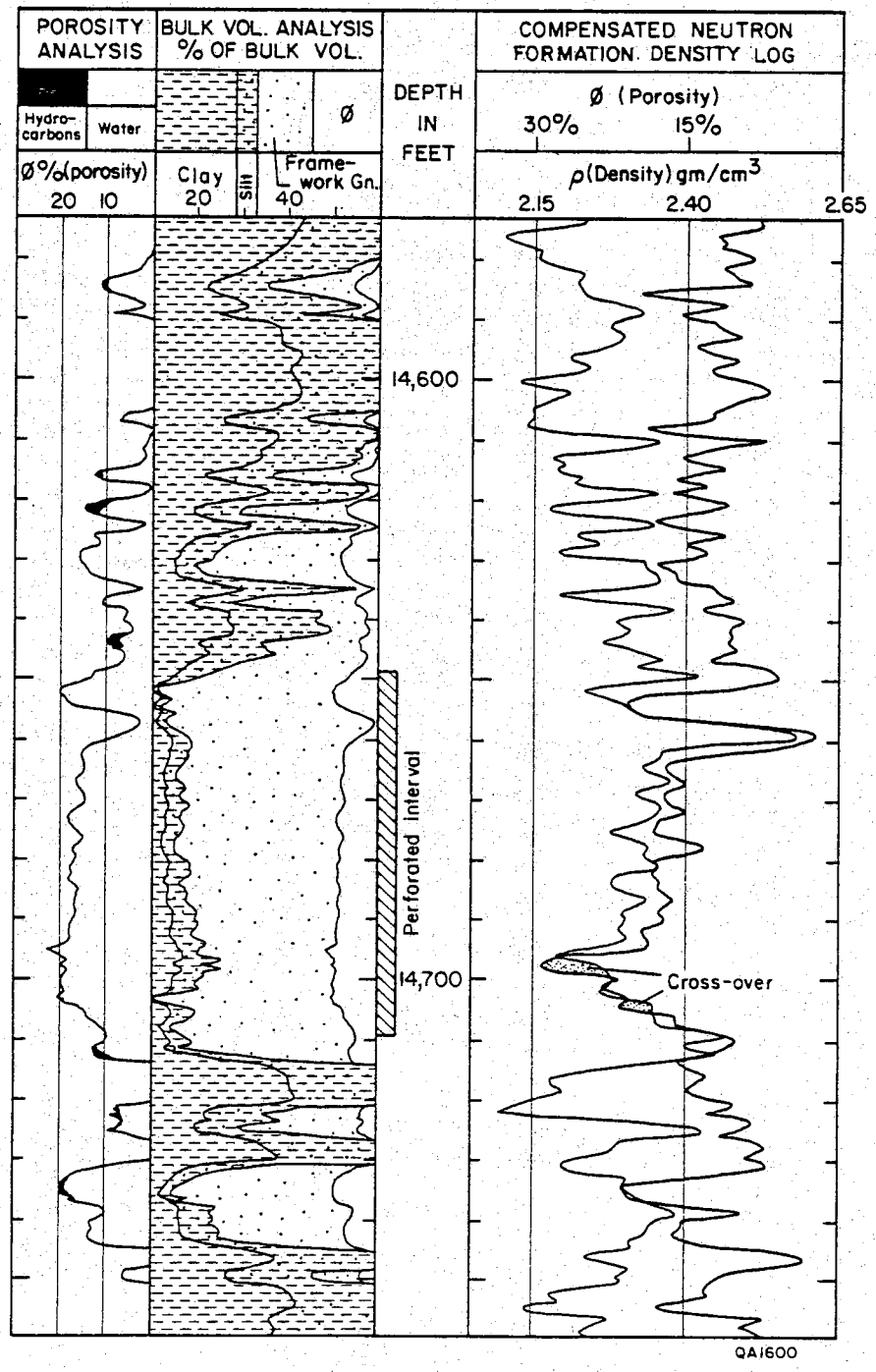

Figure IV-12A. Computer-processed log, compensated neutron log, and density log for the "C" sandstone, Pleasant Bayou No. 2 well.

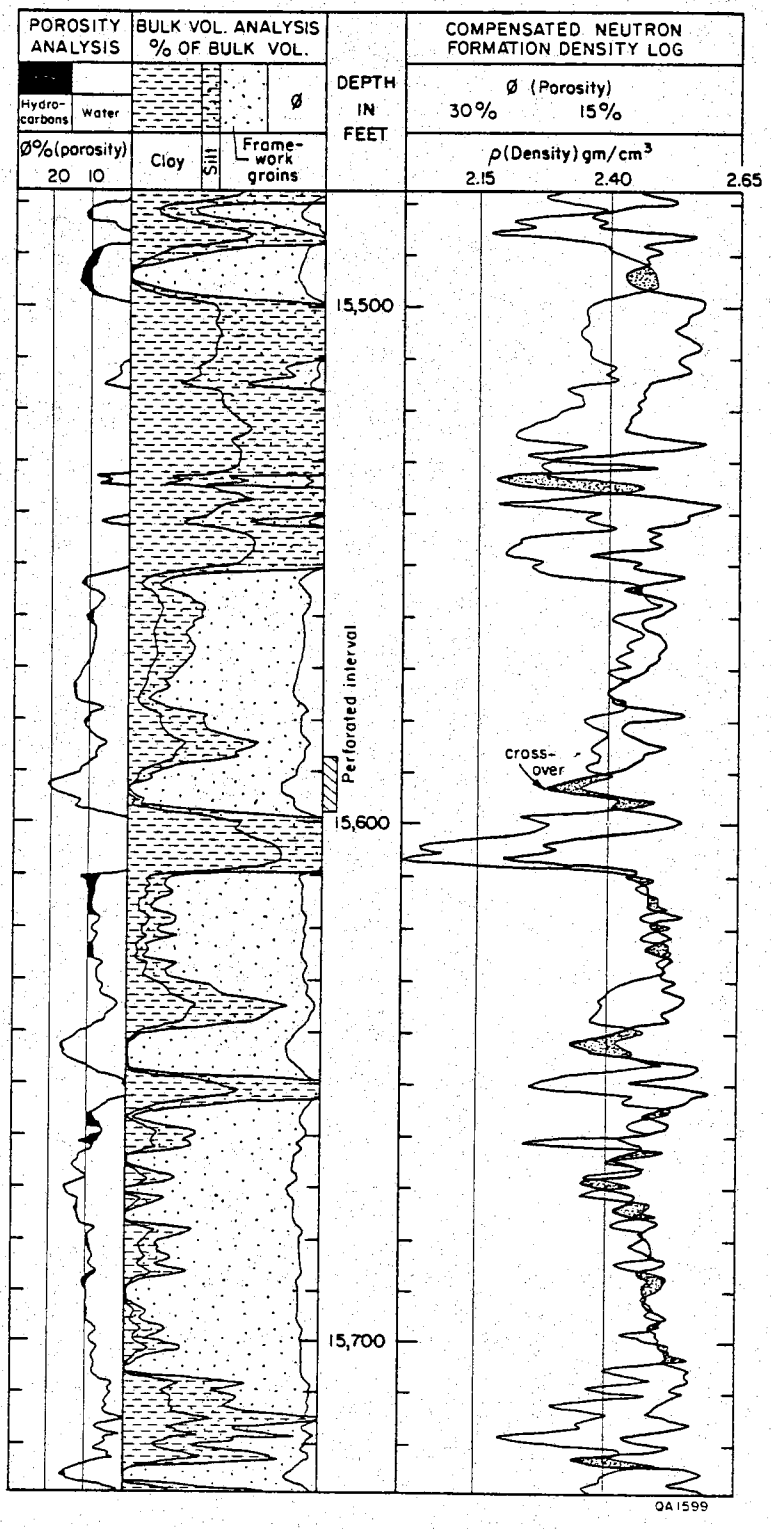

Figure IV-12B. Computer-processed log, compensated neutron log, and density log for the "F" sandstone, Pleasant Bayou No. 2 well.

thermal cracking of the organic debris and trapped by the tight, matrix-rich transgressive sandstones that overlie the lower channel sandstone and by mudstones that rest on the upper sandstone. Existence of such traps is suggested by indications of free gas-bearing zones in the "F" sand on the compensated neutron and density log, oil indication on computer-processed logs, and oil stain on the cores (fig. IV-12B). These trapped hydrocarbons could have inhibited continued diagenesis and porosity occlusion.

SALIENT FEATURES OF TEST-WELL DATA

Distribution of Sand and Shale Pressure

Four methods have been used to estimate the pressure profile of a well either in the well or projected from other wells: shale transit time, shale resistivity, weights of drilling mud, and drill-stem tests of sandstone units. Each of these methods has limitations for accurate determination of pressure, which will be discussed in a later section. Here we will summarize the conflicting pressure information obtained for the Pleasant Bayou test well.

Shale-transit-time data from the test wells define the top of geopressure at about 8,400 ft within the upper Anahuac shale, where transit times depart sharply from the normal compaction trend (fig. IV-13). Shale transit times within the Anahuac shale are extraordinarily long, suggesting very high fluid pressures and geostatic ratios of about 0.9--far in excess of ratios suggested by mud weight and shale resistivity (fig. IV-14). Because of this and the concomitant low seismic velocity of the Anahuac, Flanigan (1980) considered the Anahuac to be highly geopressured. Winker and others (1983), however, pointed out that because the wells were drilled with light muds through the interval without incident, the transit-time anomaly was more likely due to some lithologic change.

Pressures calculated from shale resistivity and mud weights are in general agreement, indicating a gradual rise in geostatic ratio from the upper Anahuac shale downward to about the T4 horizon (fig. IV-14). Below T4, shale pressures are high by all measurements, with geostatic ratio remaining relatively constant at about 0.80 to 0.85. It should be noted, however, that the correlation between shale resistivity and measured differential pressure in Brazoria County determined by Gregory (1979) was so poor that no reasonable trend could be established (fig. IV-15). Therefore, all estimates of pressure from shale-resistivity plots in the area are highly suspect.

Because only limited drill-stem-test data were available from the test well, formation pressures measured in the Chocolate Bayou (East) field are shown on figure IV-14, corrected for increased depth using a hydrostatic gradient of 0.465 psi/ft. This assumes that the sands at the

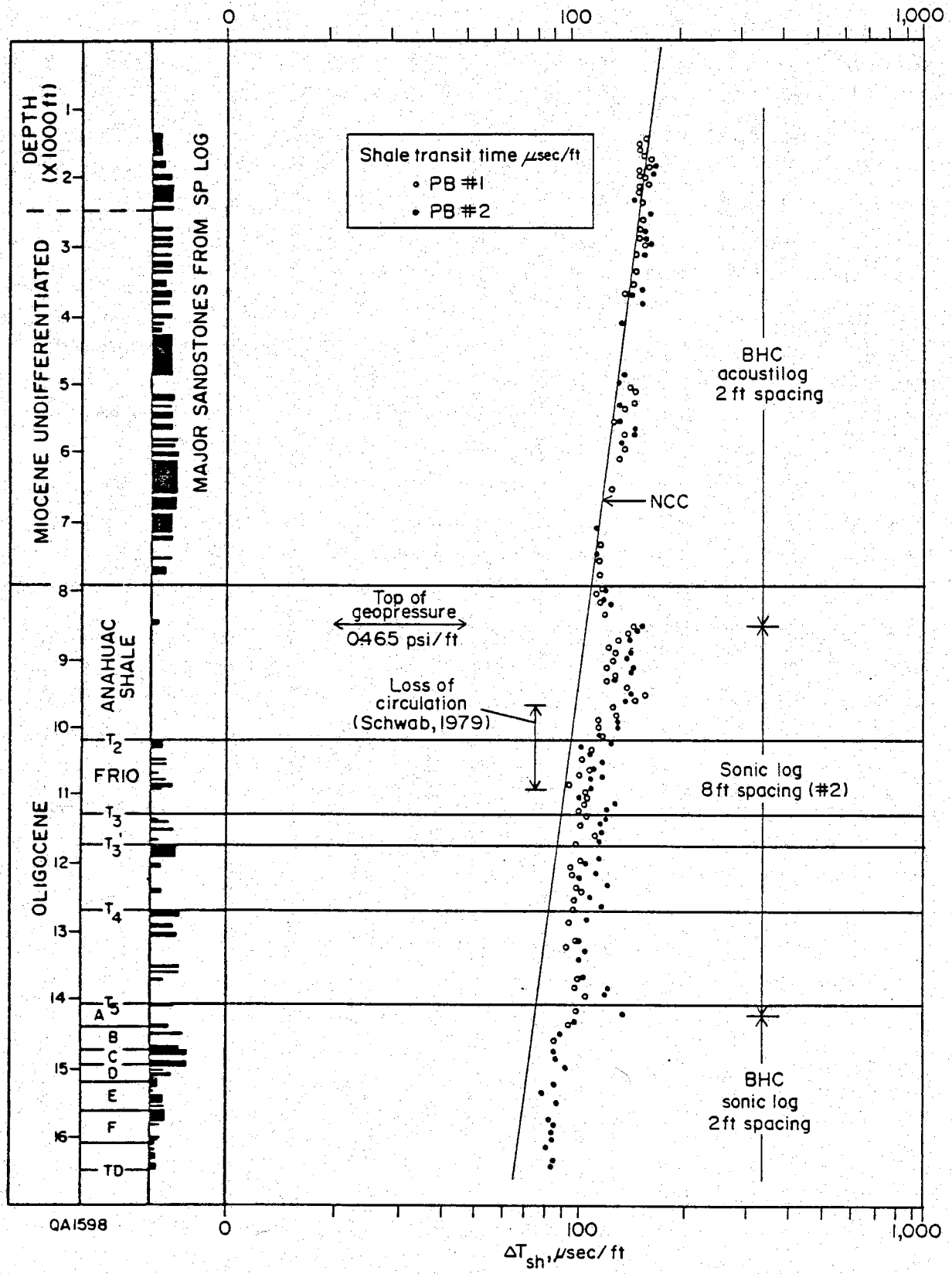

Figure IV-13. Shale transit time vs. depth for the Pleasant Bayou No. 1 and No. 2 wells, from Gregory (1979).

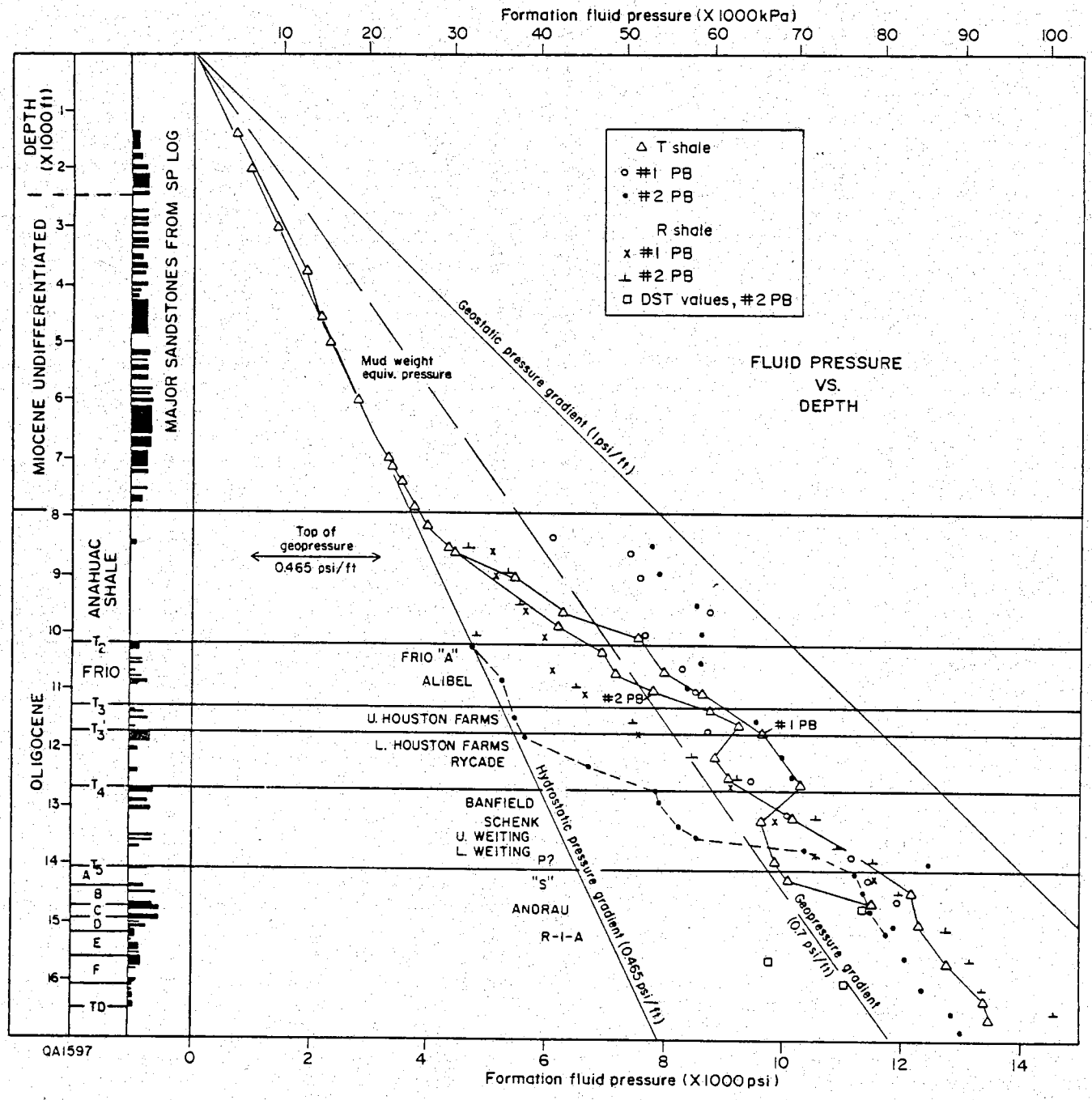

Figure IV-14. Formation fluid pressure vs. depth for the Pleasant Bayou No. 1 and No. 2 wells, as estimated from shale transit time, shale resistivity, mud weights, and drill-stem tests. Modified from Gregory (1979).

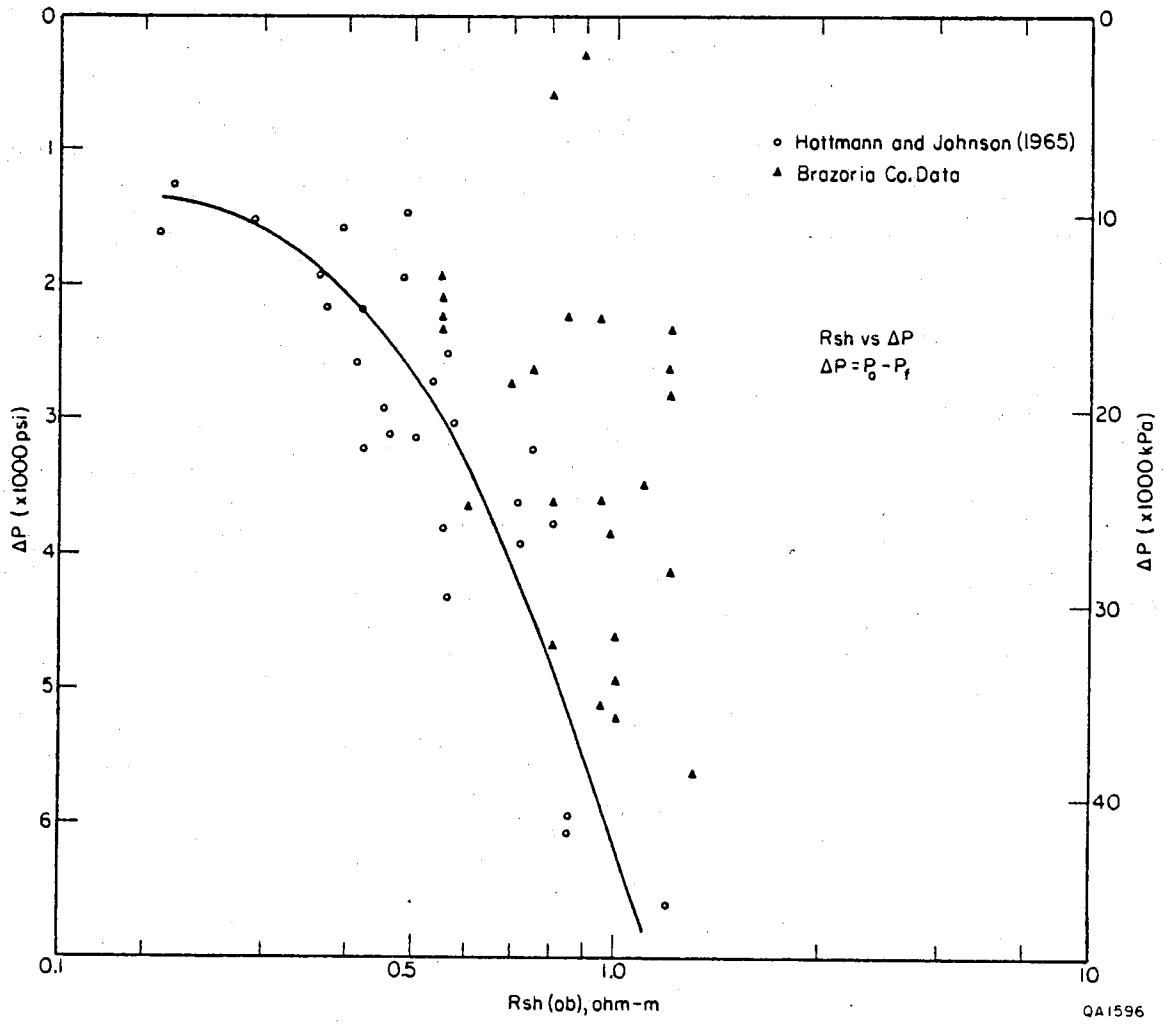

Figure IV-15. Observed resistivity vs. effective overburden pressure for Oligocene shales in Brazoria County compared to Miocene and Oligocene shales of southwestern Louisiana (Gregory, 1979).

test well are in communication with those of the Chocolate Bayou dome to the northeast. The resulting projected pressure of the Andrau sandstone is in close agreement with the drill-stem-test results, substantiating this assumption. However, the two tests made below the Andrau show initial bottom-hole shut-in pressures far less than those of the Andrau and surrounding shales. Either these data do not represent true formation pressures (Gregory, 1979) or these sub-Andrau sandstones (not completed on the Chocolate Bayou dome) have anomalously low overpressures.

The transition from normally pressured to geopressured sandstone reservoirs occurs below the T3' marker horizon, 3,400 ft deeper than the first appearance of shale geopressure (fig. IV-14). Formation pressures then rise stepwise to high geostatic ratios at and below T5 (Fowler, 1970). This suggests a division of the section into four zones:

(1) The zone of hydropressure above the top of the Anahuac.

(2) An upper zone between 8,400 and 12,000 ft that may contain highly geopressured shales but normally pressured sandstones.

(3) A middle zone between 12,000 and 13,500 ft that contains highly geopressured shale and moderately geopressured sandstones.

(4) A lower zone below 13,500 ft that contains highly geopressured shale and sandstone, with at least two sandstones having only moderate geostatic ratios. The sandstones in this zone have a calculated fracture pressure gradient (Anderson and others, 1972) less than the geopressure gradient.

Anomalous Vitrinite and Thermal Alteration Indices

The level of maturity in a subsiding basin is determined by geologic time and temperature history and is measured by vitrinite reflectance (R_o), thermal alteration indices (TAI), and other organic geochemical parameters (Bostick, 1973; Wright, 1980).

The thermal maturity profile in the Pleasant Bayou No. 1 well, based on both TAI and vitrinite reflectance measurement (Brown, 1979; Schwab, 1979), grades from immature above the T3' marker horizon (11,750 ft) to moderately mature in the lower section (fig. IV-16). The vitrinite reflectance values show low dispersion above 8,000 ft in the test well but are widely scattered below. Anomalously low reflectance values in cuttings may result from uphole caving, whereas anomalously high values result from the presence of older reworked debris. Both contaminations appear to be present in the test-well samples.

Core samples at 14,078 and 15,550 ft in the Pleasant Bayou No. 1 contain more than one vitrinite population. However, the lowest average vitrinite value in core should represent the in situ organic maturity, as caving contamination is eliminated. As shown in figure IV-16, these

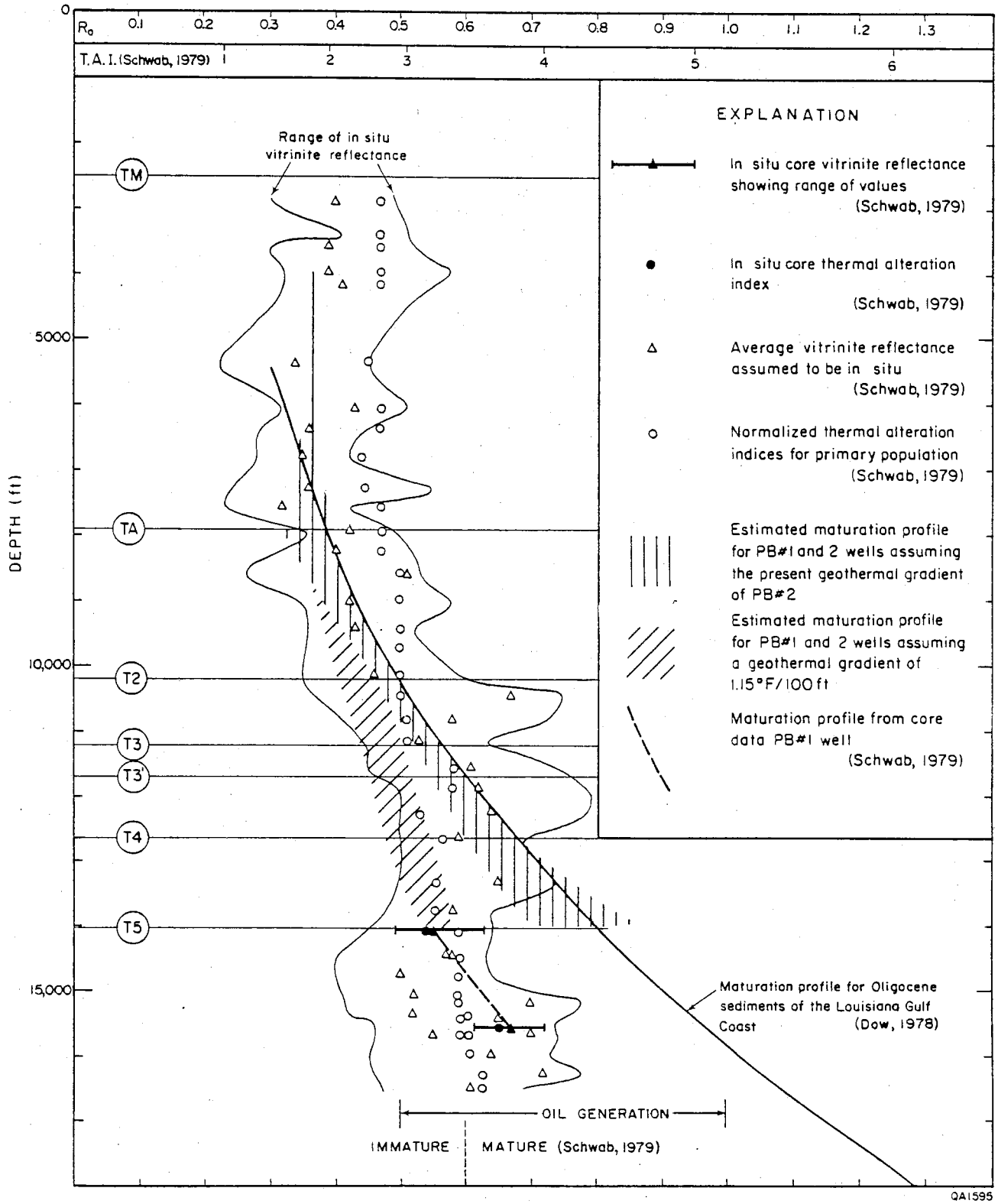

Figure IV-16. Vitrinite reflectance and thermal alteration index vs. depth for the Pleasant Bayou No. 1 well (Brown, 1979; Schwab, 1979). The reflectance profile is compared to the regional reflectance (Dow, 1978) and to calculated profiles using the present-day geothermal gradient at the test well and a low gradient of 1.15°F/100 ft.

values are 0.55 and 0.67, respectively. These values lie some 25 to 30 percent below the regional maturation profile for Oligocene sediments (Dow, 1978), as well as sediments tested in San Patricio and Cameron Counties. Cuttings analyses show that this anomalously immature section includes all strata below 12,500 ft.

Normal Present Geothermal Gradient

Temperature gradients in Brazoria County, as elsewhere in the Gulf Coast Tertiary basin, are not constant with depth but increase within the geopressured zone (Lewis and Rose, 1970; Gregory, 1979). Geothermal gradients have been estimated for the Pleasant Bayou wells (fig. IV-17) using equilibrium temperatures and the mean annual surface temperature of 70°F (McGowen and others, 1976). Temperatures for Pleasant Bayou No. 1 are consistently higher than those at equivalent depths in Pleasant Bayou No. 2 for unknown reasons (Gregory, 1979). The temperature gradient in the hydropressured Miocene to Recent strata (1.4°F/100 ft) is similar to the average for the prospect area (1.35°F/100 ft; Loucks and others, 1981) and to the average geothermal gradient for Oligocene rocks in Louisiana (Dow, 1978). The Anahuac and upper and middle Frio interval has a gradient of 1.75°F/100 ft in the Pleasant Bayou No. 2 well, similar to the gradient obtained from produced fluids in the Chocolate Bayou (East) field (1.72°F/100 ft). In the lower Frio section, the geothermal gradient is estimated at 2.04°F/100 ft, less than the average gradient for wells in Brazoria County below 11,000 ft (2.49°F/100 ft; Loucks and others, 1981).

Anomalous Silica Geothermometer Temperature

Formation water produced from the "F" sandstone in the Pleasant Bayou No. 2 well contained from 190 to 210 mg/L dissolved SiO_2 (Kharaka and others, 1979). This gives a temperature of equilibration with quartz of 178 $\pm$ 10°C, and the measured subsurface temperature is 152°C (fig. IV-18). Either the waters are sourced from a somewhat greater depth (Kharaka and others, 1979) or the solution was equilibrated to amorphous silica rather than quartz.

Uranium and Thorium Anomalies in the Lower Frio

Zones of anomalous radioactivity have been detected in the lower Frio in the Pleasant Bayou test well by logging with the Spectralog tool (described by Fertl, 1979, and Hotz and Fertl, 1981). These zones have uranium concentrations from 8 to over 21 ppm and thorium/uranium ratios of less than 2 (table IV-1), suggesting that the sediments contain a major

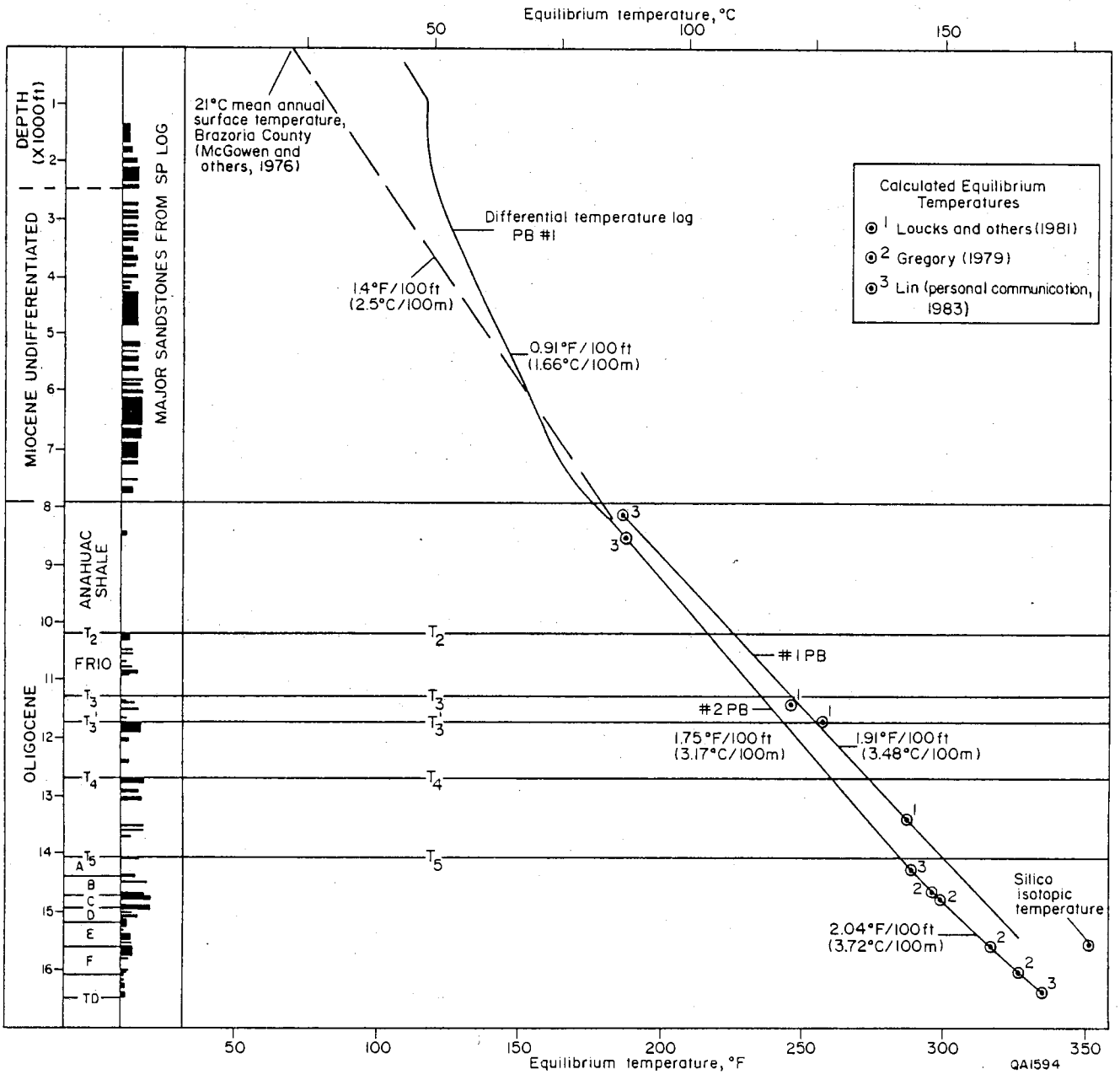

Figure IV-17. Well-log temperature corrected to equilibrium values vs. depth, Pleasant Bayou No. 1 and No. 2 wells.

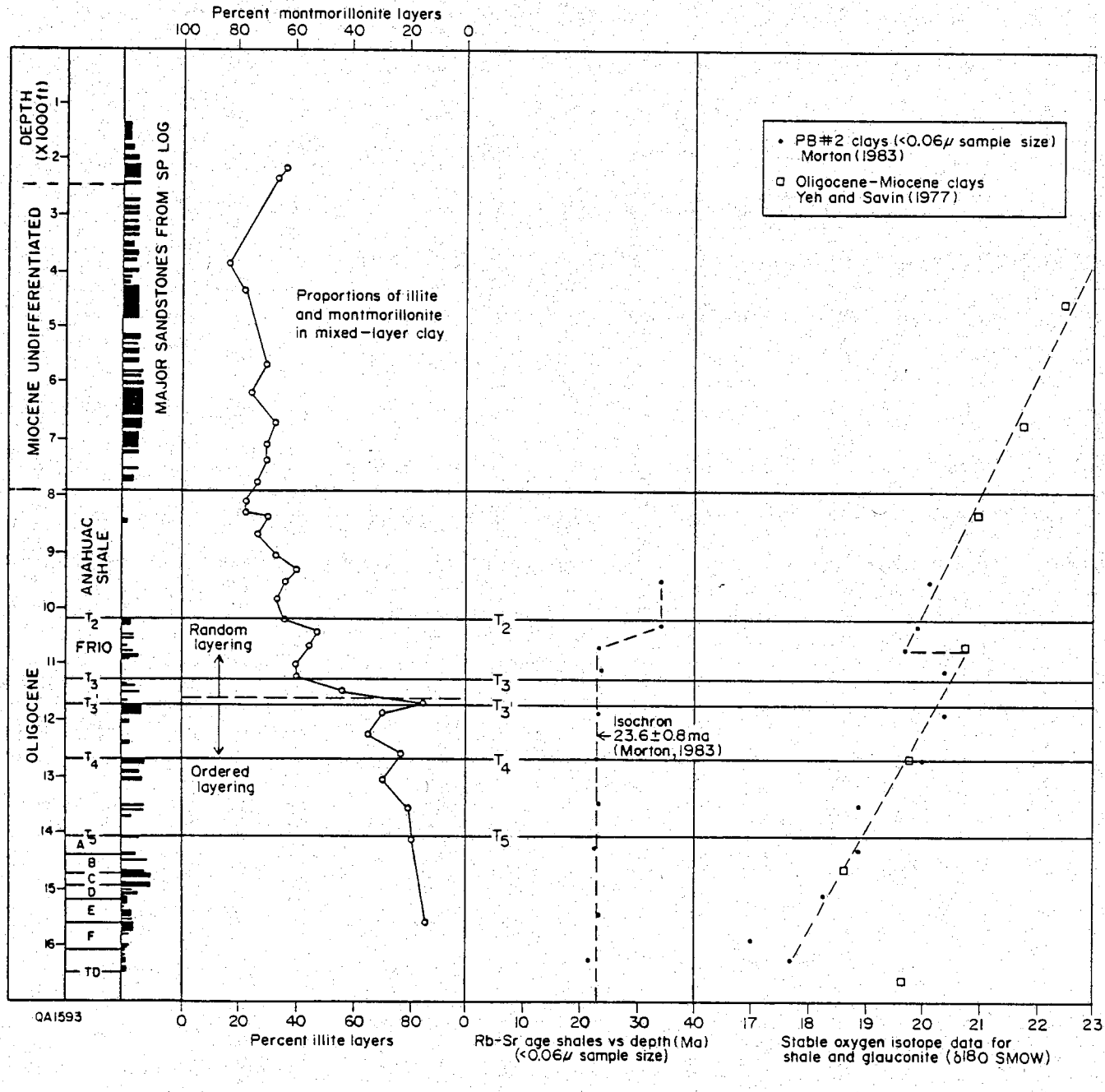

Figure IV-18. Proportion of illite and smectite in mixed-layer clays vs. depth, Pleasant Bayou No. 1 well (Freed, 1979); apparent Rb-Sr age of clays <0.06μm in diameter vs. depth in the test well (Morton, 1983); and oxygen isotope values for shale and glauconite vs. depth in the test well (Yeh and Savin, 1977; Morton, 1983).

Table IV-1. Potassium (K), uranium (U), and thorium (Th) distribution in the GCO-DOE Pleasant Bayou No. 2 well.

Lithology	Depth interval (ft)		K(%)	U (ppm)	Th (ppm)	$\frac{Th}{U}$
Sandy silt	14,316	14,321	> 14.5	21	9.5	0.45
Silty shale	14,467	14,472	> 14.5	> 21	> 20	
Silty shale	14,586	14,605	> 14.5	20	16	0.80
Sandy silt	14,967	14,971	> 14.5	18	7	0.39
Silty shale	15,466	15,469	> 14.5	16	10.5	0.66
Shale	15,590	15,600	3	11.5	16	1.39
Silty shale	15,965	15,969	> 14.5	> 21	> 20	
Silty shale	16,315	16,317	> 14.5	8	10	1.25

bentonitic or volcanic ash component (Fertl, 1979). They may be similar to fluvial and crevasse-splay muds of the updip Catahoula Formation, which contain up to 12 ppm uranium; lacustrine muds contain up to 35 ppm (Galloway, 1977).

Uranium in excess of 20 ppm in volcanic ash of the Catahoula Formation is considered to be enriched, whereas concentrations under 5 ppm are depleted (Galloway, 1977). By this standard, the ash zones detected in the Frio at Pleasant Bayou have not undergone substantial enrichment.

Smectite-Illite Transformation and Geochronometry

Smectite undergoes transformation to the ordered mixed-layer 20 percent smectite/80 percent illite as temperature and pressure increase owing to burial (Burst, 1969; Boles and Franks, 1979). Although this transformation is partly controlled by temperature (Loucks and others, 1981), other factors must also play a role. In the Pleasant Bayou No. 1 well, this transformation occurs between the T3 and T3' markers (fig. IV-18; Freed, 1979) at about 11,500 ft or 119-123°C. This is 25-30°C higher than in Hidalgo County in South Texas (Loucks and others, 1981). The transformation occurs near the uppermost major marine sandstone unit in the Frio, the uppermost appearance of geopressure in the sandstones, and the upper limit of anomalously low vitrinite reflectance.

From strontium isotope data, Morton (1983) has documented an isochron in all samples of the clay fraction less than 0.06 μm in diameter below 10,500 ft (near T2) of 23.6 ± 0.8 Ma, with an initial ratio approximating that of seawater (fig. IV-19). The highest shale sample falling on this isochron corresponds to a break in the linear trend of oxygen isotope ratios for clay minerals in the area (Morton, 1983). He interpreted this date as the age of the smectite-illite transition. The 23.6 Ma age is stratigraphically equivalent to the T2 mid-Anahuac interval, which is 500 to 2,000 ft higher. Morton suggested that at this time the Frio, which had been rapidly depressed, released a flood of potassium from K-feldspar dissolution that converted the smectite to illite. He estimated that this conversion occurred at a temperature of 65 to 75°C from oxygen isotope data.

High and Variable Salinity

Salinity values in the Pleasant Bayou wells have been measured by Kharaka and others (1979) and calculated by Z. S. Lin for this project from the SP logs using algorithms of Bateman and Konen (1977) as modified by Dunlap (1980) for lignosulfonate muds. Measured values exist only for the two completed intervals, but calculated values for those intervals show good agreement. No technique exists for measuring salinity values in shale pore water.

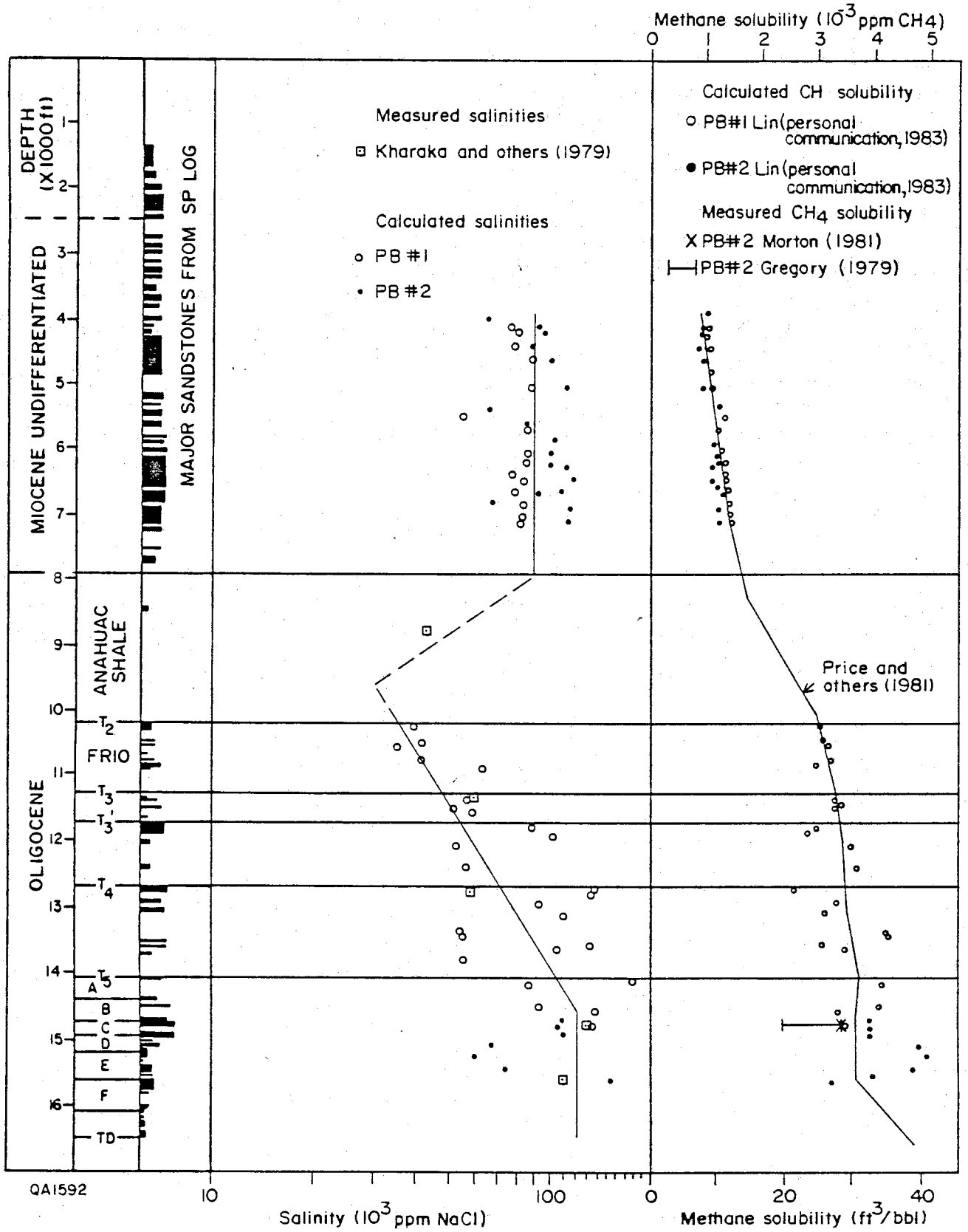

Figure IV-19. Salinity and methane solubility vs. depth, Pleasant Bayou No. 1 and No. 2 wells.

Salinity in the Miocene sandstones is nearly constant and considerably higher than that in the uppermost Frio sandstones (fig. IV-19). Below T2, the salinity increases with depth to values equal and greater than the lower Miocene values. This may result from the mixing of deep saline waters with shallower, less saline waters (Morton and others, 1983b). Hydrogen and oxygen isotope data indicate that the formation waters are modified marine connate waters of the NaCl type (Kharaka and others, 1979). Waters within the geopressured zone are not chemically compatible with waters in the overlying, normally pressured zone (Kharaka and others, 1979). These authors proposed that the high salinity of lower Frio waters (higher than waters in nearby oil and gas fields) results from dissolution of salt at Danbury Dome; Cl/Br ratios are substantially higher than the evaporation line for seawater. Concentrations of Fe, Mn, Pb, and Zn are also greater in deep Pleasant Bayou waters than in nearby oil and gas fields (Kharaka and others, 1979).

Estimated methane solubility within the Frio reservoirs ranges from 25 scf/bbl at T2 to 27-35 scf/bbl below T5, compared to the actual solubility of 29 scf/bbl for the "C," or Andrau, sandstone (Morton, 1981). Testing of sub-T5 reservoirs indicates that the water is saturated with methane (Gregory, 1979; Kharaka and others, 1979). The produced gas has a substantial CO_2 content.

A slight crossover of the neutron porosity and density logs in the Pleasant Bayou No. 2 well in two intervals of the lower Andrau sand suggests possible free gas (fig. IV-12A). This occurs below a thin matrix-rich impermeable zone seen in the core and may indicate a local stratigraphic trap. More extensive though erratic crossover in the "F" sandstones indicates free gas in the more porous and permeable units (fig. IV-12B).

Wet Gas in Lower Frio Shales

Wetness is low above T3' in the test wells and decreases further in the T3' to T5 interval, despite a hundredfold increase in C5-C7 content (fig. IV-20; Brown, 1979). The large increase in C5 to C7 corresponds to the break in the vitrinite-reflectance profile. Wetness exceeds 50 percent below T5, however, and there is an associated increase in the C15+ hydrocarbon content. Although the sub-T5 interval has reached moderate thermal maturity, the rock is too organic-poor (total organic carbon less than 5 percent) to form a major petroleum source rock.

THERMAL EVOLUTION OF THE PLEASANT BAYOU AREA

Modeling of Vitrinite and Thermal Alteration Index Data

From examination of the vitrinite-reflectance profile obtained for Pleasant Bayou test wells (fig. IV-16), it is apparent that no simple conductive model is adequate. The observed

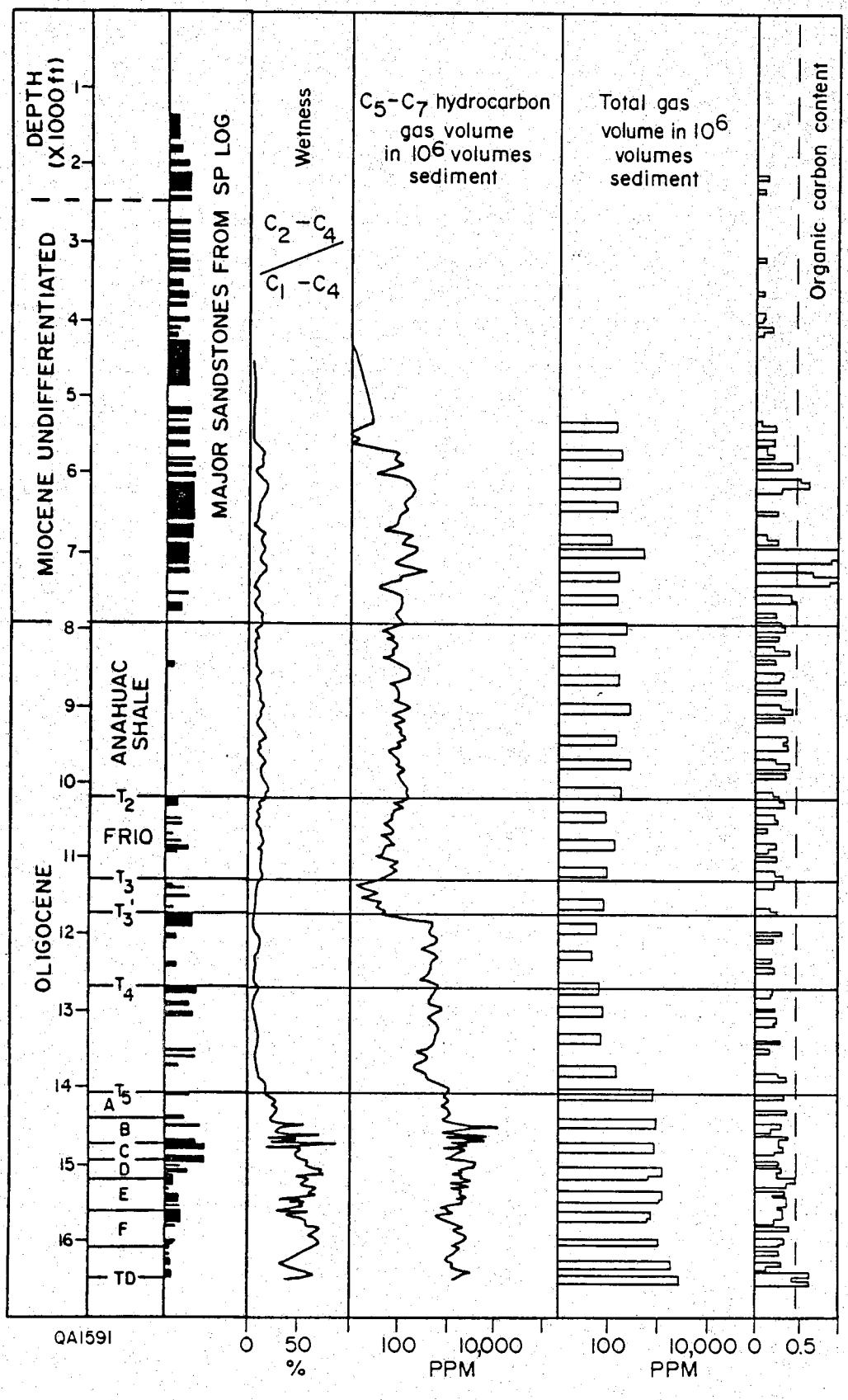

Figure IV-20. Organic geochemistry of shale extracts vs. depth, Pleasant Bayou No. 1 well (Brown, 1979).

maturity, both from core vitrinite reflectance and from TAI analyses, is lower below T4 than that which the present (and the apparent regional) geothermal gradient gives when applied over the burial history of those strata.

In order to evaluate the maturity profile of the Pleasant Bayou wells, a burial history plot (using sediment thicknesses decompacted after Sclater and Christie, 1980) was constructed (fig. IV-21). Using this plot, the maturity of the marker horizons was estimated by the methods of Cooper (1977), Waples (1980), and Royden and others (1980) for various geothermal regimes.

Successful models fall into two main groups. The first group assumes a uniform heat flux through time, represented by the present geothermal gradient of Pleasant Bayou No. 2, upon which was superimposed a cooling effect caused by shallower waters passing through the lower Frio sandstones (fig. IV-21A). These models demand that the water flow be stopped in the last 5 Ma (millions of years) so that the temperature gradient could rise to its present value.

The second group of models assumes an initially low geothermal gradient (1.15°F/100 ft) upon which was superimposed a heating effect caused by the flow of deeper basinal waters through sandstones between T2 and T4 (fig. IV-21B). This low temperature gradient continued for some 17 to 20 Ma and then increased in the last 10 Ma to reach the observed gradient in the test well.

The first group of models is consistent with the fairly uniform burial rate of the Frio (Galloway and others, 1982b). Maturation profiles derived for Oligocene sediments in the Gulf Coast and for wells in Cameron and San Patricio Counties use an average geothermal gradient of 1.4°F/100 ft (fig. IV-16) (Dow, 1978; Dow, 1981; Dow and Page, 1981). However, this requires cooling of the undermature lower Frio interval in the test well. Such cooling could only come from fluids descending from areas at least 2,000 to 3,000 ft shallower. Such fluids could have been derived from the crest of the Chocolate Bayou dome, for example, but only if there were some outlet to the west or southwest. The low-pressure outlet in this case could be Danbury piercement salt dome, where the Andrau may intersect the zone of deformation surrounding the dome. Ascending fluid flow around salt domes is known elsewhere and is inferred to form both false cap rock and metal deposits in cap rock (Price and Kyle, 1983). A similar flow system is currently active within the sub-T5 Andrau sand in the Chocolate Bayou (West) field, as attested by tilted gas-water contacts (Fowler, 1970). Hydrodynamic flow of the magnitude required would demand an essentially hydropressured lower Frio interval until the Pliocene.

A fluid source for such a model is more difficult to find. Burst (1969) calculated that the amount of interlayer water expelled during clay diagenesis is 10 to 15 percent of the compacted bulk volume. This water is thought to be less saline than aquifer brines. However, in a

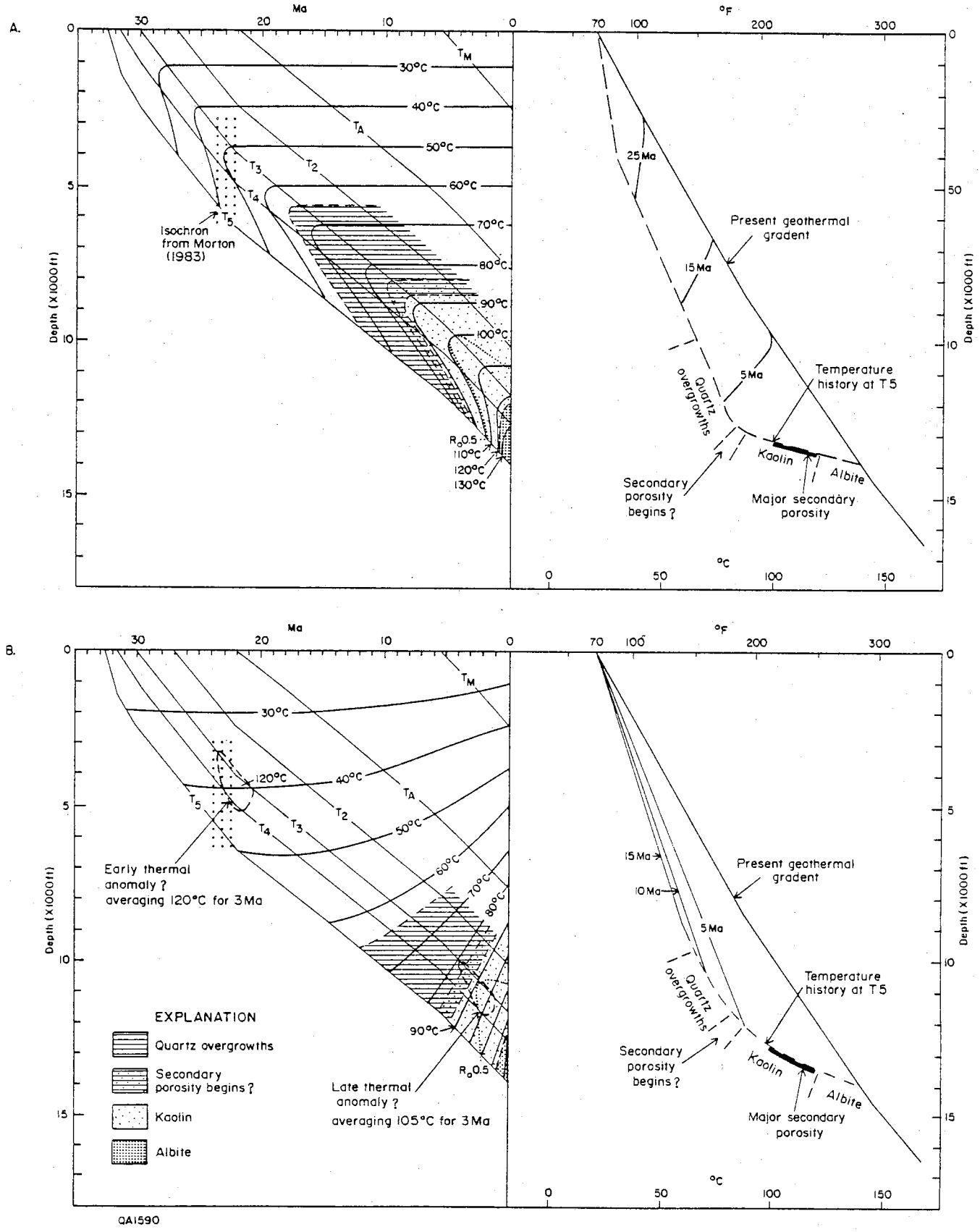

Figure IV-21. Models for thermal and diagenetic evolution of the Pleasant Bayou No. 2 well, constrained by burial history, present geothermal gradient, and observed vitrinite reflectance. (A) Model with present gradient and flow of cool fluids. (B) Model with low past gradients and flow of hot fluids.

geopressured system, lithostatic pressure is reduced, which inhibits the expulsion of interlayer water (Loucks and others, 1981). This water is one source of aquifer fluids to support a hydrodynamic system. However, the present-day waters in the sub-T5 sandstones are highly saline and Br-depleted, indicating that these waters are not largely derived from shale dewatering and may have a component of halite dissolution. Thus either the present-day waters are different from those that occurred before 5 Ma, or the fluid source was something other than compaction.

The second group of models poses two anomalies. Why the Pleasant Bayou area should have remained anomalously cool for 17 to 20 Ma and then heated up to the regional normal gradient is not evident. Early depression of isotherms caused by rapid loading should have been recouped gradually since deposition; but cool temperatures to recent times are needed to produce the observed maturities. Also, an additional flow of hot fluids must be superimposed on this anomalously low background gradient to produce the present profile; however, these fluids must not have flowed through the highly transmissive Andrau and other lower Frio sandstones. To fit the observed anomaly, these fluids could have affected the section either early in the burial history, at the time suggested by the illite isochron, or late, within the last 3 to 6 Ma. The late event requires a lower temperature, only 20°C greater than the estimated background temperature at that time.

Significance of the Illite Geochron

The temperature range of the smectite-illite transition (65 to 75°C, according to Morton, 1983) could not have been reached at the T5 horizon before 16 Ma ago, according to either class of models (fig. IV-21). The highest shale sample showing the 23.6 Ma date was taken some 1,000 ft above the top of the major smectite-illite transition (Morton, 1983). The lack of correspondence between the top of the 23.6 Ma clays, the depth of the Anahuac sediments deposited at about that time, and the depth of the main smectite-illite transition suggests that the setting of the Rb-Sr clock and the formation of illite may be separate diagenetic events. In calculating the temperature of illite formation, Morton (1983) assumed that the clay in the shales and the quartz overgrowths in the interbedded sandstones were formed in isotopic equilibrium. If this is not valid, the smectite-illite transition may have occurred at temperatures as low as 45°C (W. R. Kaiser, personal communication, 1983) and earlier than the quartz overgrowths.

The 23.6 Ma isochron may represent the time of effective sealing of recharge and discharge areas of the early Frio meteoric system by the transgressive upper Frio and Anahuac shale. This isolation would result in the reequilibration of the stagnant ground-water flow

system from an early, more oxidizing environment to a reducing environment (Garrels and Christ, 1965; Galloway, 1977). An increase in K/Na ratio could then lead to illite formation. Deep saline waters in Brazoria County are characterized by high K/Na (Kaiser and Richmann, 1981).

Expulsion of the compaction waters from shale transports cations released in the smectite-illite transition into sandstones, where they may precipitate as authigenic phases (Loucks and others, 1981). The plots of time, temperature, and depth for the two maturity models of figure IV-21 suggest that the major diagenetic phase of quartz overgrowths may have begun some 8 to 13 Ma ago in the sub-T5 strata. The formation of secondary porosity below 10,000 ft, which postdates quartz overgrowth development and predates major kaolin formation, must be even younger, as shown on the temperature profiles of figure IV-21. The late albitization, which has the highest isotopic temperatures, is very late (after 2 Ma) and still continuing.

It has been proposed that the release of Ca^{2+} ions from the albitization of feldspar and the release of CO_2 from humic organic matter are chiefly responsible for the occlusion of primary and secondary porosity at depth. If so, the preservation of very high porosity and permeability in the lower Frio aquifers at Pleasant Bayou may depend on the anomalously cool thermal history of the area. In more "normal" areas, extensive albitization would have caused calcite occlusion of porosity at the depths of the lower Frio strata.

Implications for the Origin of Geopressure

As described above, the pressure profile of the Pleasant Bayou area falls into four divisions: (1) an upper zone of normally pressured sandstone and shale overlying (2) a zone of normally pressured sandstones and overpressured shales, (3) a zone of moderately overpressured sandstones and more greatly overpressured shales, and, deepest, (4) a zone of highly overpressured sandstones and shales. This last zone is thermally undermature. The sandstones in zone 2 have a sufficiently high permeability and continuity updip across the growth fault (Fowler, 1970) that they are maintained at hydrostatic pressure. Fowler (1970) correlated the increasing overpressures in zone 3 sandstones to upward fluid flow through relatively impermeable shales (and linked this to observed salinity variations); however, log-derived shale-fluid pressures are greater than those of the sandstones, indicating pressure sealing. Therefore, upward flow is unlikely in zones 2 and 3 at Chocolate Bayou dome, except along the many small faults. The sandstones of zones 3 and 4 have a decreasing ability to bleed off overpressure, owing to generally lower porosity and permeability and increasing geometric isolation.

The zone 4 Andrau sandstone is the conspicuous exception. Although it is currently highly geopressured (and therefore sealed), it is highly permeable. As noted above, one model for the thermal history of Pleasant Bayou requires that this high geopressure is a recent development. At an earlier stage, it may have been similar to the present-day Andrau system in the Chocolate Bayou (West) fault compartment, which forms a normally pressured channel within geopressured units draining towards Danbury Dome (Fowler, 1970). If this is true, then geopressure in the Andrau aquifer is not the result of primary geometric isolation but of repressurization. The anomalously low-pressure "F" sand intervals might represent part of the early system that has been incompletely repressurized. Part of this repressurization must have been from the surrounding shales, although their smectite water may have been liberated somewhat earlier (fig. IV-21). The water chemistry suggests that repressurization may have occurred by equilibration with basinal brines, possibly across the South Chocolate Bayou growth fault.

The second model requires an initially low geothermal gradient. Because the thermal conductivities of the sediments are not likely to be abnormal, this implies a lower than usual heat flux. The transgressive Anahuac shales effectively sealed the recharge and discharge areas of the previous Frio meteoric system, perhaps at 23.6 Ma. Under these circumstances, the K/Na ratio of the fluids rose, as they were linked to regions of active feldspar dissolution. Isolation of the sands and shales simultaneously led to geopressuring and the formation of 80 percent illite. After 13 Ma hot, saline, acidic fluids migrating laterally through the system introduced hydrocarbons and produced secondary porosity and anomalous maturity. This migration may have been connected with elevation of heat flux to the present values.

POSSIBLE HYDRODYNAMIC MODELS

Several workers in recent years have attempted to chart the migration of fluids, especially hydrocarbon-bearing basinal brines, within moderately geopressured zones in the Gulf Coast Basin (Kumar, 1977; Harrison, 1980). For the most part, these studies have relied entirely on maps and sections showing pressure (or head; Hanor and Bailey, 1983), temperature, and salinity. In order to determine if such an attempt is warranted at Chocolate Bayou, we have examined the sources of error inherent in these maps and have tried to predict what variations are significant.

Pressure

Three methods are used to determine pressures. The drill-stem test is measured after drilling and completion in a sandstone reservoir. Before 1970, measurements of formation fluid

pressure (bottom-hole shut-in pressure, or BHSIP) had instrumental errors of 20 to 30 psi. Recent instrumentation has improved this accuracy to a few psi (Z. S. Lin, personal communication, 1983). Because most of the wells in the Pleasant Bayou area were drilled before 1970, pressure variations of 60 psi are expected to be meaningful on instrumental grounds. However, what is of interest is the virgin pressure of the aquifer--or of a hydrocarbon field, especially at the hydrocarbon-water contact. Typically, BHSIP is obtained in a productive gas (or oil) reservoir, which often has been produced for some time and has been drawn down by an amount that depends on the reservoir drive. Therefore, only those pressure measurements taken before any significant production from a reservoir (or its attached aquifer) can be used. This generally limits the usable data to one per productive sandstone of each fault compartment.

The other two methods calculate pressures from geophysical logs and determine the fluid pressures within shale units. The first, using shale-resistivity plots, involves first the determination of a normal compaction curve for the area, against which the undercompacted and hence less resistive geopressured shales can be compared (Hottman and Johnson, 1965). This is subject to numerous uncertainties, as this normal curve varies from area to area, is not easily extrapolated, and is a fit of a scatter plot. Furthermore, as normally pressured units are rarely found at geopressured depths in a given area, the normal curve cannot be empirically located at depths of primary interest. Also, it is assumed that normally pressured sandstones have normally pressured shales above and below them, which does not appear to be true at Chocolate Bayou. In addition, the calculation of a geostatic ratio is based on an empirical fit of the ratio (or effective stress) against a resistivity ratio. This plot has much scatter, and no adequate line could be drawn in the Brazoria County area (fig. IV-15). Also, the onset of geopressure at Chocolate Bayou is transitional and occurs near the bend in the assumed normal compaction curve (fig. IV-22). This makes the calculation of geostatic ratio by this method virtually meaningless in zone 2. Gregory (1979) suggested an error of about 2,000 psi in the method; pressures need to vary more than 2,000 to 4,000 psi to be meaningful.

The other calculation method uses travel times within shale (from sonic log data) to calculate pressure; overpressured shales are undercompacted and hence have longer acoustic travel times. The method shares many of the problems of shale resistivity but is improved because the normal curve is based on a straight-line extrapolation of shallow, normally pressured shales. However, the difference between the normal line and the undercompacted shales is slight (fig. IV-13), so that residual extrapolation errors or well-specific errors (note the variation between the No. 1 and No. 2 wells on fig. IV-13) can occur, and possible mineralogic or structural changes in shale (Winker and others, 1983) can create large errors. Gregory (1979) estimated an error of 1,500 psi at depths of interest.

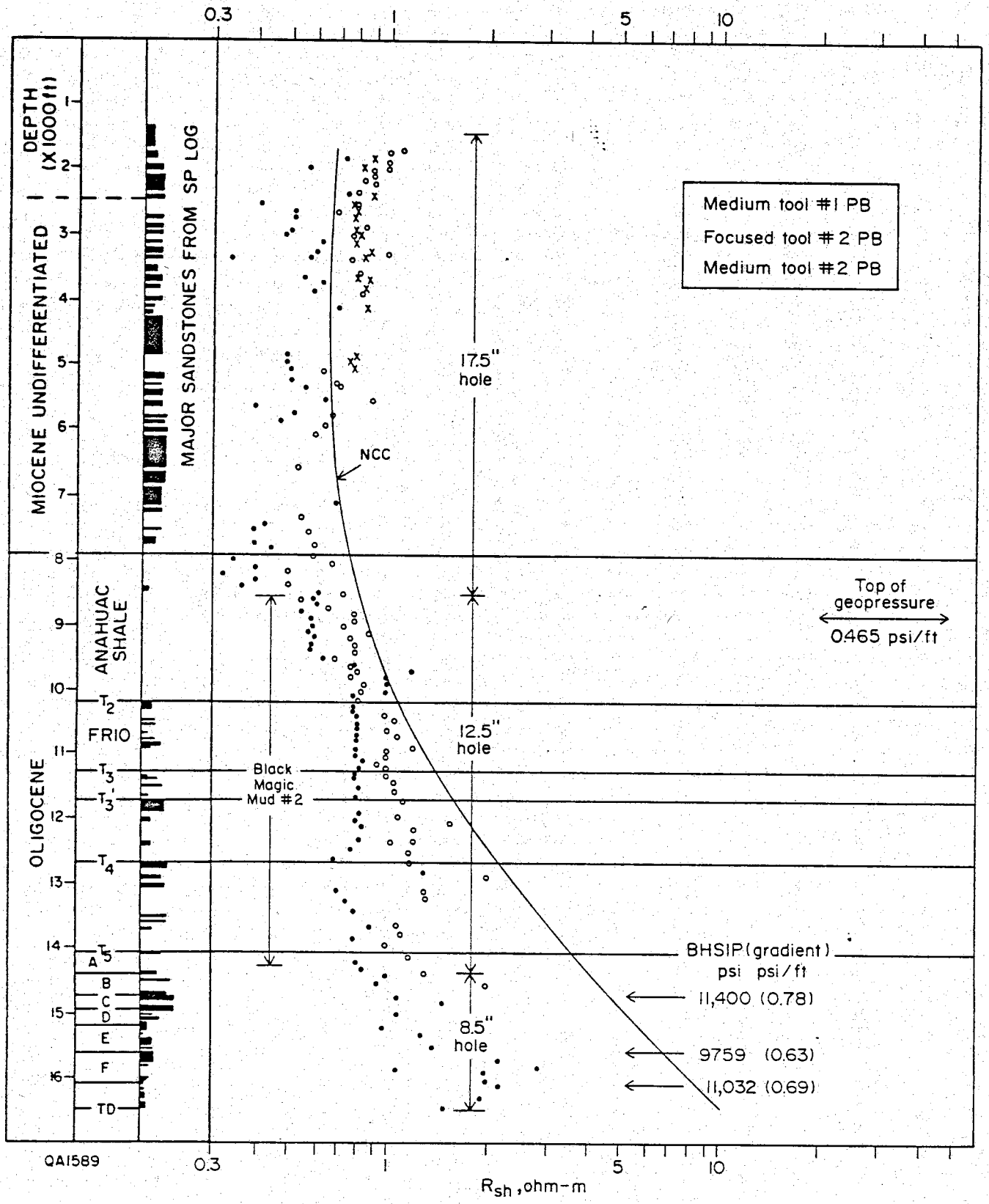

Figure IV-22. Shale resistivity vs. depth, Pleasant Bayou No. 1 and No. 2 wells (from Gregory, 1979).

From this it is evident that pressure, the critical element in a hydrodynamic model, is elusive. Although qualitative ideas and trends may be obtained, contouring in any detail seems unreasonable. In particular, the conversion to head advocated by Hanor and Bailey (1983), although technically preferred, yields an insignificant improvement in the quality of interpretation over geostatic ratio plots. Pressure data from sandstones is reliable but generally not sufficiently abundant for two- or three-dimensional modeling.

Temperature

Temperature values can be obtained by two methods. One method, actual wellhead measurement, is generally only possible for completed wells. It may be affected by some cooling in the wellbore and minor measurement errors, but it is probably reliable. However, the data are limited to completed intervals.

More generally, equilibrium temperature values are obtained by correcting well-log temperatures by the method of Kehle (1971). Comparing these corrected temperatures against measured values shows that the calculated temperatures underestimate the true temperatures by up to 40°F (Bebout and others, 1978) and show a large scatter of 20° to 30°F (fig. IV-23). The calculated temperatures from the test wells show a systematic difference of about 17°F throughout the Frio section (fig. IV-17). This indicates that only temperature variations in excess of 40°F can be realistically mapped in the Chocolate Bayou area.

Also, to draw up the temperature maps used in migration detection, the sparse BHT data must be interpolated to yield enough values. This interpolation, generally done without any evaluation of variable conductivities, must also introduce errors. If there were pronounced fluid flow, as suspected in the Andrau aquifer, these errors could be severe.

Salinity

Salinity, like temperature, can be either measured or calculated. Measured wellhead salinities are subject to some errors, particularly resulting from condensation, as discussed by Morton and others (1981). Those authors indicated that salinity variations of 10 percent or less are attributable to sampling and analytical error.

More generally, salinity is calculated from the resistivity of formation water. These calculations have been shown in the past to be subject to serious mud-dependent errors in the geopressured zone. In the Chocolate Bayou area, the measured salinity values (total dissolved solids) have been compared to salinities calculated using the algorithm of Bateman and Konen (1977), with adjustments for the mud system used. This comparison (fig. IV-24) shows a rather good correlation, with a standard deviation of about 8,000 ppm. This, at the data centroid, is

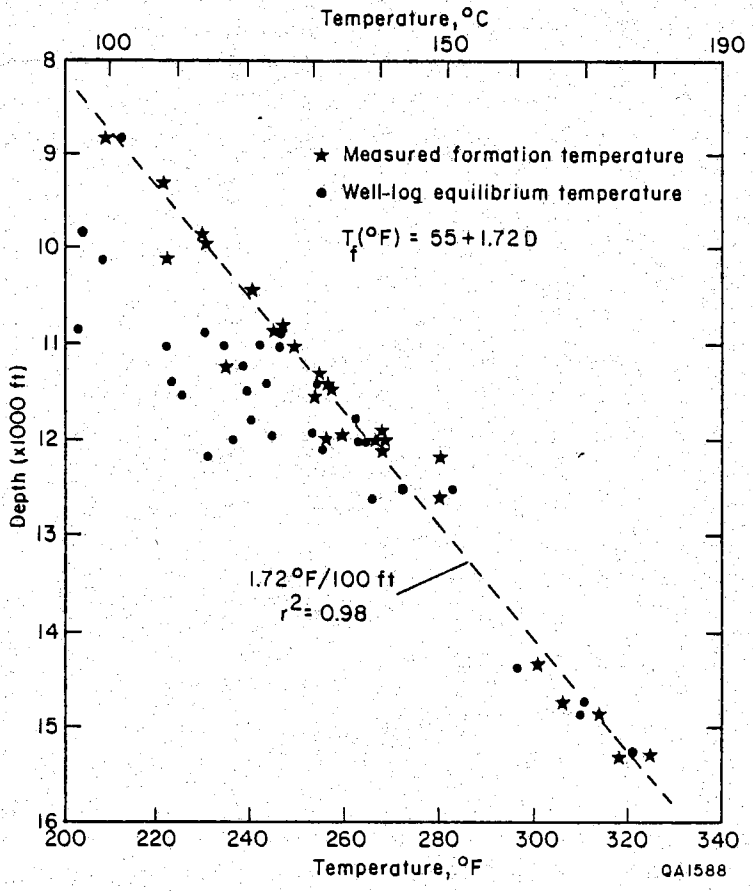

Figure IV-23. Temperature vs. depth for Chocolate Bayou area wells; measured fluid samples vs. corrected well-log temperatures.

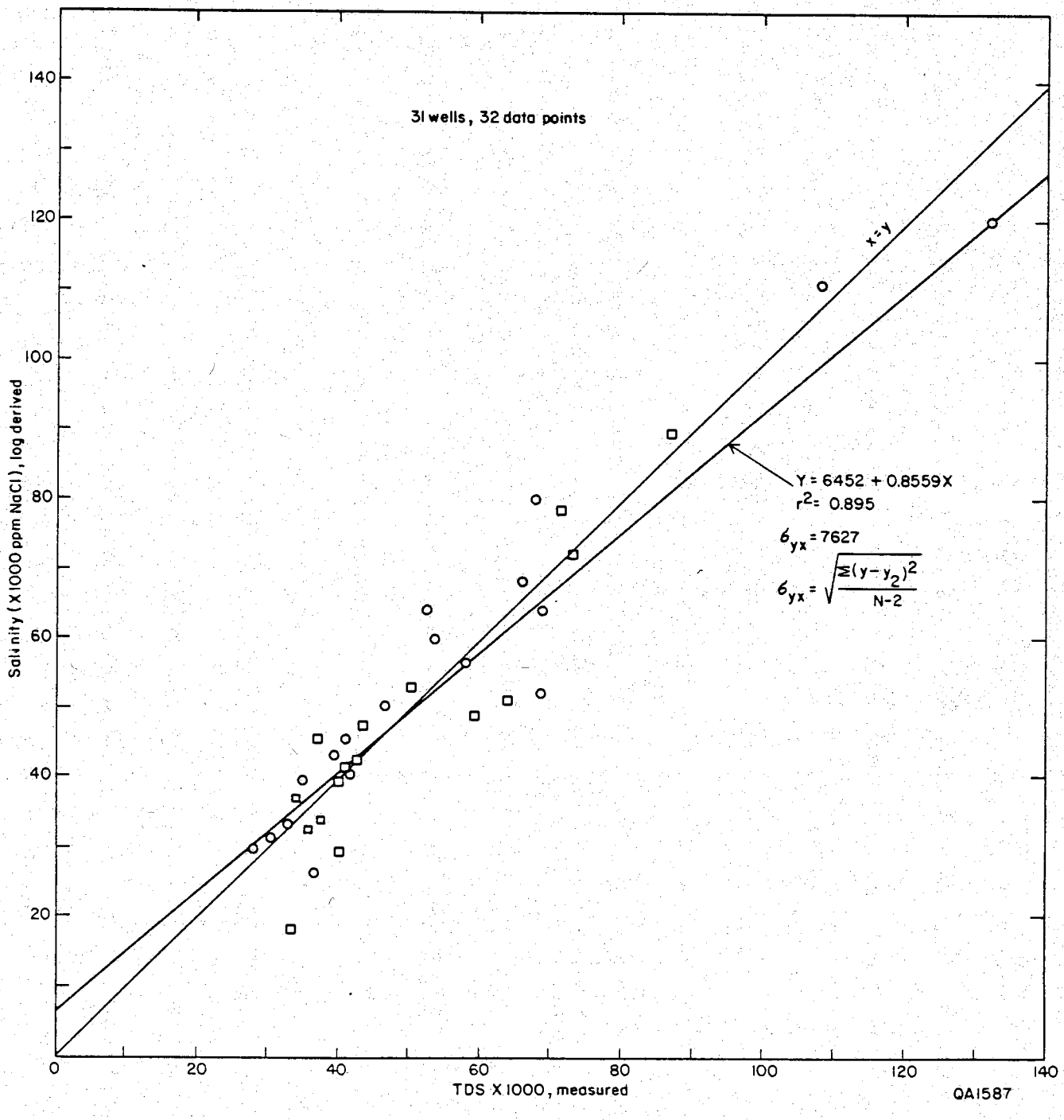

Figure IV-24. Measured vs. calculated salinities in the Chocolate Bayou area.

about 15 to 20 percent error, perhaps twice the error estimate in the measured values. It is unknown, however, if a similarly small error would hold elsewhere on the Gulf Coast.

It appears, then, that salinity variations (using calculated values) of more than about 10,000 ppm may be considered to reflect real differences in waters of the Chocolate Bayou area but should be treated with caution.

In summary, of the three parameters generally used to define fluid migration, the most important (pressure) is the least certain; any anomalies must be viewed with great suspicion unless based on initial BHSIP data from aquifers. Temperature is somewhat better, but has uncertainties of up to 40°F. Salinity may have the best resolution to define fluid flow, with sensitivity of about 10,000 ppm in the Chocolate Bayou area.

ACKNOWLEDGEMENTS

We wish to thank R. A. Morton, W. E. Galloway, and W. R. Kaiser for valuable discussions; Z. S. Lin for calculation of salinity data and general engineering concepts; and W. A. Fowler for discussion of maturity data. The text was typed by Dottie C. Johnson under the direction of Lucille C. Harrell. Illustrations were drafted by John T. Ames, Mark T. Bentley, Thomas M. Byrd, and Jeff Horowitz under the direction of R. L. Dillon. Funding for this research was provided by the U.S. Department of Energy, Division of Geothermal Energy, under Contract No. DE-AC08-79ET27111.

REFERENCES

Anderson, R. A., Ingram, D. S., and Zanier, A. M., 1972, Fracture pressure gradient determination from well logs: Society of Petroleum Engineers, preprint of paper SPE4135 presented at 47th annual meeting, 15 p.

Bateman, R. M., and Konen, C. E., 1977, The log analyst and the programmable pocket calculator: Log Analyst, v. 18, no. 5, p. 3-11.

Bebout, D. G., Loucks, R. G., Bosch, S. C., and Dorfman, M. H., 1976, Geothermal resources--Frio Formation, Upper Texas Gulf Coast: The University of Texas at Austin, Bureau of Economic Geology Geological Circular 76-3, 47 p.

Bebout, D. G., Loucks, R. G., and Gregory, A. R., 1978, Frio sandstone reservoirs in the deep subsurface along the Texas Gulf Coast--their potential for production of geopressured geothermal energy: The University of Texas at Austin, Bureau of Economic Geology Report of Investigations No. 91, 92 p.

_____ 1980, Geologic aspects of Pleasant Bayou geopressured geothermal test well, Austin Bayou prospect, Brazoria County, Texas, in Proceedings, Fourth Congress on Geopressured Geothermal Energy: The University of Texas at Austin, p. 11-45.

Boles, J. R., and Franks, S. G., 1979, Clay diagenesis in Wilcox sandstones of southwest Texas: implications of smectite diagenesis on sandstone cementation: Journal of Sedimentary Petrology, v. 49, no. 1, p. 55-70.

Bostick, N. H., 1973, Time as a factor in thermal metamorphism of phytoclasts (coaly particles): Septième Congrès International de stratigraphie et de géologie du Carbonifère, v. 2, p. 183-192.

Boulden, C. W., and Walk, H. G., 1979, General Crude No. 1 and No. 2 Pleasant Bayou geothermal test, Chocolate Bayou area, Brazoria County, Texas: unpublished reports by Eco-Pal.

Brown, S. W., 1979, Hydrocarbon source facies analysis, Department of Energy and General Crude Oil Company Pleasant Bayou No. 1 and 2 wells, Brazoria County, Texas, in Proceedings, Fourth Conference on Geopressured Geothermal Energy: The University of Texas at Austin, p. 132-152.

Burst, J. F., 1969, Diagenesis of Gulf Coast clayey sediments and its possible relationship to petroleum migration: American Association of Petroleum Geologists Bulletin, v. 53, no. 1, p. 73-93.

Coleman, J. M., and Prior, D. B., 1980, Deltaic sand bodies: American Association of Petroleum Geologists Continuing Education Course Note Series No. 15, 171 p.

Cooper, B. S., 1977, Estimation of the maximum temperatures attained in sedimentary rocks, in Hobson, G. D., ed., Developments in petroleum geology: London, Applied Science Publishers, p. 127-146.

Dow, W. G., 1978, Petroleum source beds on continental slopes and rises: American Association of Petroleum Geologists Bulletin, v. 62, p. 1584-1606.

_____ 1981, Geochemical analysis of selected samples from Kelly Bell No. D-1 well, San Patricio County, Texas: Report No. 357 prepared for The University of Texas at Austin, Bureau of Economic Geology, by Robertson Research (U.S.), Inc., 25 p.

Dow, W. G., and Page, M. M., 1981, Geochemical evaluation of the Cameron Park and Development Company #1, Cameron County, Texas: Report No. 284 prepared for The University of Texas at Austin, Bureau of Economic Geology, by Robertson Research (U.S.), Inc., 36 p.

Dunlap, H. F., 1980, Study of log derived water resistivity data in Geo^2 Formations; Third Progress Report: The University of Texas at Austin, Department of Petroleum Engineering, p. 2-10.

Fertl, W. H., 1979, Gamma ray spectral data assists in complex formation evaluation, in Transactions, SPWLA Sixth Formation Evaluation Symposium: London, Dresser Atlas Publication No. 3335.

Flanigan, T. E., 1980, Pore fluid pressure regimes, Brazoria County, Texas: a preliminary study: The University of Texas at Austin, Master's thesis, 118 p.

Fowler, W. A., 1970, Pressures, hydrocarbon accumulation and salinities--Chocolate Bayou field, Brazoria County, Texas: Journal of Petroleum Technology, v. 22, p. 411-423.

Frazier, D. E., 1974, Depositional episodes: their relationship to the Quaternary stratigraphic framework in the northwestern portion of the Gulf Basin: The University of Texas at Austin, Bureau of Economic Geology Geological Circular 74-1, 28 p.

Freed, R. L., 1979, Shale mineralogy of the No. 1 Pleasant Bayou geothermal test well: a progress report, in Proceedings, Fourth Conference on Geopressured Geothermal Energy: The University of Texas at Austin, p. 153-167.

Galloway, W. E., 1977, Catahoula Formation of the Texas Coastal Plain--depositional systems, composition, structural development, ground-water flow history, and uranium distribution: The University of Texas at Austin, Bureau of Economic Geology Report of Investigations No. 87, 59 p.

Galloway, W. E., Garrett, C. M., Jr., Tyler, N., Ewing, T. E., and Posey, J. S., 1982a, Geological characterization of Texas oil reservoirs: The University of Texas at Austin, Bureau of Economic Geology, final report to the Texas Energy and Natural Resources Advisory Council, Energy Development Fund, Project No. 82-OU-1, 96 p.

Galloway, W. E., Hobday, D. K., and Magara, K., 1982b, Frio Formation of the Texas Gulf Coast Basin--depositional systems, structural framework, and hydrocarbon origin, migration, distribution, and exploration potential: The University of Texas at Austin, Bureau of Economic Geology Report of Investigations 122, 78 p.

Garrels, R. M., and Christ, C. M., 1965, Solutions, minerals and equilibria: New York, Harper and Row, 450 p.

Gregory, A. R., 1979, Geopressured formation parameters, geothermal well, Brazoria County, Texas, in Proceedings, Fourth Conference on Geopressured Geothermal Energy: The University of Texas at Austin, p. 235-311.

Hanor, J. S., and Bailey, J. E., 1983, Use of hydraulic head and hydraulic gradient to characterize geopressured sediments and the direction of fluid migration in the Louisiana Gulf Coast: Gulf Coast Association of Geological Societies Transactions, v. 33, p. 115-122.

Harrison, F. W., III, 1980, The role of pressure, temperature, salinity, lithology and structure in hydrocarbon accumulation in Constance Bayou, Deep Lake and Southeast Little Pecan Lake fields, Cameron Parish, Louisiana: Gulf Coast Association of Geological Societies Transactions, v. 30, p. 113-129.

Hottman, C. E., and Johnson, R. K., 1965, Estimation of Formation Pressures from Log-Derived Shale Properties: Journal of Petroleum Technology, v. 17, p. 717-723.

Hotz, R. F., and Fertl, W. H., 1981, Spectralog applications in complex formation evaluation, in Spectralog, Dresser Atlas, reprinted from Drilling-DCW: 3 p.

Kaiser, W. R., 1983, Predicting reservoir quality and diagenetic history in the Frio Formation (Oligocene) of Texas, in Morton, R. A., Ewing, T. E., Kaiser, W. R., and Finley, R. J., Consolidation of geologic studies of geopressured geothermal resources in Texas: The University of Texas at Austin, Bureau of Economic Geology, report prepared for the U.S. Department of Energy, Contract No. DE-AC08-79ET27111, p. 137-170.

Kaiser, W. R., and Richmann, D. L., 1981, Predicting diagenetic history and reservoir quality in the Frio Formation of Brazoria County, Texas, and Pleasant Bayou test wells, in Proceedings, Fifth Conference on Geopressured Geothermal Energy: The University of Texas at Austin, p. 67-74.

Kehle, R. O., 1971, Geothermal survey of North America: Annual report to Research Committee of the American Association of Petroleum Geologists, 31 p.

Kharaka, Y. K., Lies, M. S., Wright, V. A., and Carothers, W. W., 1979, Geochemistry of formation waters from Pleasant Bayou No. 2 well and adjacent areas in coastal Texas, in Proceedings, Fourth Conference on Geopressured Geothermal Energy: The University of Texas at Austin, p. 11-45.

Kumar, M. B., 1977, Geothermal and geopressure patterns of Bayou Carlin - Lake Sand area, south Louisiana: implications: American Association of Petroleum Geologists Bulletin, v. 61, p. 65-78.

Land, L. S., and Milliken, K. L., 1981, Feldspar diagenesis in the Frio Formation, Brazoria County, Texas Gulf Coast: Geology, v. 9, p. 314-318.

Lewis, C. R., and Rose, S. C., 1970, A theory relating high temperatures and overpressures: Journal of Petroleum Technology, v. 22, no. 1, p. 11-16.

Lindquist, S. J., 1977, Secondary porosity development and subsequent reduction, overpressured Frio Formation sandstone (Oligocene), South Texas: Gulf Coast Association of Geological Societies Transactions, v. 27, p. 99-107.

Loucks, R. G., Bebout, D. G., and Galloway, W. E., 1977, Relationship of porosity formation and preservation to sandstone consolidation history--Gulf Coast lower Tertiary Frio Formation: Gulf Coast Association of Geological Societies Transactions, v. 27, p. 109-120.

Loucks, R. G., Dodge, M. M., and Galloway, W. E., 1979a, Importance of secondary leached porosity in lower Tertiary sandstone reservoirs along the Texas Gulf Coast: Gulf Coast Association of Geological Societies Transactions, v. 29, p. 164-171.

_____ 1979b, Sandstone consolidation analysis to delineate areas of high-quality reservoirs suitable for production of geopressured geothermal energy along the Texas Gulf Coast: The University of Texas at Austin, Bureau of Economic Geology, report prepared for the U.S. Department of Energy, Contract No. EG-77-5-05-5554, 97 p.

_____ in preparation, Factors controlling porosity and permeability of hydrocarbon reservoirs in lower Tertiary sandstones along the Texas Gulf Coast.

Loucks, R. G., Richmann, D. L., and Milliken, K. L., 1980, Factors controlling porosity and permeability in geopressured Frio sandstone reservoirs, General Crude Oil/Department of Energy Pleasant Bayou test wells, Brazoria County, Texas, in Proceedings, Fourth Congress on Geopressured Geothermal Energy: The University of Texas at Austin, v. 1, p. 46-82.

_____ 1981, Factors controlling reservoir quality in Tertiary sandstones and their significance to geopressured geothermal production: The University of Texas at Austin, Bureau of Economic Geology Report of Investigations No. 111, 41 p.

Lundegard, P. D., Land, L. S., and Galloway, W. E., in press, The problem of secondary porosity: Frio Formation (Oligocene), Texas Gulf Coast: Geology.

McGowen, J. H., Brown, L. F., Jr., Evans, T. J., Fisher, W. L., and Groat, C. G., 1976, Environmental geologic atlas of the Texas Coastal Zone--Bay City - Freeport area: The University of Texas at Austin, Bureau of Economic Geology, 98 p.

Milliken, K. L., Land, L. S., and Loucks, R. G., 1981, History of burial diagenesis determined from isotopic geochemistry, Frio Formation, Brazoria County, Texas: American Association of Petroleum Geologists Bulletin, v. 65, p. 1397-1413.

Morton, J. P., 1983, Age of clay diagenesis in the Oligocene Frio Formation, Texas Gulf Coast: The University of Texas at Austin, Ph.D. dissertation, 33 p.

Morton, R. A., 1981, Pleasant Bayou #2--a review of rationale, ongoing research and preliminary test results, in Proceedings, Fifth Conference on Geopressured Geothermal Energy: The University of Texas at Austin, p. 55-57.

Morton, R. A., Ewing, T. E., and Tyler, Noel, 1983a, Continuity and internal properties of Gulf Coast sandstones and their implications for geopressured fluid production: The University of Texas at Austin, Bureau of Economic Geology Report of Investigations No. 132, 70 p.

Morton, R. A., Garrett, C. M., Jr., Posey, J. S., Han, J. H., and Jirik, L. A., 1981, Salinity variations and chemical compositions of waters in the Frio Formation, Texas Gulf Coast: The University of Texas at Austin, Bureau of Economic Geology, report prepared for the U.S. Department of Energy, Contract No. DE-AC08-79ET27111, 96 p.

Morton, R. A., Han, J. H., and Posey, J. S., 1983b, Variations in chemical compositions of Tertiary formation waters, Texas Gulf Coast, in Morton, R. A., Ewing, T. E., Kaiser, W. R., and Finley, R. J., Consolidation of geologic studies of geopressured geothermal resources in Texas: The University of Texas at Austin, Bureau of Economic Geology, report prepared for the U.S. Department of Energy, Contract No. DE-AC08-79ET27111, p. 63-136.

Price, L. C., Blount, C. W., MacGowen, D., and Wenger, L., 1981, Methane solubility in brines with application to the geopressured resource: Proceedings, Fifth United States Geopressured Geothermal Energy Conference, Louisiana State University, p. 205-214.

Price, P. E., and Kyle, J. R., 1983, Metallic sulfide deposits in Gulf Coast salt dome caprocks: Gulf Coast Association of Geological Societies Transactions, v. 33, p. 189-193.

Royden, L., Sclater, J. G., and von Herzen, R. P., 1980, Continental margin subsidence and heat flow--important parameters in formation of petroleum hydrocarbons: American Association of Petroleum Geologists Bulletin, v. 64, p. 178-187.

Schmidt, V., and McDonald, D. A., 1979, The role of secondary porosity in the course of sandstone diagenesis: Society of Economic Paleontologists and Mineralogists Special Publication 26, p. 175-207.

Schwab, K. W., 1979, Visual kerogen and vitrinite reflectance analyses of the Pleasant Bayou No. 1 well, Brazoria County, Texas, in Proceedings, Fourth Conference on Geopressured Geothermal Energy: The University of Texas at Austin, p. 85-131.

Sclater, J. G., and Christie, P. A. F., 1980, Continental stretching: an explanation of the post mid-Cretaceous subsidence of the Central North Sea Basin: Journal of Geophysical Research, v. 85, p. 3711-3739.

Tyler, Noel, 1981, Deltaic and associated shallow marine deposits in the deep Frio Formation, Brazoria County, Texas: Society of Economic Paleontologists and Mineralogists, Gulf Coast Section, Second Annual Research Conference, p. 68-74.

Tyler, Noel, and Han, J. H., 1982, Elements of high-constructive deltaic sedimentation, lower Frio Formation, Brazoria County, Texas: Gulf Coast Association of Geological Societies Transactions, v. 32, p. 527-540.

Walker, R. G., 1979, Turbidites and associated coarse clastic deposits, in Walker, R. G., ed., Facies models: Geological Association of Canada, Geoscience Canada Reprint Series 1, p. 91-104.

Waples, D. W., 1980, Time and temperature in petroleum formation: application of Lopatin's method to petroleum exploration: American Association of Petroleum Geologists Bulletin, v. 64, no. 6, p. 916-926.

Winker, C. D., Morton, R. A., Ewing, T. E., and Garcia, D. D., 1983, Depositional setting and structural style of three geopressured geothermal areas: The University of Texas at Austin, Bureau of Economic Geology Report of Investigations No. 134, 60 p.

Wright, N. J. R., 1980, Time, temperature and organic maturation--the evolution of rank within a sedimentary pile: Journal of Petroleum Geology, v. 2, no. 4, p. 411-425.

Yeh, H. W., and Savin, S. M., 1977, The mechanism of burial metamorphism of argillaceous sediments: 3. Oxygen isotopic evidence: Geological Society of America Bulletin, v. 88, p. 1321-1330.

DISC DOCUMENT INDEX

INDEX: 148

TITLE	TYPE	CREATED	REVISED	PAGES	SECTORS
ETE therm cr caps	WP	6/ 6/84	6/11/84	6	27
ETE therm cr III t-1	WP	6/ 6/84	6/ 8/84	1	4
ETE therm cr t-1	WP	6/ 6/84	6/ 8/84	1	3
ETE therm cr ttp	WP	6/ 6/84	6/ 8/84	1	3
ETE therm cr discl	WP	6/ 8/84	6/ 8/84	2	6
ETE therm cr tcon	WP	6/ 6/84	6/ 8/84	8	37
ETE therm cr IV txt	WP	6/ 6/84	6/ 7/84	26	152
ETE therm cr III txt	WP	6/ 6/84	6/ 7/84	20	115
ETE therm cr II txt	WP	6/ 6/84	6/ 6/84	4	23
ETE therm cr I txt	WP	6/ 6/84	6/ 6/84	15	92
ETE therm cr III app	WP	6/ 6/84	/ /	4	18

STORAGE LEFT 306

END OF DOCUMENT LIST